Stabilisation of lipolytic enzymes for industrial applications

Submitted by Simone Antonio De Rose to the University of Exeter

as a thesis for the degree of Doctor of Philosophy in Biological Science

in October 2017

I certify that all material in this thesis which is not my own work has been identified and that no material has previously been submitted and approved for the award of a degree by this or any other University.

Simone Antonio De Rose

Abstract

The use of enzymes as industrial catalysts is a very promising alternative to conventional synthetic chemistry since enzymes are very specific, selective and display very high activity under mild experimental conditions. This research is focused on lipases, which are widely used in several industrial sectors and especially in the laundry industry. Enzymes in laundry formulation are exposed to alkaline pH, high concentrations of detergents and the presence of proteases. These harsh conditions have a negative effect on the stability and activity of the enzymes and can eliminate the benefits of adding enzymes to formulation entirely.

This study aimed to investigate the stabilisation of existing commercial lipases and the characterisation of a novel cold-adapted lipase for industrial applications.

The commercial lipase Lipex 16L is a variant of the *Thermomyces lanuginosus* lipase and is the current benchmark lipase for application in laundry products. Lipex 16L has been used to develop an improved method for carrier-free immobilisation, using Cross-Linked Enzyme Aggregates (CLEAs). The CLEAs production protocol has been modified by introduction of an activator step to obtain a higher number of individual lipase molecules in the "open lid" conformation and by the introduction of a terminator step to quench the cross-linking reaction at an optimal time to obtain smaller and more homogenous cross-linked particles. This improved immobilisation method has been compared to a commercially available immobilised enzyme and has been shown to be made up of smaller and more homogenous particles with higher activity than the Lipex 16L. The CLEAs produced show improved features for commercial applications such as an enhanced wash performance comparable with the free enzyme, improved stability to proteolysis and a higher activity after long-term storage.

The stabilisation of Lipex 16L has also been investigated through the introduction of two additional glycosylation sites on the protein surface. The commercial Lipex 16L has only one glycosylation site on asparagine 33. A tri-glycosylated mutant has been generated with the introduction of two further glycosylation sites on asparagine 37 and asparagine 99. This recombinant enzyme and a mono-glycosylated wild-type enzyme have been cloned and expressed in *Pichia*

pastoris while a non-glycosylated variant has been expressed in *Escherichia coli*. The enzymatic activities of the glycosylated and non-glycosylated lipases have been compared under various conditions such as temperature, pH, detergents, and incubation with proteases. The results have demonstrated that while the additional glycans do not affect the lipase activity and cleaning performance, they do improve its resistance to proteases and its overall stability with an increase of the melting temperature of + 4 °C.

A novel lipase from the psychrophilic bacteria *Psychromonas ingrahamii* (PinLip) has been biochemically characterised. The enzyme shows activity towards short and medium chain fatty acids and has a good fat stain cleaning performance which makes it attractive for industrial applications. Structural characterisation of the PinLip has been attempted by using crystallisation trials for X-ray crystallography and NMR spectroscopy with limited success. A 3D homology model has been generated using the server I-TASSER using the most closely related known structures, *Gibberella zeae*, *Rhizomucor miehei* and *Rhizopus microspores* lipases, all with a sequence identity to PinLip between 20 and 24%.

The different lipases studied in this thesis have been tested for their stability in the presence of traditional laundry formulation ingredients and new novel biosurfactants using differential scanning fluorimetry (DSF). The results have shown an improved stability of all the Lipex variants in presence of mono-rhamnolipids based biosurfactant, while the cold-adapted PinLip was stabilised by a small concentration of a polymer (EPEI) and few other compounds (Tinopal CBS-CL, and Triethylamine).

The improved CLEAs method and the use of the PinLip enzyme have been patented (Patent no: WO2017/036901, WO2017/036902, WO2017/036915, WO2017/036916, and WO2017/036917).

Table of contents

List of figures

Chapter 1

Chapter 3

Chapter 4

Chapter 5

Chapter 6

List of tables

List of equations:

Abbreviations:

AOX: Alcohol Oxidase

BMG: Buffered Minimal Glycerol

BMMY: Buffered Methanol-complex Medium

CBPG: Cyclic 2,3-bisphosphoglycerate

C-CON: Carbon-Carboxylic Carbon Nitrogen correlation

CD: Circular Dichroism

CIE: Commission International de l'Eclairage

CLEAs: Cross-linked enzyme aggregates

CLECs: Cross-linked enzyme crystals

CLEs: Cross-linked enzymes

COOH: group Carboxylic acid group

CSPs: Cold Shock Proteins

ddH2O: Double distilled water

DDT: Dithiothreitol

DEAE: Diethylaminoethyl Cellulose

DIP: di-*myo*-inositol-1,1′-phosphate

DMSO: Dimethyl sulfoxide

DNA: Deoxyribonucleic acid

DPG: Diglycerol phosphate

DQD: Digital Quadrature Detection

DSF: Differential Scanning Fluorimetry

EC: Enzyme commision

EDTA: Ethylenediaminetetraacetic acid

ER: Endoplasmatic Reticulum

GlcNAc: N-acetyl- glucosamine

HEPES: 4-(2-hydroxyethyl)-1-piperazineethanesulfonic acid

HIC: Hydrophobic Interaction Chromatography

HSQC: Heteronuclear Single-Quantum Coherence

IMAC: Immobilised Metal Affinity Chromatography

IPTG: Isopropyl β-D-1-thiogalactopyranoside

I-TASSER: Iterative Threading ASSEmbly Refinement

LAS: Linear Alkylbenzene sulphonate

LB: Luria-Bertani

LC: Liquid Chromatography

LiAc: Lithium Acetate

LOMETS: Local Meta-Threading-Server

MALDI-TOF: Matrix-assisted laser desorption/ionisation – Time of Flight

Man: Mannose

MBP: Maltose Binding Protein

MEL: Mannosylerythritol lipid

MG: Mannosylglycerate

MGA: Mannosylglyceramide

MtL: *Myceliophthora thermophila* Laccase

MTP: Microtitre plates

MW: Molecular Weight

MWCO: Molecular Weight Cut Off

NMR: Nuclei Magnetic Resonance

PAGE: Polyacrylamide gel electrophoresis

PCR: Polymerase Chain Reaction

PDB: Protein Data Bank

PinLip: Psychromonas ingrahamii Lipase

PMF: Peptide Mass Fingerprint

PMSF: Phenylmethylsulfonyl fluoride

pNP: Para-nitrophenyl

RDB: Regeneration Dextrose Medium

RMDS: Root Mean Square Deviation

RPM: Rotation per Minute

SAX: Strong Anionic eXchange

SCX: Strong Cationic eXchange

SDS: Sodium dodecyl sulphate

SEC: Size Exclusion Chromatography

SLES: Sodium Laureth Sulphate

SOC: Super optimal broth

SRI: Stain Removal Index

SW: Spectrum Width

TfB: Transformation Buffer

TLL: *Thermomyces lanuginosus* Lipase

TROSY: Trans-verse Relaxation-Optimised Spectroscopy

YASARA: Yet Another Scientific Artificial Reality Application

Acknowledgements

I would like to express my special appreciation and thanks to my supervisors Jennifer Littlechild and Dietmar Lang, your constant support and advice have made this thesis possible.

Thanks to Unilever and the University of Exeter for funding this project.

Thanks to Sukriti Singh and Mark Thompson for their help in preparing, running and analysing wash performance experiments during my time at Unilever, to Alfonso De Simone and Jay Patel for the opportunity to perform NMR experiments at Imperial College London University.

I would also like to thank Misha Isupov, Halina Novak, Chris Sayer, and Mirella Vivoli for their friendly advice and useful discussion.

A big thank you to everyone in the Biocatalysis Centre you made my time in Exeter special.

Finally, I would like to thank my parents and my sister who always believed in me, and my dear Simona whose energy and happiness supported me through hard times and pushed me to be the best version of myself.

Chapter 1 - Introduction

1.1 Biocatalysis

Biocatalysis refers to the use of enzymes to catalyse different biotransformations. The term enzyme was first used in 1877 by Professor Wilhelm Friedrich Kühne, however, enzymes had been used for thousands of years for fermentation processes to produce and preserve food such as cheese, beer, vinegar, and wine and for the manufacture of commodities, such as leather and linen (Reetz, 2013). The first example of modern biocatalysis dates back to 1858 when Louis Pasteur treated an aqueous solution of racemic tartaric acid ammonium salt with a culture of the mould *Penicillium glaucum*, which leads to the consumption of (+)-tartaric acid and the concomitant enrichment of the (−)-enantiomer (Pasteur, 1858; Bordenave, 2003). Biocatalysis has since then been applied to many other reactions, such as the biological synthesis of lactic acid in 1880 and the production of optically active molecules using yeast by Neuberg and Hirsch in 1921 (Powell et al., 2001; Reetz, 2013). However, it is only in the past few decades, that biocatalysis has expanded to include hundreds of industrial applications and processes in multiple areas such as food, feed, detergent, tanning, textiles, laundry, pharmaceuticals, cosmetics, and fine-chemicals industries as reviewed by Kumar et al., 2014. The enzyme industry, in its current form, is the result of a rapid development of modern biotechnology, including the use of recombinant DNA, high throughput screening, and protein engineering technologies. The advances in recombinant gene technology have further improved manufacturing processes and allowed the commercialisation of enzymes that were not previously amenable to being produced in sufficient quantities.

Much of the catalytic power of enzymes comes from the binding of their substrates in a favourable orientation to promote the formation of the transition states of enzyme-substrate complexes (Brown 1902; Donald van Slyke et al., 1913; Cornish-Bowden 2013). Indeed, like chemical catalysts, enzymes only accelerate reactions by the reduction of the activation energy needed to carry out the reactions at ambient temperatures. They carry out their reactions in a stereoselective manner and are not used up during in the reaction allowing them to be used for several cycles if they are sufficiently stable.

Enzymes can be classified into six different classes by the Enzyme Commission (EC) from the International Union of Biochemistry and Molecular Biology according to the type of the chemical reaction they catalyse (Table 1.1). Lipases, the enzymes studied in this thesis, belong to the class 3 of hydrolases, and they catalyse the hydrolysis of triglycerides in nature.

Table 1.1**:** The six classes of enzymes (Nomenclature Committee of the International Union of Biochemistry and Molecular Biology (NC-IUBMB)).

Name	**Reaction catalysed**	**Description**
EC 1. Oxidoreductase	$A_{red} + B_{ox} \rightarrow A_{ox} + B_{red}$	Catalyse oxidation-reduction reactions
EC 2. Transferase	A-B+C → A+B-C	Transfer a functional group (e.g. a methyl or phosphate group)
EC 3. Hydrolase	$A\text{-}B + H_2O \rightarrow A\text{-}H + B\text{-}OH$	Catalyse the hydrolysis of various bonds
EC 4. Lyases	A(XH)-B → A-X + B-H	Cleave various bonds by means other than hydrolysis and oxidation
EC 5. Isomerases	Ax ↔ xA	Catalyse isomerisation within a molecule
EC 6. Ligases	A+B+ ATP → A-B + ADP + Pi	Join two molecules with covalent bonds.

The enzyme industry is expanding with the industrial enzyme market growing from 1.6 USD billion in 1998 to 5.1 USD billion in 2009, and it has steadily increased since then (Illanes et al., 2012; DiCosimo et al., 2013).

The use of enzymes presents several advantages in comparison to traditional chemical processes:

I.) Non-toxic catalysts.
II.) High selectivity and high product purity.
III.) Decrease in waste production.
IV.) Operate at mild reaction conditions such as at ambient temperature, at physiological pH and low pressure resulting in lower energy consumption.
V.) Operate in both aqueous and organic solvent based reaction media (Meyer et al., 2012).
VI.) The use of biocatalytic approaches usually shortens synthesis time (Wenda et al., 2011).

These advantages can enhance the efficiency and decrease the cost of many industrial processes making the biocatalytic route a greener process in comparison to traditional synthesis (Posorske, 1984).

However, enzymes are generally unstable under most industrial conditions making biocatalysis challenging to apply in many cases (Novak et al., 2013). In industrial processes elevated temperatures, extremes of pH and the use of organic solvents are often a limitation to the lifetime and the functionality of many enzymes (Powell et al., 2001). Nevertheless, there are enzymes which naturally show very high stability. For example, the xylose isomerase enzyme, used in the production of D-fructose from D-glucose, is stable and active at temperatures up to 70 °C for prolonged reaction times of several months (Schoemaker et al., 2003).

The limitations of biocatalysis have been overcome in many ways. Screening for enzymes in organisms isolated from extreme environments is a popular method for identifying new stable enzymes. These environments include volcanic hot springs, deep ocean black smokers, hypersaline and soda lakes and permanently frozen soil.

However, screening for novel enzymes can be a long and not always successful process. It is estimated that less than 1% of micro-organisms can be cultivated using standard laboratory techniques. Metagenomics has appeared as an alternative strategy to conventional microbial screening techniques. This involves the preparation of a genomic library from environmental DNA and systematically screening such a library for open reading frames that potentially encode novel

enzymes (Lorenz et al., 2002; Kennedy et al., 2008; Uchiyama and Miyazaki 2009).

1.2 Extremophiles

Extremophilic microorganisms represent a tremendous source of many new enzymes, the extremozymes. Extremophiles are adapted to live at high temperatures in volcanic springs, at low temperatures in the cold polar regions, at high pressure in the deep sea, at very low and high pH values (pH 0-3 or pH 10-12), or at very high salt concentrations (5%-30%)(Iyer and Ananthanarayan, 2008).

Over the past decades, a number of hyperthermophilic archaea have been isolated that are able to grow at 100 °C. The organisms with the highest growth temperatures (103-113 °C) are members of the genera *Pyrobaculum, Pyrodictium*, *Pyrococcus* and *Methanopyrus* (Stetter, 1996; Stetter, 2006). Within the bacteria, *Thermotoga maritima* and *Aquifex pyrophilus* exhibit the highest growth temperatures of 90 °C and 95 °C respectively. A review reported in 2006 that there were more than 90 species of hyperthermophilic bacteria and archaea (Stetter 2006) and since that time this number has grown to 156 (Global catalogue of microorganism http://gcm.wfcc.info, Wu et al., 2013)

Running biotechnological processes at elevated temperature has many advantages. The high temperature changes the bioavailability and solubility of the substrates decreasing viscosity and increasing the diffusion coefficient of organic compounds used as enzyme substrates (Niehaus et al., 1999). Although in some industrial applications, the enzymatic reactions need to be carried out at low temperature. In such cases, cold-adapted enzymes could be more applicable rather than mesophilic or thermophilic enzymes. Psychrophilic enzymes present numerous advantages such as energy saving and easy inactivation at the end of the process. Some examples of high/low-temperature enzymatic processes are displayed in table 1.2

Table 1.2**:** Examples of Biocatalysis processes at high and low temperature.

High-temperature processes	**Low-temperature processes**
Glucose isomerase has been used for the catalytic conversion of glucose to high fructose syrup at 60/65 °C (Visuri and Klibanov, 1987)	Cold washing in the detergent industry reduces energy consumption and fabric wear and tear (Maiangwa et al., 2015)
α-Amylase (85–110 °C) and glucoamylase (55–65 °C) used for starch hydrolysis (Riaz et al., 2012)	The lactase from *P. halaktoplanktis* is used to remove lactose from cow milk during storage at 4 °C (Hoyoux et al., 2001)
Cellulase degradation of cellulose at 65–70 °C (Bilen et al., 1998)	Bioremediation of soil and wastewater in mild or cold climate conditions (Kuddus, 2014)

Thermophilic proteins usually share similar three-dimensional structures with their mesophilic counterparts. The differences are usually seen within the primary structure in regions distant from the active site which is more conserved. High diversity is found primarily in loop regions and on the protein surface (Gerday et al. 2000; Iyer and Ananthanarayan 2008).

Primary sequence comparisons have led to a few general observations. Generally, in thermophilic enzymes lysine is replaced by arginine, proline content is higher in some bacterial species such as *Thermus* species, and asparagine/glutamine content is lower compared to their mesophilic counterparts (Ó'Fágáin, 2003). Proline residues exhibit unique dihedral angles in the polypeptide backbone. The cyclic proline residue lowers the entropy of unfolding and stabilises the protein. Proline substitutions have been made in *Thermomyces lanuginosus* lipase in positions where the dihedral angles are appropriate for a Pro residue. The temperature stability has been increased by 2 °C for the mutation G225P in *T. lanuginosus* lipase measured by differential scanning calorimetry (Svedsen et al., 1991).

1.2.1 Enzymes from psychrophiles

A large part of the earth is occupied by permanently cold environments including the Antarctic, Arctic and alpine regions. . Even under such harsh conditions, many cold-adapted microorganisms can grow at 4 ^{o}C or lower (Suzuki et al., 2001).
The cold temperatures place severe physicochemical constraints on cellular functions due to the increase in cell rigidity, and water viscosity.There is subsequently a reduction in solute diffusion rates, membrane fluidity, enzyme kinetics and macromolecular interactions (Rodrigues and Tiedje 2008; Piette et al., 2011).
Psychrophiles have evolved mechanisms to successfully counteract additional stress factors associated with the cold environments, such as desiccation, radiation, excessive UV, high or low pH, high osmotic pressure and low nutrient availability (Morgan-Kiss et al., 2006). In 2014 De Maayer et al. reviewed some of these mechanisms. Low temperature and psychrophilic adaptation profoundly affect membrane fluidity resulting in increased polyunsaturated to saturated fatty acids ratios in membrane phospholipids and a reduced size and charge of the lipid head groups. Cold exposure also induces the up-regulation of genes involved in membrane biogenesis, such as fatty acids and lipopolysaccharide biosynthesis.

Other psychrophilic adaptive mechanisms are the production of cold-shock proteins (CSPs), a family of small, single-stranded nucleic acid binding proteins that regulate a variety of cellular processes, including transcription, translation, protein folding and membrane fluidity (Casanueva et al., 2010). CSPs are also expressed in mesophilic organisms as a response to cold exposure but are constitutively rather than transiently expressed in psychrophiles (D'Amico et al., 2006). Some psychrophiles are also able to produce antifreeze and ice-nucleating proteins. Antifreeze proteins have the ability to modify ice crystal structure and inhibit recrystallisation of ice by adsorbing onto the surface of ice and lowering the temperature at which it grows (thermal hysteresis) (DeVries 1986; Gilbert et al., 2004), while Ice-nucleating proteins can prevent supercooling of water by facilitating ice crystal formation at temperatures close to the melting point (Kawahara, 2002).

The thermostability of thermophilic enzymes has been extensively investigated, and several possible determinants of this stability have been proposed (Georlette

et al., 2004; Littlechild et al., 2013). By contrast, there is little information about the structural determinants of adaptation in cold-adapted enzymes. From 1995 onwards only 56 psychrophilic protein structures have been deposited in the Protein Data Bank (PDB), which is relatively few when compared to the thousands of mesophilic and thermophilic structures deposited in the same period.

Cold-adapted enzymes are characterised by high flexibility, thermolability, and specific activity at low temperatures (Feller and Gerday 2003; D'Amico et al., 2006), while thermostable enzymes are structurally rigid and have low or no activity at low temperatures (Fields, 2001; Vieille and Zeikus 2001). The low stability and high activity of cold-adapted enzymes at low temperatures imply a flexible enzyme structure. The temperature dependence of chemical reactions is commonly described by the Arrhenius equation:

$$k = Ae^{-Ea/RT}, \qquad (1.1)$$

in which the rate of a reaction, k, decreases exponentially with temperature, T (where R is the universal gas constant, A is a reaction specific pre-exponential constant and Ea represents the Arrhenius activation energy of the reaction). According to Equation 1.1, at very low temperatures (0–4 °C), lower kinetic energy is available in the system to overcome reaction barriers therefore only highly favourable reactions can proceed (Siddiqui and Cavicchioli, 2006) however psychrophilic organisms are able to compensate for a very slow metabolic rate and are able to exhibit higher catalytic activities at low temperatures (Margesin and Schinner, 1994).

The analysis of the available 3D structures reveals some general characteristics. Firstly, psychrophilic enzymes seem to have a larger and more accessible catalytic pocket which is often obtained by the replacement of bulky amino acid side chains by smaller groups at the active site entrance or by the deletion/rearrangement of loops bordering the active site. Examples of a psychrophilic enzyme with large catalytic pockets are the protease from *Pseudomonas sp*. TACII18 (Aghajari et al., 2003) and the lipase from *Proteus mirabilis* (Korman and Bowie, 2012) which is homologous with lipases from *Pseudomonas aeruginosa*, *Burkholderia cepacia*, and *Burkholderia glumae.* The

structural comparison shows remarkable differences in the active site pocket as it is much more exposed and solvent accessible than the active site seen in other lipases of known structure, even though *Proteus mirabilis* lipase structure otherwise appears to be in a closed conformation. It is likely that a larger active site is required to reduce the energy necessary for the substrate binding step (D'Amico et al., 2003). However, a larger active site seems to not be the complete explanation for the catalytic activity of the psychrophilic enzymes. In 2006 Siddiqui and Cavicchioli reviewed the adaptation of psychrophilic enzymes to their cold environment and suggested that improved accessibility and enhanced flexibility should not only reduce the energy required to access large substrates but also decrease substrate binding strength increasing the K_m and lowering the potential energy barrier to reaction (Georlette et al., 2004; Siddiqui and Cavicchioli 2006; Fields et al., 2015). This strategy is referred as ground-state destabilisation, and it opposes the classic transition-state stabilisation proposed by Pauling (Pauling, 1946). However while the role of the transition-state stabilisation in enzyme catalysis has been clearly demonstrated by extensive studies, the ground-state destabilisation has limited experimental evidence and remains a controversial hypothesis (Phillips et al., 2016).

Also, sequence comparison with mesophilic enzymes has shown an increased number and clustering of glycine residues (providing local mobility) and a decrease of proline residues in loops (providing enhanced chain flexibility between secondary structures) (Georlette et al., 2004). Aromatic interactions are helpful in promoting stabilisation and they are often missing in psychrophilic enzymes in comparison to their mesophilic homologues (Kennedy et al., 2008).

A major difference between psychrophilic, mesophilic and thermophilic proteins is that the thermophilic proteins retain their structures to higher temperatures. The thermophilic proteins are stabilised by additional interactions resulting in a more robust overall structure (more rigid, higher packing efficiency, reduced entropy of unfolding, conformational strain release and stability of α-helices). Different extremophilic proteins must, therefore, balance the demands of molecular flexibility (for efficient catalysis) and stability (which requires extra interactions and rigidity) (Ó'Fágáin, 2003).

Due to difficulties faced in isolation and cultivation of many extremophilic organisms, a more convenient approach is to clone the gene encoding the required protein into a suitable mesophilic host. This gives the advantages of easy cultivation and high productivity. The recombinant proteins can be further optimised for their specific applications by protein engineering, chemical modification, or immobilisation techniques.

1.3 Protein stabilisation

The first industrial processes that were developed using enzymes found stability to be the major challenge. Although the stability of a protein is not something absolute and depends on several factors, it can be said that each enzyme is stable in its optimum conditions. However, during the biotransformation reaction the enzyme can be exposed to conditions that depart significantly from their physiological environment (Illanes et al., 2012). The main critical factors are the temperature, pH, and hydrophilicity/hydrophobicity of the industrial process but there are many different factors that must be considered for each protein.

Stability of proteins *in vitro* remains a critical issue in their applications in biotechnology. Both storage and operational stabilities affect the usefulness of enzyme application. Storage stability, or shelf life, refers to an enzyme maintaining its catalytic abilities in the period between manufacture and eventual use. Industrial applications are requiring an ever-increasing demand for new and more stable enzymes.

There are different approaches to deal with enzyme stabilisation. Enzyme stability can be studied from the point of view of the different denaturation processes that occur, the kinetics involved therein and the intended industrial use and potential storage of an enzyme-based product.
To improve enzyme stability, two major routes of research have been pursued:

(1) Production of more stable protein mutants by protein engineering
(2) Stabilisation of unstable enzymes by chemical modification, immobilisation and the use of molecule additives.

1.3.1 Protein engineering

Historically the first approach to be used to change or enhance a specific protein's characteristic was rational design. Developed in the early 1970s (Richardson and Richardson, 1989) rational design refers to the construction of protein variants based on the knowledge of the protein structure. The technique has benefited from the new methodology for site-directed mutagenesis and the ability to synthesise an entire gene encoding the desired mutations.
Examples of the application of rational design include the bacterial laccase from *Bacillus sp.* HR03, The variant E188K showing a 3-fold higher thermal activation with respect to the native enzyme (Mollania et al., 2011) and the yeast triose phosphate isomerase that was made 25% more resistant to thermal inactivation by a N78I or N78T substitution (Ahern et al., 1987). Estell and co-worker modified the *Bacillus amyloliquefacien* subtilisin primary oxidation site (Met 222) by saturation mutagenesis, when the methionine was substituted by a non-oxidable residue such as serine the resulting enzyme was resistant to oxidative inactivation (Estell., et al 1985).

The effectiveness of enzyme design can be improved with the use of specific algorithms to target the mutations (Lippow and Tidor 2007; Karanicolas and Kuhlman 2009). However, it has limitations and cannot be used for proteins that have no structural information (Powell et al., 2001).

Directed evolution is a method used in protein engineering that mimics the process of natural selection to evolve proteins towards a defined goal (Lutz, 2010). In directed evolution the design of the library is often critical since for a protein that is composed of 400 amino acids, there are approximately 20^{400} different possible sequences that could exist (Turner, 2009). Since libraries of this size are impossible to be screened, the researchers had to develop a way to successfully screen a well randomised library to maximise the chances to identify good mutants. The earlier techniques involved the application of bacterial mutator strains and subjecting DNA to UV radiation or chemical mutagens. Error-prone PCR, which produces random mutations during the PCR reaction by reducing the DNA polymerase fidelity, is perhaps the most widely used method (Jäckel et al., 2008). After the generation of the libraries is completed a selection screen is necessary to sort positive mutations from the others. The screening method should be highly specific and possibly high-throughput to minimise the time

necessary to screen the library.

There are many examples of directed evolution strategies to improve enzyme stability. In 2003, Butler and co-workers described the directed evolution of a thermophilic laccase from *Myceliophthora thermophila* (MtL). The MtL gene was subjected to random error-prone PCR, expressed in yeast, and screened through nine rounds of *in vivo* shuffling (Pompon and Nicolas 1989). Directed evolution improved the over-expression in *E.coli* eightfold to the highest yield reported for a laccase in yeast (18 mg/litre) (Bulter et al., 2003). In 2013, Sideri and co-worker used directed evolution to obtain a mutant of the bacterial cytochrome P450 BM3 capable of hydroxylation of unnatural substrates such non-substituted polycyclic aromatic hydrocarbons. In contrast to rational design, directed evolution techniques do not require prior knowledge of the protein structure which is a significant advantage in many cases.

In addition to protein engineering methods, there are many other ways to obtain a more stable protein through protein immobilisation or chemical modifications.

1.3.2 Other methods of protein stabilisation

Enzymes used for industrial applications often have to be immobilised to be used efficiently for extended time periods for biotransformation reactions. In addition, some other critical enzyme properties have to be improved like stability, activity, inhibition by reaction products, and selectivity (Mateo et al., 2007). Enzyme immobilisation needs to be carefully designed in order to balance improved stability versus activity loss.

There are a variety of methods used to immobilise enzymes, the three of the most common being (i) adsorption, (ii) entrapment and (iii) covalent immobilisation or cross-linking to a support (Spahn and Minteer, 2008; Singh et al., 2013).

Immobilisation of enzymes by adsorption involves the binding of the enzyme to a support matrix by weak attractive forces, such as van der Waals, hydrophobic interactions and hydrogen bonds. The immobilisation is achieved simply by incubation of the enzyme solution within the support. For the case of lipases, the interaction of the enzyme with a hydrophobic support which resembles an oily interface can activate the lipase through the phenomenon of interfacial activation (Balcão and Malcata 1998; Paiva et al., 2000). Immobilisation by adsorption may

stabilise the enzyme against interaction, aggregation, autolysis or proteolysis by proteases from the extract (Spahn and Minteer, 2008).

.

Due to the weak forces which regulate the adsorption of this kind of immobilisation it is a reversible process. The enzyme can be detached from the support with an appropriate buffer changing pH and ionic strength to disrupt the weak interactions between support and enzyme. This method is highly attractive since when the enzymatic activity has decayed, the support can be regenerated and reloaded with a fresh enzyme (Mohamad et al., 2015).

Entrapment is caging of enzymes by covalent or non-covalent bonds within gels or fibres. This technique presents the advantages of physically separating the enzyme from the reaction environment and minimising enzyme leaching while improving its stabilisation. Drawbacks of this method include the limitation of transport of the substrate to the enzyme active site (Spahn and Minteer, 2008). There are several types of matrices for entrapment, and the most commonly used are alginate, polyacrylamide, polyurethane, polyvinyl alcohol and k-carrageenan. The entrapment process may be a purely physical caging or involves covalent binding. The surface lysine residue may be derivatised and the enzyme can then be copolymerised with acrylamide and bisacrylamide to form a gel. *Thermomyces lanuginosus* xylanase has been immobilised by entrapment in alginate, the activity of the non-covalently linked enzyme was higher and showed higher thermal stability than the free enzyme at 70 °C (Edward et al., 2015). Chymotrypsin covalent entrapment in polymethacrylate and polyacrylamide gels gave heat stability increases of up to 1000 fold (Klibanov, 1983).

Covalent immobilisation presents the advantages of being stable and highly specific, and the technique allows for excellent control of enzyme orientation and activity. The formation of covalent bonds is commonly achieved through ester, ether, thioether, amide or carbamate bonds between the enzyme and support material involved (Brena and Batista-viera, 2006; Homaei et al., 2013). By contrast to the adsorption, this method is irreversible meaning that the support and the enzyme need to be discarded when the enzyme activity decays.

Cross-linking of the enzyme is a type of covalent immobilisation which doesn't require a support, but instead, the enzyme molecules are covalently bound to

each other with a cross-linker, commonly glutaraldehyde a cheap and very versatile agent (Schoevaart et al., 2004). The technique of protein cross-linking using the reaction of glutaraldehyde with reactive amine residues on the protein surface was initially developed in the 1960s (Doscher and Richards, 1963; Schmidt and Bornscheuer, 2005). However, this method had several drawbacks, such as low activity retention, poor reproducibility, low mechanical stability and difficulties in handling the gelatinous Cross-Linked Enzymes (CLEs). Subsequently, cross-linked enzyme crystals (CLECs) were developed and successfully commercialised into industrial biocatalysts (Clair and Navia, 1992). An inherent disadvantage of CLECs is the need to crystallise the enzyme, which is often a laborious procedure requiring enzyme of high purity. Cross-linked enzyme aggregates (CLEAs) solve this issue with the precipitation of enzymes from aqueous solution followed by the cross-linking of the protein aggregates (Sheldon et al., 2005). The mechanical resistance of the CLEAs particle is lower that of the CLECs (Garcia-Galan et al., 2011), but it has the advantage of using less pure enzyme preparations and can be carried out more rapidly.

The other commonly used approach is to introduce additives to the protein to stabilise it and increase its long-term storage. Under extreme conditions microorganisms produce small organic compounds called osmolytes, which are zwitterionic uncharged or anionic molecules (Lentzen and Schwarz, 2006; Littlechild et al., 2013). Their natural role is to maintain homeostasis however osmolytes are also produced in response to environmental changes such as high temperature and can reach concentrations up to 2 M (da Costa et al., 1998; Lentzen and Schwarz, 2006). These molecules include amino acids, sugars, polyols, betaine and ectoines (Littlechild et al., 2013). However, extremophiles produce alternative osmolytes named extremolytes. Amino acids, betaine and ectoines are not found in hyperthermophiles but mannosylglycerate (MG), mannosylglyceramide (MGA), di-*myo*-inositol-1,1′-phosphate (DIP), diglycerol phosphate (DGP), di-mannosyl-di-*myo*-inositol phosphate, and cyclic 2,3-bisphosphoglycerate (cBPG) (Borges et al., 2002) seem to play a role not only in the osmotic adaptation of thermophilic and hyperthermophilic organisms, but also in their adaptation to high temperature (Ciulla et al., 1994; Martins and Santos, 1995; Silva et al., 1999). Osmolytes act by increasing protein hydration and consequently reducing protein unfolding (Littlechild et al., 2013). Osmolytes are

being used for their stabilising effect. Some of the many applications are highlighted in a review by Lentzen and Schwarz (2006) and include stabilisation of enzymes against thermal stress and freeze-drying (Borges et al., 2002), inhibition of aggregation and neurotoxicity of Alzheimer's beta-amyloid (Kanapathipillai et al., 2005) and prevention of UVA-induced photoaging (Buenger and Driller, 2004).

1.3.2.1 Protein glycosylation

In addition to the widely used immobilisation techniques, other natural stabilisation methods involve glycosylation of the protein at specific sites on its surface. Using genetic modification techniques, it is possible to introduce new glycosylation sites in the protein sequence. The glycosylation of a specific protein can be achieved by chemical modification or heterologous expression coupled with rational design. The two approaches have their pro and cons. The chemical approaches offer greater flexibility and control in the choice of the defined glycan, and the chemical modification of potential glycosylation sites.

The other approach to produce glycosylated proteins is to use the heterologous expression of eukaryotic hosts that have the machinery to glycosylate their proteins. This approach is simpler but has the disadvantage of limited control over the type and order of sugars which is determined by the host selected for the expression. A conventional approach is to over-express the enzyme in a fungal host system. The attraction of fungi as production hosts is based on the high yield of protein obtained and the ease of purification due to their natural ability to secrete large amounts of proteins into the growth medium (Nevalainen et al., 2005). The rational design can be used when a protein has none or few of the naturally occurring glycosylation sites found in fungal proteins. Site-directed mutagenesis can be applied to introduce new glycosylation sites on the protein surface.

Glycosylated proteins have interesting biological properties along with increased stability to proteolysis, heat, storage and chemical denaturants (Schwarz and Datema 1980), which, in many cases are thought to be due to the carbohydrate addition to the protein surface.

1.3.2.2 Addition of additives

Most enzyme formulations on the market are using different small molecule additives used as stabilisers (Iyer and Ananthanarayan 2008). Using additives is a good approach towards enhancing enzyme storage stability however in some applications such as in the detergent industry the formulation is designed for another purpose rather than the stabilisation of the enzyme itself, such as removing a stain. In these cases, if the formulation design is co-operative, the ingredients can play not only their own specific role but can also result in an overall synergy to improve the washing effect. Conversely, if an improper formulation is produced, components will offset each other, and result in adverse effects (Zhang et al., 2014).

1.4 Lipases

Lipases (EC 3.1.1.3) are ubiquitous enzymes that can hydrolyze long-chain acyl-triglycerides to di- and monoglycerides, glycerol, and free fatty acids at a water/oil boundary (Maurer, 2004). The lipase enzyme was first identified by Sarda and Desnuelle (1958) as an esterase with a peculiar mechanism of activation in the presence of substrate emulsions called interfacial activation that deviates from classical Michaelis-Menten kinetics. The essential role of lipases in all living organisms is to transport and process dietary lipids (triglycerides, fats, oils). Besides their role in lipid metabolism lipases are widely used in biotechnology applications such as being additives in detergents, involved in the manufacture of food ingredients, in pitch control in the pulp and paper industry, in biopolymers and in biodiesel production, in biotransformation reactions (Jaeger and Eggert, 2002). The properties of lipases such as their stability in organic solvents, catalytic activity without cofactors, broad substrate specificity and high enantio-selectivity make them the most widely used class of enzymes in a number of biocatalytically crucial chemical reactions including esterification, transesterification, regioselective acylation of glycols and menthols, and synthesis of peptides and other chemicals (Sharma et al., 2001). A Table listing many of the industrial application of lipases is shown below (Table 1.3).

Table 1.3: Examples of Industrial applications of microbial lipases (adapted from Vulfson, 1994).

Industry	**Action**	**Product or application**
Detergents	Hydrolysis of fats	Removal of oil stains from fabrics
Dairy foods	Hydrolysis of milk fat, cheese ripening, modification of butter	Development of flavouring agents in milk, cheese, and butter
Bakery foods	Flavour improvement	Shelf-life prolongation
Food dressings	Quality improvement	Mayonnaise, dressings, and whippings
Fats and oils	Transesterification, hydrolysis	Cocoa butter, margarine, fatty acids, glycerol, mono-, and diglycerides
Chemicals	Enantioselectivity, synthesis	Chiral building blocks, chemicals
Pharmaceuticals	Transesterification, hydrolysis	Speciality lipids, digestive aids
Biofuels	Transesterification, hydrolysis	Biodiesel
Leather	Hydrolysis	Leather products
Paper	Hydrolysis	Paper with improved quality

Lipases represent the third most commercialised enzymes, after proteases and amylases (Hasan et al., 2006). The primary commercial application for hydrolytic lipases is their use in laundry detergents. In 1998 it was estimated that 1000 tonnes of lipases were added to approximately 13 billion tonnes of detergents produced each year (Jaeger and Reetz, 1998), and this has continued to increase.

1.4.1 Structure and mechanism of lipases

The three-dimensional structure of many lipases has been well studied over the past decades, and many structures are now available. In terms of the overall amino acid sequence lipases can show very limited similarity(Jaeger et al., 1994;

Anobom et al., 2014) however all lipases share the same structural architecture called α/β hydrolase fold (Schrag and Cygler, 1997). The α/β hydrolase fold family includes proteases, lipases, esterases, dehalogenases, peroxidases and epoxide hydrolases, making it one of the most versatile and widespread protein folds known (Nardini and Dijkstra, 1999). The α/β fold is characterised by a highly conserved catalytic triad consisting of a nucleophile (serine, cysteine, or aspartic acid) positioned after strand β5, an aspartic or glutamic acid almost always positioned after strand β7 and a conserved histidine residue located after the last β strand (Fig. 1.1).

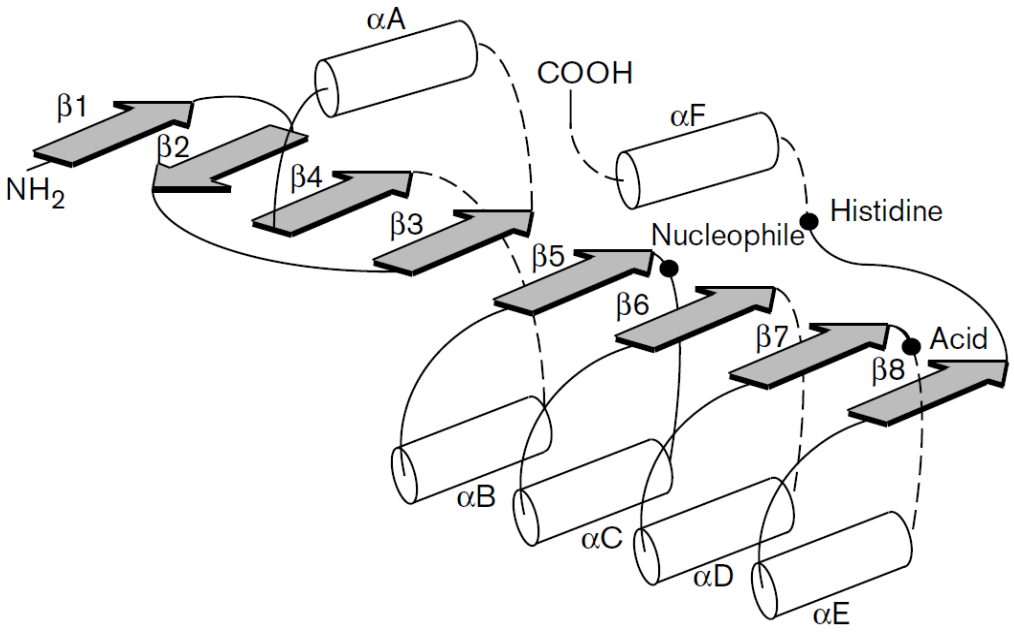

Fig. 1.1: Secondary structure diagram of the 'canonical' α/β hydrolase fold. α helices and β strands are represented by white cylinders and grey arrows, respectively. Black dots indicate the location of the catalytic triad. Dashed lines indicate the location of possible insertions (Image taken from Nardini and Dijkstra, 1999).

The nucleophile residue is usually located in a sharp turn towards the C-terminal end of the β5 strand, named the 'nucleophile elbow', where it is accessible to the substrate and water (Anobom et al., 2014). The nucleophile is encoded by a consensus sequence shared by almost all lipases, Gly-X-Ser-X-Gly. The geometry of the nucleophile elbow also contributes to the formation of the oxyanion binding site, which is termed 'oxyanion hole' and stabilises the negative charge that occurs during hydrolysis. In most lipases, the active site is buried under a lid, making it inaccessible to the substrate in the so-called closed conformation (Schmid and Verger, 1998).

The lid is a distinguishing feature of lipases (Fig. 1.2) (Schrag et al., 1997; Jaeger and Reetz 1998; Jaeger et al., 1999) and gives a structural explanation for their peculiar property, that the activity of lipases, but not esterases, is enhanced upon contact with a lipid-water interface, which triggers the opening of the lid (Nardini and Dijkstra, 1999). Upon opening, the active site becomes accessible, and the lid exposes a large hydrophobic surface, whereas the previously exposed hydrophilic domain becomes buried inside the protein, in the so-called open conformation (Schmid and Verger, 1998). This process is termed interfacial activation, and it has been observed in many lipase enzymes (Derewenda et al., 1992; Verger, 1997). However, there are exceptions such as *Candida antarctica* lipase B which is a widely used commercially available enzyme which lacks the lid domain and is not activated at a water-lipid interfacial surface (Martinelle et al., 1995). A better distinction between lipases and esterases would be to consider lipases as esterases that act on long-chain triacylglycerol (Verger, 1997; Jaeger et al., 1999).

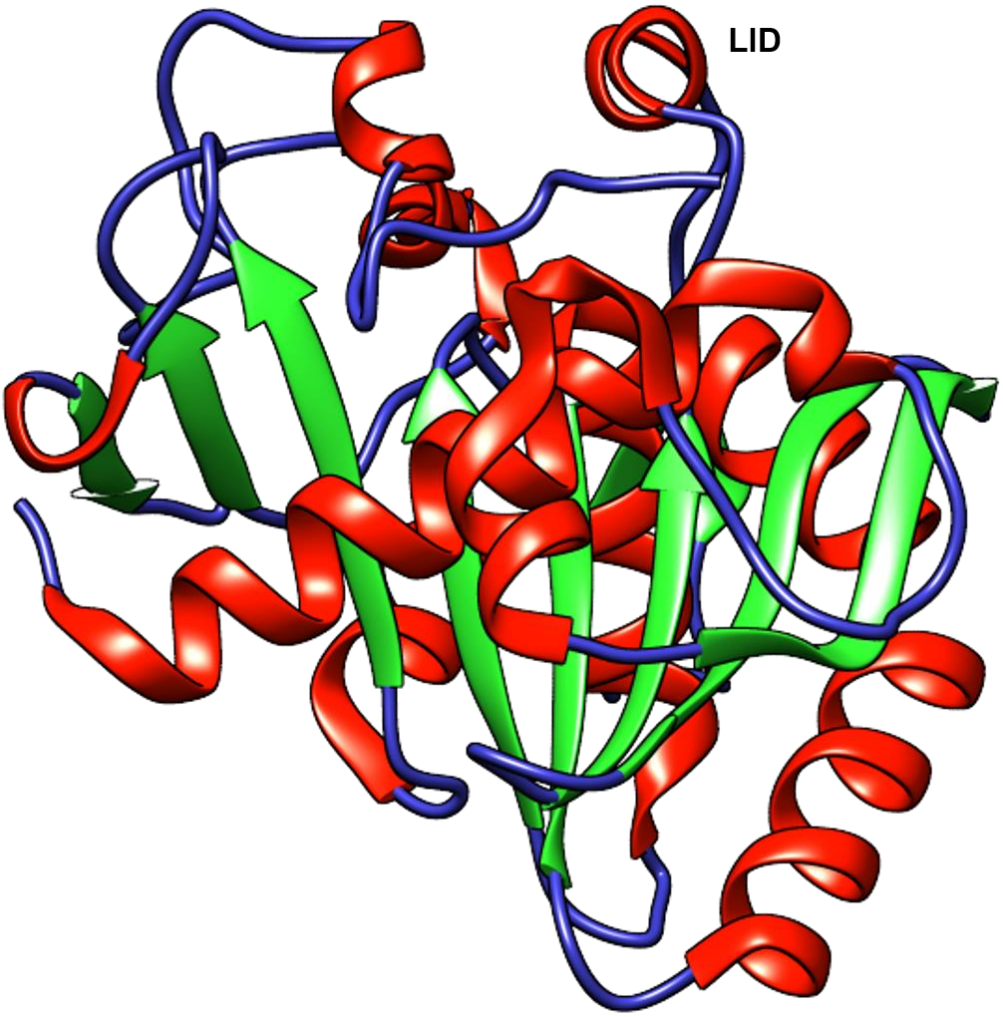

Fig. 1.2: Example of a lipase structure using the *Thermomyces lanuginosus* lipase(PDB: 1TIB)which shows the enzyme in the closed conformation (Image produced with the program UCSF Chimera (Pettersen et al., 2004)).

The catalytic mechanism of a lipase is described in Fig. 1.3. The hydrolysis of the substrate takes place in two steps. In the first step, the oxygen atom of the catalytic serine attacks the carbon atom of the ester linkage carbonyl group, this proton transfer is facilitated by the presence of the catalytic acid, which precisely orients the imidazole ring of the histidine and partly neutralises the charge that develops on it. A transient tetrahedral intermediate is formed, that makes hydrogen bonds with backbone nitrogen atoms in the “oxyanion hole.” Next, the alcohol part (**R^2OH**) is liberated from the intermediate while the acid component of the substrate remains covalently attached to the serine residue in the acyl-enzyme intermediate (**R^1CO-E**), which is ultimately hydrolysed releasing free fatty acid and regenerating the enzyme.

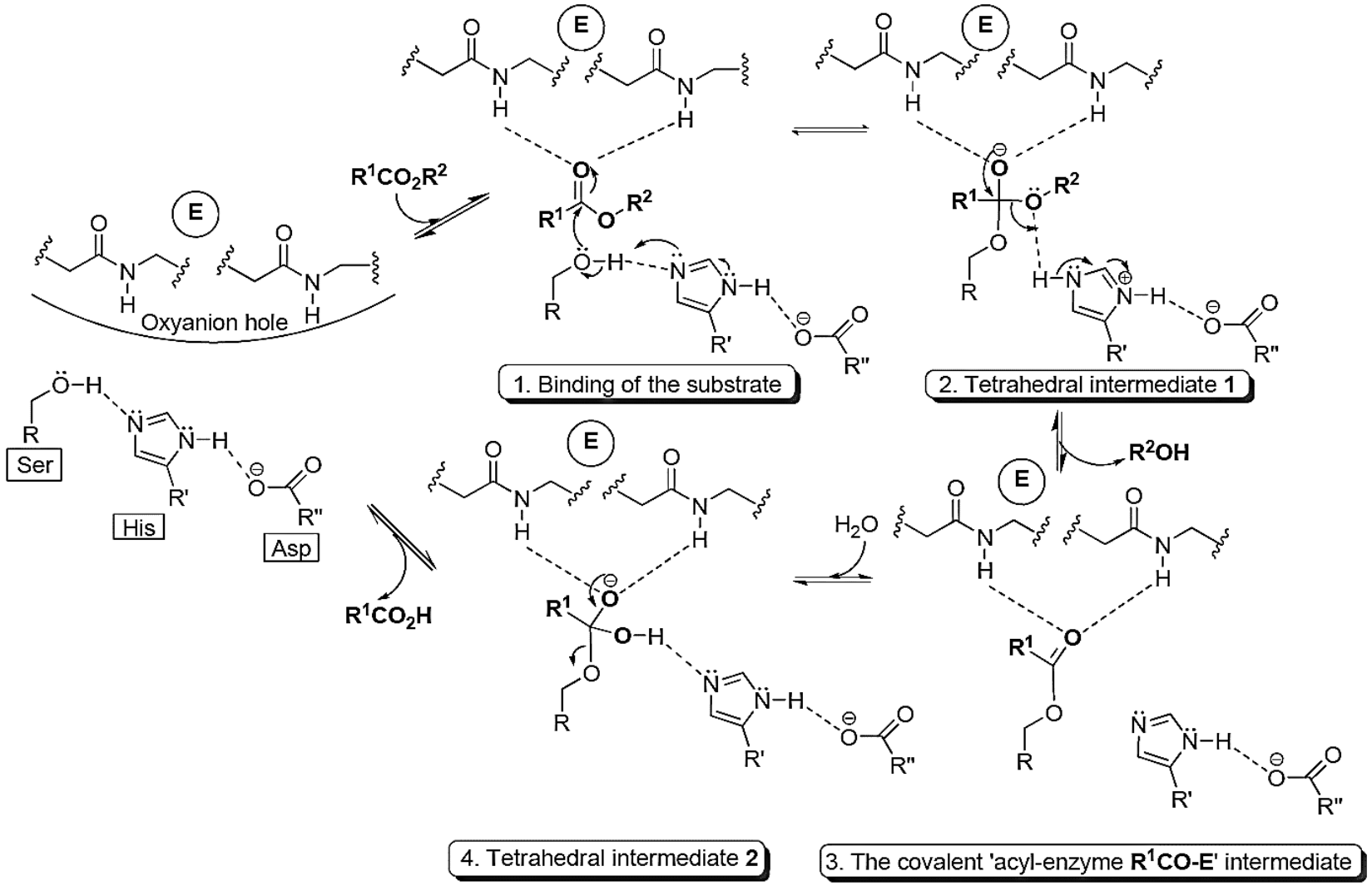

Fig. 1.3**:** The catalytic cycle of a lipase catalysed hydrolysis of an ester bond (Image taken from Turcu, 2010)**.**

Evidence for this mechanism has come from various studies (Jaeger and Reetz, 1998; Nardini and Dijkstra, 1999; Gupta et al., 2003; Anobom et al., 2014). In addition, crystallographic data from other α/β hydrolase enzymes such as proteases, haloalkane dehalogenases and carboxylesterases, has provided definitive evidence for the occurrence of a covalent intermediate (Verschueren et al., 1993; De Simone et al., 2004; Liu et al., 2004).

1.4.2 Lipases in the detergent industry

Both in terms of volume and value detergent industries are a large consumer of enzymes. Dirt on clothes is a complex mixture of inorganic and organic compounds. Inorganic dirt like dust can be removed easily with the assistance of surfactants and chelating agents in the detergent. Whereas organic dirt such as the body secretion of sebum or blood, which is mainly composed of organic compounds, for example, protein, fat, etc. are often insoluble in water and are highly adhesive to the surface of textiles, which makes them difficult to remove thoroughly with surfactants and co-surfactants (Zhang et al., 2014).

The application of enzymes in detergents enhances the detergents ability to remove tough stains and also makes detergents more eco-friendly (Gurung et al., 2013).

Enzymes have been used as catalysts in detergents since the 1960s. The first detergent containing a bacterial protease was introduced by Novo Nordisk (now Novozymes) in 1956. The presence of lipases in detergent formulations is needed to remove fat-containing stains. In contrast with other biocatalytic processes where an enzyme is selected for its high selectivity of the reaction. Lipases used in detergent formulations are chosen on the basis of their broad substrate specificity, and their resistance to harsh washing conditions at alkaline pH and high temperatures, to oxidizing and chelating agents, and to damage induced by surfactants and other enzymes, such as proteases, which are found in many detergent formulations (Hasan et al., 2006; Borrelli and Trono 2015). The first lipase introduced into detergent formulations in 1988 was known as Lipolase®, the enzyme was cloned and expressed into *Aspergillus oryzae* by Novo Nordisk. In the 1990s, more recombinant lipases were introduced onto the market for detergent applications and these enzymes have been subjected to protein engineering to improve their stabilities and catalytic properties under washing

conditions (Wolff and Showell 1997). In particular, two lipases from *Pseudomonas mendocina* and *Pseudomonas alcaligenes*, which are known as Lumafast® and Lipomax®, respectively, were recombinantly expressed in *Bacillus subtilis* and commercialised by Du Pont while a lipase from *Pseudomonas glumae* was commercialised by Unilever. For the *P. glumae* lipase, an engineered variant with improved resistance to proteases was produced (Frenken et al., 1993).

More recently, a whole-cell biocatalyst has been applied to real-life laundry process. Lipase from *Burkholderia cepacia* and its chaperone were co-expressed on the surface of *E. coli* by autodisplay. The whole-cell biocatalyst and the outer-membrane preparations were used in standardised laundry tests that imitated regular machine washing. Both of these preparations appeared to be stable enough to endure the standard European laundry test, while they showed the same lipolytic activity as the purified lipase from *B. cepacia* and the commercial Lipex® (Kranen et al., 2014; Borrelli and Trono, 2015).
In recent years, the trend of lower washing temperatures and an economical and more sustainable laundry procedure has made the removal of fatty stains more difficult. The use of cold-active lipases in the formulation of detergents could solve this problem, with the additional advantages of a reduction in energy consumption and wear and tear of the textiles (Feller and Gerday, 2003).

1.4.3 Cold-adapted lipases

Cold-adapted lipases have become important biocatalysts due to their high activity, and specific regioselectivity in organic solvents with broad substrate specificities at low temperatures (Gerday et al., 2000). They have a wide range of potential applications for the esterification, transesterification and hydrolysis, of triglycerides and in the chiral selective synthesis of esters (Hardwood, 1989).
In the past decade, several attempts have been made to isolate cold adapted lipases from microorganisms isolated in Antarctic and Polar Regions or from deep-sea sediments. The bacteria isolated include *Pseudoalteromonas sp*., *Psychrobacter sp*. (Zeng et al., 2004) and *Photobacterium lipolyticum* (Ryu et al., 2006). A soil bacterium *Oceanobacillus rekensis* isolated from saline soil produced a cold-active lipolytic enzyme (Jiewei et al., 2014). Other bacterial

species including *Pseudomonas fragi* (Alquati et al., 2002), *Pseudomonas fluorescens* (Dieckelmann et al., 1998) *Serratia marcescens* (Abdou, 2003) and *Yersinia enterocolitica* (Ji et al., 2015) which produces cold active lipases were isolated from refrigerated milk and food samples.

Cold-active lipases can also be found in psychrophilic fungi and yeast. Some examples are *Candida lipolytica, Geotrichum candidum* and *Penicillium roqueforti* isolated from frozen food samples for cold active lipase production (Alford and Pierce, 1963).

On the structural point of view so far only two structures of cold-adapted lipases have been solved. In 2008 Jung and co-worker determined the crystal structure of the *P. lipolyticum* M37 lipase at 2.2 Å resolution (PDB: 2ORY) and compared it to that of non-adapted *Rhizomucor miehei* lipase (RML) (PDB: 3TGL) (Jung et al., 2008). Next in 2012 Korman and Bowie solved the structure of *Proteus mirabilis* lipase (PDB: 4GW3), which is homologous with lipases from *P. aeruginosa*, *B. cepacia*, and *B glumae*. Both the M37 lipase and the *P. mirabilis* lipase showed a wide oxyanion hole when compared to the respective closest mesophilic homologues. Both the enzymes seemed to utilise a unique solution to improve their catalytic efficiency. The M37 structure revealed some interesting features, a lid composed of two helices and a wide active site that is solvent accessible even in the closed conformation. The structural analysis revealed that M37 lipase adopted a folding pattern similar to that observed for other lipase structures. However, comparison with RML revealed that the region beneath the lid of the M37 lipase included a significant and unique cavity that would be occupied by a lid helix upon substrate-binding. In addition, the oxyanion hole was much wider in M37 lipase than RML. The author proposed that these distinct structural characteristics of M37 lipase might facilitate the lateral movement of the helical lid and subsequent substrate hydrolysis, which might explain its low activation energy and high activity at low temperatures (Babu et al., 2008).

In the case of *P. mirabilis* lipase comparison showed longer loops connecting the helices and an active site pocket much more exposed and solvent accessible than the active site seen in other lipases of known structure, even though the lipase structure otherwise appeared to be in a closed conformation. Moreover *P. mirabilis* lipase lacked a conserved disulphide bond (between 181 and 238) suggesting the possibility of increased conformational flexibility for folding and catalysis at low temperature (Korman and Bowie, 2012).

Balancing the stability of an enzyme with its activity and flexibility is fundamental to understanding the functional and structurally adaptive properties (Margesin and Häggblom, 2007; Buzzini et al., 2012; Struvay and Feller, 2012).

1.5 Lipases investigated in this project

1.5.1 Lipase from *Psychromonas ingrahamii*

The extreme psychrophile *P. ingrahamii* was isolated from sea ice from the Arctic. It grows exponentially with a doubling time of 240 hours at -12 °C and may well grow at even lower temperatures (Breezee et al., 2004).

The single, circular chromosome of 4.56 Mb constituting the genome of *P. ingrahamii* has been sequenced. The GC content of *P. ingrahamii* DNA was determined experimentally to be 40% and verified by the composition of the total genome sequence (40.1%). The amino acids isoleucine, asparagine, lysine, phenylalanine and tyrosine all are present at a higher percentage in *P. ingrahamii* compared to those of *Vibrio cholerae*, *Shewanella oneidensis and E. coli* (Breezee et al., 2004; Riley et al., 2008).

P. ingrahamii belongs to the family of gamma-proteobacteria and like all proteobacteria is Gram-negative. Like other marine organisms, *P. ingrahamii* appears to have the capability of utilising macromolecules in the environment for nutrition and energy. *P. ingrahamii* has genes for 48 peptidases and proteases and has a complete general secretion system capable of excreting such degradative enzymes to the environment. To take up the digestion products of proteolysis, there are ABC-type transporters for peptides and amino acids. There is also evidence that *P. ingrahamii* is capable of hydrolysing fats as there are three lipases and five phospholipases (Riley et al., 2008).

Cold-active lipases offer new opportunities for biotechnological exploitation based on their high catalytic activity at low temperature and low thermostability and unusual specificities. Indeed, the cold enzymes, along with the host microorganisms cover a broad spectrum of biotechnological applications. They include additives in detergents (cold washing), additives in food industries (fermentation, cheese manufacture, bakery, meat tenderising), and environmental bioremediations.

1.5.2 Lipase from *Thermomyces lanuginosus*

The *T. lanuginosus* lipase is a single-chain protein consisting of 269 amino acids. It has a molecular weight of 31,700 Da and an isoelectric point of 4.4 (Jha et al., 1999).The T. lanuginosus lipasestructure has been solved at 1.8 Å resolution (Derewenda et al., 1995). It is approximately spherical, (35Å×45Å×50Å), and contains a central eight-stranded, β-sheet structure with five interconnecting α-helices (Fig. 1.4 shows the open and closed structures of this enzyme).

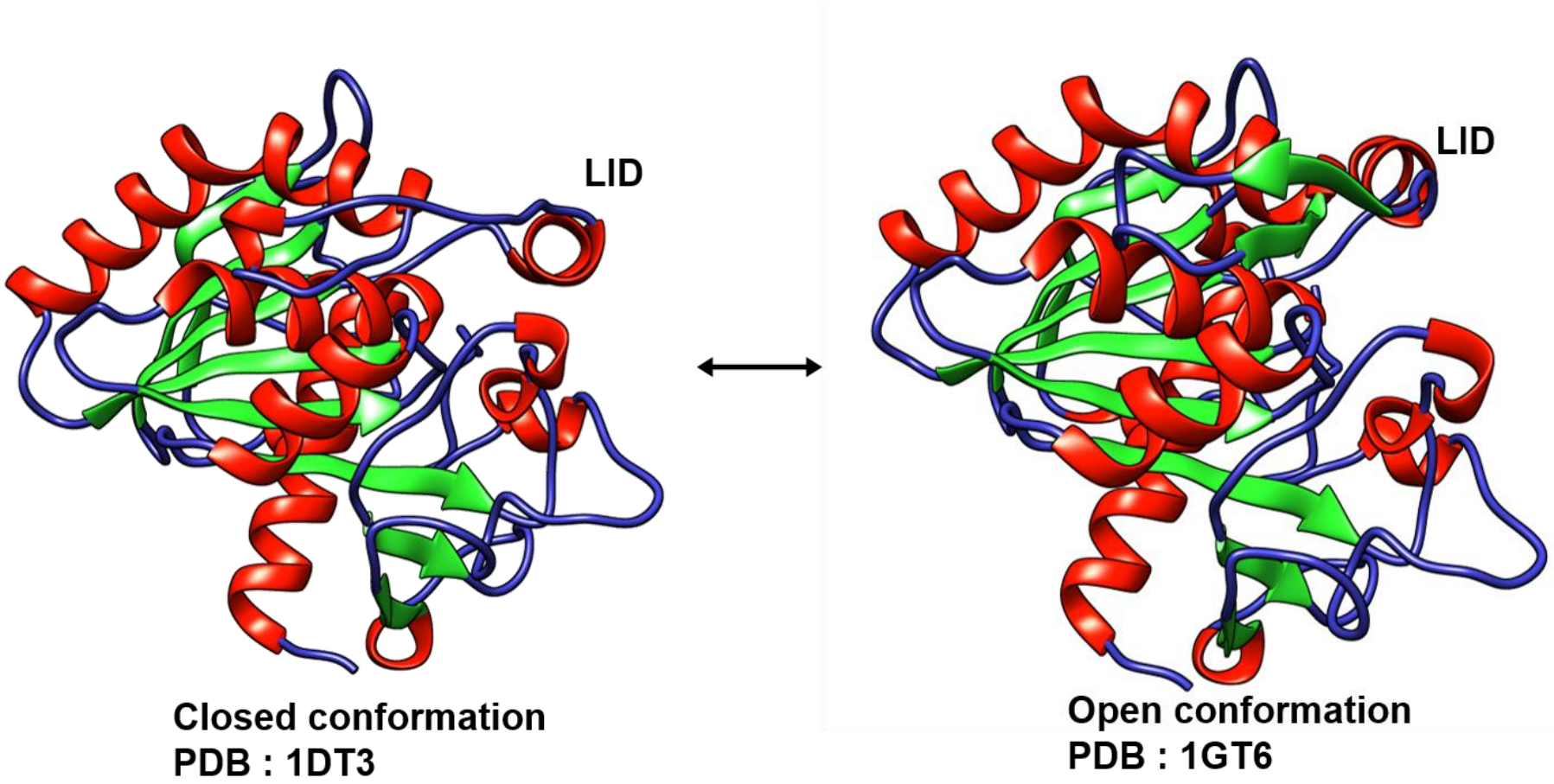

Fig.1.4: Structure of the open (PDB: 1GT6) and closed (PDB: 1DT3) forms of *T. lanuginosus* lipase.. The structures are displayed using the program UCSF Chimera (Pettersen et al., 2004).

The lid is an α-helical mobile surface loop consisting of amino acids 86–93 that covers the active site (Derewenda et al., 1995). The active site includes the typical Ser-His-Asp catalytic triad, and it is important to notice one of the four Trp residues of *T. lanuginosus* lipase, Trp89, is located in the lid region (Martinelle et al., 1995). This residue has been demonstrated to be very important for efficient hydrolysis since site-directed mutagenesis at Trp 89 decreases the activity of *T. lanuginosus* lipase (Martinelle et al., 1995).

The *T. lanuginosus* lipase is quite stable and it maintains activity at 55–60 °C (Fernandes et al., 2005), with the maximum of activity at pH 9.0 (Rodrigues et al., 2009).

Even though *T. lanuginosus* lipase is a relatively stable enzyme, any further improvement in its stability is of interest to further increase its range of applications. The high activity and stability of *T. lanuginosus* lipase have permitted the use of this enzyme in different solvent conditions. From biphasic water-organic–solvent media to solvent-free reactions (Dominguez de Maria et al., 2009), there are many processes catalysed by this enzyme. The lipase from *T. lanuginosus* was the first to be commercialised on a large scale in 1988 under the name Lipolase®, and due to its versatility, it has been used in many industrial applications (Fernandez-Lafuente, 2010). Over the years different variants of Lipolase® have been produced using site-directed mutagenesis. Lipolase® Ultra showed improved binding towards fatty acids due to the substitution of an acidic residue in the region that binds the substrate with a uncharged leucine residue. LipoPrime® (S216W), showed better performances in the first wash and Lipex® (T231R - N233R) showed better performances in the first wash at temperatures as low as 20 °C and showed beneficial synergistic results when combined with bleach catalysts (Borrelli and Trono, 2015). Lipex® is still widely used in the laundry industry where it is considered one of the benchmark enzymes to which new lipase enzymes should be compared in term of performance.

1.6 Aims and Objectives

This project is part of a collaboration between the University of Exeter and Unilever R&D Port Sunlight focused on the stabilisation of existing commercial lipase enzymes and on the discovery of a novel psychrophilic lipase that could be applied to cleaning applications such as laundry and household care.

The first aim of this project is to investigate the stabilisation of the industrial *T. lanuginosus* lipase variant named Lipex 16L. Lipex 16L is used in the laundry formulation to overcome the issue of long-term storage stability in the presence of a companion enzyme such as protease which could impair lipase activity by proteolysis. A carrier-free immobilisation method will be used in developing a more stable biocatalyst for application in laundry detergents. This will include the design of a new protocol and the characterisation of stability and wash performance of the new biocatalyst (Chapter 3). In Chapter 4 a different approach is pursued with the study of the effect of glycosylation profile on proteolysis resistance. Lipex 16L naturally has just one glycosylation site on N33 in order to better understand how different glycosylation may affect stability and activity a mutant with three glycosylation sites has been generated expressed and characterised.

The second aim is to investigate the use of a novel psychrophilic lipase for new catalysts at low temperature. Cold-adapted enzymes are an attractive prospect for biocatalysis which may allow substantial economic benefits such as energy savings. A novel psychrophilic lipase from the arctic bacteria *Psychromonas ingrahamii* (PinLip) has been overexpressed and subsequently characterised biochemically and in terms of wash performance (Chapter 5). Structural characterisation will be attempted with the aim of elucidating the three-dimensional structure of the enzyme using X-ray crystallography (Chapter 6).

The third aim is to investigate the impact of the individual laundry formulation ingredients on the psychrophilic and mesophilic lipases (Lipex 16L and in-house generated variant) and then translation of the findings into the establishment of the best formulation plus enzyme combination for better cleaning performance.

This will include the exploration and evaluation of next-generation bio-surfactants (e.g. Rhamnolipid) which have the potential to substitute some of the current formulation ingredients (Chapter 7).

In summary, this work seeks to investigate novel stabilisation methods for industrial enzymes which will allow their improved performance in the laundry detergents application (Chapter 3, 4 and 7) and to characterise a novel cold-adapted lipase for its potential industrial applications (Chapter 5 and 6).

Chapter 2 - General Materials and Methods

Lipex 16L™ and Coronase™ were obtained from Novozymes (Bagsværd, Denmark), Lipase-sensitive stains: CS61–Beef fat stain, and C46B-Used fry fat were from Warwick Equest Ltd (Durham, United Kingdom). Laundry detergent formulations and individual formulation ingredients were kindly donated by Unilever (Port Sunlight, UK). All other chemicals were obtained from Sigma-Aldrich (Irvine, UK) unless otherwise stated. All chemicals used were of analytical grade. All solutions were made using double distilled purified water (ddH_2O) unless otherwise stated. All media and buffers used in microbiology were sterilised by autoclaving at 121 °C and 15 psi for 20 minutes, or by filter sterilisation using a Sartorius Stedim, minisar 0.2 µm single-use filter unit (Stonehouse, UK).

2.1 Microbiology

2.1.1 Growth media

Table 2.1: Media used in this study

***E. coli* Media**	**Components (for 1 L)**
Luria-Bertani (LB) broth	10 g Tryptone 10 g NaCl 5 g Yeast extract
LB agar	1 L LB Broth 8 g Agar
Super-Optimal broth (SOC)	20 g Tryptone 5 g Yeast Extract 4.8 g $MgSO_4$ 3.603 g Glucose 0.5 g NaCl 0.186 g KCl
M9 minimal media (pH 7.4)	6 g Na_2HPO_4-$7H_2O$ 3 g KH_2PO_4 0.5 g NaCl 3 g Glucose 0.7 g NH_4Cl 1 mL 1M $MgSO_4$, 1 ml 40 mg/mL thiamine, 1 ml 50 mg/mL carbenicillin, 200 µL 1 M $CaCl_2$

***P. pastoris* Media**	**Components (for 1 L)**
Yeast Extract Peptone Dextrose (YPD)	10 g Yeast extract 20 g Peptone 20 g Dextrose
Buffered Minimal Glycerol (BMG)	100 mM Potassium phosphate, pH 6.0 13.4 g Yeast Nitrogen Base 4×10^{-5} % Biotin 1% Glycerol
Regeneration Dextrose Medium (RDB)	1 M Sorbitol 20 g Dextrose 13.4 g Yeast Nitrogen Base 4×10^{-5} % Biotin 0.005% Amino acids
RDB Agar	1 L RDB 20 g Agar
Buffered Methanol-complex Medium (BMMY)	10 g Yeast extract 20 g Peptone 100 mM Potassium phosphate, pH 6.0 13.4 g Yeast Nitrogen Base 4×10^{-5} % Biotin 0.5% Methanol

2.1.2 Strains

Table 2.2: Bacterial and fungal strains used in this study

Strain	Use
E. coli XL10-Gold	High efficiency cloning strain
E. coli BL21(DE3)	Gene over-expression
E. coli Rosetta BL21 (DE3)	Gene over-expression
E. coli SoluBL21 (DE3)	Gene over-expression
P. pastoris GS115	Gene over-expression
P. pastoris KM17	Gene over-expression

2.1.3 Antibiotics

Antibiotics were prepared at a 1000 X concentration in ddH_2O. Stocks were stored at -20 °C and fully defrosted before use. Final working concentrations were 100 µg/ml and 50 µg/ml for Ampicillin and Kanamycin respectively.

2.1.4 *E. coli* growth

An overnight starter culture was prepared by adding 20 µL of bacterial glycerol stock or inoculating a single colony to 100ml of LB broth followed by incubation at 37 °C in a shaking incubator (200 rpm).

2.1.5 *P. pastoris* growth

An overnight starter culture was prepared by adding 20 µL of bacterial glycerol stock or inoculating a single colony into BMG medium (Table 2.1) in a 1 litre baffled flask followed by incubation at 28 °C in a shaking incubator (250 rpm) until the culture reaches an OD_{600} = 2–6 (approximately 16–18 hours).

2.1.6 Microorganism preservation

Equal volumes of cell culture and 50% glycerol stock solution were mixed, flash frozen in liquid nitrogen and stored at -80 °C.

2.2 Molecular biology

2.2.1 DNA gel electrophoresis

All agarose gels were made with 0.8% w/v of solid agarose dissolved in a solution of TAE 1 x made from a 50 x stock, 50 x TAE buffer was made up of 142 g/L Tris base, 57 ml/L acetic acid and 19 g/L EDTA (Final pH 8.6). A 2.5 µl aliquot of Midori Green Advance (Nippon Genetics, Dueren, Germany) was also added to the gel before pouring, to a final concentration of 0.5 µg/mL, as a highly sensitive stain for DNA visualisation. DNA samples were loaded onto the gel, and an appropriate DNA ladder was run alongside to estimate the molecular weight. The gel was run in a Sub-Cell GT Cell (Bio-Rad, Watford, UK) at 100 V in 1 x TAE buffer for 45 minutes before visualisation of the DNA under UV light using a Bio-Rad BioDoc-It imaging system.

2.2.2 Primer design

Primers were designed using the software SnapGene (GSL Biotech, Chicago, IL, USA; available at http://www.snapgene.com). All primers were ordered from Eurofins Genomics (Ebersberg, Germany) as a 10 nM salt-free pellet. Primers were re-suspended in sterile ddH_2O to make a 100 µM solution and stored at -20 °C.

2.2.3 PCR reaction

PCR reactions were carried out in a final volume of 50 µl containing: 10 µM of each of the primers (forward and reverse), 0.4 µl of template (50 ng/µL), 1 mM of $MgSO_4$, 0.2 mM of dNTPs, 2 µL of 10 x Buffer (200mM Tris-HCl pH 8.4 ,15mM $MgSO_4$,100mM KCl, 60mM $(NH_4)_2SO_4$, 0.1% Triton X-100 (Merck, Darmstadt, Germany)), 0.5 U of Phusion polymerase (New England BioLabs, Ipswich, MA, USA) and made up to 50 µL with ddH_2O.

PCR reactions were performed in a Bio-Rad thermocycler T100 using the following program:

- 98 °C for 1 minute
- 35 cycles of:
    - 98 °C for 30 seconds
    - 55 °C for 30 seconds (other annealing temperatures were used where appropriate)
    - 72 °C for 30 seconds per 1 kb
- 72 °C for 5 minutes

2.2.4 Restriction enzyme digestion

This following reaction was used to digest both PCR product and Plasmid.

- 5 µL PCR product or purified plasmid
- 1 µL of each restriction enzyme
- 2 µL 10 x Fast Digest Green buffer
- ddH_2O to 20 µL

The digestion reaction was mixed and incubated at 37 °C for 15 minutes.

2.2.5 DNA Extraction

The DNA bands of interest were excised from the gel using a sterile scalpel. The DNA gel extraction was performed using a QIAquick gel extraction Kit (Qiagen, West Sussex, UK) and was used for plasmid purification following the manufacturer's instructions. All procedures were carried out at room temperature. The DNA was eluted in 50 µL ddH_2O.

2.2.6 Cloning

2.2.6.1 Ligation into pLATE31

For ligation into the expression vector pLATE31, the aLICator LIC Cloning and Expression System Kit (Thermo Fisher Scientific, Waltham, MA, USA) was used

following the manufacturer's instructions. The constructs obtained were stored at 4 °C before transformation.

2.2.6.2 Ligation into pET-22b and pHIL-S1

For ligation into the expression vectors pET-22b and pHIL-S1, the following reactions in Table 2.2 were used.

Table 2.3: Ligation reactions used with pET-22b and pHIL-S1 vectors. DNA Ligase buffer consisted of 50 mM Tris-HCl pH 7.5, 10 mM $MgCl_2$, 1 mM ATP and 10 mM DTT.

Components	**Reaction 1**	**Reaction 2**	**Reaction 3**
Vector	20 ng	20 ng	20 ng
Insert	20 ng	80 ng	180 ng
T4 DNA Ligase	1 U	1 U	1 U
DNA Ligase Buffer 2 x	10 µL	10 µL	10 µL
ddH_2O	To 20 µL	To 20 µL	To 20 µL

Reactions were incubated at 22 °C for 1 hour and the ligation products stored at 4 °C before transformation.

2.2.6.3 Site-directed mutagenesis

Site-directed mutagenesis was performed using the Quick-change II site-directed mutagenesis kit (Agilent Technologies, Santa Clara, CA, US) as described by the manufacturers'. The construct obtained were stored at 4 °C before transformation.

2.2.6.4 Competent *E. coli* preparation and transformation

Competent *E. coli* cells were prepared using the rubidium chloride method (Hanahan, 1983). *E. coli* cells from a glycerol stock were streaked onto an LB-agar plate and incubated at 37 °C for 16 hours. A single colony from the plate was picked and grown in 5 mL of LB for 16 hours at 37 °C. The overnight culture was then diluted 40-fold into 200 mL of LB and grown at 37 °C to an optical density at 600 nm (OD_{600}) of 0.3/0.5. The LB culture was then incubated on ice for five minutes and harvested by centrifugation at 4000 g for 20 minutes at 4 °C The cells were suspended in 80 mL of transformation buffer I (Tfb I), incubated on ice for 1 hour and then harvested by centrifuged at 4000 g for 20 minutes at 4 °C. The cell pellet was then suspended in 8 mL of resuspension buffer II (Tfb II)

and incubated on ice for 2-3 hours. The cells were flash frozen in dry ice in 100 µL aliquots and stored at -80 °C until use.

Transformation Buffer I (Tfb I) contained per litre 2.94 g of potassium acetate, 1.209 g of rubidium chloride, 2.19 g of calcium chloride hexahydrate, 9.9 g of manganese chloride hexahydrate and 150 mL of glycerol. The final pH was adjusted to 5.8 with 200 mM acetic acid and the solution filter sterilised before storage at -20 °C. Transformation buffer II (Tfb II) containing per 200mL 0.42 g of MOPS, 0.24 g of rubidium chloride, 3,29 g of calcium chloride hexahydrate and 30 mL of glycerol. The final pH was adjusted to 6.5 using 1M potassium hydroxide and the solution filter sterilised before storage at -20 °C.

2.2.6.5 *E. coli* Transformation protocol

A heat shock protocol was used for the transformation of the plasmid into a chemically competent *E. coli* strain (Table 2.4).

Table 2.4: Summary of the competent cell lines used and heat shock time necessary for the transformation reaction.

***E. coli* strain**	**Application**	**Heat shock duration (sec)**
XL10-Gold	Cloning	30
BL21 (DE3)	Expression	45
Rosetta BL21 (DE3)	Expression	45
SoluBL21	Expression	45

An aliquot of 50 µL of competent *E. coli* cells stored at -80 °C was transferred to ice. Then the ligation products were gently added to the cells and left on ice for 30 minutes. Cells were heat-shocked at 42 °C for the appropriate amount of time (Table 2.4) and placed back on the ice for 5 minutes. The cells were mixed with 200 µL of pre-warmed SOC media (Table 2.1) and incubated at 37 ºC and 200 rpm for one hour. The transformation reaction was plated onto LB agar plates (Section 2.2.1) supplemented with the appropriate antibiotics. The plates were incubated at 37 °C overnight. The control plasmids pUC18 or pUC19 were used as a positive control to test the transformation efficiency.

2.2.6.6 Plasmid extraction

Plasmid extraction was performed from overnight cultures of *E. coli* grown in 10 ml of LB media with the appropriate antibiotics. A QIAprep Spin Miniprep Kit

(Qiagen) was used for plasmid purification following the manufacturer's instructions. The DNA was eluted into 50 µL of ddH_2O.

2.2.6.7 *P. pastoris* Electroporation Protocol

The *P. pastoris* strains GS115 and KM17 were purchased from Invitrogen (Carlsbad, CA, USA). The yeast was grown overnight in YPD medium (Table 2.1). Twenty microliters of yeast culture were transferred to 100 mL of YPD medium and incubated at 30 °C until the cell density reached OD_{600} = 1.5. The cells were collected by centrifugation at 3000 g at 4 °C. The cells pellet was washed two times with ice-cold ddH_2O. The *P. pastoris* cells were pre-treated for 30 minutes with 0.6 M sorbitol, 10 mM Tris-HCl pH 7.5, with 100 mM lithium acetate (LiAc) and 10 mM dithiothreitol (DDT)(Wu and Letchworth, 2004), and then washed two times with 20 mL of ice-cold 1M sorbitol. Finally, the cells were collected by centrifugation and re-suspended in ice-cold 1M sorbitol in a volume of 1.5 mL. An aliquot of 80 µL of cells was mixed with 3 ng of linearised plasmid and 7 ng of sonicated calf thymus DNA in 1 µL of ddH_2O transferred to a 0.2 cm pathlength electroporation cuvette and incubated for 5 minutes on ice.

The electroporation pulse was applied at 1.5 kV, 25 µF, 186 Ω using a Gene Pulser Xcell™ Electroporation Systems (Bio-Rad). The electroporated cells were immediately diluted in 1 mL of ice-cold 1 M sorbitol, and 50 µL aliquots were spread on plates containing RDB agar and incubated at 30 °C for 4 days.

2.2.6.8 DNA Sequencing

All DNA samples for sequencing analysis were prepared in ddH_2O at a concentration of 50-100 ng/µL for a final volume of 15 µL. The samples were sent to Eurofins Genomics for sequencing. The AOX 3' and AOX 5' primers (Table 2.4) were used for pHIL-S1 sequencing, and T7 Promoter and T7 Terminator primers were used for pLATE31 and pET-22b sequencing.

Table 2.5: Primers used for sequencing.

Primer	**Sequence**
AOX 3' (Forward)	GACTGGTTCCAATTGACAAGC
AOX 5' (Reverse)	GCAAATGGCATTCTGACATCC
T7 Promoter (Forward)	TAATACGACTCACTATAGGG
T7 terminator (Reverse)	GCTAGTTATTGCTCAGCGG

2.3 Biochemistry

2.3.1 *E. coli* protein expression

An overnight starter culture was prepared by adding 20 µL of bacterial glycerol stock or inoculating a single colony to 100 ml of LB broth followed by incubation at 37 °C in a shaking incubator (200 rpm). A 10 mL aliquot of the starter culture was diluted 1:100 in a 2 L Erlenmeyer flask containing 1 L of LB broth (Section 2.2.1) supplemented with antibiotics. Cultures were incubated under various conditions to determine the best expression protocol. The conditions varied and included the induction at OD_{600} value ranging between 0.4 -1.2; the incubation temperature 37, 28, 20, and 12 °C. The isopropyl β-D-1-thiogalactopyranoside (IPTG) concentration for induction ranged from 0.1 to 2 mM and the incubation time after induction ranged between 3 and 48 h. Afterwards, the cell pellet was collected by centrifugation at 4700 g at 4 °C for 30 minutes and stored at -20 °C before protein purification.

2.3.1.1 Cell lysis

Bacterial cell paste was suspended in the appropriate homogenisation buffer and treated with a Soniprep 150 Sonicator (MSE, London, UK) at 10 µm amplitude with short bursts of 30 seconds followed by 1 minute rest on ice to prevent overheating. The treated cells were harvested by centrifugation at 24000 g and 4 °C for 30 minutes and the supernatant containing soluble proteins was saved for protein purification.

2.3.2 *P. pastoris* protein expression

An overnight starter culture was prepared by adding 20 µL of yeast glycerol stock or inoculating a single colony in 10 mL of BMG medium (Section 2.2.1) in a 100 mL baffled flask followed by incubation at 30 °C in a shaking incubator (250 rpm) until the culture reached OD_{600} = 3. The culture was diluted 1:100 in a 3 L baffled flask containing 1 L BMG medium (Section 2.2.1) and incubated at 30 °C in a shaking incubator (250 rpm) until the culture reach OD_{600} = 3. The cells were collected by centrifugation at 3000 g for 10 minutes at 4 °C and suspended in 200 mL of BMMY to induce the expression. The culture was incubated in a 1 L baffled flask at 30 °C in a shaking incubator (250 rpm) adding 1 mL of 100% methanol every 24 hours to maintain the induction for 4 days. The culture was collected by centrifugation at 3000 g at 4 °C for 30 minutes. The supernatant was saved for

protein purification and immediately concentrated by ammonium sulphate precipitation.

2.3.2.1 Ammonium sulphate precipitation

The soluble protein supernatant was made 80% ammonium sulphate (w/v) (enzyme grade) by gradually added the salt while being stirred at 4 °C for one hour. The protein solution was harvested by centrifugation at 24000 g for 30 minutes. The precipitated proteins were then suspended in the appropriate homogenisation buffer to a final concentration of 10% (w/v) and stored at 4 °C prior to purification.

2.3.3 Protein purification

All protein samples were purified using a ÄKTA Purifier (GE Healthcare, Cincinnati, OH, USA). All the buffers used in the purification (Table 2.5) were vacuum filtered with a 0.2 nylon membrane filter (Whatman, Maidstone, UK). The protein concentration was monitored by measuring the absorbance at 280 nm. The protein parameters necessary for the development of the different purification protocols were calculated using the online tool ProtParam available online at the following address: http://web.expasy.org/protparam/.
This tool calculates several protein parameters from the amino acid sequence including theoretical pI, extinction coefficient and theoretical stability of the protein.

Protein concentration was determined by measuring OD_{280} nm using a Nanodrop 2000c (Thermo Scientific), utilising an extinction coefficient and molecular weight calculated by the Expasy ProtParam tool.

Table 2.6: A list of the purification buffers used and their components.

Buffer	**Composition (for 1 L)**
Hydrophobic Interaction chromatography (HIC) Buffer A	100 mM Tris-HCl pH 8.5 1 M Sodium Chloride 1 mM Calcium Chloride
Hydrophobic Interaction chromatography (HIC) Buffer B	100 mM Tris-HCl pH 8.5 1 mM Calcium Chloride
Diethylaminoethyl Cellulose (DEAE) Buffer A	100 mM Tris-HCl pH 8.5 1 mM Calcium Chloride
DEAE Buffer B	100 mM Tris-HCl pH 8.5 500 mM Sodium Chloride 1 mM Calcium Chloride
Ion Exchange Chromatography Buffer A	25 mM Sodium Phosphate pH 9.0 5 mM Sodium Chloride
Ion Exchange Chromatography Buffer B	25 mM Sodium Phosphate pH 9.0 1 M Sodium Chloride
Size Exclusion Chromatography (SEC) Buffer 1	25 mM Sodium Phosphate pH 9.0 25 mM Sodium Chloride
Immobilised Metal Affinity Chromatography (IMAC) Buffer A	50 mM HEPES pH 8.0 100 mM Sodium Chloride 1 mM Calcium Chloride 20 mM Imidazole
IMAC Buffer B	50 mM HEPES pH 8.0 100 mM Sodium Chloride 1 mM Calcium Chloride 250 mM Imidazole
SEC Buffer 2	50 mM HEPES pH 8.0 100 mM Sodium Chloride 1 mM Calcium Chloride

2.3.4 Dialysis

Protein samples were dialysed using a cellulose dialysis tubing membrane (Thermo Fisher Scientific) with a molecular weight cut-off (MWCO) of 8 kDa. Dialysis membranes were rinsed with ddH_2O before use and the protein dialysed in 4 L of the appropriate buffer at 4 °C with gentle stirring.

2.3.5 SDS-PAGE

SDS-PAGE was performed using a Bio-Rad mini-Protean cell. The protein samples were initially boiled for 10 minutes at 100 °C after being diluted with Laemmli loading buffer (Laemmli, 1970) in order to denature the protein. Samples were then cooled and loaded onto a 4-12% ExpressPlus™ PAGE Gels (GenScript, Piscataway, NJ, USA). 5 µL of Spectra Broad range multicolour protein ladder (Bio-Rad) were loaded onto the gel to allow measurement of protein molecular weights in the sample.

The protein separation was performed in a MOPS running buffer (50 mM Tris-Base, 50 mM MOPS, 1 mM EDTA and 0.1 % SDS (w/v), pH 7.7) with the following running condition: 140 V, 400 mA, 50 minutes at room temperature. Protein bands on SDS-PAGE gels were revealed by staining in Quick Coomassie Stain (Generon, Slough, UK) following the manufacturer's protocol. Destaining was performed in warm (50/60 °C) ddH_2O at room temperature for 30 minutes to remove the unbound stain.

2.3.6 SDS Page sample preparation for protein mass spectrometry

Protein bands were excised from the SDS-Page gel using a sterile scalpel and transferred into a sterile Eppendorf tube.

2.3.7 Protein mass spectrometry

The samples for protein mass spectrometry measurements were sent to the University of Bristol Proteomics facility for proteolytic digestion and fractionation of the resulting peptides by reverse phase (RP) chromatography. Each fraction was then analysed by RP nano-LC MSMS. A database search for peptide identity with known proteins was performed using the 'in-house' Mascot server.

2.3.8 Glycoprotein staining

Proteins were analysed by SDS-PAGE which was stained with a glycoprotein staining kit (GelCode®, Thermo Fisher Scientific) as described by the manufacturer's instructions. The gel was treated with a periodate solution, which oxidised the cis-diol sugar groups in any glycoproteins. The resulting aldehyde groups were detected through the formation of Schiff-bases with a reagent that produces magenta bands.

2.3.9 Western Blot

The Western blot procedure was carried out after SDS-PAGE electrophoresis on some samples without staining.

The separated proteins were transferred to a nitrocellulose membrane (Sartorius Stedim) using a Pierce G2 Fast Blotter (Thermo Fisher Scientific) with a current of 25 V, 1.3 A, for 15 minutes. The experiment was completed with the use of an iBind Western system (Thermo Fisher Scientific). The iBind Western system uses lateral flow capillary diffusion to automatically perform all of the Western blot steps.

The membranes were soaked in 6 mL of the iBind mix (6 mL iBind Buffer, 300 µL additive and 23.7 mL ddH_2O) and placed on an iBind card pre-equilibrated with 6 mL of the iBind mix. The antibody solutions were prepared according to the manufacturer's suggested dilution in the iBind mix for a final volume of 2 mL. The iBind system was closed and the iBind solution added to slot 1 to 4 as follows:

1. 2 mL primary antibody solution
2. 2 mL iBind mix
3. 2 mL secondary antibody solution
4. 6 mL iBind mix

Incubation was carried out at room temperature for 2.5 hours or at 4 °C overnight. The results were analysed using an Odyssey CLx Imaging System (LI-COR, Lincoln, NE, USA).

2.3.10 Lipase Activity Assay

The p-nitrophenol (pNP) assay is based on the method described by Shirai and Jackson, 1982. It measures the release of pNP as the lipase turns over the pNP-substrate by cleaving the ester bond. The standard activity test was performed in

a Greiner 655101 96-well microtitre plate (Greiner Bio-One, Stonehouse, UK) with different pNP esters (pNP-valerate, pNP-laurate) as the substrate.

The assay was conducted in 100 mM Tris-HCl pH 8.5 and 1 mM $CaCl_2$. 20 µL of diluted enzyme sample (final concentration of 3 nmol) was transferred to 160 µL of buffer on a 96-well microtiter plate followed by 20 µL of 1mM pNP-ester.

The activity was measured by monitoring the release of free pNP at 410 nm during the 15 minutes incubation at room temperature in a TECAN Infinite M200 PRO plate reader (TECAN, Männedorf, Switzerland). All activity measurements included a reading for the blank rate of hydrolysis which was subtracted from the observed activity, compensating for any auto-hydrolysis of the pNP-ester.

2.3.11 Differential scanning fluorimetry

Differential scanning fluorimetry (DSF) was used as a method to monitor protein unfolding with increasing temperature (T_m). In this method, proteins are incubated with a fluorescent dye which alters its fluorescence upon binding to the hydrophobic regions of the proteins. The protein dye mixture is then heated, and the fluorescence monitored as the heat rises. The unfolding of the protein and exposure of hydrophobic parts of the protein gives rise to a characteristic pattern of the fluorescence as a function of temperature (Vivoli et al., 2014). The DSF samples were prepared at the following concentrations in a final volume of 20 µl: 0.4 mg/ml protein, 10 mM HEPES pH 7.0, 150 mM NaCl, 8 x SYPRO Orange dye (Invitrogen). The addition of the different compounds to be tested were added to a final concentration of between 0.1 µM and 1 mM. All samples were prepared in triplicate. The fluorescence was measured using a StepOne quantitative PCR machine (Applied Biosystems, Foster City, CA, USA) while heating the samples in a gradient from 25 to 99 °C over a period of 40 minutes. Measurements were taken every 0.37 °C. The DSF curves obtained were used to calculate the midpoint temperature of the unfolding transition (T_m) using the differential of each DSF curve calculated using the Protein Thermal Shift software package (Applied Biosystems).

2.4 Wash performance methods

These experiments were carried out with the assistance of Dr Sukriti Sing and Dr Mark Thompson at Unilever, Port Sunlight. The laundry detergent formulations

used in this study were provided by Unilever, the details of their composition are listed in table 2.6.

Table 2.7: Formulations used in this study. F1 and F2 are current commercial formulations while F3 is an experimental formulation which is not yet available on the market.

Formulation	Linear alkylbenzene sulphonate (LAS) (%)	Sodium laureth sulphate (SLES) (%)	Neodol (Non-ionic surfactant) (%)	Dequest 2010 (Chelating agent) (%)	Total surfactant level%
F1	4.5	13.5	0	0	18
F2	5.8	4.37	4.37	0.1	15.4
F3	11.2	8.4	8.4	0.1	31.5

2.4.1 Micro-titre End-point stain removal assays

Fabric lipase sensitive stains, CS61 (Beef fat on cotton) and C46B (Used fry fat and violet dye on cotton), were hole-punched into discs and transferred to 96 well microtitre plates (MTP). The stained clothes were washed to remove any residual free stain. The wash liquor contained the following reagents: Enzyme 10 mg/L final; 20 µL of laundry formulation containing no enzymes 0.8 g/L final; ddH_2O 160 µL.

The reaction was incubated at 40 °C for one hour with shaking at 250 rpm. The clothes were washed by adding 200 µL of ddH_2O to each well, followed by shaking at 900 rpm for 1 minute. The wash liquor was then removed. This procedure was repeated three consecutive times then the clothes were dried overnight at room temperature. After drying, the stain plates were digitally scanned and their deltaE measured. This value is used to express the cleaning effect and is defined as the colour difference between a white cloth and that of the stained cloth after being washed. Mathematically, the definition of deltaE is:

$$\text{deltaE} = [(\Delta L)\,2 + (\Delta a)\,2 + (\Delta b)2]\,½ \qquad (2.1)$$

Where in ΔL is a measure of the difference in darkness between the washed and white cloth; Δa and Δb are measured for the difference in redness and yellowness respectively between both cloths. From this equation, it is clear that the lower the

value of deltaE, the whiter the cloth will be. With regard to this colour measurement technique, reference is made to Commission International de l'Eclairage (CIE); Recommendation on Uniform Colour Spaces, colour difference equations, psychometric colour terms, supplement no. 2 to CIE Publication, no. 15, Colorimetry, Bureau Central de Ia CIE, Paris 1978.

The cleaning effect is expressed in the form of a stain removal index (SRI):

$$SRI = 100 - deltaE \quad (2.2)$$

The higher the SRI the cleaner the cloth, SRI = 100 (white).

2.4.2 Terg-O-Tometer wash performance

To better simulate home washing condition a Terg-O-Tometer (Testfabric Inc., West Pittston, PA, US) has been used. Terg-O-Tometer is a laboratory scaled multiple washing device that is used for laboratory evaluation of perfumes and fragrances, soaps, detergents, dyes, and surfactants. This instrument simulates the action of an agitator type washer and performs the wash in all its six beakers (wash vessels) under controlled conditions of temperature and speed of agitation. Terg-O-Tometer experiments have been performed, using stain cloths and the clean ballast cloths. Ballast was a mixture of woven cotton (10x10) and polyester squares (10x10). In the Terg-O-Tometer wash study frying fat with violet dye (CS46B) and beef fat with dye (CS61) cotton stains were used with a dimension of 7.0”x 3.5” cm^2. After washing, the cloths were removed from the wash liquor and the cotton stain cloths were separated from the ballast cloths. The ballast cloths were discarded and the cotton stain cloths were retained. Further cotton stain cloths were rinsed in 1 L of water and allowed to dry flat at room temperature in the dark overnight. The dried cotton stain cloths were read using an X-Rite instrument (Pantone, Carlstadt, NJ, US) with a UV excluded light source and the deltaE whiteness measured relative to an unwashed white fabric.

Chapter 3 - Stabilisation of Lipase from *Thermomyces lanuginosus* through Cross-Linked Enzyme Aggregates (CLEAs)

3.1. Background

The process of protein cross-linking using the reaction of glutaraldehyde with reactive amine residues on the protein surface was initially developed in the 1960s. These enzyme aggregates were found to be more stable than the free enzyme when stored for long period of time (Doscher and Richards, 1963). However, these Cross-Linked Enzymes had many disadvantages including low activity retention and poor stability. To overcome these problems in 1964 Quiocho and Richards developed the first Cross-Linked Enzyme Crystals (CLECs) which became a successful industrial biocatalyst (Clair and Navia, 1992; Zelinski and Waldmann, 1997). The CLECs were active in environments that were otherwise incompatible with enzyme function, including prolonged exposure to high temperatures, near-anhydrous organic solvents, and aqueous-organic solvent mixtures. The CLECs were also highly stable against exogenous protease degradation (Persichetti et al*.,* 1995). Disadvantages were that the CLECs required highly purified enzyme in crystalline form, making the whole process expensive and not applicable to most enzymes. In 2001 Sheldon and co-workers patented the method for the production of Cross-Linked Enzyme aggregates (CLEAs)(Cao et al., 2000). The preparation of CLEAs involved the precipitation of the enzyme followed by crosslinking of the precipitated enzyme aggregates with a bifunctional crosslinking agent such as glutaraldehyde (Sheldon, 2007; Kartal and Kilinc, 2012)(Fig. 3.1). It is well known that the addition of salts, to aqueous solutions of proteins, leads to their precipitation as physical aggregates, held together by non-covalent bonding without perturbation of their tertiary structure (Sheldon, 2007). The cross-linking occurs between amino groups of the lysine residues on the surface of the enzyme and the aldehyde group. The cross-linking reagent which is usually glutaraldehyde (Migneault et al*.,*2004), results in the formation of covalent bonds, rendering the CLEAs permanently insoluble. This method is robust and straightforward, and the CLEAs are significantly more stable to denaturation by proteolysis, heat and organic solvents than the corresponding soluble enzyme (Sheldon, 2007; Ju et al*.,* 2013). The leading

causes for the stabilisation of CLEAs are ascribed to the rigidification of the tertiary structure due to massive crosslinking (Cui and Jia, 2015).

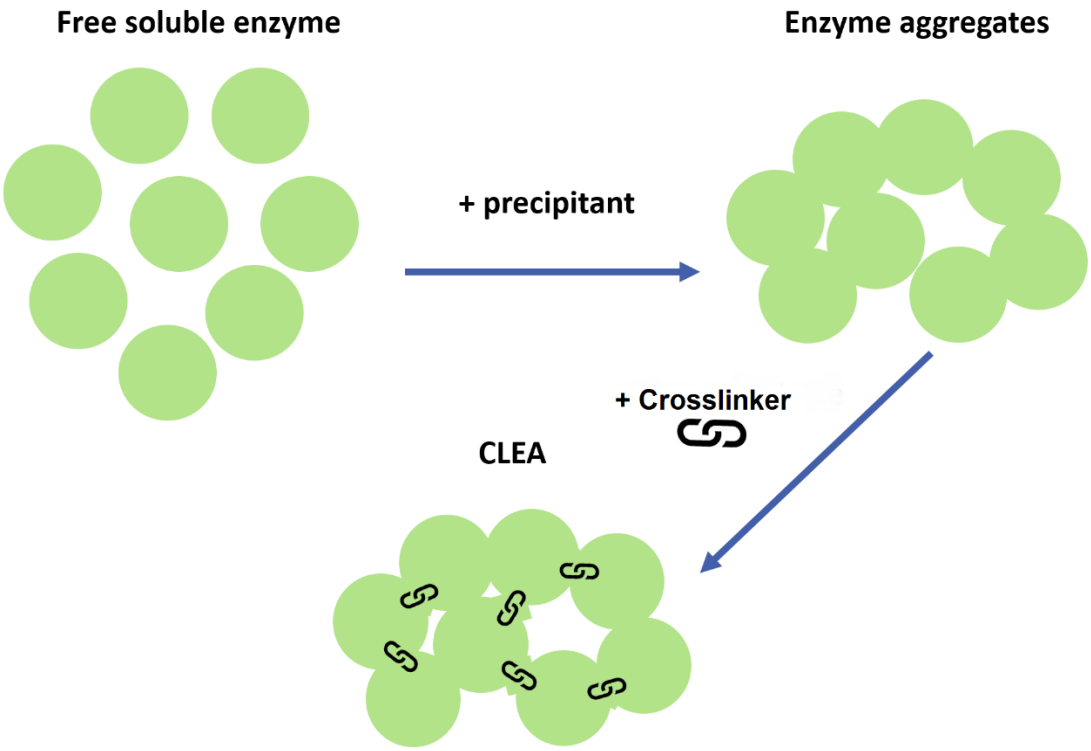

Fig. 3.1: Schematic representation of the CLEAs production process.

However, the CLEAs technology has also some disadvantages. The CLEAs are fragile for many industrial applications, and it is difficult to isolate and recover CLEAs from the reaction system (Wang et al., 2010). CLEAs also present extended diffusional limitations in mass transfer (Czichocki et al., 2001), and the cross-linking efficiency thus rigidity is dependent on the number of lysine residues in the protein making it not an ideal method for some proteins. This issue may be overcome by different methods such as precipitating the protein with a polymer containing numerous free amino groups, such as (i) poly-lysine or polyethylene imine (López-Gallego et al., 2005), (ii) by modifying the target protein in order to introduce more lysine residues into the sequence by site-directed mutagenesis or (iii) by adding bovine serum albumin as a “proteic feeder” during the preparation of the CLEAs to facilitate their formation (Shah et al., 2006). Regardless of the choice, those immobilisation strategies have a common feature of not requiring an immobilisation support since the biocatalyst is predominantly the enzyme (Rodrigues et al., 2011).

Hyperactive lipase CLEAs have been made in the presence of surfactants and detergents (Kartal and Kilinc, 2012; Guauque Torres et al*.,* 2013). These compounds are added to the enzyme prior to cross-linking and initiate the process of interfacial activation, opening the lipase 'lid', by binding to the hydrophobic active site of the enzyme (Derewenda et al*.,* 1992). Cross-linking of the enzyme molecules in this 'open' conformation can produce lipase CLEAs with more than 100 % activity when compared to the non cross-linked enzyme (Kartal et al*.,* 2011). It is assumed that these "activating" molecules are washed out of the lipase active site when the CLEAs are washed after the cross-linking reaction since enzymatic activity towards known substrates can be readily detected. The CLEAs technology offers many advantages for industrial applications as it is simple and amenable to rapid optimisation, which translates to low costs and a short time to market processes (Sheldon, 2007).

Since enhanced activity and stability are good requisites for industrial enzymes these technologies have received increasing interest in recent years from the industry (Mateo et al*.,* 2007; Fernandez-Lafuente, 2010). This is particularly true for the production of 'bio-based' liquid laundry detergent where the detergent enzymes have to remain stable during the shelf life of the product and remain active when used in the wash process.

This chapter describes the use of a carrier-free immobilised enzyme technique to determine if CLEAs generated from the commercially available Lipex 16L lipase will have improved stability in detergent surfactants and will be more resistant to proteolysis.

3.2. Materials and Methods

Lipex 16L™ and Coronase™ were obtained from Novozymes Bagsværd, lipase-sensitive stains: CS61–Beef fat stain, and C46B-Used fry fat were from Warwick Equest. All other chemicals were obtained from Sigma-Aldrich. All chemicals used were of analytical grade. The laundry formulation used in this chapter is F1 (Table 2.6).

3.2.1. Synthesis of Lipex CLEAs

The Lipex 16L was diluted to a final concentration of 0.69 µM in 30 mM MES-NaOH, pH 7.5, 150 mM NaCl, and 1 mM $CaCl_2$ to a final volume of 5 mL in a 50 mL Falcon tube at room temperature. Tween 80 was added to a final concentration of 19 mM in order to activate the Lipex by locking the lid in the open conformation, and the solution was left stirring at room temperature on a magnetic plate at 150 rpm for 5 minutes. Ammonium sulphate was slowly added to a final concentration 80% (w/v) and the solution stirred at 150 rpm for 30 seconds before the addition of glutaraldehyde at a final concentration of 5 mM. The CLEAs reaction was stirred for 17 hours at 4 °C at 150 rpm in a clear 50 mL Falcon tube. The reaction was stopped with 27 mL of amine buffer (1 M Tris-HCl pH 8.0). The Lipex CLEAs was mixed for 5 minutes with the amine buffer using a Pasteur pipette and centrifuged at 24000 g for 40 min at 4 °C. To wash the Lipex CLEAs, 27 ml of ddH_2O was added to the sample. The Lipex CLEAs was mixed for 5 minutes with the water using a Pasteur pipette and centrifuged at 24000 g for 40 minutes at 4 °C. The supernatant was decanted and 30 ml of dH_2O was added to the CLEAs pellet. The CLEAs samples were mixed with the dH_2O using a Pasteur pipette until the CLEAs particles were dispersed evenly, followed by centrifugation at 24000 g for 40 min at 4 °C. This was repeated three times in order to wash the CLEAs thoroughly. The CLEAs pellet was dispersed in 5 ml of 30 mM MES-NaOH, pH 7.5, 150 mM NaCl, 1 mM $CaCl_2$ or in 5 mL of Unilever formulation and mixed at 150 rpm overnight at 4 °C in order to obtain a homogeneous preparation of the CLEAs particles in suspension. The final enzyme preparation was stored at 4 ± 1 °C. At the end of the process, 57% the enzyme was cross-linked with a final concentration of Lipex in CLEAs of 0.40 µM. It is important to note that the enzyme that is not cross-linked enzyme is still active and can be used for further applications which would make the process more cost-efficient.

3.2.2 Size determination of the CLEAs

The different samples were measured with a Turbiscan MA 2000 sedimentometer (Sci-Tec Inc, Princeton, NJ, US) to scan a vertical cylinder of the sample over a distance not exceeding 80mm with 40um resolution. The rate of scanning was varied from 1 minute up to several hours and can follow the kinetics of

sedimentation. The temperature was set to 21 °C. The scanning frequency was varied according to the rate of sedimentation, initially set at the minimum of one scan per minute. From the rate of change of the sedimentation height of the material in the tube, the particle velocity was calculated, from which the particle size was calculated using the Stokes-Einstein equation (3.1).

$$D = \frac{kT}{6\pi\eta R} \quad (3.1)$$

Where *D* is the hydrodynamic diameter, *k* is the Boltzmann constant, *T* is the temperature *η* is the viscosity and *R* is the hydrodynamic radius of the particle.

As this is related to particle size and phase volume, it is possible to evaluate the maximum and minimum sizes of the particles contained in the material.

3.2.3 Activity assay

The standard Lipase activity assay (section 2.3.10) was carried out. The *p*-nitrophenol (pNP) assay is based on the method described by Shirai and Jackson, 1982. It measures the release of pNP as the lipase turns over the pNP-substrate compound breaking the ester bond. This can be visualised by eye as the assay solution turn to yellow while the pNP is released. The assay can also be followed spectrophotometrically at 410 nm. The enzyme activity is either shown as a percentage compared to a control reaction or in µM of product produced by 1 mg of protein in 1 minute.

3.2.4 Storage stability

The long-term stability of the different Lipex variants was evaluated in buffer (100mM Tris-HCl pH 8.5) and in three commercial laundry formulations (Table 2.6). The experiment was carried out incubating the samples at 37◦C for four weeks with/without protease being present (0.08 mg/mL enzyme sample in 0.8 g/L laundry formulation without enzymes and 0.2 mg/mL of protease). The activity was measured with the standard activity assay (section 2.3.10), taking the activity measured at time 0 as 100%.

3.2.5 Wash performance

Wash performances were evaluated by Micro-titre End-point stain removal assays (section 2.4.1).

3.3 Results

3.3.1 Preliminary studies

The preliminary experiments reported in this section were performed by Dr Halina Novak, Dr Andrew Dowd and Dr Sukriti Singh at Unilever, Port Sunlight, and represent the starting point on which this section of the thesis was developed.

In a typical biological laundry detergent formulation, there are at least three types of enzymes which address different types of stains which include proteases, amylases, and lipases however additional enzymes can be added such as mannanases and cellulases. Detergent enzymes are always being challenged for their stability in laundry application because of the presence of the added proteases (Galante and Formantici, 2003).

Preliminary studies analysed the effect of short-term incubation (5 days at 37 °C) of lipase and protease in laundry formulation either in their free form or their Cross-linked form. The results show that joint incubation with protease is detrimental for lipase activity and demonstrates that the use of Cross-linked lipase could be beneficial to improve the storage stability of these enzymes (Fig.3.2).

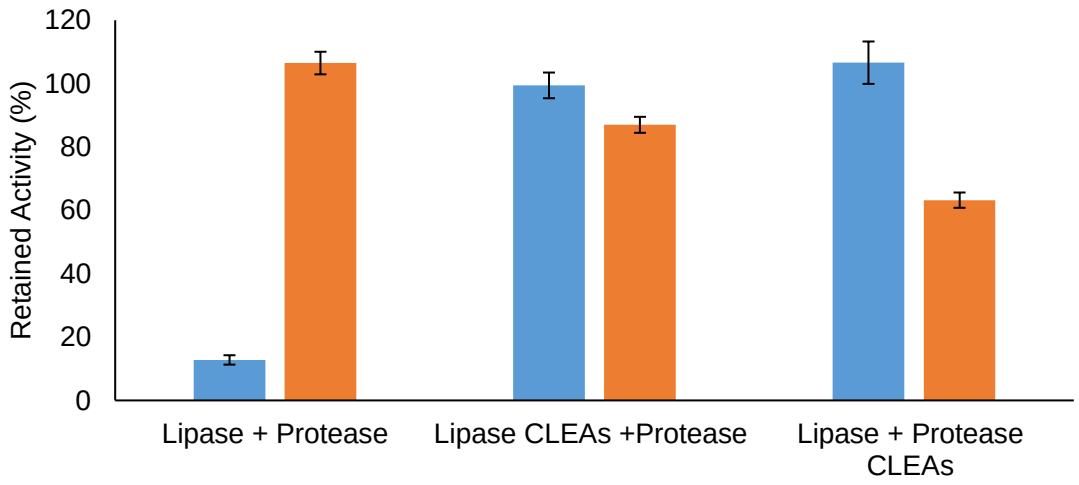

Fig. 3.2: Lipase (Lipex 16L (Blue)) and protease (Coronase (Orange)) retained activities following a 5-day storage in laundry formulation liquid at 37 °C. The retained activities were calculated from the equivalent zero time sample in the laundry formulation liquid. The error bars display the standard deviation between eight replicates (Data from Unilever internal report, 2014).

Lipase CLEAs were able to retain up to 99 % activity when exposed to free protease for 5 days at 37 ˚C. On the contrary protease CLEAs lost 40% of their activity when compared to free protease, indicating that the cross-linking had a negative effect on protease activity. However further investigation showed an issue in reproducibility and consistency of this result. In particular, Fig 3.3, shows how different product batches show different enzyme activities indicating batch release criteria weaknesses. This problem will impair the wash performance making it difficult to develop a formulation with reproducible performance characteristics.

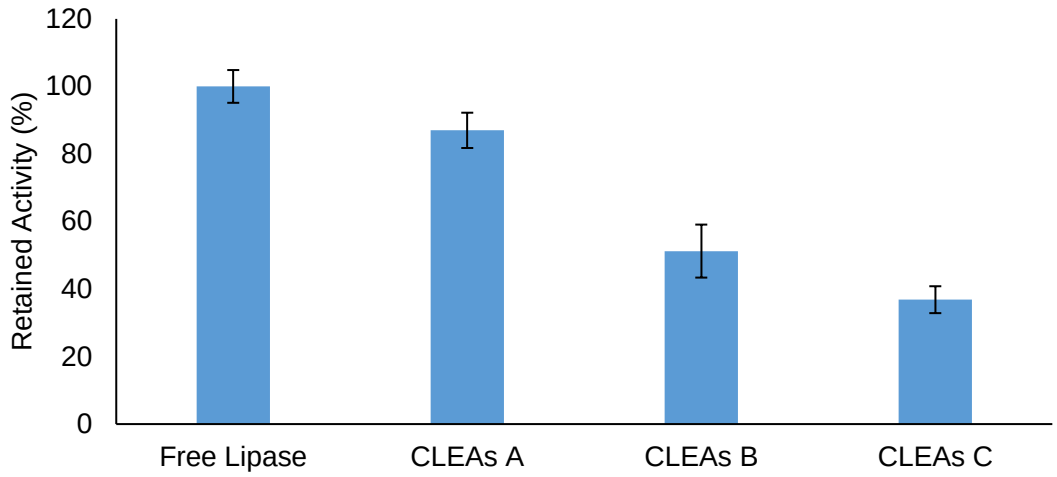

Fig 3.3: A graph showing the activity of three batches of commercial Lipase CLEAs purchased from by the same supplier but corresponding to different production batches show how there is great variability in the activity of the commercially available CLEAs. The error bars display the standard deviation between eight replicates (Data from Unilever internal report, 2014).

These differences could be explained by the fact that the preparation of reproducible CLEAs is difficult. It requires the fine tuning of the preparation conditions such as stirring rates, precipitant addition rates, and protein concentrations, which are parameters which can affect the final CLEAs activity (Kartal and Kilinc, 2012). Furthermore, additional parameters such the enzyme spatial orientation, the activation state and the size of the particles can all affect how the enzyme can interact with its substrate and have an impact on its activity. The results presented above represent a problem for the commercial application of enzyme in general, but for lipases in the laundry industry in particular. Taking this into account there is a need for an improved protocol for the preparation of Lipase CLEAs.

3.3.2 Optimisation of CLEAs production process

The CLEAs production protocol was optimised and continued the work of Dr Halina Novak who was working in the Littlechild group until 2014. The conditions varied included the cross-linker concentration value ranging between 1 and 15 mM; incubation temperature (4 and 22 °C); and incubation time between 2 and 17 hours. Assays were carried out in triplicate (section 2.3.10) and a positive control of Lipex 16L was taken as 100% activity. The best condition to CLEAs production was found to be, incubation with 5 mM of cross-linker at 4 °C on a stirring plate for 17 hours.

3.3.2.1 Screening of additives

A selection of compounds was identified which may have potentially beneficial effects on the activity retained by the Lipex CLEAs (Table 3.1). These included various non-ionic surfactants, ether compounds, waxes and oils, natural fats, natural detergents, inhibitors and amino acids. These compounds were added at varying concentrations to the CLEAs for 5 minutes prior to precipitation. The surfactant, oil, and wax may trigger the opening of the active site lid and allow the bind of the substrate into the hydrophobic active site.

Table 3.1: A list of the compounds tested as "activator molecules" in the Lipex CLEAs production highlighting the concentration range tested, the final concentration of the compound where highest activity was observed and the value of the highest activity retained. Activity was assayed using the pNP assay describe in section 2.3.10.

Compound	**Final concentration test (Concentration that shows the highest activity retained)**	**Highest activity retained (%)**
Lipex 16L	--	100.0 ± 3.6
T. lanuginosus lipase CLEAs (Sigma-Aldrich)	--	86.9 ± 5.3
Lipex CLEAs without compound	--	86.3 ± 4.1
Tween 85	2.4% v/v	47.5 ± 3.2
Tween 80	**6.5-50.4 mM (19 mM)**	**129.7** ± 2.2
Tween 40	19.5 mM	55.6 ± 3.4
Tween 20	6.7-27.1 mM	57.8 ± 4.5
Span 20	72.1 mM	35.0 ± 8.1
Span 60	58.1 mM	55.4 ± 3.3
Span 80	58.3 mM	61.2 ± 4.7
Tributyrin	110-661 mM (220 mM)	36.2 ± 3.7
SDS	5.8-115.6 mM (5.8 mM)	21.6 ± 5.3
Orlistat	67-336 µM (67 µM)	45.7 ± 4.1

Arginine	1.9-9.6 mM (1.9 mM)	3.5 ± 3.3
Coconut oil	1.65-3.3% v/v (1.65 v/v)	31.6 ± 2.7
Rhamnolipid	1.6-9.9% v/v (3.3 v/v)	51.8 ± 5.6

The interfacial activation is a well-documented phenomenon in lipase enzyme (Schmid and Verger, 1998), and what stands out in Table 3.1 is that the Lipex CLEAs have shown the highest retained activity after pre-treatment of the enzyme with Tween 80 before the cross-linking. The Tween 80 seems to bring the maximum number of lipase molecules into its active conformation prior to the cross-linking process so that the cross-linking process locks them in a favourable position and thereby increasing the overall activity of Lipex CLEAs.

3.3.3 CLEAs particle size determination

The particle size distribution of differently produced CLEAs might have an impact on the activity performance of the resulting products. Kartal and Kilinc (Kartal and Kilinc, 2012) showed that increasing the particle size of the CLEAs resulted in lower activity because of the loss of enzyme flexibility caused by excessive cross-linking and/or diffusion limitations (Kartal and Kilinc, 2012). The CLEAs particle size gradually increased as a result of the cross-linking times and the process needed to be fine-tuned in order to obtain a positive effect. Too short cross-linking times can lead to a low activity because of insufficient cross-linking whereas too long cross-linking times may lower activity due to increasing CLEAs particle size. If the particle size of the CLEAs is too large, the enzyme molecules inside the CLEAs particle would have no chance to reach the substrate due to limited diffusion and/or steric hindrance (Kartal and Kilinc, 2012).

Thus, a particle size comparison of Lipex CLEAs produced with and without the introduction of a termination step to control particle size, could reveal the impact on the improved stability of the enzyme and improved wash performance (Section 3.2.2) (Table 3.2). The different CLEAs samples were equally prepared for these experiments with a controlled, repeatable aggregation process (Section 3.2.1) before the measurement and were analysed with a sedimentometer (Section 3.2.2). The resulting data have provided evidence for the crucial role of the incubation with 1 M Tris-HCl pH 8.0 as terminator step for the production of

smaller CLEAs with higher activity because more enzyme molecules are able to interact with the substrate.

Table 3.2: Comparison of the particle size distribution across the different CLEAs preparation. Sizes were measured with a Turbiscan MA 2000 sedimentometer as described in section 3.2.2

Sample	Velocity (cm/s)	Diameter (µm)	Mean diameter (µm)	Retained activity compared to free enzyme (%)
T. lanuginosus lipase CLEAs (Sigma-Aldrich)	8.24E-04	12.3	6.67	86.9 ± 2.5
	2.63E-04	6.95		
	1.07E-04	4.44		
	4.86E-05	2.99		
Lipex CLEAs without terminator step	4.86E-05	2.99	4.01	67.9 ± 4.5
	8.96E-05	4.05		
	9.05E-05	4.07		
	8.33E-05	3.91		
Lipex CLEAs with terminator step	1.43E-05	1.62	1.85	123.8 ± 8.0
	1.32E-05	1.56		
	2.84E-05	2.28		
	2.08E-05	1.96		

3.3.4 Lipex CLEAs Stability

The Lipex CLEAs stability in different storage conditions was studied and after each time point, the residual activity of each sample was determined by measuring the hydrolytic enzyme activity of the enzyme using the substrates as described in Material and Methods.

To simulate the storage of the Lipex CLEAs in a commercial laundry formulation, further stability tests have been performed by incubating the samples at 37 °C for 4 weeks in a liquid laundry formulation with and without protease (Coronase^{TM}) (Fig. 3.4).

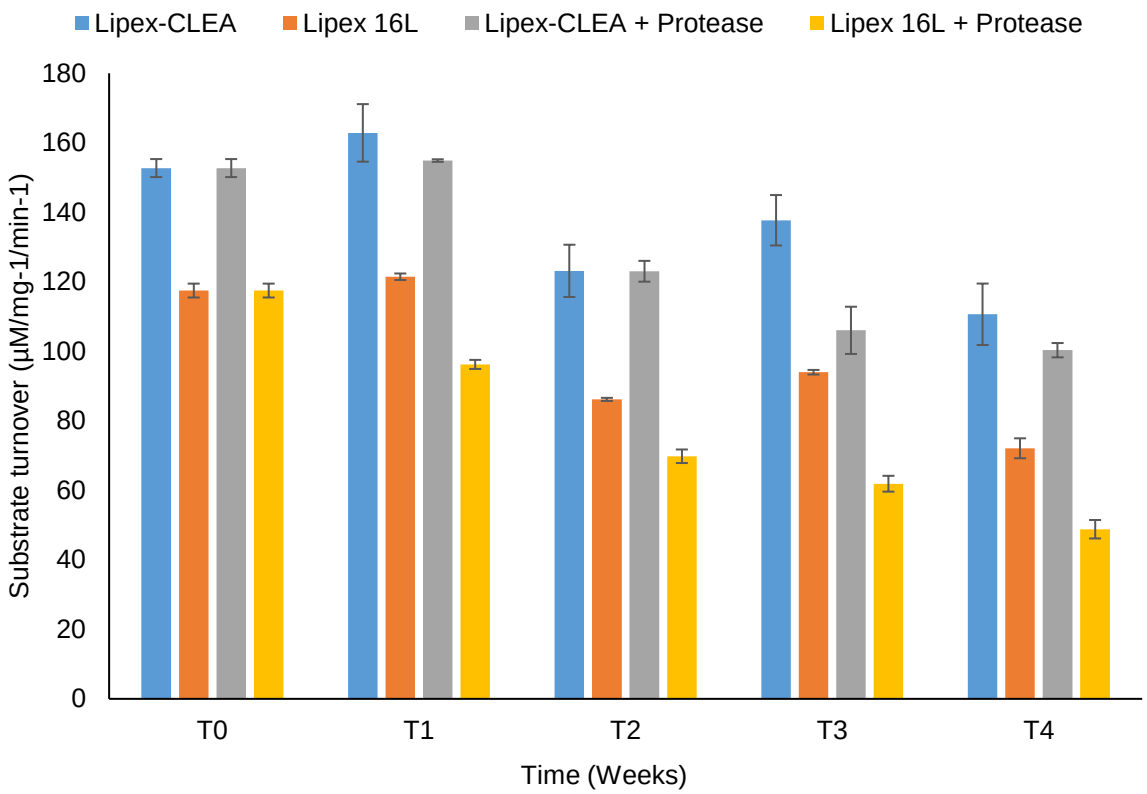

Fig. 3.4: The Lipex-CLEAs absolute activities. The assay used 0.4 mg/mL of each lipase with pNP-laurate as the substrate following a 4-week storage at 37 °C in liquid laundry formulation with and without 0.08 mg/mL of protease (Coronase™). The error bars display the standard deviation between threeee replicates.

The results in Fig. 3.4 shows that the residual activities of the Lipex-CLEAs which had been stored for 4 weeks (without protease) was higher than that observed for the soluble Lipex. The difference in activities between the CLEAs and the soluble lipase was approximately 30%. In addition to the increased enzyme activity, an increase in enzyme stability was also observed with the cross-linked lipases in the presence of the protease. The Lipex CLEAs was found to be more stable in comparison to soluble lipase in the presence of the protease. After 4 weeks, the Lipex-CLEAs possessed a residual activity of ≥ 70% while a substantial drop in residual activities was observed with Lipex 16L (~35%). It can be concluded that the Lipex CLEAs possesses a superior stability and improved activity in the presence and absence of protease in laundry formulation compared to soluble non-activated Lipex 16L.

3.3.5 Wash Performance

The microtiter end-point stain removal assays (section 2.4.1) have been performed using the freshly prepared Lipex CLEAs and the soluble enzyme against two types of lipid stain and the results show that the cleaning effect is comparable (Fig. 3.5) with a slight advantage for the Lipex-CLEAs on beef fat stains.

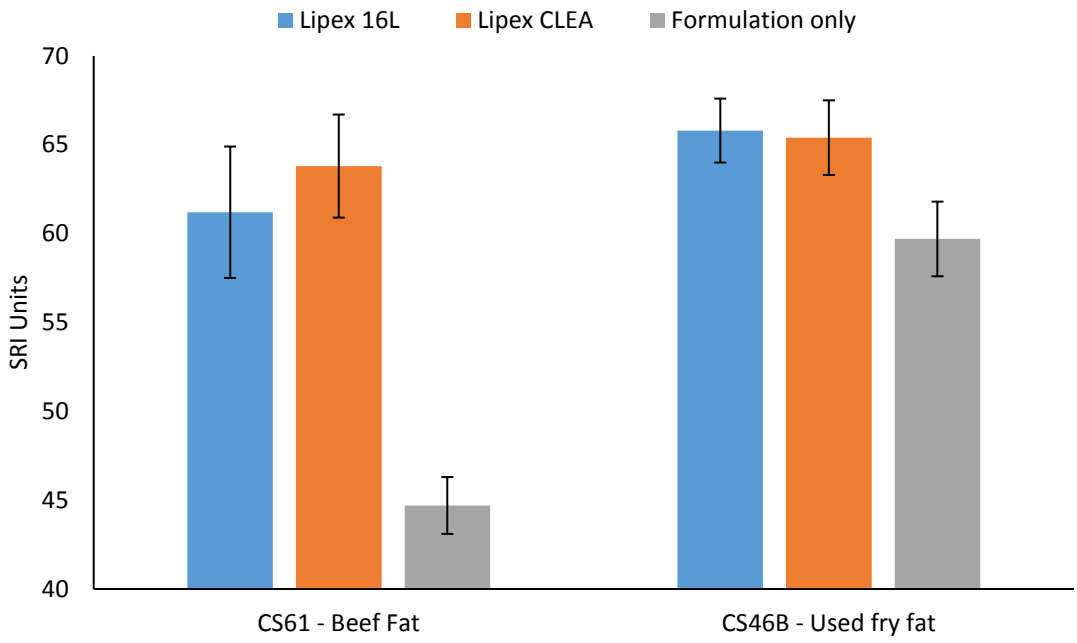

Fig. 3.5: The Lipase microtiter end-point stain removal assays was performed on both CS61 (Beef Fat stained cloth) and CS46B (Used Fry Fat stained cloth). The stained cloths were treated with 10 mg/L of Lipex 16L, or Lipex CLEAs in combination with liquid laundry formulation (0.8 g/L), or liquid laundry formulation with no enzyme. The error bars display the standard deviation between eight replicates.

CS61 - Beef fat is composed of triglycerides, whose major constituents are derived from stearic and oleic acids whereas the CS46B is composed of shorter fatty acid (≤ 12C). Since Lipex 16L has a substrate specificity for triglycerides containing medium-long chain fatty acids it is expected to perform better against the beef fat stain, however short chain fatty acids are more soluble in water and easier to remove from cloths.

Further wash performance experiments have been carried out using a Terg-O-Tometer which is an instrument able to reproduce washing conditions on a laboratory scale (1L liquid container). Adapting a real laundry product condition,

the cleaning effect of lipases/enzyme CLEAs were screened following storage at 37 °C for 4 weeks in the presence of protease as described in section 2.4.2.

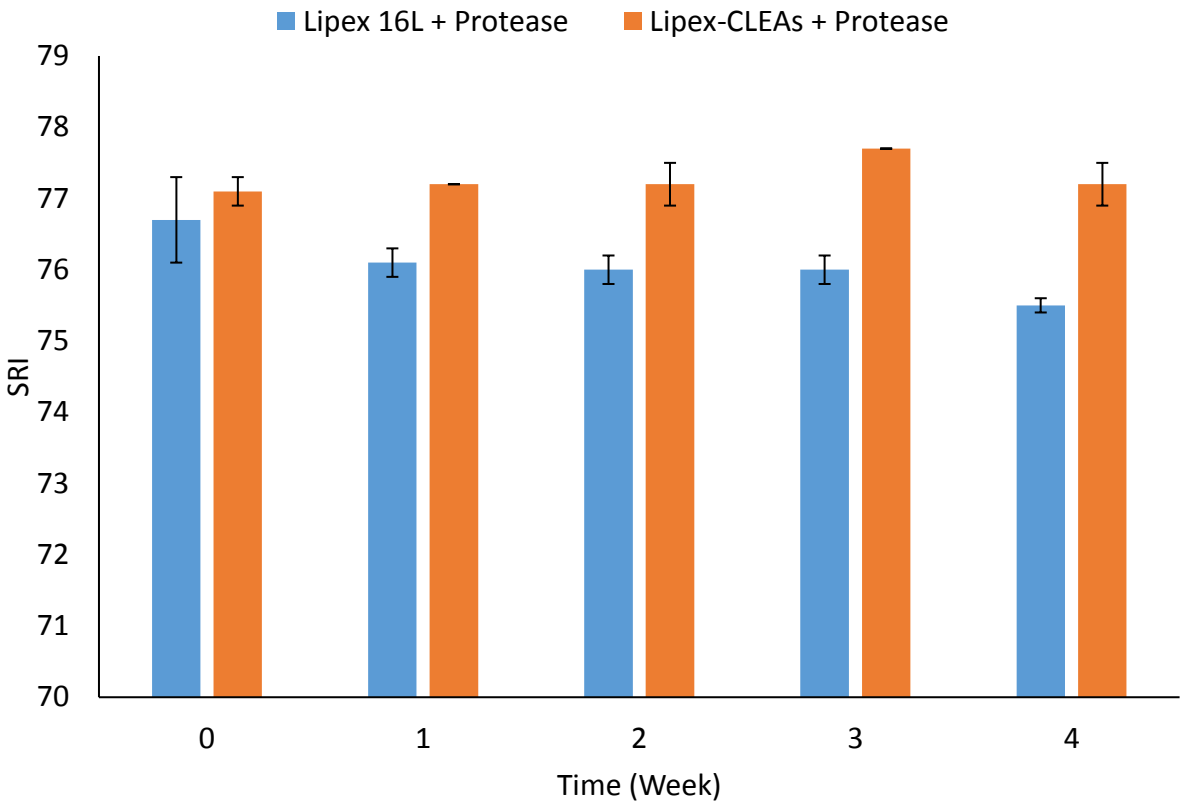

Fig. 3.6: The results of the Terg-O-Tometer wash performance assay. The assay used 10 mg/L of Lipex-CLEAs or Lipex 16L in a 1 L bottle under constant agitation in the presence of 10 mg/L of protease (Coronase™) using beef fat (CS61) stained cloths over 4 weeks storage at 37 °C. The error bars display the standard deviation between eight replicates.

The above figure shows that with Lipex-CLEAs (in the presence of protease), a cleaning effect on the CS61 stain was obtained after 4 weeks of incubation. In comparison to the soluble Lipex, the Lipex-CLEAs showed ~2 SRI units better cleaning than soluble-Lipex on CS61 stains.

3.4 Discussion

The CLEAs technology has many advantages in the context of industrial applications of enzymes. The method is simple and amenable and can be rapidly optimised which translates to low development costs and to shorter time-to-market (Schoevaart et al*.,* 2004). This project aimed to develop and optimise the production of a cross-linked enzyme aggregate lipase. This has led to the development of a Lipex CLEAs which has been shown (i) to be more conformationally homogenous, (ii) to be more stable in wash formulation, (iii) to be less protease sensitive and (iv) to have a better wash performance after long time storage when compared with Lipex 16 L. The overall product yield by the process is 57% which still requires optimisation for a commercial process to be economically viable. There is the opportunity that the remaining amount of unmodified enzyme material, which is still active, could be fed back into the cross-linking process to enhance the total overall product yield.

The Lipex CLEAs have been obtained by improving the cross-linking method in the presence of Tween 80 as an activator/enhancer. Detergents are suggested to be able to shift the open/closed equilibrium of lipases towards the open conformation, by coating the hydrophobic region of the lipase that surrounds the active site of the enzyme. This coating would reduce the negative interactions between this large and highly hydrophobic pocket and the environment stabilising the open form of the enzyme (Fernandez-Lorente et al*.,* 2006). The Tween 80 molecules most likely bind to the active site region of the enzyme rendering it in its ‘open’ conformation while undergoing the precipitation and cross-linking reaction. The beneficial effect of Tween 80 for lipase CLEAs hyperactivation was already described by Kartal and co-workers in 2012 (Kartal and Kilinc, 2012). These authors report a two-fold increase in activity for *Rhizopous oryzae* lipase CLEAs. However, previous studies on *T. lanuginosus* lipase CLEAs (López-Serrano et al*.,* 2002; Gupta et al*.,* 2009) reported increased activity only in the presence of SDS and Triton X-100, while Tween 80 caused a 20 % decrease in activity which was not observed in this study. These differences may be explained by the different method of CLEAs production. The introduction of a reaction step to stop the cross-linking reaction, using amine buffer, into the process has led to highly homogeneous CLEAs with a small particle size distribution as shown by the sedimentometer experiments (section 3.3.3). Smaller CLEAs are more active

because they are less affected by diffusional problems and because of their larger surface area available to react with the substrates.

A technology has been developed to stabilise the Lipex enzyme to make it more appropriate for commercial applications in the detergent industry. This methodology could be applied to help stabilise other enzymes that are used in commercial detergents. As result of this investigation a scientific paper has been published (De Rose et al., 2017) and three patent applications filed (Patent no: WO2017/036915, WO2017/036916, and WO2017/036917).

Chapter 4: Effect of different glycosylation profiles on the stability of *Thermomyces lanuginosus* Lipase

4.1 Background

As already mentioned in the previous chapter (section 3.3.1), detergent enzymes are always being challenged for their stability in laundry application because of the presence of the added proteases (Galante and Formantici, 2003). The presence of proteases in the laundry formulation is detrimental for lipase activity. The present investigation is aimed to assess how glycosylation affects the overall stability of the Lipex 16L enzyme and its sensitivity to protease.

Glycosylation is one of the naturally occurring covalent modifications of eukaryotic proteins. It has been estimated that over half of all the proteins found in nature are glycosylated, and more than three quarters are N-glycosylated (Apweiler, 1999).

Glycosylated proteins have interesting biological properties along with increased stability to proteolysis, heat, storage, and chemical denaturants, which in many cases are thought to be due to the carbohydrate addition to the protein surface. An example is the human erythropoietin commercialised by Amgen where the fully deglycosylated version of the protein lost 89 % of it's *in vitro* activity after heat treatment when compared to the wild-type recombinant enzyme. Whereas the darbepoetin alfa, an engineered hyperglycosylated analogue of erythropoietin that contains two additional N-linked carbohydrates, showed a three-fold increase in its serum half-life and an increased *in vivo* activity (Sinclair and Elliott, 2005).

Two recent papers demonstrate that the N-glycosylation of a β-glucuronidase and a *Pseudomonas aeruginosa* elastase expressed in *Pichia pastoris* gave the proteins an improved structural stability without affecting the enzymes activities when compared to the chemically de-glycosylated enzymes (Zou et al., 2013; Han et al., 2014). The expression of glycosylated proteins can be carried out in different eukaryotic hosts from yeast to insect and mammalian cells. However, the most used hosts in industrial biotechnology are filamentous fungi such as *Aspergillus niger*, *Aspergillus oryzae* and *Pichia pastoris* due to their broad use by the enzymes market leader Novozymes. The attraction of filamentous fungi as production hosts is based on their natural ability to secrete large amounts of proteins (mainly hydrolytic enzymes) into the growth medium (Nevalainen et al.,

2005). To achieve a high level of expression a commonly applied strategy is to introduce multiple copies of the gene of interest, expressed under a strong gene promoter in a high protein secreting mutant strain. Integration of the incoming genetic material can be targeted to a particular gene locus, often encoding a major endogenous secreted protein such as glucoamylase A in *A. niger* (Nevalainen et al., 2005). The sugar post-translational modifications on the expressed proteins are an added bonus which makes filamentous fungi particularly interesting for production of recombinant proteins for therapeutic application where the glycosylation is often essential for biological function.

The first steps for the synthesis of N-glycans is conserved across all domains of life and consists of the transfer of the core lipid-linked oligosaccharide unit $Glc_3Man_9GlcNAc_2$ (where GlcNAc = N-acetyl- glucosamine and Man = mannose)in the endoplasmic reticulum where it is connected to the amide side chain of an asparagine in the recognition sequence Asn-X-Ser/Thr (Gemmill and Trimble, 1999), with the formation of a N-glycosidic linkage (Macauley-Patrick et al., 2005).

There are three classes of N-linked glycans that are synthesised by the co-translational addition of $Glc_3Man_9GlcNAc_2$ to the polypeptide chain by oligosaccharyl transferase. These are composed of Man5–6GlcNAc2 (high mannose), a mixture of several different sugars (complex) or a combination of both (hybrid) (Fig 4.1) (Macauley-Patrick et al., 2005).

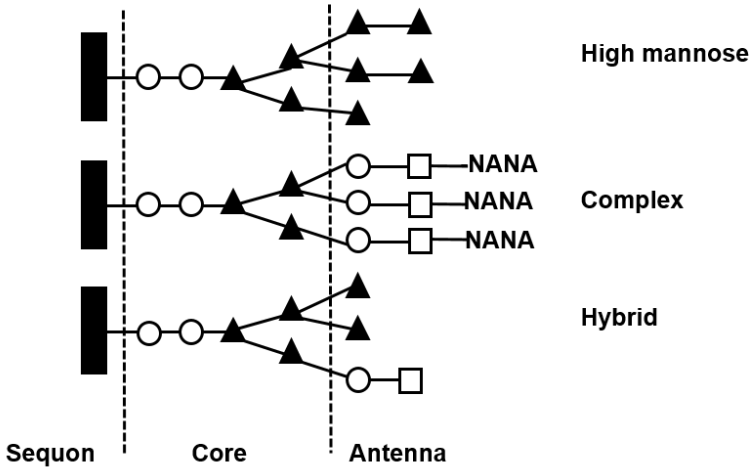

Fig. 4.1: Protein glycosylation patterns. Oligosaccharide chains consist of a sequon, which is attached to the core at an Asn residue. The core is attached to the antenna, which can be high-mannose, complex or hybrid. GlcNAc, ○; mannose, ▲: galactose, □. Image adapted from Macauley-Patrick et al., 2005.

A possible disadvantage of the protein glycosylated by filamentous fungi is the heterogeneity of the final protein due the fact that naturally glycosylation is an effective way of generating diversity in proteins with respect to the site of glycan attachment (macroheterogeneity) and with respect to the glycan's structure (microheterogeneity) (Petersen et al., 1998). It is well known that in certain species the processing of the attached glycan can vary even between different molecules of the same protein (Gemmill and Trimble, 1999).

The expression of proteins from *T. lanuginosus* in fungal systems in order to obtain glycosylated proteins has been explored by several researchers. There are systems that can be considered efficient especially for the expression of proteins with hydrolase activity. In 1998, Berka and co-workers successfully expressed an extracellular phytase from *T. lanuginosus* in *Fusarium venatum*. The *T. lanuginosus* phytase retained activity at assay temperatures up to 75 °C and demonstrated a superior catalytic efficiency to any known fungal phytase at 65 °C (the temperature optimum) (Berka et al., 1998). Another case was the highly efficient production of a *T. lanuginosus* xylanase in *P. pastoris* under the control of the AOX1 promoter by Damaso and co-workers (Damaso et al., 2003). The lipase from *T. lanuginosus* was expressed in a filamentous fungi system, *A. oryzae* to study the effect of the glycosylation at the N33 on the catalytic activity. The results showed that the glycosylation enhanced surface binding towards phospholipids, but did not have any effect on the lipase activity (Peters et al., 2002).
In 2010 Pinholt and co-workers studied the impact of glycosylation on the adsorption behaviour of *T. lanuginosus* lipase to hydrophobic and hydrophilic surfaces Three glycovariants were used, namely the mono-glycosylated wild-type TLL, a non-glycosylated variant and a penta-glycosylated variant, the latter two containing one and nine amino acid substitutions, respectively. However, no previous studies have addressed the role of glycosylation on stability and activity of the *T. lanuginosus* lipase.

4.1.1 The *Pichia pastoris* expression system

The *P. pastoris* expression system has been used extensively over the past decade for generation of recombinant proteins for several reasons. Firstly, the

expression can be regulated by the efficient and tightly regulated promoter from the alcohol oxidase I gene (AOX1). The AOX1 promoter is strongly repressed in cells grown on glucose and most other carbon sources but is induced over 1000-fold when cells are shifted to a medium containing methanol as a sole carbon source (Ahmad et al., 2014). Secondly, such a popular expression system is physiologically favourable since *P. pastoris* prefers a respiratory rather than a fermentative mode of growth. Fermentation products include ethanol and acetic acid, which quickly reach toxic levels in the high cell density environment of a fermenter with strongly fermentative organisms (Cereghino and Cregg, 2000). Moreover, *P. pastoris* can be genetically manipulated with the same techniques developed for *Saccharomyces cerevisiae*, one of the best characterised experimental systems in modern biology (Cereghino et al., 2002).

Regarding the glycosylation profile, *Pichia* derived proteins have in majority N-linked glycosylation of the high-mannose type (Fig 4.1) with very little O-glycosylation observed (Bretthauer and Castellino, 1999). The outer oligosaccharide chain of secreted proteins is mostly unaltered and consists of $Man_{8–9}GlcNAc_2$ (Montesino et al., 1998). In *P. pastoris* the hyper-mannosylation is not as prominent as in other yeasts with an average of only 8–14 mannose residues per side chain and is much shorter than those in *S. cerevisiae* (50–150 mannose residues). In addition, *α*-1,3-linked mannose units are found to be absent in *P*. *pastoris* derived proteins (Bretthauer and Castellino, 1999). It is believed that the α-1,3 glycan linkages in glycosylated proteins produced from *S. cerevisiae* are primarily responsible for the hyper-antigenic nature of these proteins making them particularly unsuitable for therapeutic use (Nevalainen et al., 2005).

In this chapter two gene constructs of the Lipex enzyme have been cloned and overexpressed in *P. pastoris* while another Lipex construct has been expressed in *E. coli* in order to have a non-glycosylated control for comparative studies.

4.2 Material and methods

4.4.1 Cloning

The gene for Lipex (see appendix) was purchased from GeneArt (Life Technologies, Carlsbad, CA, US) both as wild-type for expression in *P. pastoris* and the codon optimised version for expression in *E. coli*.

4.2.1.1 Cloning in *E. coli*

The synthetic gene encoding the codon optimised Lipex was cloned into the pET-22b vector PCR-amplified using the In-Fusion Cloning Kit (Takara-Clonetech, Kusatsu, Japan) as suggested by the manufacturer's instructions. The Lipex gene was PCR amplified without the stop codon using the primers shown in table 4.1, containing 15bp overhangs complementary to the vector. The pET-22b vector was linearised with the restriction enzyme *Xho*I and *Bam*HI allowing the Lipex gene to be 'in frame' with the pel B periplasmic secretion signal peptide and a 6x His Tag. The generated PCR product and the linearised vector were incubated for 30 min at 50 °C with the In-Fusion enzymes (Appendix Fig. 10.4). The resulting construct was transformed into DH5α and plated on LB plates supplemented with ampicillin for selection.

Table 4.1: Forward and reverse primer sequences for the amplification and cloning of Lipex in *E. coli* cells. The 15bp overhangs complementary to the pET-22b vector are highlighted in yellow.

LipFor (Forward Primer)	5'- GAATTAATTCGGATCGTGAAGTTAGCCAGGACCTGT- 3'
LipRev (Reverse Primer)	5'-GGTGGTGGTGCTCGAAATGCAGCTGGCACGAC-3'

Transformants were tested for the presence of the gene with colony PCR and the positive transformants were used for plasmid amplification (section: 2.2.6.5-6).

4.2.1.2 *P. pastoris* cloning

The synthetic gene encoding the wild-type Lipex was PCR-amplified, without its stop codon, using the primers shown in table 4.2 introducing a *Xho*I and *Bam*HI restriction site. The generated PCR product was digested with *Xho*I and *Bam*HI and the product was purified and ligated into the *P. pastoris* expression vector

pHIL-S1 (Life Technologies) in frame with the secretion signal PHO1 and a 6x His Tag, resulting in the plasmid pHIL-S1/Lipex (Appendix Fig.10.5).

Table 4.2: Forward and reverse primer sequences for the amplification and cloning of Lipex in *P. pastoris* cells. The bases in bold show the restriction site introduced with these primers

PichiaFor (Forward Primer)	*Xho*I 5'- ATTATTATTC**TCGA**GAAGTTAGCCAGGACCTGTTTAAT-CAGTT- 3'
PichiaRev (Reverse Primer)	*Bam*HI 5'- ATTATTG**GATC**CTTAATGATGATGATGATGATGCAGCT-GGCACGACAG-3'

4.2.1.3 Site-directed mutagenesis

One mutant containing four single amino acid mutations was generated through site-direct mutagenesis (T37N, N39S, E99N and N101S) in order to introduce two additional glycosylation sites (N-X-S) in the Lipex gene. Site-directed mutagenesis was performed using the Quick-change II site-directed mutagenesis kit (Agilent Technologies) as described by the method provided by the manufacturer using the primers in Table 4.3.

The site-directed mutagenesis protocol takes advantage of high fidelity polymerases such as *Pfu*ULTRA to obtain single point mutagenesis by a simple PCR protocol using the plasmid to mutate in the presence of two complementary primers containing the desired mutation. After the PCR the product was treated with the enzyme *Dpn*I which targets the parental plasmid, and the mutated product was transformed into competent *E. coli* cells.

Table 4.3: Forward and reverse primer sequences for the site-directed mutagenesis of Lipex in *P. pastoris* cells with the mutated bases highlighted in red.

N37 FW	5'-TCAGTTTAACCTGTTTGCA**AAC**TAT**AGC**GCAGCAGCA-TATTGTGG-3'
N37 REV	5'-CCACAATATGCTGCTGC**GCT**ATA**GTT**TGCAAACAGGTTAAACTGA-3'
N99 FW	5'-TACCAACAAACTGATT**AAC**CTG**AGC**TTTCGTGGTAGCCGTAGCATTG-3'
N99 REV	5'-CAATGCTACGGCTACCACGAAA**GCT**CAG**GTT**AATCAGTTTGTTGGTA-3'

The mutagenesis sites were chosen based on the work of Pinholt and co-workers (Pinholt et al., 2010) in order to not block the active site cavity of the Lipex enzyme (Fig.4.2) hence maintaining full catalytic activity.

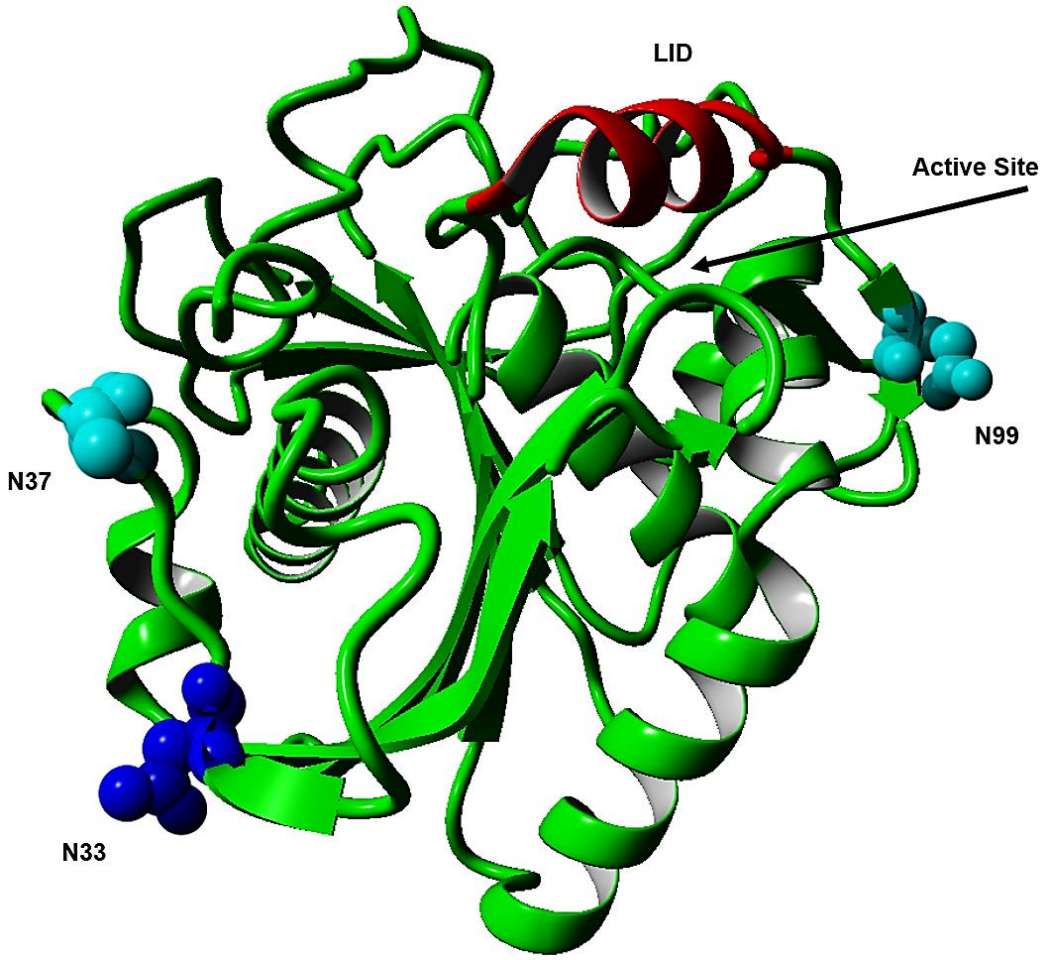

Fig. 4.2: Structure of the closed wildtype *T. lanuginosus* lipase (PDB: 1DT3 (Brzozowski et al., 2000)) showing the glycosylation sites with blue and cyan space filled spheres and the lid region is shown in red. The N33 is the glycosylation site in the wildtype *T. lanuginosus* lipase (blue), and the two other glycosylation sites (cyan) are the additional glycosylation sites in the tri-glycosylated variant of *T. lanuginosus.* The active site pocket is indicated by the black arrow (Image created with the program YASARA (Krieger et al., 2009)).

4.2.1.4 Electroporation into *P. pastoris*

The *P. pastoris* cells for electroporation were grown as described by Wu and co-worker (Wu and Letchworth, 2004). For electroporation into the *P. pastoris* genome, the expression construct was linearised with the restriction enzymes *Sal*I and *Sac*I. The linearised plasmid was run on a 0.8% agarose gel, and the bands of interest were excised and purified by gel extraction (Section 2.2.5). The electroporation was performed as described in section 2.2.6.7. The

electroporated cells were spread on plates containing RDB agar (section 2.1.1) and incubated at 30 °C for 4 days. Transformant colonies were lysed in 10 µL of water with a combination of freezing, thawing and with the addition of 5µL of a 5 U/mL lyticase enzyme for 10 min at 30 °C as described by Linder and co-workers (Linder et al., 1996) and screened by PCR (section 2.2.3) using the 5' AOX and 3' AOX primers (Table 2.4).

4.2.2 Lipex expression *E. coli*

Protein over-expression conditions were optimised (section 2.3.1). The best over-expression of the Lipex was observed using *E. coli* SoluBL21 (DE3) induced with 0.5 mM IPTG at an OD_{600} of 0.6 for 18 hours at 25 °C with agitation 200 rpm. The resulting bacterial cell pellets were harvested by centrifugation at 4750 g for 30 min at 4 °C. The supernatant was removed and the cell pellets stored at -20 °C.

4.2.3 Purification of non-glycosylated Lipex

Cell pellets over-expressing the Lipex enzyme were gently defrosted on ice in a water bath for 1 hour and re-suspended in 25% sucrose, 30 mM Tris-HCl, 1 mM EDTA, pH 8.0 and left on ice for 20 minutes to increase the osmotic gradient across the cell membrane. The resuspended pellets were centrifuged at 4750 g at 4 °C for 10 minutes. The supernatant was decanted and the cell pellets were re-suspended in ice cold H_2O containing 100 mM magnesium chloride, 5 mM sodium phosphate and left on ice for 20 minutes to disrupt the membrane and release the protein within the periplasm. A final centrifugation step of 24000 g at 4 °C for 30 minutes was applied. The resulting supernatant was immediately loaded onto a 1 mL His Trap FF column previously equilibrated with three column volumes of IMAC buffer A (Table 2.5). The unbound protein was washed from the column with five column volumes of IMAC buffer A. The bound protein was eluted using a 30 column volume step gradient to 100% IMAC buffer B (Table 2.5). The fractions corresponding to the recombinant protein were pooled together and concentrated with a 10 kDa Amicon Ultra-15 Centrifugal Filter (EMD Millipore).

4.2.4 Expression and purification of the mono and tri-glycosylated Lipex

Over-expression in *P. pastoris* was performed as described in section 2.3.2 and the best conditions were found using *P. pastoris* strain KM17 at 30 °C and 250 rpm, adding 1 mL of 100% methanol every 24 hours to maintain the induction for

96 hours. The culture was collected by centrifugation at 3000 g at 4 °C for 30 minutes. The supernatant was saved for protein purification and immediately concentrated by ammonium sulphate precipitation (Section 2.3.2.1). The precipitated proteins were re-suspended in 10 mL 50 mM Tris-HCl pH 8.5 with 1 mM calcium chloride and loaded into an 8 kDa cut-off dialysis tube (Thermo Fisher Scientific) and dialysed against 4 litres of 50 mM Tris-HCl pH 8.5 with 1 mM calcium chloride overnight at 4 °C (section 2.3.24). The dialysed protein was mixed with 1 mL of glycerol and 500 µL aliquots were stored at -20 °C prior characterisation.

4.2.5 Glycosylation analysis

Protein samples were run on SDS-PAGE (section 2.3.5) and then analysed by glycoprotein staining (section 2.3.8).

4.2.6 Biochemical characterisation

4.2.6.1 Activity assay

The standard Lipase activity assay (section 2.3.10) was carried out.

4.2.6.2 Differential Scanning Fluorimetry

The melting temperature (T_m) of the enzymes investigated in this chapter has been calculated through DSF performed as described in section 2.3.11.

4.2.6.3 Storage stability

The long-term stability of the different Lipex variants was evaluated in buffer (100mM Tris-HCl, pH 8.5) and with three commercial laundry formulations (Table 2.6). The experiment was carried out by incubating the samples at 37 °C for four weeks with and without protease (3 nmol enzyme sample in 0.8 g/L laundry formulation and 0.2 mg/mL of protease). The activity was measured with the standard activity assay (section 2.3.10), taking the activity measured at time 0 as 100% residual activity.

4.2.6.4 Wash performance

Wash performances were evaluated as described in section 2.4.

4.3 Results

4.3.1 Cloning and expression in *E. coli*

PCR was used to amplify the synthetic codon-optimised Lipex gene and a band of the correct size was observed on a 0.8% agarose gel (Fig. 4.3). The amplified gene was cloned into the expression pET-22b expression vector.

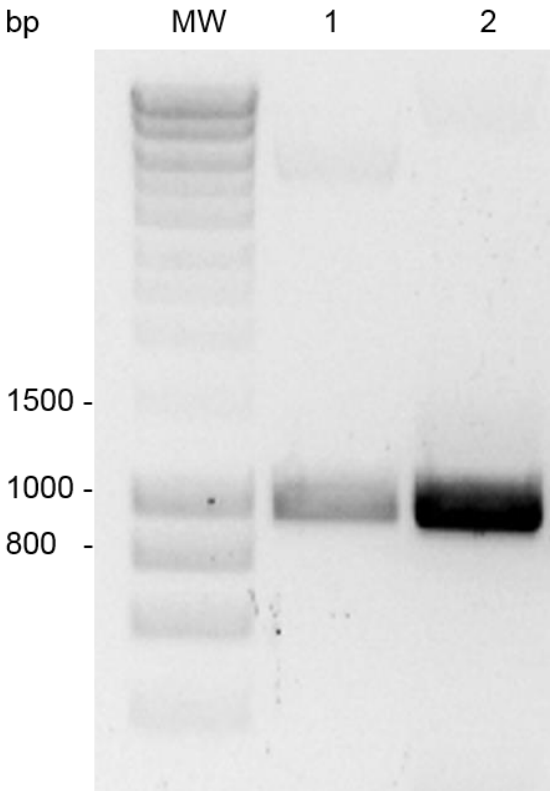

Fig. 4.3: A 0.8% agarose gel showing the amplified Lipex codon optimised gene (MW: Molecular weight marker, Lane 1 and 2: Lipex gene (expected molecular weight 924 bp).

Over-expression trials of the Lipex were conducted by varying the *E. coli* expression strain and induction condition as described in section 2.3.1. The best over-expression of the Lipex was observed using *E. coli* SoluBL21 (DE3) induced with 0.5 mM IPTG at an OD_{600} of 0.6 for 18 hours at 25 °C with agitation 200 rpm.

4.3.2 Purification of non-glycosylated Lipex

The protein was purified using a 1 ml HisTrap FF column, using a linear elution gradient (Fig 4.4).

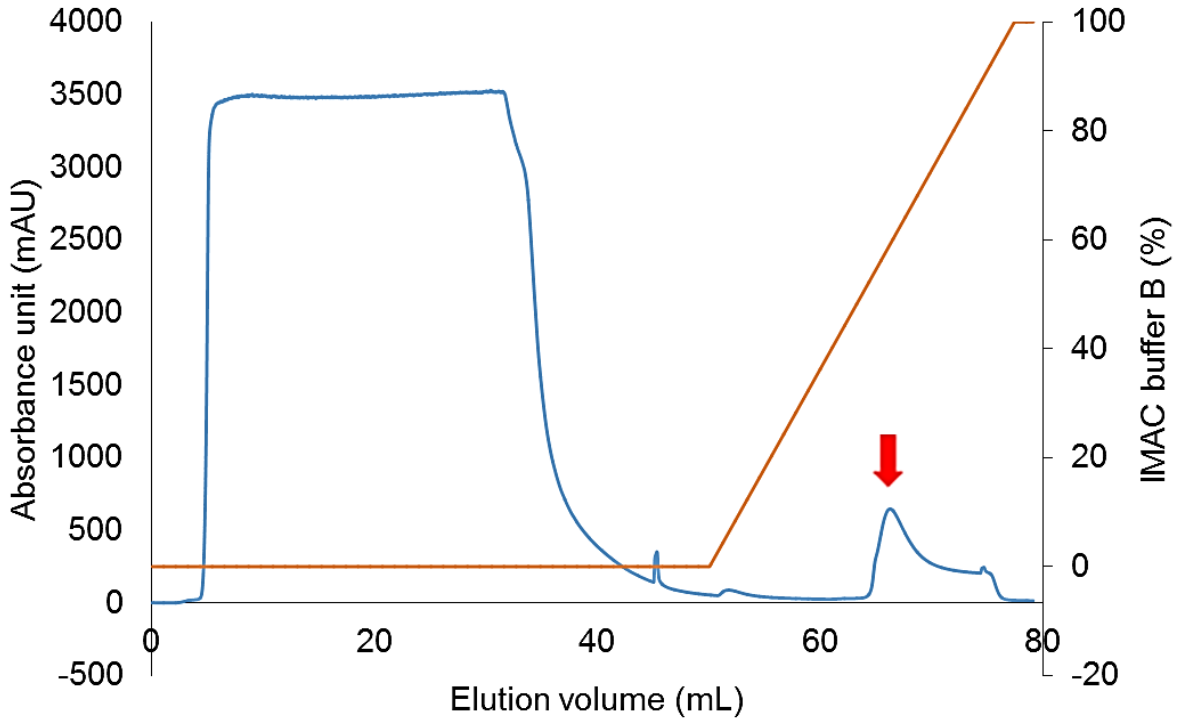

Fig. 4.4: The elution profile from the Nickel IMAC column. The non-glycosylated Lipex eluted between 63 – 68 mL as highlighted by the red arrow.

The purity of the final product was confirmed by SDS-PAGE (Fig. 4.5). A yield of 2.6 mg of purified Lipex was obtained from a 3 L culture of recombinant *E. coli* SoluBL21 (DE3).

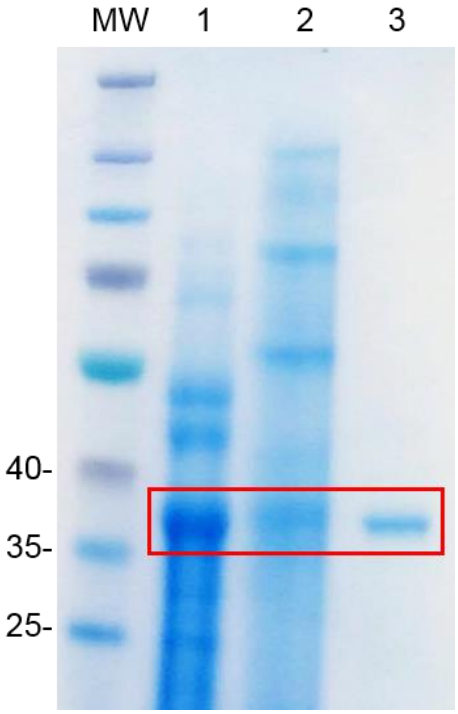

Fig.4.5: SDS-PAGE gel of fractions eluted from the Nickel IMAC column. Protein bands of interest (30 kDa) are highlighted by the red box. Lane 1: Crude protein extract, 2: Flow through and 3: Pooled peak of the non-glycosylated Lipex eluted with the imidazole gradient.

The fractions that tested positive for lipase activity (section 2.3.10) from the IMAC were pooled together and mixed with 10 % of glycerol. Aliquots of 500 µL were stored at -20 °C before further characterisation.

4.3.3 *P. pastoris* cloning

PCR was used to amplify the synthetic Lipex gene and a band of the correct size was observed on a 0.8% agarose gel (Fig.4.6). The amplified gene was cloned into the expression pHIL-S1 expression vector.

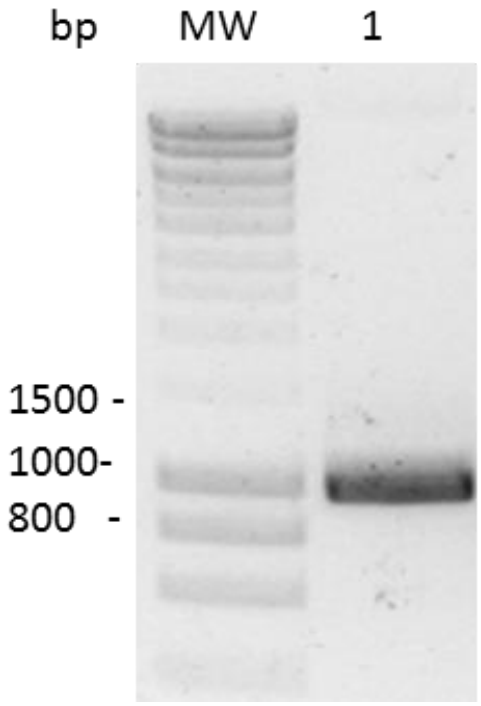

Fig 4.6: A 0.8% agarose gel showing the amplified Lipex gene (MW: Molecular weight marker, Lane 1 and 2: Lipex gene Lane 2 (expected molecular weight 935 bp)).

4.3.2.1 Site-directed mutagenesis

In order to evaluate the effect of different levels of glycosylation on activity and stability of the Lipex, four amino acid substitutions (T37N, N39S, E99N and N101S) have been introduced into the sequence of mono-glycosylated Lipex by site-directed mutagenesis (section 4.2.1.3) in order to introduce two extra N-glycosylation sites (N-X-S/T) in the Lipex sequence. The mutations were confirmed by DNA sequencing (section 2.2.6.8).

The two constructs were transformed into *P. pastoris* KM17 cells by electroporation (section 2.2.6.7). Integration into the *P. pastoris* genome was verified by colony PCR (Fig. 4.7) and DNA sequencing.

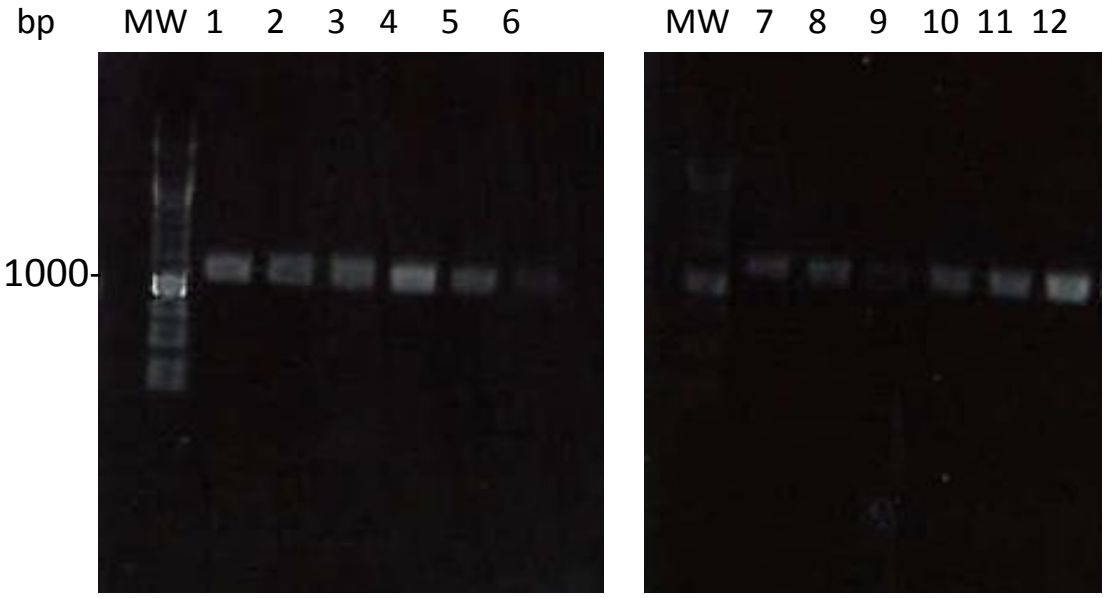

Fig. 4.7: Agarose gels showing the Colony PCR results of six randomly selected colonies of the mono (1-6) - and tri-glycosylated (7 -12) Lipex constructs. The presence of the expected molecular weight bands confirm integration in the *P. pastoris* genome.

Over-expression trials of the Lipex were conducted as described in section 2.3.1. The best over-expression conditions were found using *P. pastoris* strain KM17 at 30 °C and 250 rpm induced with 1 mL of 100% methanol every 24 hours to maintain the induction for 96 hours. These conditions were optimal for both the mono, and the tri-glycosylated Lipex.

4.3.4 Purification of the mono and tri-glycosylated Lipex

Both the Lipex variants expressed in *P. pastoris* were purified as described in section 2.3.2.1 by ammonium sulphate precipitation followed by dialysis. The dialysed protein samples were run on an SDS-PAGE gel to evaluate purity (Fig. 4.8). Due to the low amount of native *P. pastoris* proteins secreted into the media no further purification step was required. Both the mono-glycosylated and tri-glycosylated Lipex were obtained with a yield of ~75 mg from a 1 L culture of recombinant *P. pastoris* KM17.

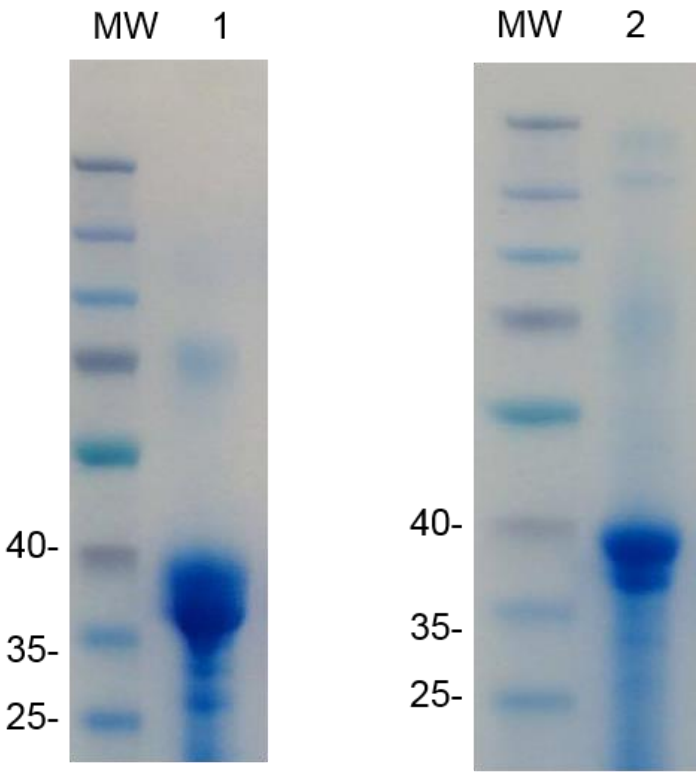

Fig.4.8: SDS-PAGE gel of Lipex variants expressed in *P. pastoris* and purified by ammonium sulphate precipitation followed by dialysis. Lane 1: 10 µg of mono-glycosylated Lipex; Lane 2: 10 µg of tri-glycosylated Lipex.

The purified lipases were mixed with 10% of glycerol and 500 µL aliquots were stored at -20 °C prior to further characterisation.

4.3.5 Glycoprotein staining

To visualise the presence of protein glycosylation the SDS-PAGE was stained as described in section 2.3.8 Glycosylated proteins are shown (Fig. 4.9) as a magenta band. The intensity of the band depends on the extent of glycosylation and the protein size and abundance.

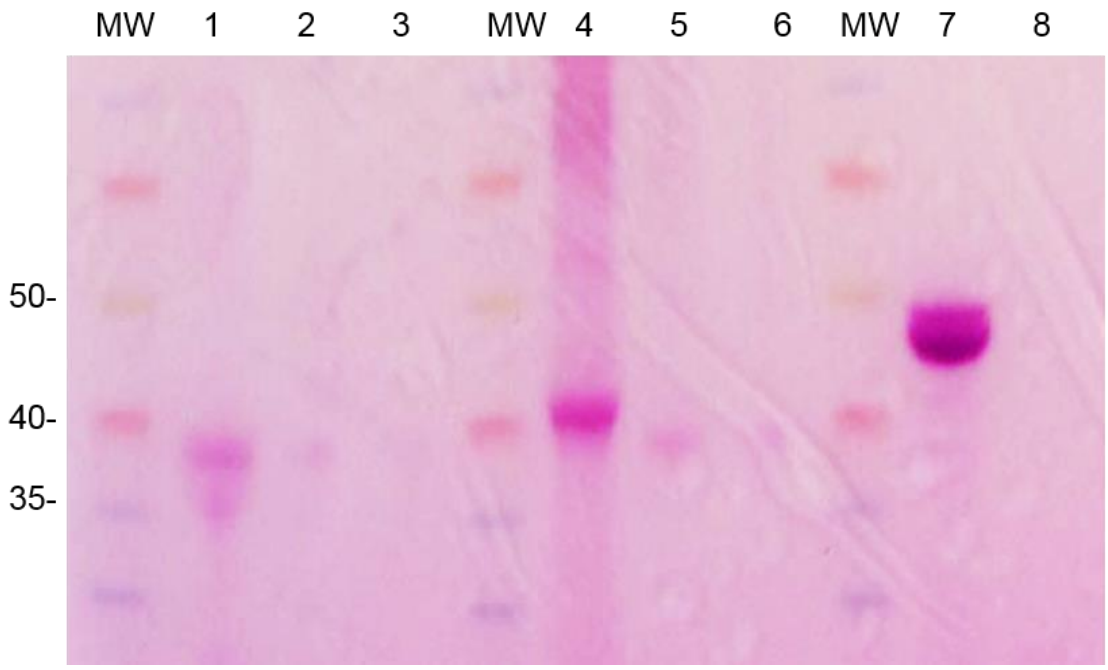

Fig. 4.9: SDS-PAGE gel of Lipex variants expressed in and purified by ammonium sulphate precipitation followed by dialysis. Samples stained with glycoprotein stain Lane 1, 2 and 3: Mono-glycosylated Lipex (10, 5, and 1 µg); Lane 4, 5 and 6: Tri-glycosylated Lipex (10, 5, and 1 µg); Lane 7: Positive control (10 µg of horseradish peroxidase); Lane 8: Negative control (10 µg soybean trypsin inhibitor).

4.3.6 Biochemical characterisation

To investigate the role of glycosylation on stability and activity of the Lipex enzyme, the biochemical characterisation was carried out on the three enzymes produced in this investigation plus the commercial Lipex 16L which was used as a control.

4.3.6.1 Lipase activity

To evaluate how the different lipases produced in this investigation compared to the commercial enzyme Lipex 16L the standard lipase activity assay (section 2.3.10) was performed (Fig 4.10).

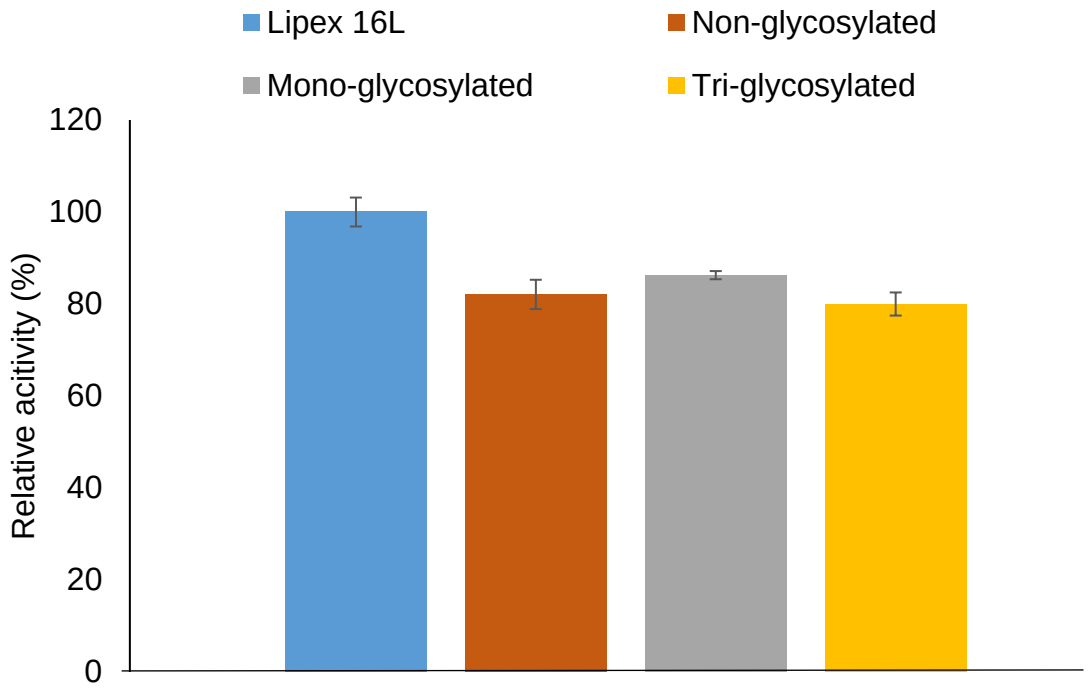

Fig. 4.10: Lipase activity assay of the different Lipex variants assayed using the pNP-laurate substrate as described in section 2.3.10. Activities are expressed relative to the maximum activity of the commercial Lipex 16L. The error bars display the standard deviation between three replicates.

From the graph in Fig. 4.10 it is clear that the commercial Lipex 16L is the most active enzyme. The other 'in-house' produced proteins show similar levels of activity between each other and ~20 % less activity than the commercial Lipex 16L. The difference between the mono-glycosylated Lipex and the commercial Lipex 16L (which is also glycosylated on N33) could be explained by the difference in the expression host (*P.pastoris* vs *Aspergillus niger*) which have different glycosylation machinery. *P. pastoris* favours a low amount of mannose units (< 20 on average) in the glycan chain as described in section 4.1.1 while *A. niger* produces hyper-mannosylated proteins with up to 100 mannose molecules for a single glycan chain (Kainz et al., 2008).

Another reason of the activity difference could be related to the formulation of the commercial enzyme. Commercial enzyme formulations are designed to stabilise and improve the activity of the enzymes, which is a commercial secret of the supplier.

4.3.6.2 Temperature and pH

The effect of temperature on lipase activity was examined by performing the assay at different temperatures (20–90 °C). To determine their stability at different

temperatures, the enzymes were incubated at 20–90 °C for 1 hour. The residual activity after treatment was determined with pNP laurate as the substrate using the lipase assay method (Fig. 4.11).

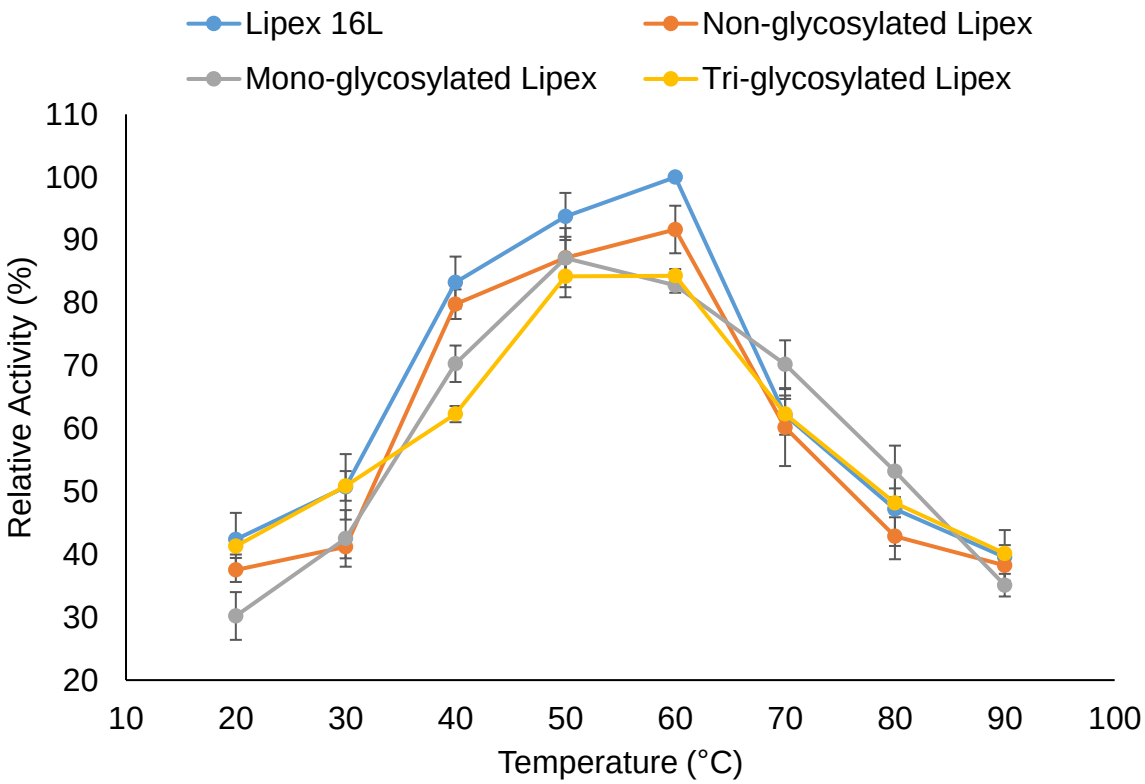

Fig. 4.11: The effect of temperature on the Lipase enzymes. Hydrolytic activity at various temperatures was assayed using pNP laurate as a substrate. Activities are expressed relative to the maximum activity of the commercial Lipex 16L (60 °C). The error bars display the standard deviation between three replicates.

Similarly, for the determination of optimum pH, the lipase activity was monitored over a pH range of 4.0–11.5 by using pNP laurate as the substrate (Fig 4.12).

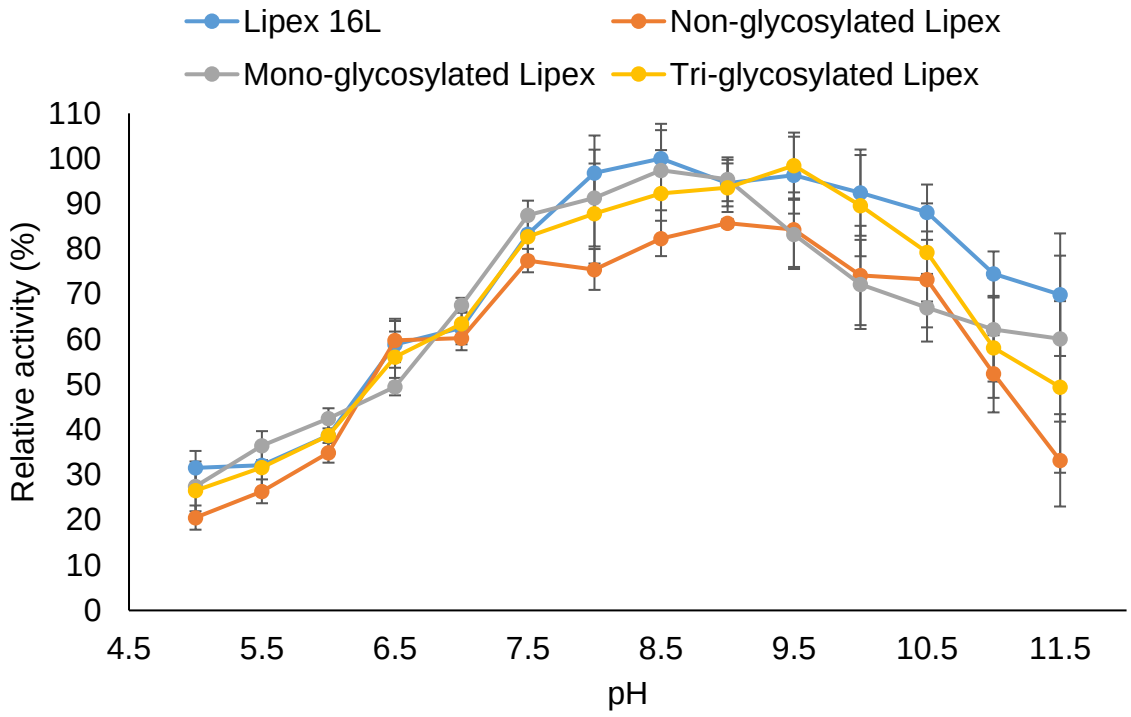

Fig. 4.12: The effect of pH on the activity of the Lipex variants. The optimum pH was assayed after incubation for one hour at room temperature in the following buffers covering a range of pH values from 5 to 12: 100 mM sodium phosphate pH 5.0 and pH 6.0, 100 mM Tris-HCl pH 7.0, pH 8.0 and pH 9.0, 100 mM glycine-NaOH pH 10.0, 100 mM sodium dihydrogen orthophosphate-NaOH pH 11.0 and pH 12.0. Activities are expressed relative to the maximum activity of the commercial Lipex 16L (pH 8.5). The error bars display the standard deviation between three replicates.

These results show an optimum pH ranging between 8.0 and 9.5 with little differences between the different Lipex variants.

4.3.6.3. Melting temperature determination

The melting temperature (T_m) of a protein is defined as the temperature at which the free energy of the unfolded and folded states is equal and half of the population is unfolded and the other half is folded. The general behaviour of the stability curves for the proteins suggests that, on average, increases in T_m are associated with increases in the free energy of maximal stability, an increase in maximal stability of ~0.008 kJ/mole/residue is, on average, associated with a 1°C increase in T_m (Rees and Robertson, 2001).

To measure the melting temperature of the different Lipex variants the DSF assay (section 2.3.11) was performed (Fig 4.12).

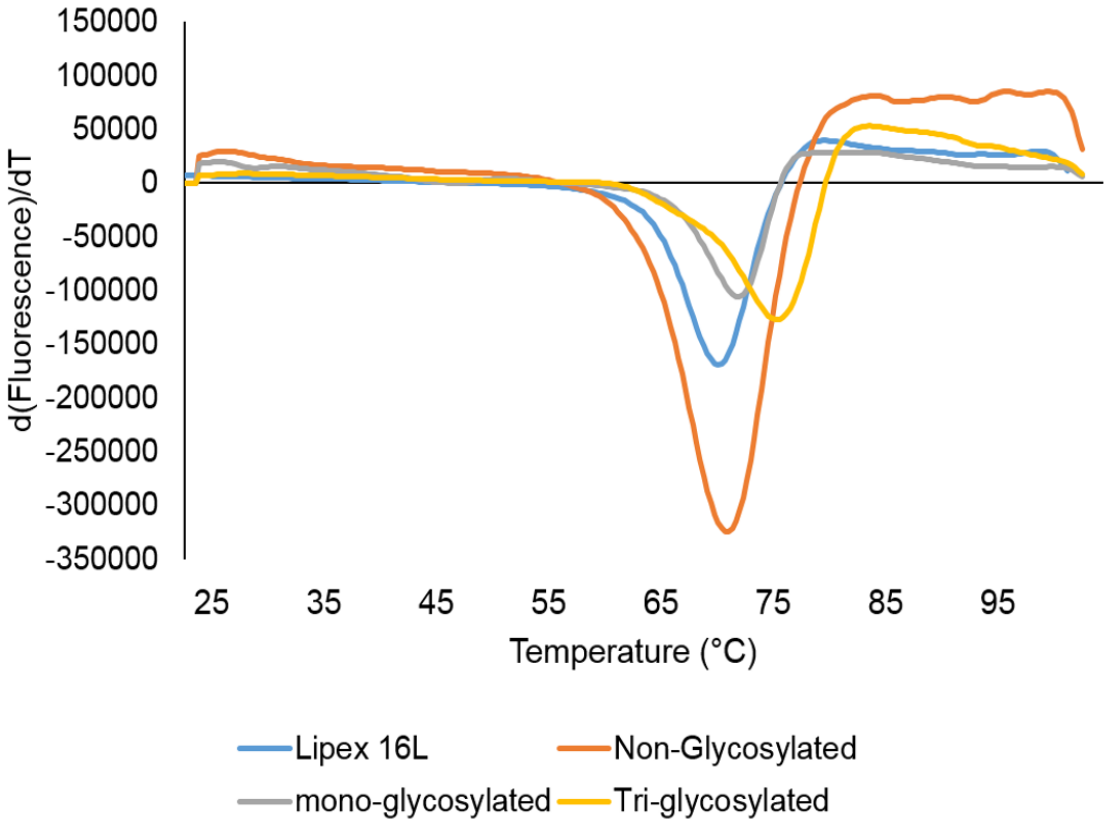

Fig 4.13: Representation of the melting curve of the Lipex variants. The characteristic shape of the raw data shows the derivative of the fluorescence with a progressive rise in fluorescence to a maximum, followed by a shallow decline. The minimum of the curve indicates the melting temperature of the protein.The data in Fig 4.13 shows that Lipex 16L and the non-glycosylated Lipex share a similar T_m of 69.3 and 69.4 ˚C respectively while the two variants expressed in *P. pastoris* are more stable with the mono-glycosylated enzyme having a T_m of 69.8 ˚C and the tri-glycosylated enzyme having a T_m of 73 ˚C.

Also in this case the differences between the commercial Lipex 16L and the mono-glycosylated Lipex may be explained by the different expression host of these two proteins that leads to different glycosylation profiles.

4.3.6.4 Long-term stability

The storage stability of the Lipex variants was tested in the buffer over 28 days in order to evaluate if the additional glycosylation had an additional enzyme stability effect in the form of higher retained activity (Fig.4.14).

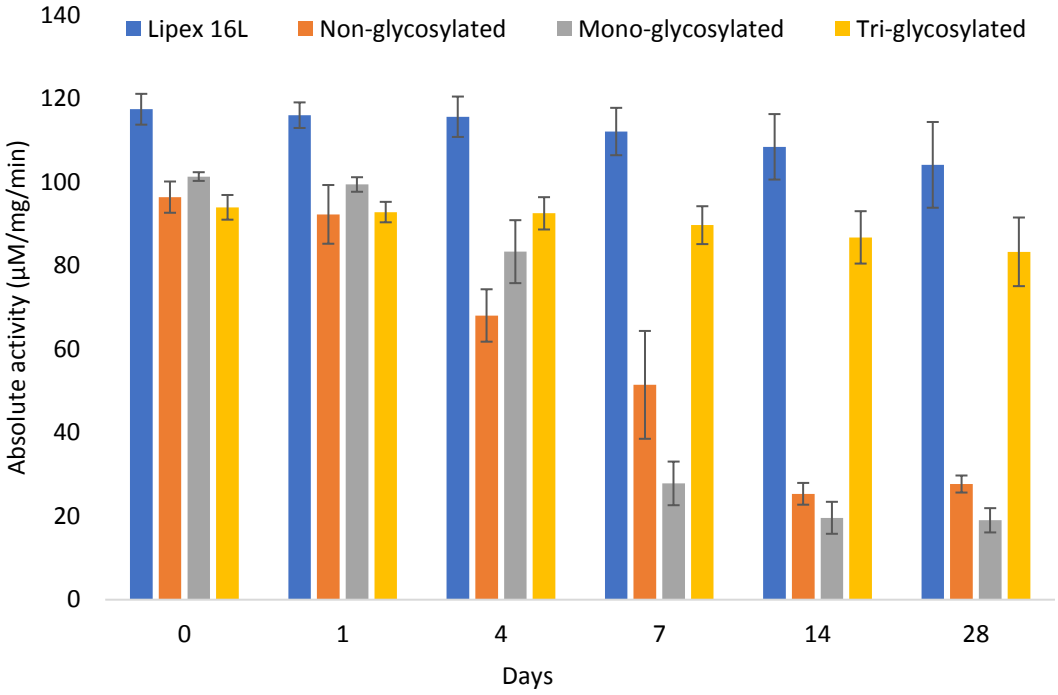

Fig. 4.14: The residual Lipex activities with pNP-laurate as the substrate following a 4-week storage at 37 °C in aqueous buffer (100 mM Tris–HCl, pH 8.0, 100 mM NaCl, 1 mM $CaCl_2$). The error bars display the standard deviation between three replicates.

The above figure shows that the commercial Lipex 16L is the most active after 28 days. However, a substantial difference was found between the activity of the glycosylated variants (mono-, tri-glycosylated Lipex and Lipex 16L) and the non-glycosylated Lipex. This data shows that the extra N-linked glycosylations did have a positive effect on long-term stability.

4.3.6.5 Protease stability

The same experiment of the previous section was repeated in three different laundry detergent formulations (Table 2.7) with and without the addition of a commercial protease (Carnival 100L, Novozymes) (Fig. 4.15).

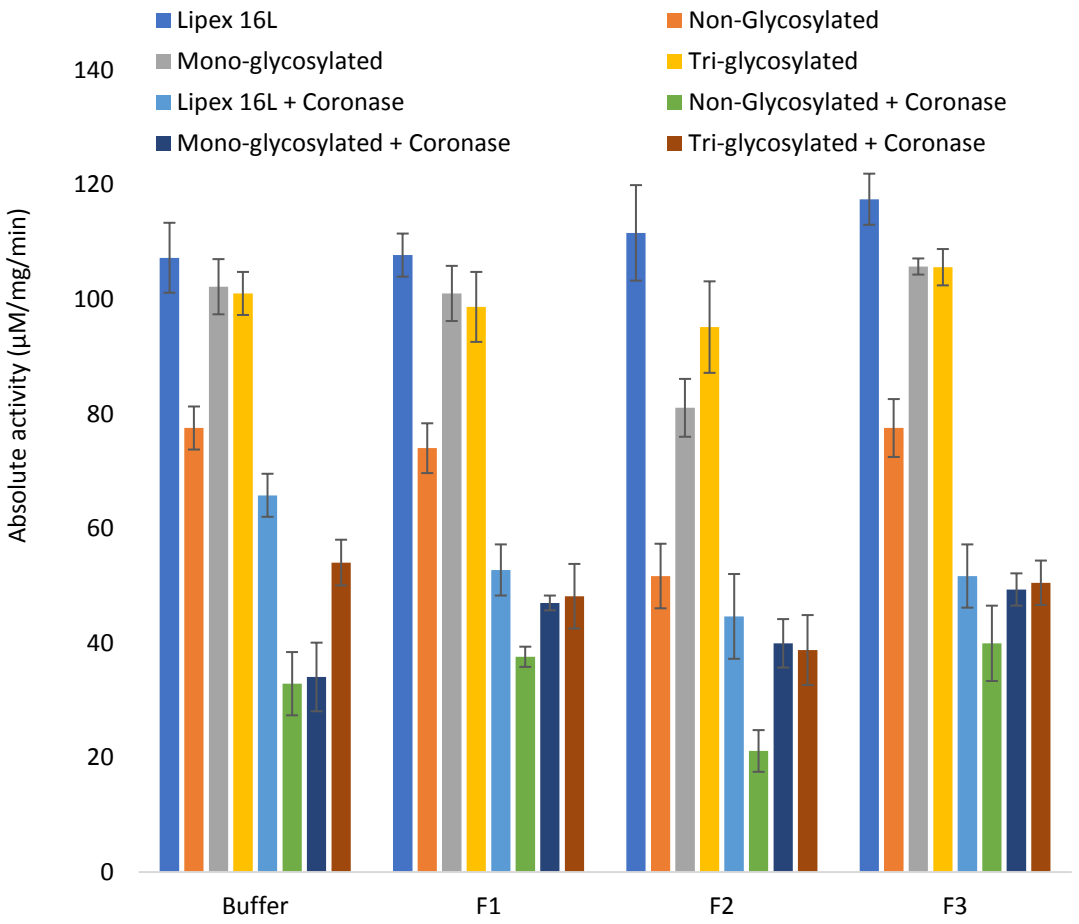

Fig 4.15: Lipase absolute activity measured after 28 days incubation at 37°C with and without 0.08 mg/L protease in Buffer (100 mM Tris–HCl, pH 8.0, 100 mM NaCl, 1 mM $CaCl_2$), or in F1, F2 or F3 formulations. The error bars display the standard deviation between the three replicates.

The results in the figure above confirms that the non-glycosylated enzyme is the most unstable in all the conditions tested. On the contrary, all the glycosylated enzymes performed well during long-term storage without protease, retaining more than 70% of their activity over 28 days even in formulation with a high percentage of total surfactant (F3). This result demonstrates the importance of glycosylation for the stability of this enzyme. However the same cannot be said for the results from formulation plus protease, where all the enzymes dropped below 50% of retained activity. In particular no major difference could be observed between the three glycosylated enzymes.

4.3.7 Wash performance

Preliminary wash performance studies were performed as described in section 2.4.1 of the Materials and Methods section, (Fig. 4.16). Due the low yield of the

non-glycosylated Lipex expressed in *E. coli* only the commercial enzyme and the two *P. pastoris* variants were tested.

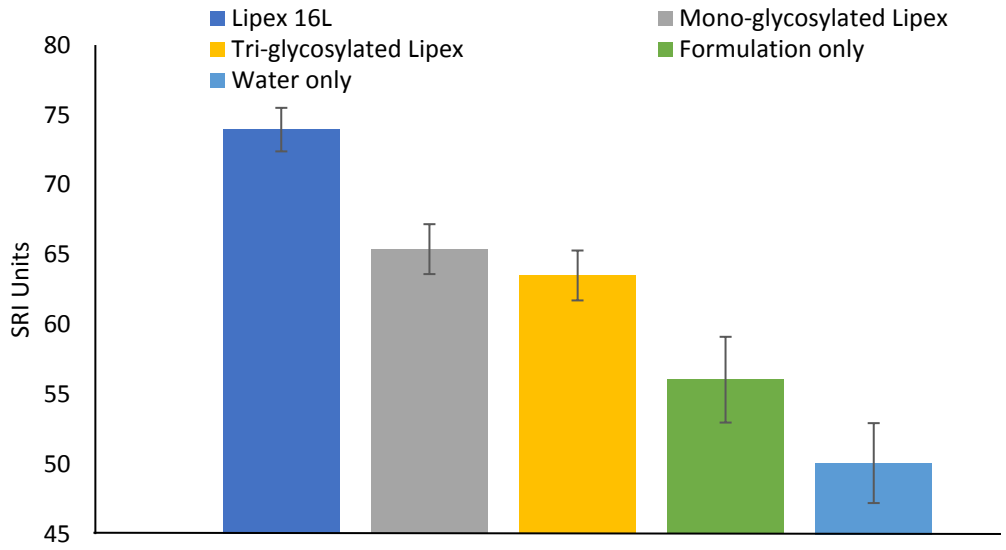

Fig 4.16: The Lipase end-point stain removal assays using CS61 (Beef Fat stained cloth) treated with Lipex 16L, mono-glycosylated Lipex, tri-glycosylated Lipex, laundry formulation with no enzyme and water. The error bars display the standard deviation between eight replicates.

The wash performance studies showed that the two *P. pastoris* Lipex variants were less effective than the commercial enzyme Lipex 16L. Furthermore, the tri-glycosylated Lipex did not show better performance than the mono-glycosylated Lipex.

4.4 Discussion

In the present study, we have explored the possibility of increasing the stability of the *T. lanuginosus* variant Lipex by glycosylation of the enzyme. Three Lipex variants were studied: a non-glycosylated, a mono-glycosylated (wild type) and a tri-glycosylated, in addition the commercial Lipex 16L was used as a comparison. The mono and tri-glycosylated Lipex were expressed in *P. pastoris*, reaching a high yield of secreted protein, while the non-glycosylated Lipex was expressed in *E. coli* which is not able to glycosylate proteins.

All three enzymes were characterised and the overall activity was found to be lower than the Lipex 16L (Fig 4.10). The tri-glycosylated variant did not show any increase in activity compared to the non and mono-glycosylated Lipex proving that the increase of protein glycosylation did not affect the enzyme activity which

is in agreement with previous studies (Peters et al., 2002; Pinholt et al., 2010). In the same way wash performances were comparable for the mono- and tri-glycosylated variant with the commercial Lipex 16L being more efficient. The expressed lipases were relatively stable from pH 8.0 to 12.0 and showed maximum activity between pH 8.5 and 10, and a temperature optimum around 55 °C for all the three Lipex variants which is consistent with previously reported data (Rodrigues et al., 2009).

The DSF data (Fig. 4.13), showed a noticeable improvement in stability of the tri-glycosylated Lipex compared to the other enzymes which is particularly relevant in comparison with the mono-glycosylated variant, which is expressed in the same organism thereby reducing the differences between the two enzymes to the amount of glycosylation only. The long-term stability experiment with and without protease shows that the tri-glycosylated Lipex has an advantage over the mono-glycosylated and non-glycosylated Lipex in the presence of protease (Table 4.2) with the tri-glycosylated Lipex being able to retain up to 46% of activity after 28 days in the presence of protease compared to 28% and 29% of the non-glycosylated Lipex and tri-glycosylated Lipex, respectively. The results are different when the incubation was performed in laundry formulation instead of aqueous buffer (Fig 4.15). In this set of experiments there were no clear differences between the mono- and tri-glycosylated Lipex and the Lipex 16L.

The commercial Lipex 16L performed better than the ‘in-house’ produced Lipex variants in all of the experiments however, it needs to be considered that the Lipex 16L is sold together with a formulation that is optimised for industrial applications, which could have a positive effect on stability and wash performances.

The Lipex 16L shown better stability to long storage (28 days) with and without the presence of Coronase and retained around 55% of its initial activity after 28 days of incubation in aqueous buffer in presence of Coronase. However when the incubation was performed in laundry formulations F1, F2 or F3 the differences between the commercial and the ‘in house’ produced glycosylated enzyme were minimal demonstrating the importance of the formulation components on protein stability.

To summarize, the DSF data proved that the tri-glycosylated Lipex was the most stable variant with a T_m shift of 4 ˚C demonstrating a direct stabilisation effect based on the abundance of glycan on the surface of the enzyme which is consistent with that found in previous studies (Benoit et al., 2006; Deshpande et al., 2008; Zou et al., 2013; Han et al., 2014). The improved stabilisation did not affect the lipase activity but did improve the resistance of the Lipex to proteolysis.

These results can be considered a starting point for further investigation which will aim to improve both the activity and the stability of the lipase enzymes.

More glycosylation sites could be introduced into the enzyme for expression in different eukaryotic hosts (insect and mammalian cells) which would allow the effect of further glycosylation on the lipase properties to be studied. It could also demonstrate how the composition of the different glycans that are added by the different host cells can impact on the lipase enzyme characteristics.

Chapter 5 - Characterisation of a novel psychrophilic lipase from *Psychromonas ingrahamii*

5.1 Background

More than three-quarters of the Earth's surface is occupied by cold ecosystems, including the ocean depths, the polar regions and the high alpine areas (Rodrigues and Tiedje, 2008). These permanently cold environments have been successfully colonised by a class of extremophilic microorganisms that are known as psychrophiles. The ability to thrive at temperatures that are close to, or below, the freezing point of water requires a vast array of adaptations to maintain the metabolic rates and sustained growth which is compatible with life under these severe environmental conditions. This is the subject of a recent review by De Maayer et al., 2014.

Biocatalysis has been applied commercially under cold conditions for chemical synthesis, bioremediation of contaminants and clean-energy production. This demonstrates the potential of this technology for industrial applications that are more environmentally friendly. The high activity of psychrophilic enzymes at low and mild temperatures offers potential economic benefits, for example, substantial energy savings in large-scale processes that would not require the expensive heating of the bioreactors. An example is the industrial 'peeling' of leather by proteases, which can be performed at the temperature of tap water by cold-active enzymes instead of heating to 37 °C for the process to be carried out by mesophilic enzymes (Mehta 2010). Psychrophilic enzymes also have potential applications for domestic processes. For instance, washing clothes at low temperatures can protect the colours of the fabrics and reduce energy consumption. However, the enzymes that are currently added to detergents to hydrolyse macromolecular stains - for example, proteases, lipases and glycosidases - are poorly active at the temperature of tap water (~ 13 °C in the UK). If mesophilic enzymes could be substituted by psychrophilic enzymes this could allow efficient cleaning at lower temperatures.

Cold-active lipases are promising enzymes to replace the conventional enzyme processes of the biotechnological industries (Babu et al., 2008). Cold-active lipases are structurally adapted allowing an increased flexibility of the polypeptide chain around the active site region of the enzyme to allow turnover of substrates

at low temperature (Babu et al., 2008). A cold-adapted lipase could be a suitable enzyme for removing fat and oil stains in laundry or dishwashing applications without the need for heating the water, thereby reducing energy consumption, and reducing greenhouse gas emissions. There is a challenge to demonstrate both stain removal at low temperatures and to maintain storage stability of potential psychrophilic enzymes at ambient temperatures.

This chapter will focus on the characterisation of a novel psychrophilic lipase from the arctic bacterium *Psychromonas ingrahamii.*

The *P. ingrahamii* bacterium was isolated in 1991 from north polar sea ice cores which were collected in Alaska. This *P. ingrahamii* strain 37 is able to grow at -12 ºC with a generation time of 240 hours (Breezee et al., 2004) and has an optimal growth temperature of 5 ºC, with a generation time of 12 hours (Novak et al., 2013).

A gene encoding a potential lipase was identified within the genome of this marine gram-negative bacterium. The gene called *PinLip* has been previously cloned and over-expressed in *E. coli* by Dr Halina Novak in our laboratory as part of her PhD thesis (Novak, 2012). However, the gene construct was unstable, and it was difficult to over-express the PinLip protein in reasonable quantities (> 0.5 mg/L cell culture). Within this project, the gene has been re-cloned, and an efficient over-expression system has been developed which has allowed the enzyme to be characterised and evaluated for its application in the homecare industry, especially laundry application.

5.2 Materials and methods

5.2.1. Bioinformatics

Protein sequence alignments of the lipase from *P. ingrahamii* with other structurally characterised lipases from the Protein Data Bank (PDB) database (Berman et al., 2000) were performed using the alignment algorithm Clustal Omega (http://www.ebi.ac.uk/Tools/msa/clustalo/). This was carried out to identify the positions of the known catalytic residues within the PinLip and to see the closest known homologues.

5.2.2. Cloning and over-expression

The *P. ingrahamii* lipase (*PinLip*) synthetic gene (see appendix Fig. 10.6) was purchased from GeneArt (Life Technologies). The gene was codon optimised for expression in *E. coli*. The PinLip gene was removed from the original GeneArt vector by restriction digestion with the enzymes *EcoR*I and *Sac*I.

Two primers were designed to sub-clone the optimised gene sequence into the pLATE31 vector (Thermo Scientific). The *PinLip* gene plus the compatible vector overhangs were amplified by PCR (Section 2.2.3) using the primers shown in Table 5.1.

Table 5.1: Forward and reverse primer sequences for the amplification and cloning of *P. ingrahamii* lipase. The overhangs complementary to the pLATE 31 vector are highlighted in yellow.

PinLipFW (Forward Primer)	5'- AGAAGGAGATATAACTATGATGCCGCACAAATTT- 3'
PinLipRV (Reverse Primer)	5'- GTGGTGGTGATGGTGATGGCCCTGGGTTGAACCTTT-3'

65 ng of the resulting 1117 bp PCR amplified fragment were treated with 1 U of T4 DNA polymerase as described by the manufacture to create the compatible vector overhangs. The reaction was stopped 0.6 µL of 500 mM EDTA before being annealed to 60 ng of the vector for 1 hour at 25 °C. Restriction enzyme digestion and DNA sequencing were used to confirm the presence of the *PinLip* gene sequence in the recombinant plasmid designated pLATE31/PinLip (Appendix, Fig 10.6).

The plasmid pLATE31/PinLip was transformed into *E. coli* BL21 (DE3) (Invitrogen). The transformants were tested for the presence of the gene with colony PCR and the positive transformants were preserved as 25% glycerol stocks (section 2.1.5) at -80 °C.

5.2.3 Purification

The optimal conditions for protein over-expression were established varying several parameters (section: 2.3.1). The best over-expression of the *P. ingrahamii* lipase was observed using *E. coli* BL21 (DE3) induced with 1 mM IPTG at an OD_{600} 0.6 for 18 hours at 12 °C with agitation 200 rpm.

The bacterial cell pellets were lysed by sonication in 8 bursts of 30 seconds followed by 90 seconds rest on ice to avoid overheating. The crude extract was

clarified by centrifugation at 24000 g for 30 minutes and the supernatant containing the soluble proteins was used for PinLip purification.

5.2.3.1 Purification protocol 1:

The supernatant containing the soluble proteins was loaded onto a 1 mL HiTrap Butyl HP column (GE Healthcare) which was previously equilibrated with three column volumes of HIC buffer A (Table 2.5). The unbound protein was washed from the column with five column volumes of HIC buffer A. The bound protein was eluted using a 20 columns volume gradient to 100% HIC buffer B (Table 2.5). The fractions corresponding to the recombinant protein were pooled together and dialysed with 4 L of DEAE Buffer A (Table 2.5) overnight. The dialysed protein was loaded onto a 1 mL HiTrap DEAE FF column (GE Healthcare) previously equilibrated with three column volumes of DEAE buffer A. The unbound protein was washed from the column with five column volumes of DEAE buffer A. The bound protein was eluted using a 20 column volumes gradient to 100% DEAE buffer B (Table 2.5).

5.2.3.2 Purification protocol 2:

The soluble protein sample was loaded onto a 1 mL MBP Trap HP column (GE Healthcare) directly connected to a 1 mL His Trap FF (GE Healthcare) (Fig. 5.1) previously equilibrated with five column volumes of IMAC buffer A (Table 2.5). The unbound protein was washed from the column with five column volumes of IMAC buffer A. The bound protein was eluted using a 10 column volumes step gradient to 10% IMAC buffer B (Table 2.5), followed by a second step of 100% IMAC buffer B. The fractions corresponding to the recombinant protein were pooled together and concentrated with an Amicon Ultra-15 Centrifugal Filter Unit 10 kDa cut-off (EMD Millipore, Billerica, MA, US) to a volume of 0.5 mL. The concentrated protein was loaded onto a 120 mL Superdex 200 GF chromatography column (GE Healthcare) and eluted with an isocratic run with 1.5 column volume of SEC buffer 1 (Table 2.5).

Fig.5.1: The arrangement of the MBPTrap and HisTrap columns used for the PinLip purification protocol 2.

5.3 Results

5.3.1 Bioinformatics

A lipase from *P. ingrahamii* (PinLip) was identified using BLASTp (Altschul et al., 1990). The Pinlip protein sequence was searched against structurally characterised proteins in the PDB and showed the highest homology to the lipases from *Rhizomucor miehei* (PDB: 3TGL) and the lipase from *T. lanuginosus* (1DT3) with a sequence identity of ~22 % to them both with only 60% of query coverage. The protein sequence alignments are shown below in Fig. 5.2 and 5.3.

```
Sequence_1      MPHKFTMDHSLLEPPIKRAAYSDRTAWLMAVMSSLAYIRFEQPTPLDE-LAKVLSRETNE
Sequence_2      -------------------------------------------SIDGGIRAATSQEINE
                                                          :*  :  . *:* **

Sequence_1      RNILTKLNA------LLAAENRDQLKKELKSDLQDIGFELVDTYNISIPLVVDTQAYLAK
Sequence_2      LTYYTTLSANSYCRTVIPGATWDCIHCDATEDL-----KIIKTWS---TLIYDTNAMV--
                 .  *.*.*      :: . . * :: : ..**     :::.*:.    *: **:* :

Sequence_1      ITLQDRDPMLVLAFRGTEVTNAADIRSDVSANPMNIGPKEEGHQVHSGFYNAFKAAQSVI
Sequence_2      -ARGDSEKTIYIVFRGSSSIR--NWIADLTFVPVS-YPPVSGTKVHKGFLDSYGEVQNEL
                 :  * :  : :.***:.  .  :  :*::  *:.  *  .* :**.** :::  .*. :

Sequence_1      ELSLN--KPELKNMPLYITGHSLGGALAVVATYCISNDSV------GACYTFGGPRVGNM
Sequence_2      VATVLDQFKQYPSYKVAVTGHSLGGATALLCALDLYQREEGLSSSNLFLYTQGQPRVGNP
                  ::     :  .  : :******** *::.:  : : .          ** * *****

Sequence_1      LFGQSI---RTPVYRVINAADLVPRLPPSYLIEGITLLLRWLPIIPYNNQVADYLERFRH
Sequence_2      AFANYVVSTGIPYRRTVNERDIVPHLPPAAFGFLHAGSEYWIT-----------------
                 *.: :     *  *.:*  *:**:***: :    :    *:

Sequence_1      YRHYGDLRYLTDATRSTPEGEGMLAAYPGLQVIANPCQLSRWIWLCSRLIATYGRAGIND
Sequence_2      -----------DNSPET---VQ-------------VCTSDLETSDCSNSIV---------
                           * : .*                  *  .     **. *.

Sequence_1      HSIDIYVEKLAYWGIQRNLGKPKLVSAQAETKGSTQ
Sequence_2      -PFTSVLDHLSYFGINTGLCT---------------
                  :   :::*:*:**: .* .
```

Fig 5.2: The amino acid sequence alignment between the *P. ingrahamii* lipase (Sequence_1) and the *R. miehei* lipase (Sequence_2). The lid region is highlighted in grey, and the GXSXG motif is highlighted in yellow. The serine, aspartic acid and histidine of the catalytic triad are highlighted in red.

```
Sequence_1      MPHKFTMDHSLLEPPIKRAAYSDRTAWLMAVMSSLAYIRFEQPTPLDELAKVLSRETNER
```

```
Sequence_3      --------------EVSQDLFNQF--NLFAQYSAAAYCGKNNDAPAG-----------T
                             :.:  :.:    *:*  *: **   :: :* .

Sequence_1      NILTKLNALLAAENRDQLKKELKSDLQDIGFELVDTYNISIPLVVDTQAYLAKITLQDRD
Sequence_3      NITCTGNACPEVE---KADATFLYSFEDSG-------------VGDV---TGFLALDNTN
                **  . **   .*   : .  :  .::* *            * *.    . ::*:: :

Sequence_1      PMLVLAFRGTEVTNAADIRSDVSANPMNIGPKEEGHQVHSGFYNAFKAAQSVIELSLN--
Sequence_3      KLIVLSFRGSRSIENW--IGNLNFDLKEINDICSGCRGHDGFTSSWRSVADTLRQKVEDA
                 ::**:***:.  :     .::. :  :*.   .* : *.** .::::. ..:. .::

Sequence_1      KPELKNMPLYITGHSLGGALAVVATYCISNDS-VGACYTFGGPRVGNMLFGQSI----RT
Sequence_3      VREHPDYRVVFTGHSLGGALATVAGADLRGNGYDIDVFSYGAPRVGNRAFAEFLTVQTGG
                  *  :  : :**********.**   : .:.     :::*.*****  *.: :

Sequence_1      PVYRVINAADLVPRLPPSYLIEGITLLLRWLPIIPYNNQVADYLERFRHYRHYGDLRYLT
Sequence_3      TLYRITHTNDIVPRLPPREFGYSHSSPEYWIKSGTLVPVTRNDIVKIEGID---------
                 :**: :: *:******  :  . :    *:        . : : ::.

Sequence_1      DATRSTPEGEGMLAAYPGLQVIANPCQLSRWIWLCSRLIATYGRAGINDHSIDIYVEKLA
Sequence_3      ------ATGGNNQ---P------NIPDIPAHLWYFGLIGTCL------------------
                       * .     *      *  ::   :*  . : :

Sequence_1      YWGIQRNLGKPKLVSAQAETKGSTQ
Sequence_3      -------------------------
```

Fig 5.3: The amino acid sequence alignment between the *P. ingrahamii* lipase (Sequence_1) and the *T. lanuginosus* lipase (Sequence_3). The lid region is highlighted in grey, and the GXSXG motif is highlighted in yellow. The serine, aspartic acid and histidine of the catalytic triad are highlighted in red.

The alignments shown above allowed the identification of the consensus motif GXSXG containing the putative active-site serine, which is well conserved in other lipases (Jaeger et al., 1999). The aspartic acid from the catalytic triad was also identified but the third residue of the catalytic triad could not be identified because of very low sequence identity in the C-terminal region of the lipases. The sequence alignments also allowed the identification of the PinLip lipase lid region.

5.3.2 Cloning and over-expression

PCR was used to amplify the synthetic codon optimized *P. ingrahamii* lipase gene and a band of the correct size was observed on a 0.8% agarose gel (Fig. 5.4). The amplified gene was cloned into the expression vector pLATE31.

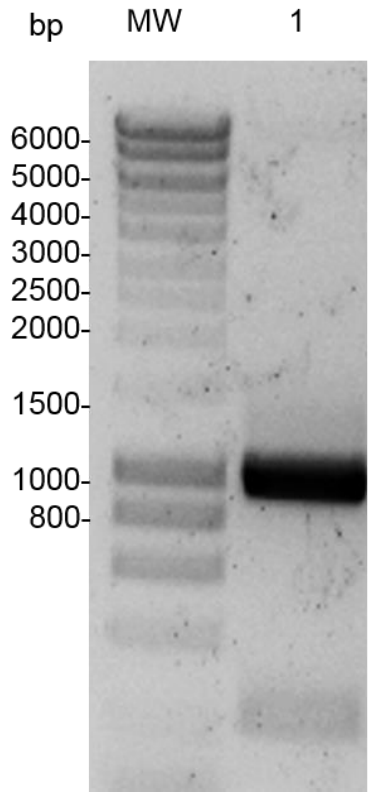

Fig 5.4: A 0.8% agarose gel showing the amplified *P. ingrahamii* lipase gene (MW: Molecular weight marker, Lane 1: *P. ingrahamii* lipase gene.

Over-expression trials of the *P. ingrahamii* lipase were conducted by varying the *E. coli* expression strain and induction conditions as described in section 2.3.1. The best over-expression of the *P. ingrahamii* lipase was observed using *E. coli* BL21 (DE3) induced with 1 mM IPTG at an OD_{600} 0.6 for 18 hours at 12 °C with agitation 200 rpm.

5.3.3 Purification

The bacterial cell paste from 3 L of recombinant *E. coli* was harvested by centrifugation. Bacterial cells were lysed by sonication and soluble protein was then purified.

Several purification processes were developed for PinLip. Initial trials with immobilised metal ion (Nickel) affinity chromatography (IMAC) failed despite the introduction of a C-terminal His-tag to the PinLip sequence to facilitate purification. Then, a two-step process comprising hydrophobic interaction chromatography (HIC) (Fig 5.5 and 5.6), and a DEAE anion exchange chromatography (Fig 5.7) yielded a protein product, which was still contaminated

with other proteins (55 % purity calculated with the ImageJ gel analyser tool (Schneider et al., 2012)). A band corresponding to the correct molecular weight (42 kD) was excised from the final SDS-PAGE gel (Fig 5.8) and sent to the University of Bristol Proteomics facility for tryptic digestion followed by Peptide Mass Fingerprint (PMF) (section 2.3.7), to confirm the identity of the over-expressed protein.

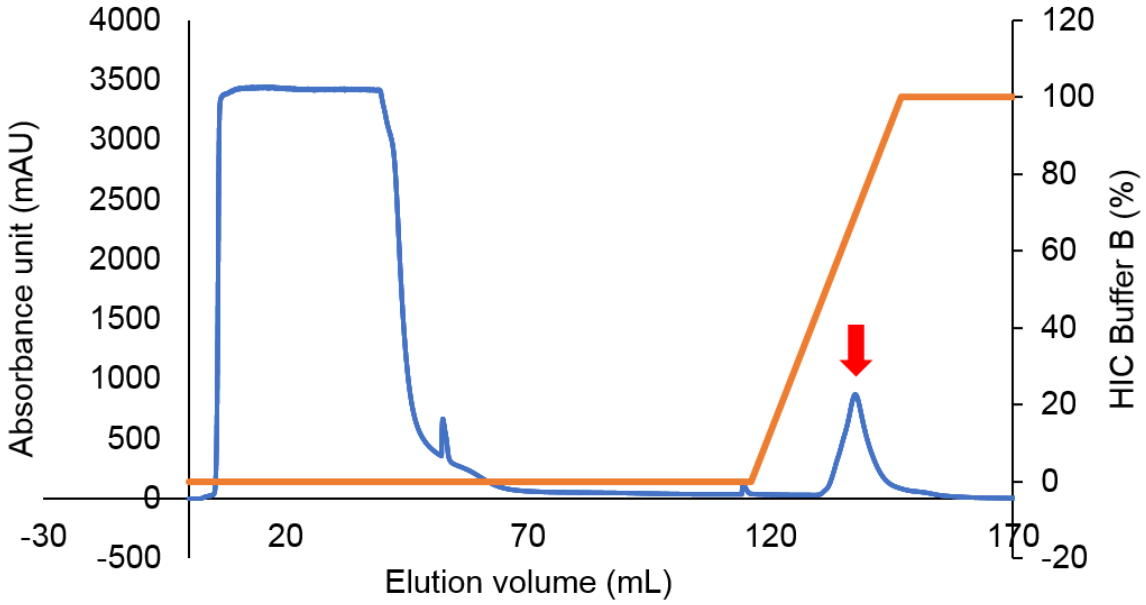

Fig. 5.5: The elution profile from the HIC column. The PinLip eluted between 130 – 150 mL as indicated by the red arrow.

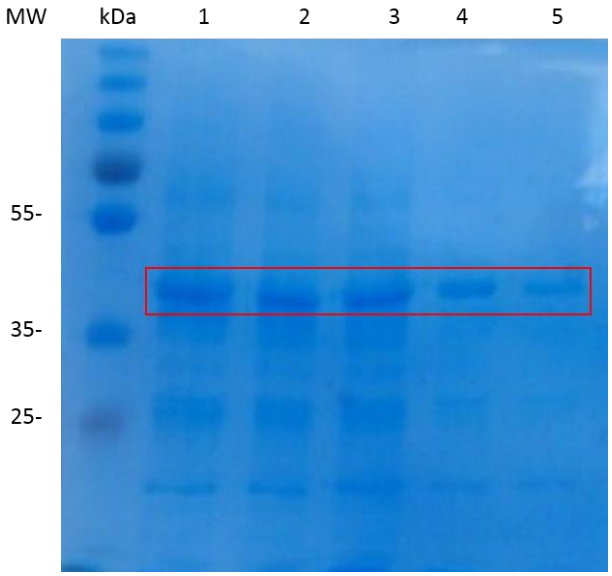

Fig. 5.6: SDS-PAGE gel across the peak fractions eluted from the HIC column. The protein bands of interest (42 kDa) are highlighted by the red box.

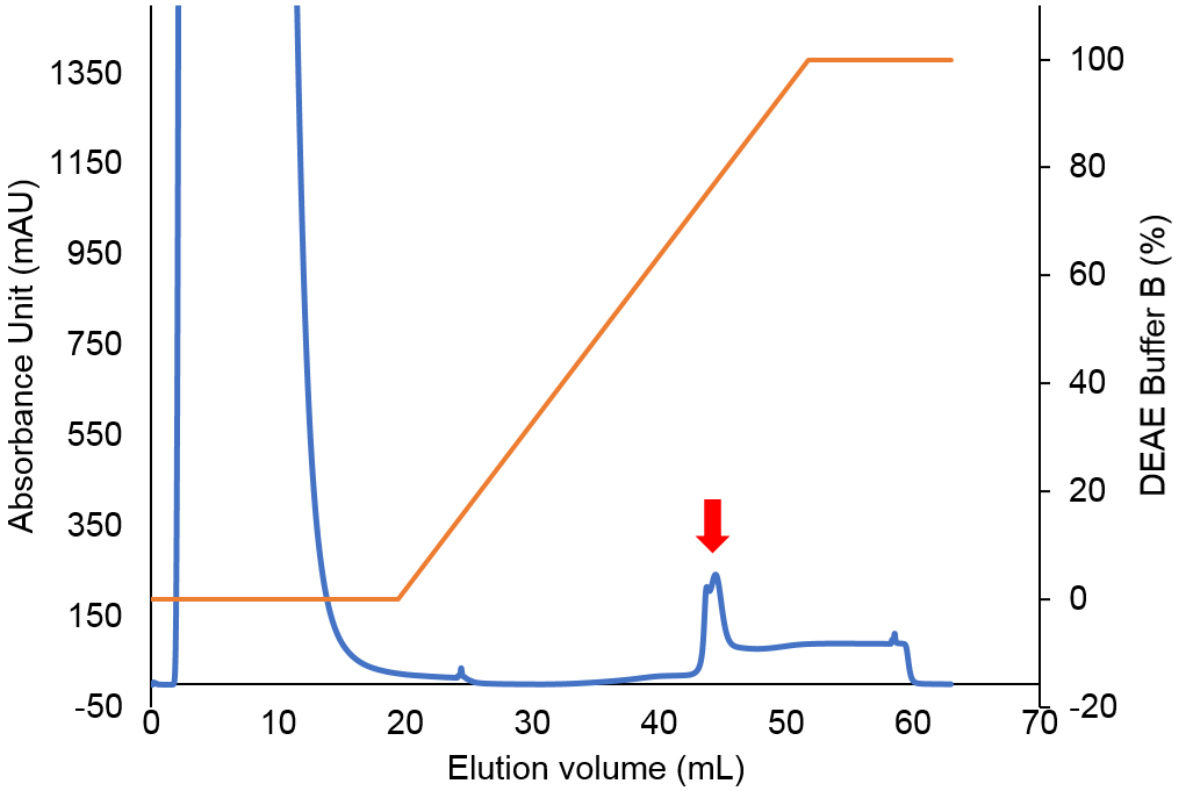

Fig. 5.7 Elution profile from the DEAE anion exchange column. The PinLip eluted between 42 and 46 mL as indicated by the red arrow.

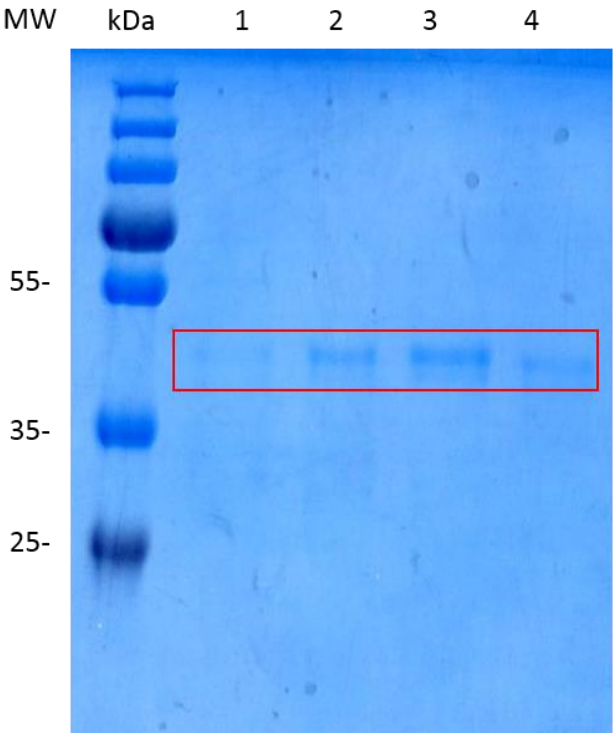

Fig. 5.8: SDS-PAGE gel of the peak fractions eluted from the DEAE anion exchange column. Protein bands of interest (42 kDa) are highlighted by the red box.

The peptide Mass Fingerprint (PMF) analysis revealed that the PinLip was contaminated with the maltose binding protein (MBP) from *E. coli.* Incidentally, the *E. coli* MBP has a molecular weight of 41.8 kDa so the two proteins were not resolved on the SDS-PAGE gel. It was proposed that the PinLip interacts with the MBP by hydrophobic interactions which masked the His-tag making it impossible to purify with Nickel-IMAC technology. This result triggered the development of a new purification protocol. A one-step process was established, (Section 5.2.3.1 Protocol 2) using a two-column tandem arrangement (MBP affinity plus Nickel – IMAC (Fig. 5.1)) to purify the PinLip by coupling a flow-through method with a binding and elute mode separation. The removal of the contaminant, MBP, allowed the C-terminal His-Tag to then bind to the nickel affinity IMAC column which could now be used for purification (Fig. 5.9).

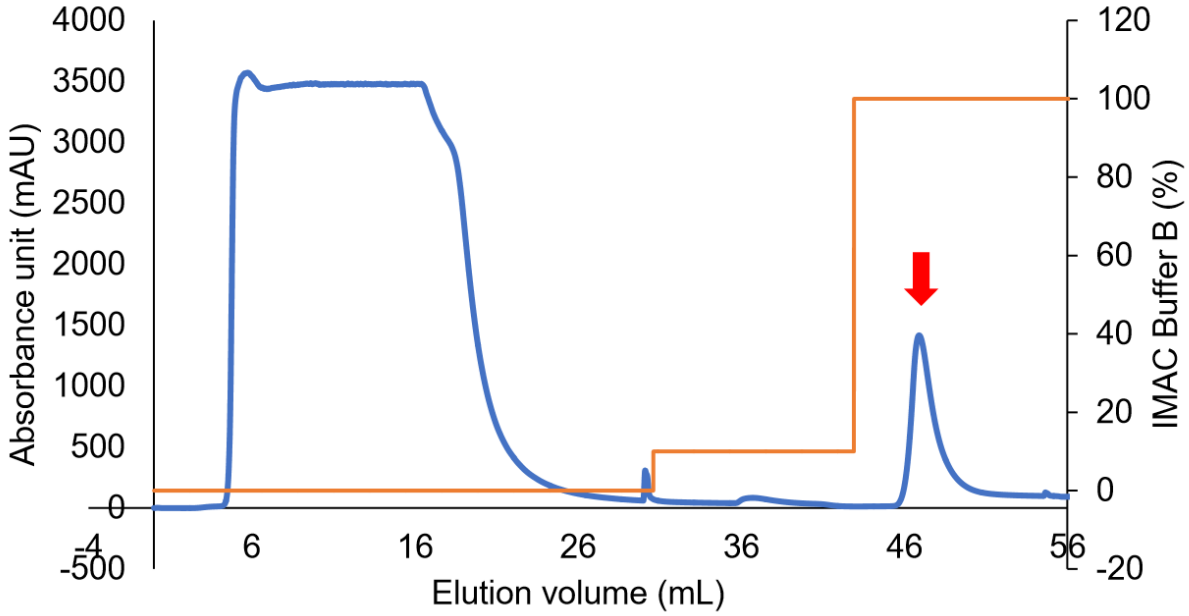

Fig. 5.9: The elution profile from the coupled MBP and Nickel IMAC columns. The PinLip eluted between 45 and 52 mL as indicated by the red arrow .

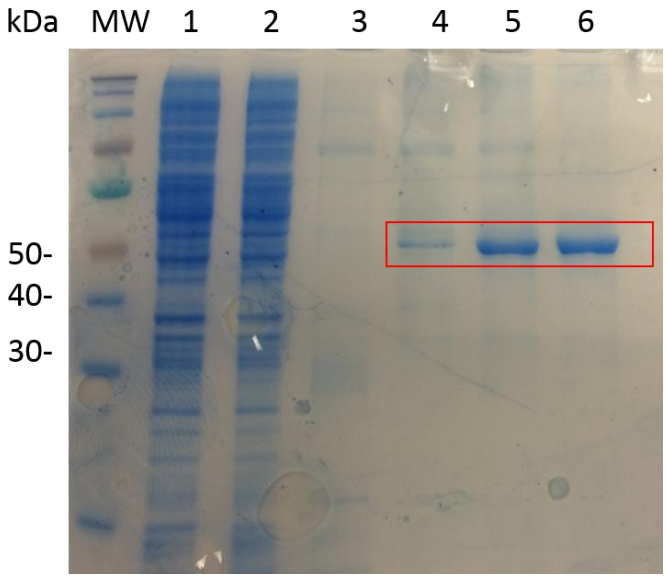

Fig. 5.10: SDS-PAGE gel of fractions eluted from the coupled MBP and Nickel IMAC columns. Protein bands of interest (42 kDa) are highlighted by the red box. Lane 1: Insoluble fraction, Lane 2: Crude protein extract, Lane 3: Flow through,Lane 4 4, Lanes 5 and 6: Purified PinLip fractions across the elution peak.

The fractions that tested positive for lipase activity (section 2.3.10) from the IMAC were pooled together and concentrated with an Amicon Ultra-15 centrifugal filter unit 10 kDa cut-off (EMD Millipore). The concentrated protein sample was further purified on a Superdex 200 GF chromatography column (Fig 5.11).

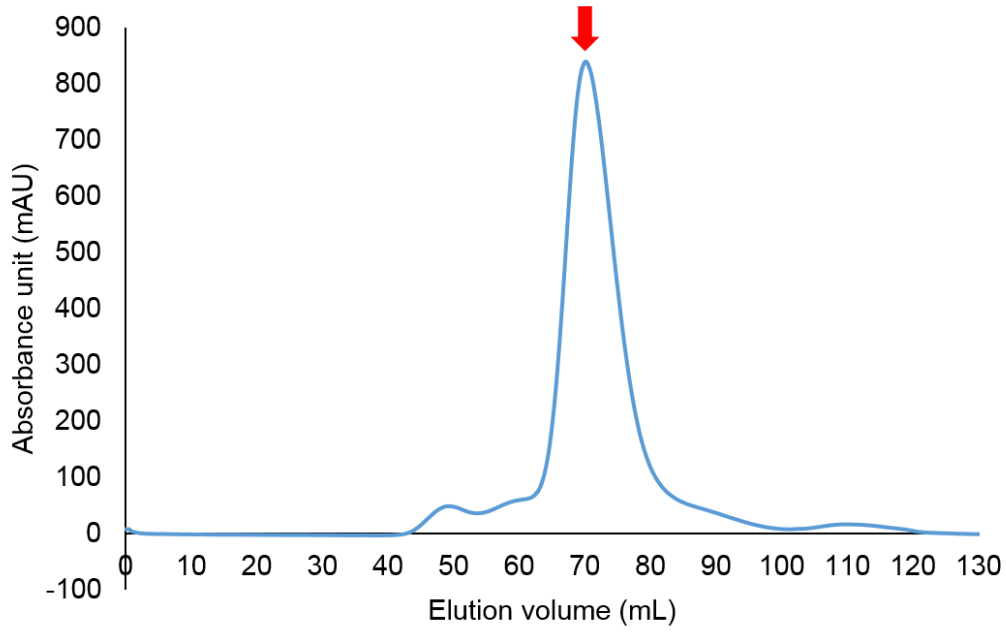

Fig 5.11: The elution profile from the Superdex 200 GF gel filtration chromatography column. The PinLip eluted between 60 – 80 mL as indicated by the red arrow.

The purity of the final product was confirmed by SDS-PAGE (Fig. 5.12) and by Western blot analysis as described in section 2.3.9 (Fig 5.13). A yield of 6 mg of purified *P. ingrahamii* lipase was obtained from a 3 L culture of recombinant *E coli* BL21 (DE3).

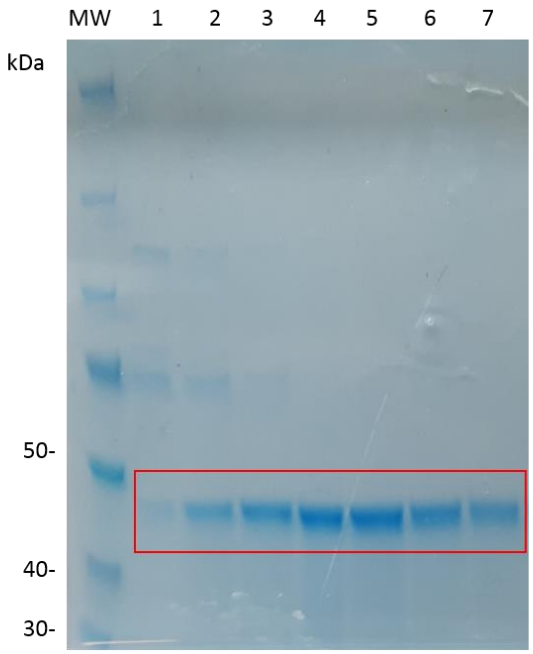

Fig. 5.12: SDS-PAGE gel of fractions (1-7) eluted from the Superdex 200 GF chromatography column. Protein bands of interest (42 kDa) are highlighted by the red box.

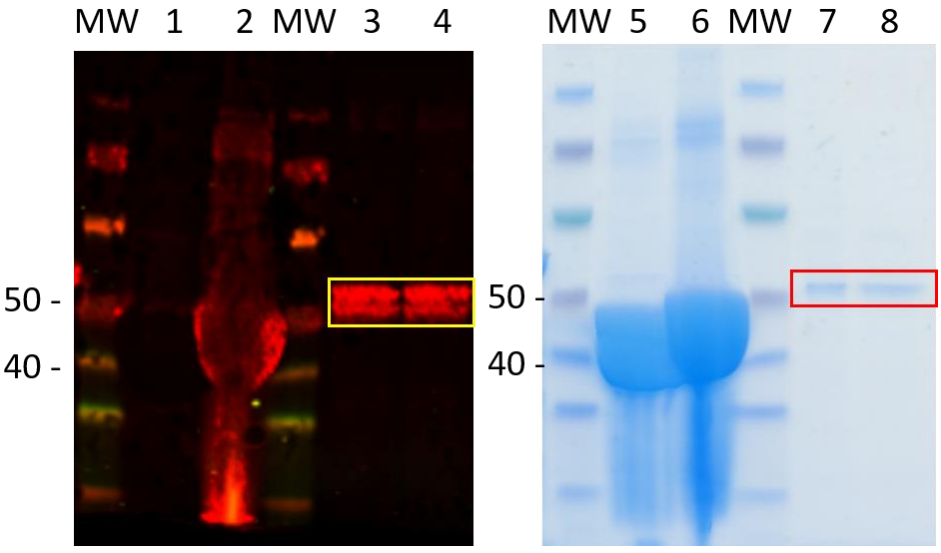

Fig.5.13: Western blot and SDS-PAGE analysis of the PinLip. Lanes 1 and 5: Western Blot negative control (*Thermogutta terrifontis* esterase); Lanes 2 and 6: Western blot positive control (*Thermogutta terrifontis* esterase with 6x C-terminal HisTag): Lanes 3, 4 7 and 8: PinLip. The Western blot was probed using mouse anti-His tag primary antibody (GenScript), and secondary antibody was goat anti-mouse IRDye 680 (Licor).

To further confirm the protein identity and exclude the presence of any remaining contamination of the MBP a band from the SDS-PAGE gel corresponding to the assumed PinLip, molecular weight of 42 kDa, was excised from the gel and sent to the University of Bristol Proteomics facility for tryptic digestion followed by Peptide Mass Fingerprint (PMF) analysis. Acquisition of the PMF data by MALDI-TOF mass spectrometry confirmed the lipase from *P. ingrahamii* with 12 positive peptide hits. No maltose binding protein was detected by this analysis which proves the efficiency of the improved purification protocol.

5.3.4 Biochemical characterisation

The quantification of hydrolytic activity was routinely measured using a spectrophotometric assay at 410 nm with p-nitrophenyl laurate (pNP laurate) as the substrate (section 2.3.10).

5.3.4.1 Substrate specificity

The substrate specificity of the PinLip lipase was examined using various pNP esters with C2 to C18 aliphatic acyl-chains (Fig. 5.14), using the standard lipase assay described in section 2.3.10.

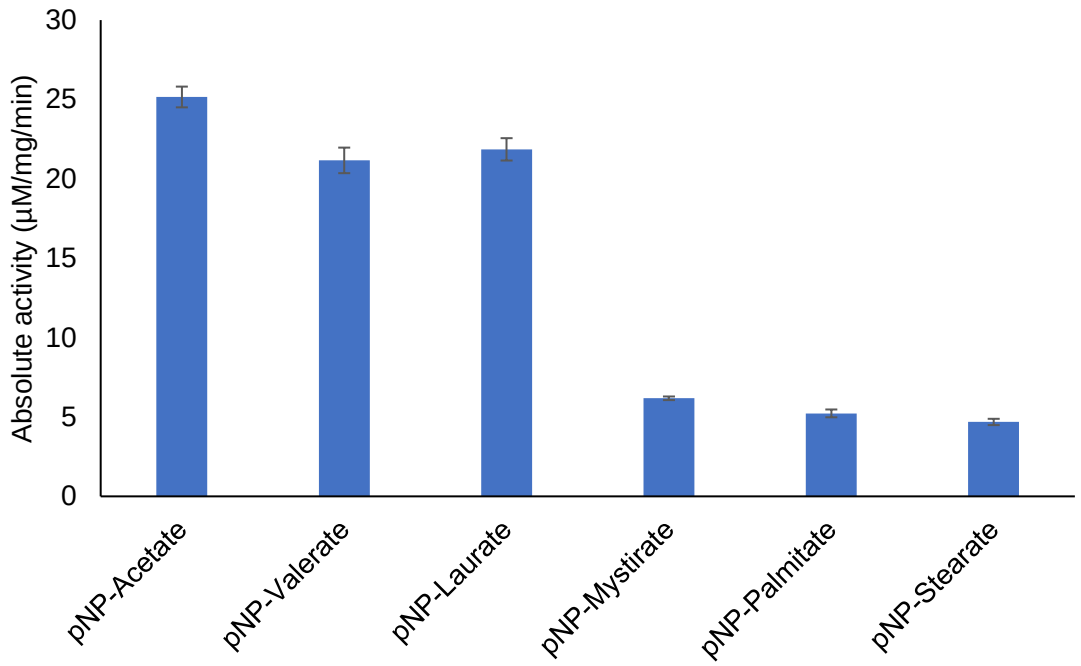

Fig. 5.14: Substrate specificity of the PinLip. The activity assay was performed using pNP esters of varying fatty acid chain length as substrates. The error bars display the standard deviation between three replicates.

The reactivity of these substrates with the PinLip enzyme depended on their acyl-chain length. The PinLip has a preference for short (< 6) and medium (6 to 12) chain fatty acids as shown in Fig, 5.13.

5.3.4.2 Effect of the temperature on the lipase activity

The purified PinLip maintained its lipolytic activity at 0–40 °C and exhibited optimum activity between 15 and 30 °C as shown in Fig. 5.15 A. When the reaction was left at 15 °C for 60min the lipase still retained almost 100% activity, whereas less than 40 % of the maximal activity was lost after incubation at 30 °C for 60min (Fig. 5.15 B). The activity was substantially reduced at temperatures higher than 30 °C, as shown in Fig. 5.14 B.

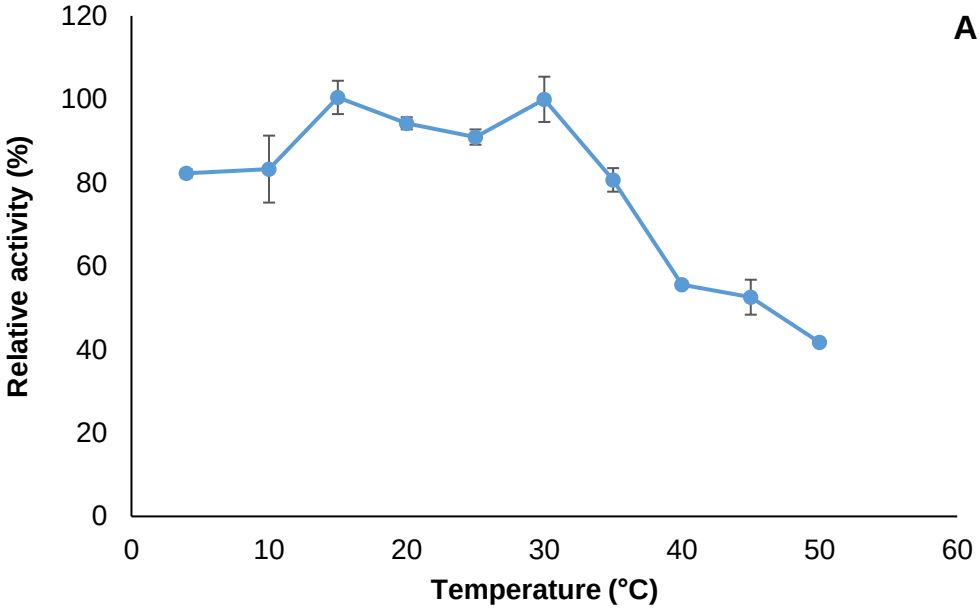

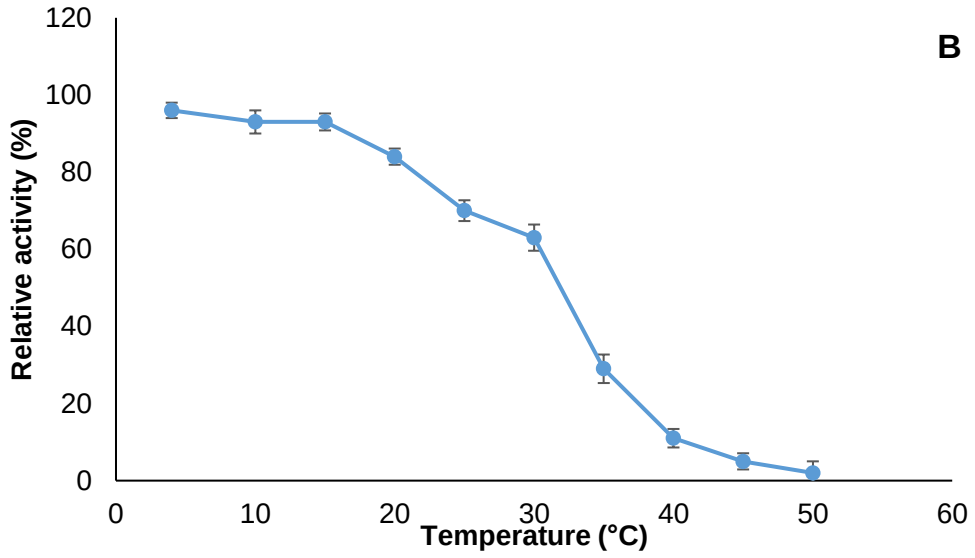

Fig. 5.15: The effect of temperature on the PinLip enzyme. (A) Hydrolytic activity at various temperatures was assayed using pNP laurate as a substrate. (B) Residual hydrolytic activity was measured after treatment for 1 hour at a range of temperatures. Activities are expressed relative to that of the most active sample. The error bars display the standard deviation between three replicates.

5.3.4.3 Effect of pH on the lipase activity

The activity of an enzyme at different pH values is an important parameter for an industrial enzyme. Therefore, the effect of pH on PinLip activity was examined by measuring activity against pNP laurate at different pH values. The optimum pH of PinLip was measured by assaying the activity at various pH values (6 - 12) for 30 minutes, and the residual activity was measured at 20 °C and pH 8.5. The lipase showed maximum activity between pH 8.5 and 10.5 when assayed at 20 °C (Fig. 5.16).

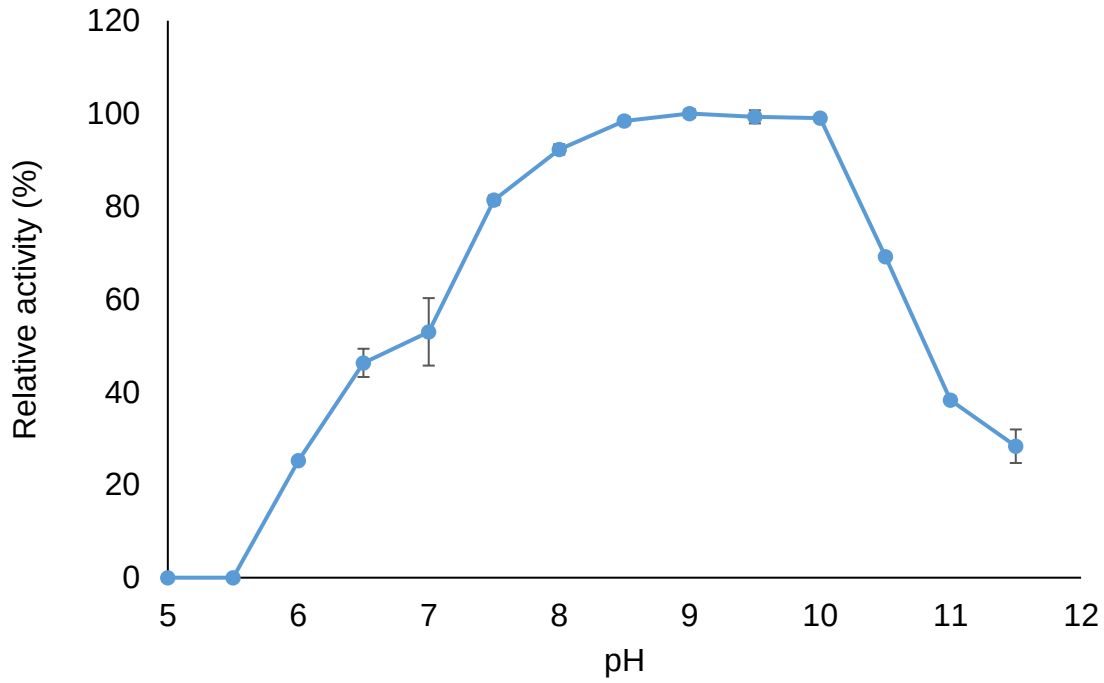

Fig. 5.16: The effect of pH on the activity of the purified PinLip enzyme. The optimum pH was determined by assays carried out after incubation for one hour at room temperature in the following buffers covering a range of pH values from 5 to 12: 100 mM sodium phosphate pH 5 and pH 6.0, 100 mM Tris-HCl pH 7.0, pH 8.0 and pH 9.0, 100 mM glycine-NaOH pH 10.0, 100 mM sodium dihydrogen orthophosphate-NaOH pH 11.0 and pH 12.0. Activities were expressed relative to that of the most active sample. The error bars display the standard deviation between three replicates.

These results agree with the range of optimal temperature and pH reported for other cold-adapted lipases by Ji et al., 2015. From the 26 characterised psychrophilic lipases, 25 had an optimum pH between 8.0 and 10.0 and 18

lipases exhibited an optimum operating temperature between 15 and 30 °C with the others not exceeding 45 °C (Ji et al., 2015).

These temperature stability results indicated that this novel PinLip lipase represented a new example of a psychrophilic lipase. The broad range of pH where the PinLip enzyme showed activity makes it an interesting candidate for industrial applications.

5.3.4.4 Effect of metal ions

To examine the effect of metal ions on the stability of the enzyme, the PinLip was incubated in 50 mM Tris-HCl pH 8.5 containing 1 mM of different metal ions (Na^+, K^+, Zn^{2+}, Ca^{2+}, Mg^{2+}, Mn^{2+} and Ni^{2+}) for 1 hour at 20 °C, and the remaining activity was determined (Fig 5.17).

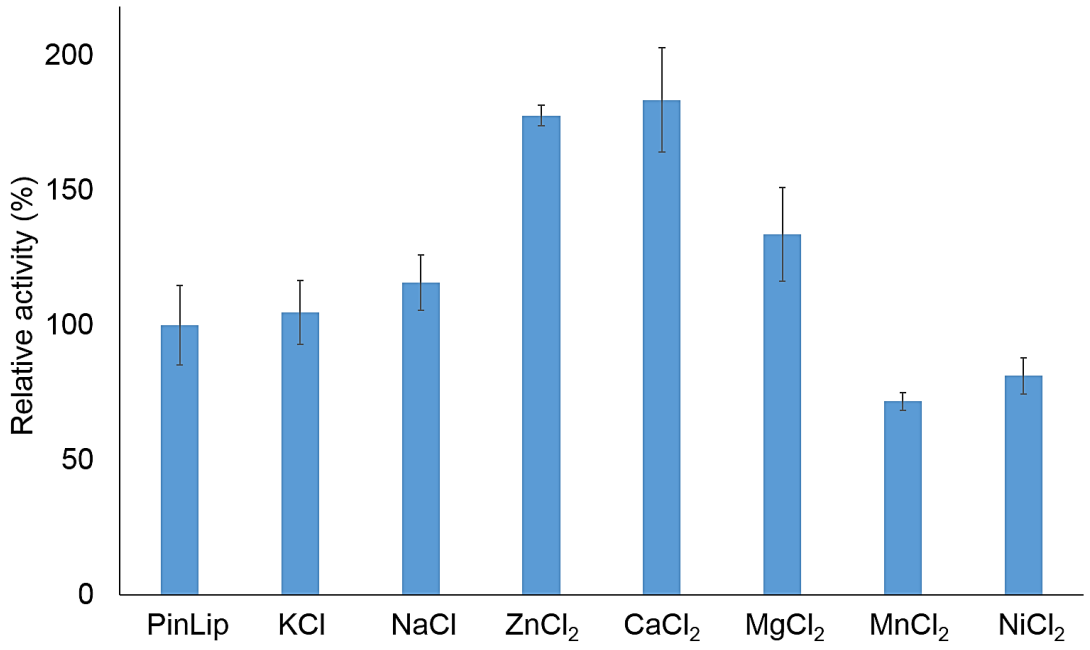

Fig 5.17: The effect of various metal ions on the lipase activity of PinLip. The lipase activity assay was performed at 20 °C, pH 8.5, in the presence of 1 mM of various metal ions. Activity of control (with no metal ions in the mixture) was taken as 100%. The error bars display the standard deviation between three replicates.

The results show the effect of various metal ions on the lipase activity. For the cations tested, Mn^{2+} and Ni^{2+} slightly inhibited the activity of the enzyme, whereas the activity was enhanced by Ca^{2+}, Zn^{2+} and Mg^{2+}. Divalent ions are known to have a stabilising effect on lipases. Particularly previous studies have proven the

presence of calcium ion in the active site of lipase to act as a stabiliser of the catalytic histidine (Kim et al., 2000; Nardini et al., 2000).

5.3.5 Wash performance studies

Wash performance studies were conducted as described in section 2.4. The objective was to identify whether the PinLip enzyme would show activity in commercial surfactant/additive formulations F1, F2 and F3 (Table 2.5), and show a cleaning benefit when compared to the industrially available Lipex 16L, the benchmark enzyme. Experiments were conducted at low temperature (20 °C) against two types of lipid stain (CS61-Beef Fat stained cloth and CS46B - Used Fry Fat stained cloth) with low and high content of short-chain triglycerides respectively (Fig 5.18 and 5.19).

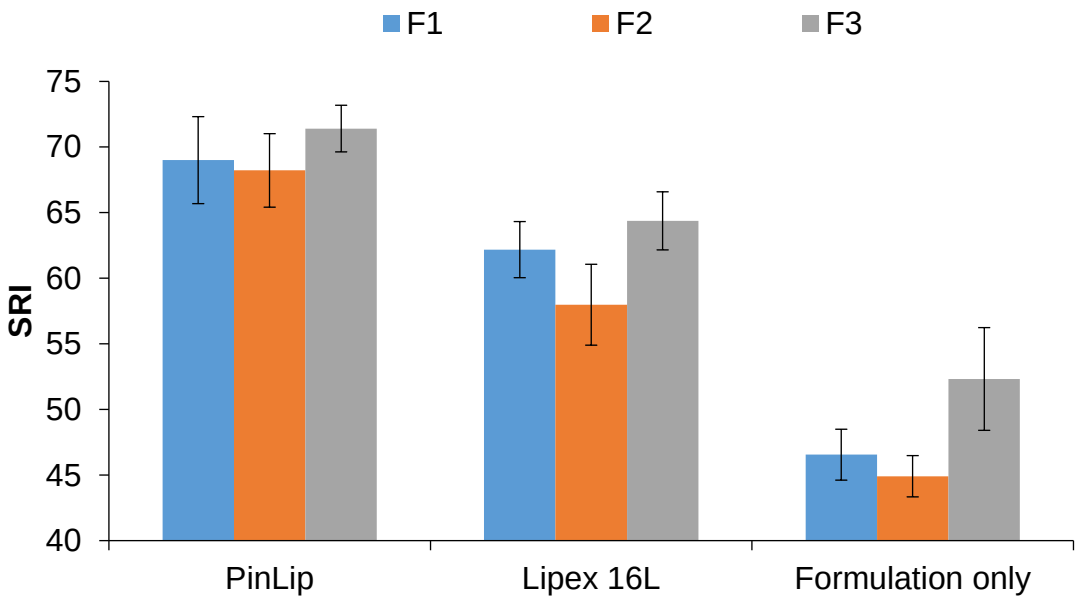

Fig. 5.18: Low temperature (20 °C) lipase end-point removal assay using CS61 (beef fat stained) cloth treated with PinLip, soluble Lipex and formulation control. The wash liquor contained 10 mg/L of enzyme and 0.8 g/L of laundry formulation. The error bars display the standard deviation between eight replicates.

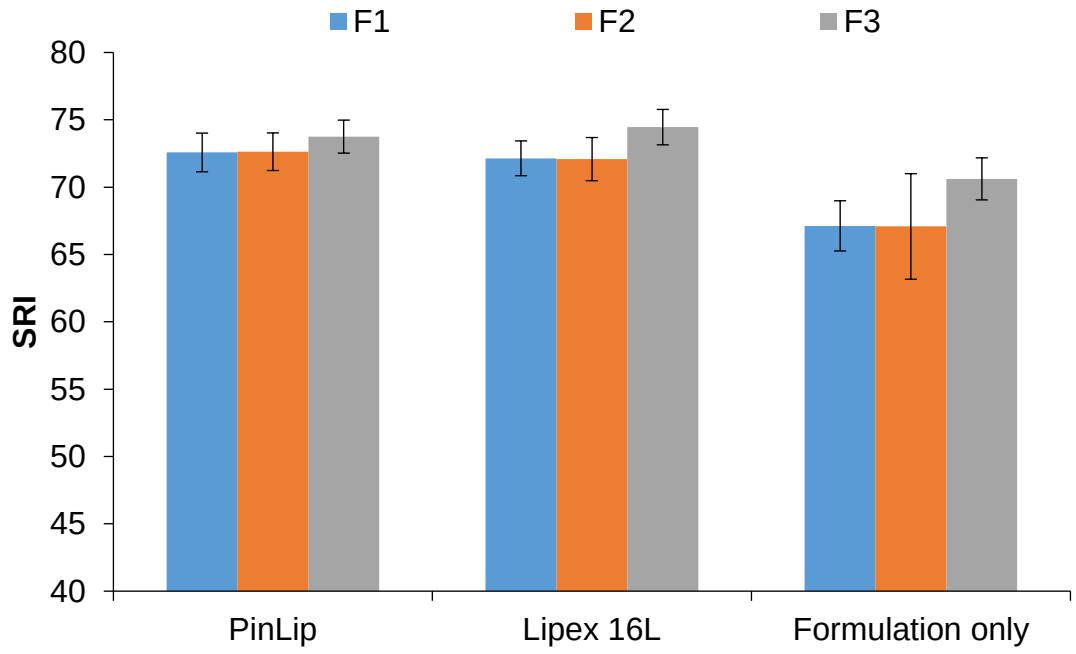

Fig. 5.19: Low temperature (20 °C) lipase end-point removal assay using CS46B (used fry fat stained) cloth treated with PinLip, soluble Lipex and formulation control. The wash liquor contained 10 mg/L of enzyme and 0.8 g/L of laundry formulation. The error bars display the standard deviation between eight replicates.

Fig 5.18 clearly shows that PinLip cleans better the CS61 Beef fat stain (+ 7-10 dSRI) than the benchmark enzyme, while neither of the lipases (PinLip or Lipex 16L) showed better activity towards the CS46B (frying fat stain, Fig 5.19). These results are a consequence of the different composition of the stains, CS61 - Beef fat is composed of triglycerides, whose major constituents are derived from stearic and oleic acids whereas the CS46B is more composed of shorter fatty acids (≤ 12C). Short-chain fatty acids are more soluble in water and therefore are easier to be removed from the cloths even in the formulation without enzyme (Fig 5.19).

The CS61 can be considered a better indicator of lipase wash performance because the laundry formulation without enzyme performs poorly when compared with the formulation with the enzyme.

5.3.5.1 PinLip wash performance in combination with biosurfactants

In an effort to reduce the environmental impact of its laundry detergent Unilever is experimenting with the introduction of natural surfactants to replace the traditional chemical surfactants that are currently used in their products.

Biosurfactants are a wide group of surface-active substances synthesised from a microorganism and excreted extracellularly. Biosurfactants are grouped as glycolipids, lipopeptides, phospholipids, fatty acids, neutral lipids, polymeric and particulate compounds (Biermann et al., 1987). Moreover, biosurfactants have good thermal and pH stability which makes them suitable for laundry applications (Bajpai and Mishra, 2016).

The biosurfactants used in this study belong to two groups: rhamnolipids and mannosylerythritol lipids (MEL). Rhamnolipids are composed of β-hydroxy fatty acids connected by the carboxyl end to a rhamnose sugar molecule. Rhamnolipids are predominantly produced by *Pseudomonas aeruginosa* and classified as mono and di-rhamnolipids (Sekhon Randhawa and Rahman, 2014). For their efficiency as natural emulsifiers rhamnolipids have potential applications in detergent compositions, laundry products, shampoos and soaps (Parry et al., 2012).

The MELs are long chain fatty acids that contain either 4-O-β-D-mannopyranosyl – erythritol or 1 -O- β -D- mannopyranosylerythritol as the hydrophilic head group, which is attached to a variety of fatty acids as the hydrophobic chain (Morita et al., 2015). The MELs are produced mostly by yeast strains of the genus *Pseudozyma* (Morita et al., 2009). The MELs have promising industrial applications due to their biodegradability, low toxicity and effectiveness in enhancing solubilisation of low solubility compounds (Mulligan, 2005).

In order to understand the effect of biosurfactants on the cleaning effects of enzymes, different compounds were screened (kindly provided by Paul Stevenson, Unilever) at different concentration levels in the presence and absence of enzymes in a Lipase end-point removal assay (section 2.4.1) (Table 5.2).

The results in the table below show that PinLip performed particularly well in combination with biosurfactants R1 across the whole concentration range. PinLip shows better synergistic cleaning performance (enzyme plus R1) than the benchmark enzyme, Lipex 16L. In the presence of MEL-B and 1614 MEL, PinLip showed over the full dosage range superior cleaning compared to the MELs Lipex 16L combinations. These biosurfactants have good potential to substitute chemical surfactants in the future. However, new formulation design is necessary

in order to produce complete formulations that can be tested with psychrophilic enzymes. This subject is treated in more details in Chapter 7.

Table 5.2: The Lipase end-point removal assay (section 2.4.1) using CS61 (beef fat stained) cloth treated with PinLip, Lipex 16L and biosurfactants only control, results are expressed in SRI percentage compared to the Lipex 16L performance without any surfactants as 100%. The conditions in which the PinLip performed better than the no surfactants control are highlighted in yellow.

Biosurfactant	Enzymes	Biosurfactant (%)					
	0	0.0125	0.025	0.05	0.1	0.2	
Rhamnolipid R2	Lipex 16L	100 ± 2.9	96 ± 1.8	102 ±3.4	84 ± 2.0	80 ± 1.5	82 ± 3.2
	PinLip	120 ± 1.9	106 ± 1.2	75 ± 1.2	77 ± 1.2	79 ± 2.2	81 ± 1.4
	No enzyme	83 ± 2.5	79 ± 1.6	78 ± 1.6	79 ± 1.2	77 ± 1.1	84 ± 1.8
Rhamnolipid 4R2	Lipex 16L		124 ± 2.9	122 ± 2.2	131 ± 3.4	131 ± 2.2	136 ± 2.6
	PinLip		123 ± 1.3	116 ± 4.2	124 ± 2.5	125 ± 6.1	111 ± 7.5
	No enzyme		88 ± 3.4	91 ± 0.7	103 ± 5.8	120 ± 7.8	123 ± 1.9
Rhamnolipid R1	Lipex 16L		106 ± 6.5	117 ± 5.2	117 ± 5.1	86 ± 5.0	87 ± 2.7
	PinLip		124 ± 3.4	130 ± 1.4	132 ± 1.4	137 ± 1.9	127 ± 1.2
	No enzyme		97 ± 1.6	91 ± 5.2	90 ± 4.2	86 ± 0.5	87 ± 3.1
MEL B	Lipex 16L		100 ± 2.1	105 ± 3.7	107 ± 4.7	112 ± 5.5	116 ± 1.8
	PinLip		116 ± 4.2	119 ± 3.4	118 ± 1.8	119 ± 2.0	123 ± 4.4
	No enzyme		77 ± 3.1	82 ± 2.5	82 ± 2.4	87 ± 3.3	104 ± 2.2
1614 MEL	Lipex 16L		104 ± 0.8	109 ± 2.2	115 ±3.4	120 ± 4.5	104 ± 2.1
	PinLip		119 ± 4.9	121 ± 4.2	124 ± 2.5	129 ± 3.2	126 ± 2.7
	No enzyme		83 ± 6.9	94 ± 0.7	103 ± 5.8	112 ± 1.6	90 ± 1.6

5.4 Discussion

In the last years, there has been a constant demand for novel enzymes for industrial applications. The use of enzymes as industrial catalysts is a very promising alternative to conventional synthetic chemistry since enzymes are specific, selective and they display high activities under mild experimental conditions. This research is focused on lipases, which are widely used in several industrial sectors and especially in the laundry industry. The use of enzymes in detergent formulations is now common in developed countries, with over half of all detergents presently available containing enzymes (Chaplin, 2014). Enzymatic cocktails containing lipases, proteases and amylases are added to the detergent formulation in order to remove soil effectively during the washing process. The addition of lipases to detergent is the biggest market for this class of enzyme, detergents are mainly used in (i) household, (ii) industrial laundry applications and (iii) in household dishwashers (Babu et al., 2008). The biological activities of current lipases used in detergent formulations are severely reduced at 20 °C, being impeded by reduced substrate availability due to decreased substrate solubility at lower temperatures and the reduced structural flexibility of the enzyme, especially around the active site which is required for activity (Gouka et al., 2011). Lowering the washing temperature improves energy conservation and reduces wear and tear of the fabrics. These are obvious benefits of using cold-active lipases in the detergent industries (Gerday et al., 2000; Lonhienne et al., 2000).

In this study, a lipase from the psychrophilic bacterium *P. ingrahamii* (PinLip) was identified using BLASTp from the sequenced genome (Altschul et al., 1990). The protein sequence was searched against structurally characterised proteins in the Protein Data Bank (PDB) and showed the highest homology to the lipase from *R. miehei* (PDB: 3TGL) and *T. lanuginosus* (PDB: 1DT3) with a sequence identity of 22% to both of these lipases. The recombinant PinLip enzyme has been successfully cloned and expressed in *E coli.* The PinLip purified protein has been characterised.

PinLip exhibits more than 80% activity at pH 8.5–10 with its maximum activity at pH 9.0, which is similar to that reported in the literature for many other cold-adapted lipases (Ji et al., 2015). The stability of PinLip at alkaline pH suggests its usefulness in laundry detergent applications where the pH of the formulations is

alkaline. The enzyme maintained over 80% activity in the low-temperature range (4-30 °C), thereby suggesting that the enzyme is a cold-active lipase. Substrate specificity analysis showed PinLip to have activity towards short-medium chain length fatty acids (C2-C12 acyl group). This substrate specificity is similar to what has been observed for other cold-adapted lipases, like the M37 lipase from *P. lipolyticum* (Jung et al., 2008), the lipase from *Pseudomonas* sp. strain B11-1 (Choo et al., 1998) and the lipase from *Yersinia enterocolitica* strain K1 (Ji et al., 2015). As for many other lipases, the presence of calcium ions improved activity, which is probably due to a stabilisation effect as reported by Kim and co-worker (Kim et al., 2000). Other divalent ions such as zinc and magnesium produced similar effects while manganese and nickel inhibited lipase activity.

The wash performance studies at low temperature (20 °C) towards two different fat stains showed an SRI increase up to 10 points higher than the commercial benchmark lipase Lipex 16L. The wash performances were also evaluated in combinations with the biosurfactants (rhamnolipids and mannosylerythritol lipid). These results showed a synergic effect with 3 compounds out of 5 (Table 3.2), which are encouraging. It proved that the psychrophilic lipase, PinLip has good application potential in the laundry industry allowing for products with improved wash performance at low temperature. Furthermore, the application of this enzyme to other processes which require lipase activity at low temperature might be the subject of a future investigation.

As a result of this investigation, two patents (Patent no: WO2017036901 and WO2017/036902) has been filed.

Chapter 6: Structural Characterisation of Lipase from *Psychromonas ingrahamii*

6.1 Background

As already discussed in section 1.2.1, in recent years, there has been a growing interest in cold-adapted enzymes, both as models in studies of protein stability and as candidates for biotechnological applications (Georlette et al., 2004). However, the structural characterisation of these type of enzymes is often difficult due to their inherent instability and flexibility at ambient temperatures. A search in the protein data bank (PDB) (Berman et al., 2000), with the keyword “psychrophilic” and “cold-adapted” revealed less than 60 unique structures. It is worth mentioning that many of these structures are closely related to their mesophilic counterparts and only differ by discrete changes that are responsible for their cold adapted properties.

As recently reviewed by Deller and co-workers (Deller et al., 2016) protein stability can be divided into compositional stability and conformational stability. Compositional stability refers to the chemical homogeneity of the protein sample. This parameter can be determined using mass spectrometry or an SDS–PAGE gel. Compositional homogeneity can be altered by post-translational modifications of the protein and its proteolysis which can lead to a non-homogeneous sample which could affect the ability to crystallise the protein.

On the other hand, conformational stability is dependent on the protein conformation, particularly for the crystallisation to be successful a specific conformation needs to be stable enough for a certain period of time to allow the protein molecules to self-organise themselves in a crystal.

However many proteins belong to the group of conformationally disordered proteins, which is common among cold-adapted proteins. In 2003 D’Amico and co-worker used conformational stability data from psychrophilic, mesophilic, and thermophilic amylases to propose an energy landscape for a family of extremophilic enzymes based on the folding funnel model, integrating the main differences in conformational energy, cooperativity of protein unfolding, and temperature dependence of the activity (Fig. 6.1).

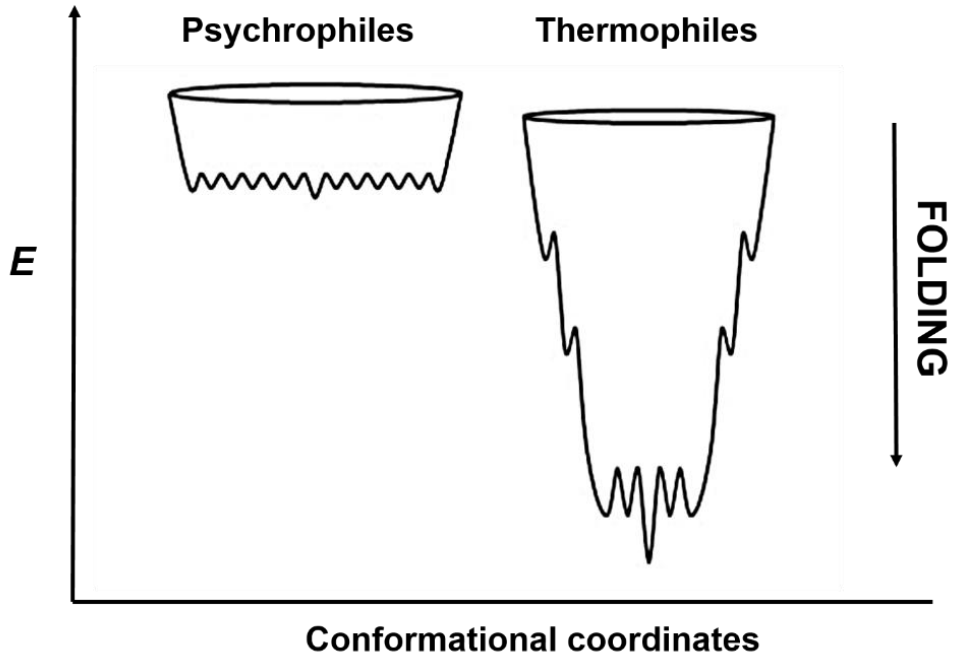

Fig. 6.1: Proposed model of folding funnels for psychrophilic and thermophilic enzymes. In these schematic energy landscapes, the free energy of folding or unfolding (E) is represented as a function of the conformational diversity (D'Amico et al., 2003).

The top of the funnels is occupied by the unfolded state in random coil conformations. The edge of the funnel for the psychrophilic protein is slightly larger (broader distribution of the unfolded state) and is located at a higher energy level (D'Amico et al., 2003). Also, other general characteristics of psychrophilic proteins such as low proline content and a reduced number of disulphide bonds have an impact on the energy level.

When the polypeptide is allowed to fold, the free energy decreases as well as the conformational ensemble. However, thermophilic proteins pass through intermediate states corresponding to local minima which are responsible for the ruggedness of the funnel slopes (Feller, 2013). While the structural elements of psychrophilic proteins generally unfold cooperatively without intermediates, as a result of fewer stabilising interactions and stable domains, and therefore, the funnel slopes are steep and smooth.

The bottom of the funnel represents the stability of the native state. The bottom of the funnel for a stable and rigid thermophilic protein can be depicted as a single global minimum or as having only a few minima with high energy barriers between them (D'Amico et al., 2003). The flexible psychrophilic protein has a large population of conformers with low-energy barriers that allow switching between them. Comparisons between the homology modelled structures of cold-active

enzymes and their mesophilic and thermophilic counterparts have identified some general trends in the structural features of cold-active enzymes: a reduced number of hydrogen bonds, salt bridges, isoleucine clusters and proline residues in loop regions; extended and highly charged surface loops; a low Arg/ (Arg + Lys) content; and an increase in the number of glycine and serine residues close to catalytic sites. All these features are proposed to lead to a higher flexibility of cold-active enzymes (De Maayer et al., 2014).

This conformational flexibility is critical for the activity of psychrophilic enzymes at low temperature however it represents a major challenge for the structural characterisation of these enzymes.

6.1.1 Introduction to protein crystallography

Macromolecular crystallography relies on the availability and quality of single crystals; these are typically obtained through extensive screening, which has a very low intrinsic success rate. Crystallisation is not a completely stochastic process and many proteins do not succumb to crystallisation because of specific features (Derewenda, 2011).

Macromolecular crystallography enables the three-dimensional (3D) structures of large biologically interesting molecules to be determined. This structural information is vital for the determination of their structure-function relationship.

Crystallisation occurs when an aqueous solution of homogeneous macromolecules reaches the solubility limit. Protein crystallisation occurs in two phases; the first phase is the formation of a nucleus, a microscopic cluster of crystal which is the starting point of successful crystallisation. The nucleus can only develop in the supersaturation condition in order to overcome the high energy barrier needed for the nucleation. The second phase is the growth from the nucleus.

The phase diagram describes the state of protein as a function of the crystallisation condition (Fig. 6.2).

There are three saturation zones in the phase diagram, the metastable zone is where crystal formation is possible, but if the supersaturation is too small, the nucleation rate will be so slow that no crystals will form in a reasonable amount of time. In the “labile” or “crystallisation” zone, spontaneous nucleation is

observable with possible formation of disordered structures, such as aggregates or precipitates. The “precipitation zone” is unfavourable for crystal formation, because precipitate will form faster than the crystals (Asherie, 2004).

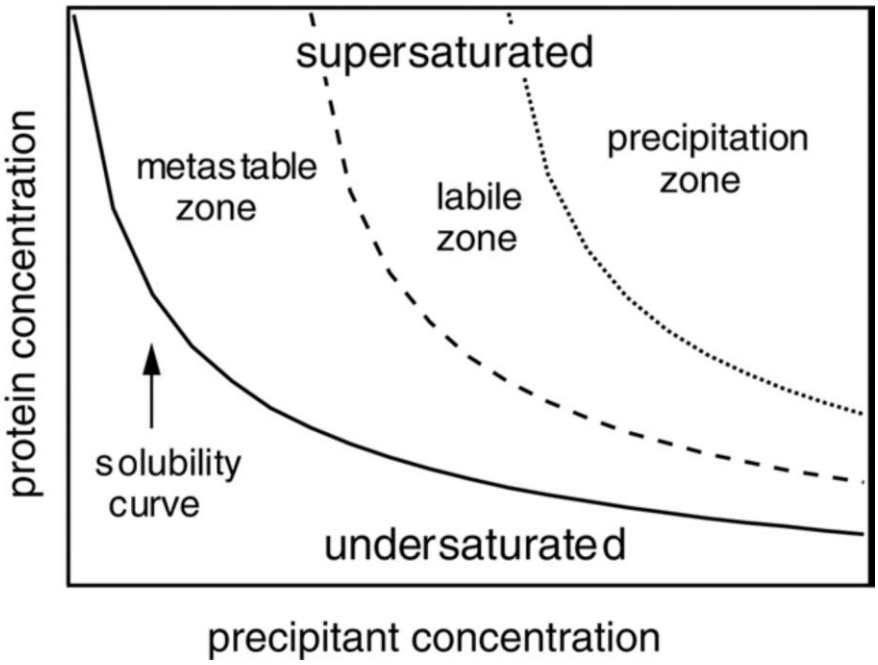

Fig. 6.2: The phase diagram showing the solubility of proteins in solution as a function of the concentration of the precipitant present (Asherie, 2004).

By changing the solution conditions, the crystallographer tries to exceed the solubility limit of the protein to produce crystals.

There are two main methods used to produce protein crystals vapour diffusion and microbatch. In the vapour diffusion method, a droplet containing purified protein, buffer, and precipitant is allowed to equilibrate with a larger reservoir containing similar buffers and precipitants at higher concentrations. Initially, the droplet of protein solution contains comparatively low precipitant and protein concentrations, but as the drop and reservoir equilibrate, the precipitant and protein concentrations increase in the drop allowing crystal formation. Microbatch is the other standard method of protein crystallisation. In this method, a small amount of highly concentrated protein is mixed with precipitant and buffer directly in a small volume drop which is covered by Al’s oil (50:50 mix of silicone and paraffin oils) to control evaporation speed.

Once crystals are obtained, they are normally mounted on a microscopic loop and flash frozen in liquid nitrogen before the X-ray crystallography experiments.

In a single-crystal X-ray diffraction experiment, the loop containing a crystal is mounted on an automated goniometer. The goniometer is used to position the crystal at selected orientations in front of the X-ray source. The X-rays are focused on the crystal in a monochromatic beam producing a diffraction pattern of regularly spaced spots known as reflections. Many thousands of two-dimensional images taken at different orientations are collected and then converted into an electron density map using the Fourier transforms, combined with chemical data known for the sample. This is possible because the X-rays have a comparable wavelength to the interatomic distances in proteins. X-ray crystallography remains the most popular method for investigating the structural properties of macromolecules. However, the overall success rate of canonical crystallisation screening is low, ranging from at best 10–30% for small prokaryotic proteins to only a few percent for a representative range of eukaryotic proteins, including those from the human proteome (Page, 2008).

6.1.2 Introduction to protein NMR spectroscopy

NMR spectroscopy and X-ray crystallography are currently the two major techniques used for the determination of the structures of biological macromolecules like proteins and nucleic acids.

NMR spectroscopy exploits the behaviour of individual atom nuclei when placed in powerful superconducting magnets (180,000 – 360,000 times stronger than the earth's magnetic field). These magnets are used to generate a constant magnetic fields B_0 and a perturbing radio frequency (RF) in order to change moment and angular momentum, of all the atoms with a spin number which is not zero (Fig. 6.3). The transition state change allows the observation of NMR absorption spectra caused by transitions between nuclear spin levels.

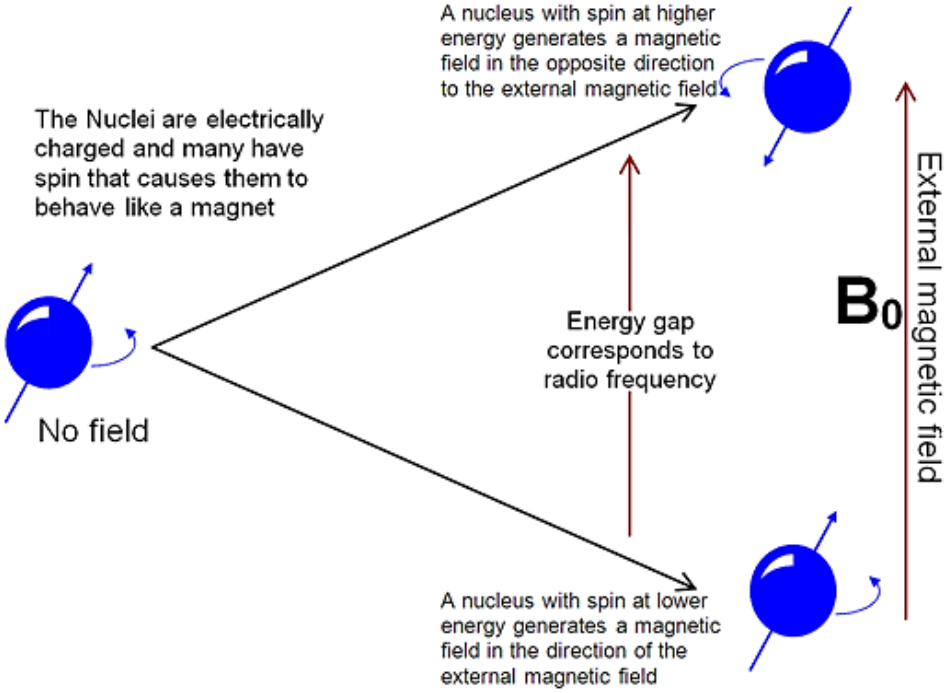

Fig. 6.3: A diagram showing the nuclei behaviour in the magnetic field B_0 with and without the radio frequency pulse. Image taken from Günther, 2013.

Heteronuclei like ^{15}N, ^{13}C and ^{2}H can be incorporated into proteins by isotopic labelling. Spectra from these samples can be drastically improved and more information about the protein structure can be determined by these methods. All of these developments currently allow the structure determination of proteins with a molecular weight of up to 50 kDa (Frueh et al., 2013). NMR spectroscopy is a powerful method for the evaluation of the stability of proteins in solution. The method can be considered complementary to X-ray structure analysis. However, NMR has the advantage to analyse structures in the solution state. NMR can easily distinguish between folded and unfolded proteins, and detect the presence of disordered and unstructured regions, makes it inherently useful as a diagnostic tool for crystallisation experiments (Deller et al., 2016).

6.1.3 Introduction to protein molecular homology modelling

Homology modelling is a powerful method of prediction for three-dimensional structures from amino acid sequences. This approach can be used to obtain structural knowledge of proteins and protein-ligand interactions. In the absence of experimental data, model building on the basis of a known 3D structure of a homologous protein is at present the only available method to obtain the

structural information (Vyas et al., 2012). Homology modelling is based on the assumption that proteins with a sequence identity of greater than 25% share a similar fold. Secondary structure is more conserved than the primary structure and, even proteins with low sequence homology may share a very similar 3D structure following the principle of divergent evolution (Lesk and Chothia, 1986).

The building of a homology model is a multi-step process, the first task to complete is the identification of a template within the PDB database of structurally characterised proteins. A search using the algorithm BLASTP (Altschul et al., 1997; Altschul et al., 1990) against the PDB is the most common method. The ideal template will have high sequence identity (> 50%) and the same biological function of the protein of interest. However, it is possible to generate a valid model with lower homology template with the current limit set around 20% of sequence identity. Models built on templates sharing low sequence identity (<20%) are often of poor quality due to evolutionary divergence between target and template structures, as well as limitations of the modelling and refinement methods (Fiser, 2010). It is not necessary to select a single template. In fact, the optimal use of several templates increases the model accuracy (Fernandez-Fuentes et al., 2007). After identification of the templates single or multiple sequence alignment is performed to be used as input for the model construction. This step is crucial since a misalignment by only one residue position will result in an error of approximately 4 Å in the model (Fiser, 2010).

The model is built based on the 3D structure of the template/s. There are a number of established software pipelines that make these techniques available to the academic community as reviewed by Schwede (Schwede, 2013). Finally, the model needs to be refined and validated. The model refinement consists of an energy minimisation step using molecular mechanics force fields and for further refinement, techniques such as molecular dynamics and Monte Carlo algorithm can be applied.

The validation process is fundamental to remove errors from the model. These errors can be estimated by superposition of the model on the template 3D structure and calculation of the RMSD of Cα atoms and a scoring algorithm server like QMEAN from the SWISS-MODEL workspace (Benkert et al., 2008).

Another fundamental determinant of model quality is the Ramachandran plot which is a way to visualise energetically allowed regions for Cα

backbone dihedral angles ψ against φ of amino acid residues in the protein structure. When the Ramachandran plot quality of the model is comparatively worse than that of the template, then it is likely that an error took place in the Cα backbone modelling (Vyas et al., 2012).

With the number of new sequences increasing at exponential rates, classical methods for the determination of the protein 3D structure cannot keep up with this increase even with the progress towards automation that has been made in recent years. Homology modelling will become increasingly important as a tool to rapidly obtain structural information on a number of proteins whose structures cannot be solved by experimental means due time and cost restraint.

This chapter describes the attempts made to study the structure of the PinLip enzyme with the means of protein crystallography, NMR spectroscopy and molecular modelling.

6.2 Materials and Methods

6.2.1 Crystallisation screening

The PinLip protein was concentrated to ~16 mg/mL using a 10 kDa MWCO spinning concentrator (EMD Millipore). The microbatch crystallisation trials were set up using an Oryx8 crystallisation robot (Douglas Instruments, Hungerford, UK). The conditions tested included the following crystallisation screening kits (Molecular Dimensions, Newmarket, UK): Clear Strategy™, JCSG Screen+™, Morpheus®, Morpheus® II, MultiXtal, Macrosol™, PACT *premier*™, SG1™ Screen, Structure Screen 1, Structure Screen 2, and Stura Footprint Screens.

The droplet size varied from 0.4 to 2 µL and contained a 50:50 or a 25:75 ratio of protein solution to crystallisation screen. After deposition, the droplet was covered with Al's oil (50:50 mix of silicone and paraffin oils) before being stored at 20 or 4 °C. Further variations of this screening protocol included the addition of additives, substrates, inhibitors and micro-seeding.

6.2.1.1 Seed stock preparation

The seed preparations were made using the 'seed-bead' kit from Douglas Instrument, as described by (Luft and DeTitta, 1999). The precipitate obtained from initial screens were placed in 50 µL of their respective reservoir solution and mechanically homogenised. These seeds were stored as 50 µL aliquots and frozen at -80 °C. Automated seeding was performed using an Oryx-8 crystallisation robot (Douglas Instruments).

6.2.2 Circular dichroism

The circular dichroism and NMR studies were carried at Imperial College, London University by Dr Alfonso Simone and Dr Jay Patel.

Protein samples for circular dichroism (CD) were prepared at 50 µM in 50 mM sodium phosphate pH 8.0 plus 50 mM NaCl. The CD spectra were recorded at 20 °C using a CD Chirascan (Applied Photophysics, Leatherhead, UK) in a Hellma 0.2 cm cuvette (Müllheim, Germany). Data were collected in triplicate and averaged.

6.2.3 Expression of isotopically labelled PinLip for NMR experiments

A single colony of *E. coli* BL21 (DE3) cells containing the PinLip plasmid was selected with antibiotic resistance and cultured in 100 mL M9 minimal media (Table 2.1). The culture was grown, shaking at 180 rpm at 37 °C overnight. The following day 20 mL of this pre-culture was used to inoculate 1 L of M9 minimal media, the culture was grown at 37 °C and induced with IPTG at a final concentration of 1 mM when the OD_{600} reached 0.8. Protein expression was carried out at 12 °C overnight. For isotopically labelled cultures 3 g/L ^{13}C labelled glucose (Cambridge Isotope Laboratories, Andover, MA, US), and 0.7 g/L ^{15}N labelled ammonium chloride (CK isotopes, Desford, UK) were used instead of ^{12}C glucose and ^{14}N ammonium chloride. The cells were harvested and purified as for unlabelled preparation (section 2.3).

6.2.4 Protein NMR

All NMR was performed with 10% (v/v) $^{2}H_2O$ for signal lock to deuterium. 5 mm Norrell tubes (Sigma Aldrich) were used as a standard with a sample volume of

500 µL. 5 mm microscale tubes (Shigemi, Allison Park, PA, US) with a minimum sample volume of 300 µL were used where sample volume was limited. All NMR measurements were performed at 4 °C. Activity assays were performed prior to NMR analysis to confirm activity of the enzyme sample. Solution NMR for PinLip was, unless stated otherwise, performed on a triple resonance (^{1}H, ^{15}N, ^{13}C) 5.0 mm probe on an 800 MHz Bruker Avance spectrometer (Billerica, MA, US). All multidimensional spectra were processed using NMRpipe (Delaglio et al., 1995).

1D ^{1}H NMR

1D ^{1}H NMR was performed with a Hahn-Echo pulse sequence (Hahn, 1950), with Shaka excitation sculpting (Hwang and Shaka, 1995) for water suppression. Spectra were acquired with 256 scans.

	^{1}H (F1)
Spectral Width (SW)	16.02
Time Domain	8192
Acquisition time (s)	0.319
Pulse length (ms)	9.65
Acquisition mode	Digital quadrature detection (DQD)

2D ^{15}N-^{1}H TROSY-HSQC

2D ^{15}N-^{1}H trans-verse relaxation-optimised spectroscopy (TROSY) - heteronuclear single-quantum coherence experiments (HSQC) were performed with a 2D [^{15}N-^{1}H] TROSY pulse sequence (Nietlispach, 2005). Spectra were centred at 4.74 and 118.60 ppm in ^{1}H and ^{15}N dimensions and acquired with 48 scans.

	^{1}H (F2)	^{15}N (F1)
SW	13.94	22.00
Offset (ppm)	4.74	118.6
Time Domain	2048	200
Acquisition time (s)	0.09	0.03
Pulse length (ms)	9.95	
Acquisition mode	DQD	Echo-Antiecho

2D ^{13}C-^{13}CON

2D ^{13}C-^{13}CON correlates the carboxylic carbon to the nitrogen atom. The experiments were performed on a 700 MHz Bruker Avance spectrometer equipped with a carbon detector TXI probe (Bruker).

	^{13}C (F2)	^{15}N (F1)
SW	40.07	34.00
Offset (ppm)	173	119
Time Domain	1024	128
Acquisition time (s)	0.06	0.03
Acquisition mode	DQD	States-TPPI

6.2.5 Protein homology modelling

The amino acid sequence of the lipase from *P. ingrahamii* strain 37 (PinLip) was obtained from the NCBI protein sequence database (Accession number: ABM03668.1). The primary sequence of PinLip protein, which was used for modelling, consists of 378 amino acids. Homology modelling was performed using the Iterative Threading ASSEmbly Refinement (I-TASSER) server based on the ab initio/threading method (Zhang, 2008), the Phyre^{2} server (Kelley et al.,

2015) and the SWISS-MODEL workspace (Arnold et al., 2006). Only the I-TASSER results were utilised because they were considered more reliable.

To predict the three-dimensional structure of PinLip, 4L3W (*Rhizopus microspores* Lipase), 3TGL (*Rhizomucor miehei* Lipase), 3NGM (*Gibberella zeae* Lipase) structures were chosen as the templates.

These template structures were selected by multiple threading approach Local Meta-Threading-Server (LOMETS) (Wu and Zhang, 2007) based on sequence similarity to PinLip. A total of five three-dimensional (3D) models were generated by I-TASSER; among them, the best model was identified based on confidence score (C-Score). The C-score is a confidence score for estimating the quality of predicted models by I-TASSER. It is calculated based on the significance of threading template alignments and the convergence parameters of the structure assembly simulations. C-score is typically in the range of [-5,2], where a C-score of higher value signifies a model with a high confidence and vice-versa (https://zhanglab.ccmb.med.umich.edu). The protein structures generated using I-TASSER server were then validated by the SAVES server (http://services.mbi.ucla.edu/SAVES) (Eisenberg et al., 1997; Laskowski et al., 1993). The quality of the structure was determined using QMEAN6 program of the SWISS-MODEL workspace (Arnold et al., 2006). The energy levels were minimised with the YASARA force fields (Krieger et al., 2009), and evaluated again by the same software. Finally, the modelled structures were visualised using the software CHIMERA UCSF (Pettersen et al., 2004) and YASARA view (Krieger et al., 2009).

6.3 Results

6.3.1 Protein crystallography

Crystallisation trials were performed as described above. Several variables were tested including PinLip concentration, gel filtration buffers, incubation temperature and ligands. Despite a large number of conditions tested so far only some ordered precipitates have been obtained (Fig 6.4) which were used for micro-seeding (section 6.2.1.1) (D'Arcy et al., 2007).

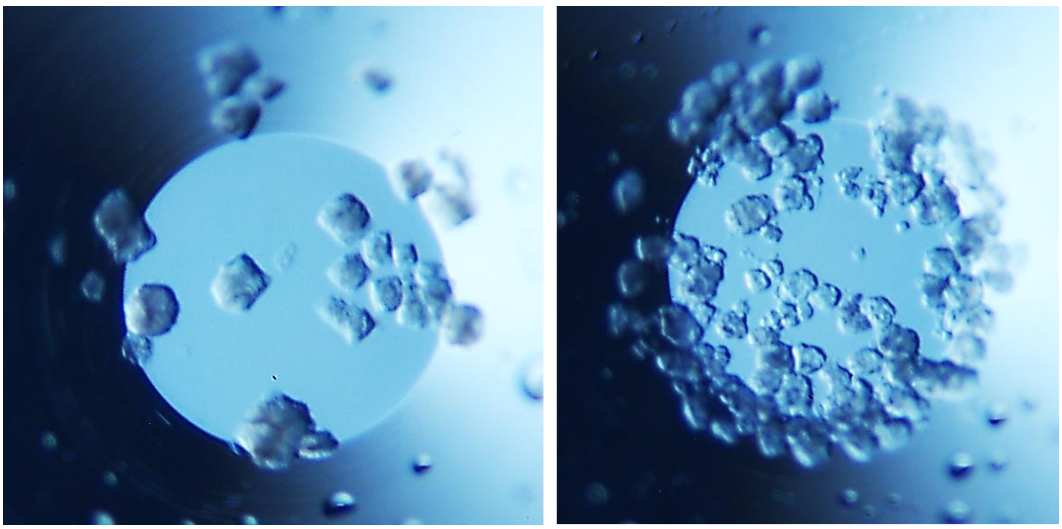

Fig. 6.4: Examples of ordered precipitates obtained during PinLip crystallisation trials which have been used for micro-seeding experiments.

To date, no protein crystal of PinLip have been produced and crystallisation trials are still going on.

6.3.2 Protein NMR

Circular dichroism spectroscopy (CD) and NMR studies were conducted in collaboration with the group of Dr Alfonso De Simone at the Imperial College (London, UK).

Initially, one-dimensional NMR spectra were produced to assess the protein conformational status. A good discrimination in the backbone amide region below 8.3 ppm., as well as peaks at around 1 ppm. are indicative of folded protein (Rehm et al., 2002). The PinLip 1D NMR spectra are shown in Fig 6.5.

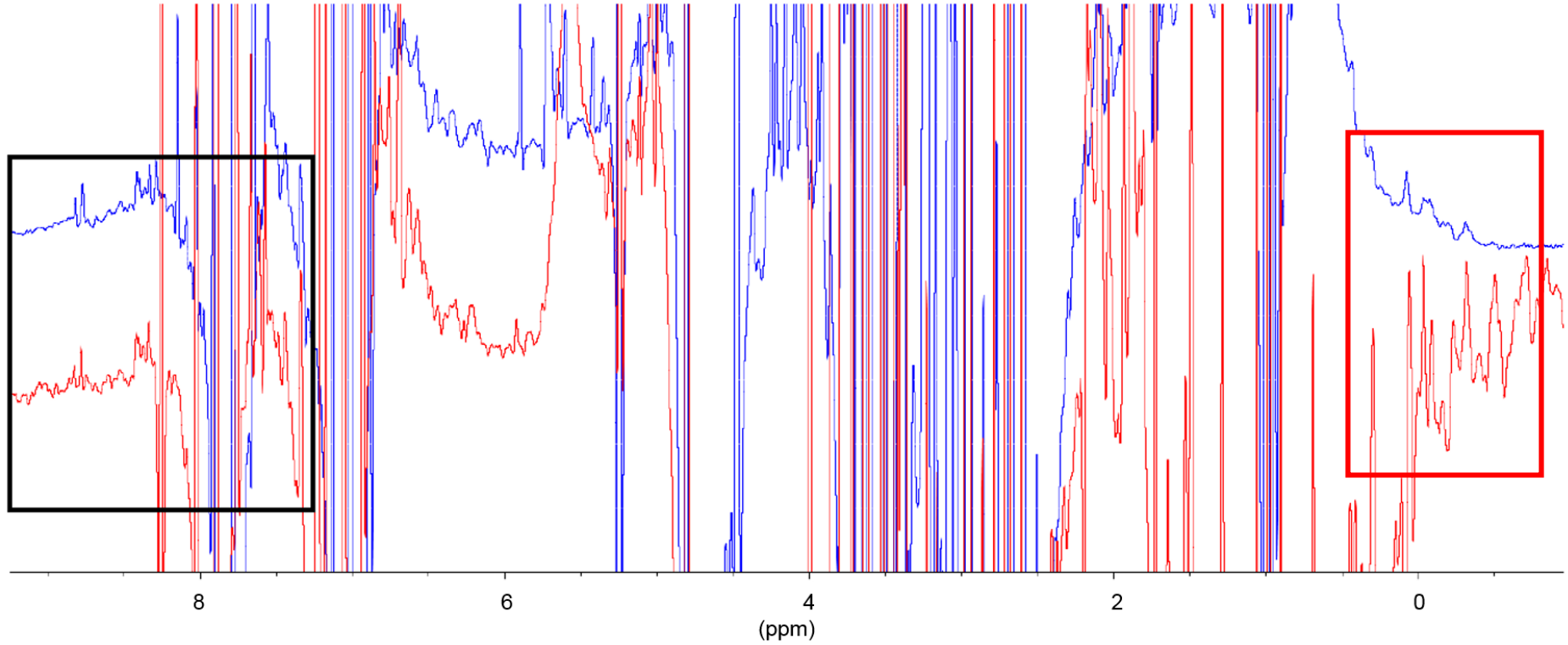

Fig 6.5: 1D ^{1}H NMR spectra of PinLip in presence and absence of 0.02% PMSF (blue: PinLip; red PinLip + PMSF) limited dispersion of peak in the amide region is indicated by the black box, folded methyl peaks are indicated by the red box.

The 1D ^{1}H NMR analysis shows that a limited dispersion in the amide region (^{1}H ppm = 7 –10 ppm) combined with folded methyl peaks found below 0 ppm indicates a protein with low levels of folded structure. Slight improvement in the amide region of the spectrum of PinLip is observed with the addition of PMSF at 0.02% (red trace). There are also changes detected at 0 ppm. This could be due to PinLip being stabilised or locked into a conformation upon binding of serine protease inhibitor PMSF to the active site serine of the lipase enzyme.

These initial findings were confirmed by circular dichroism spectroscopy (Fig. 6.6).

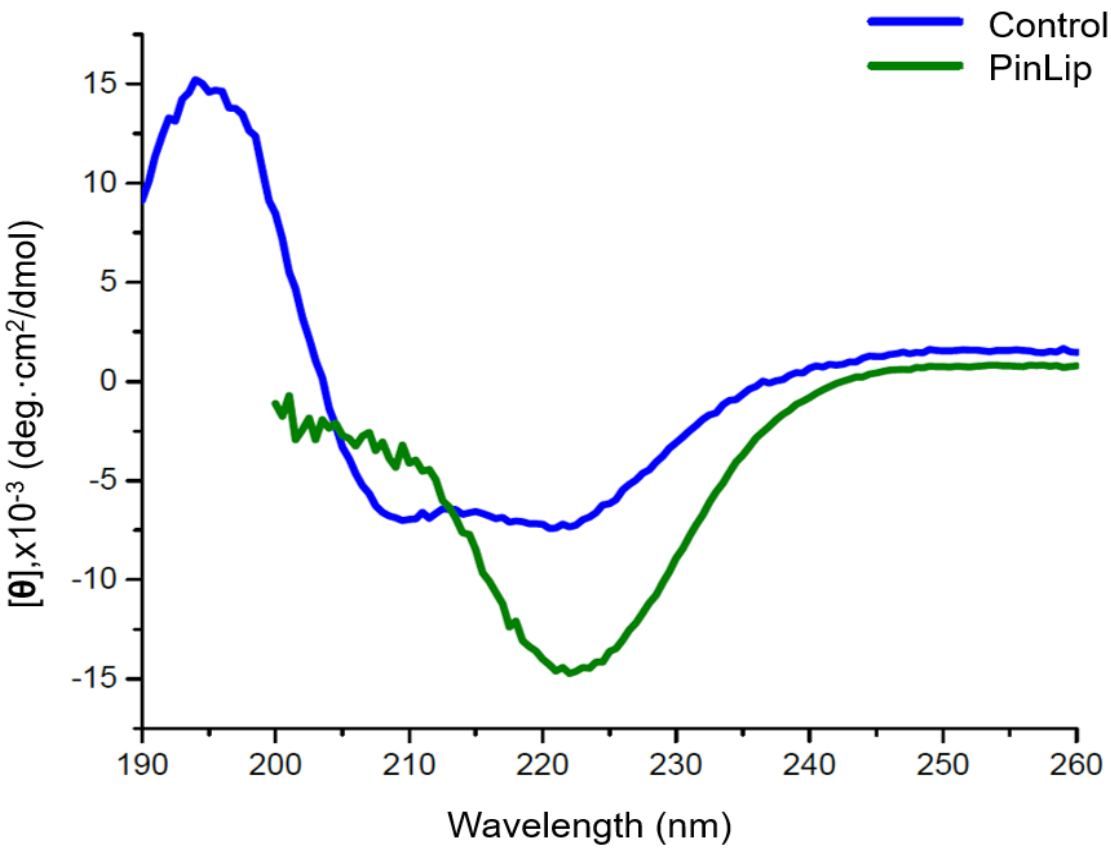

Fig.6.6: The CD spectra of PinLip (green) and *T. lanuginosus* lipase as a control (blue) recorded at 20 °C.

In Fig 6.6, the control exhibits an exemplary α-helical profile with the two minima at 208 and 222 nm, indicating the α-helical structure.

The CD spectrum for PinLip is not comparable to the *T. lanuginosus* lipase control. It begins to follow the profile of a α-helical with a minimum at 225 nm but

rises to 0. This spectrum behaviour does not agree with the spectrum of a folded secondary structure suggesting an unfolded state.

However, it is worth mentioning that the activity assay was performed before and after those experiments confirming the PinLip lipase was active. The NMR study which shows a spectrum characteristic of an unfolded protein for PinLip when the enzyme still shows activity could be explained by the PinLip being in a molten globule state. In 2002 Vassilenko and Uversky (Vassilenko and Uversky, 2000) reported the CD spectra of several proteins in their native and induced molten globule state (Fig.6.7). The molten globule is an equilibrium state of a protein molecule, which is intermediate between the folded and unfolded states. The molten globule can be induced in mildly denaturing conditions. A visual examination of the CD spectra reported in Fig 6.7 reveals that the spectra of molten globule show that the two minima 208 and 222 nm are less pronounced than in the folded protein due to reduced secondary structure.

A comparison of the spectra shown in Fig. 6.7. with the spectrum obtained for PinLip in Fig 6.6 show a similar trend.The PinLip spectrum is similar to the denatured spectra E and F which belong to the retinol binding protein and carbonic anhydrase B respectively.

The 2D ^{15}N-^{1}H HSCQ (Fig 6.5) is a useful ‘fingerprint’ of protein NMR analysis since it allows a greater level of detailed information and resolution compared to the 1D ^{1}H spectra, since the amide region is separated out in a second dimension (^{15}N). A good quality spectrum should show well dispersed and resolved peaks. Each peak corresponds to the amide group on each amino acid residue and all non-proline residues should be detected.

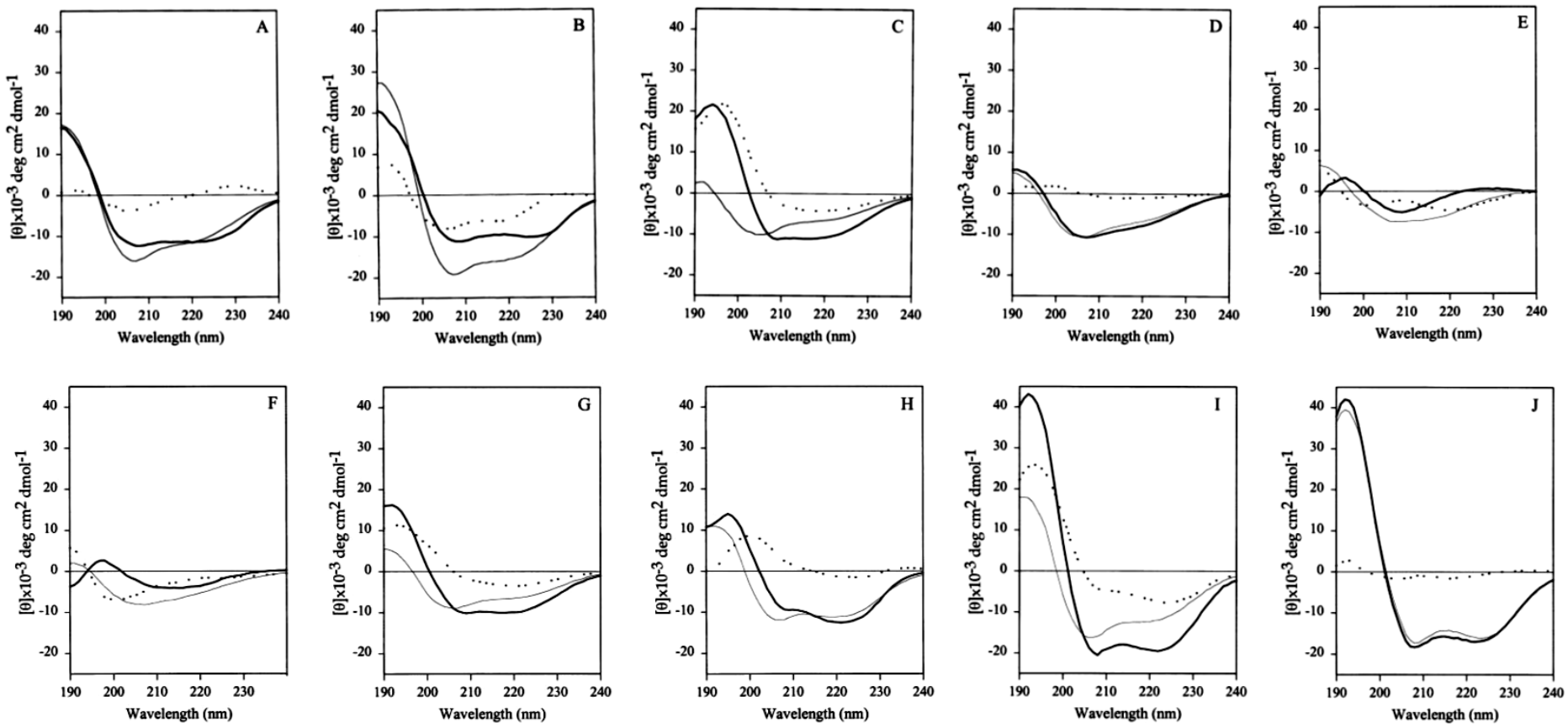

Fig 6.7: Far-UV CD spectra of nine proteins in the native and the pH-induced molten globule states. Bold curves show native proteins, thin curves are molten globules, dotted curves indicate the di¡erence between the spectra of the native protein and the molten globule: (A) K-lactalbumin (bovine); (B) K-lactalbumin (human); (C) L-lactamase; (D) ribonuclease A; (E) retinol-binding protein, apo-form;(F) carbonic anhydrase B; (G) phosphoglycerate kinase; (H) cytochrome c; (I) apomyoglobin; (J) leptin. Image taken from Vassilenko and Uversky, 2002.

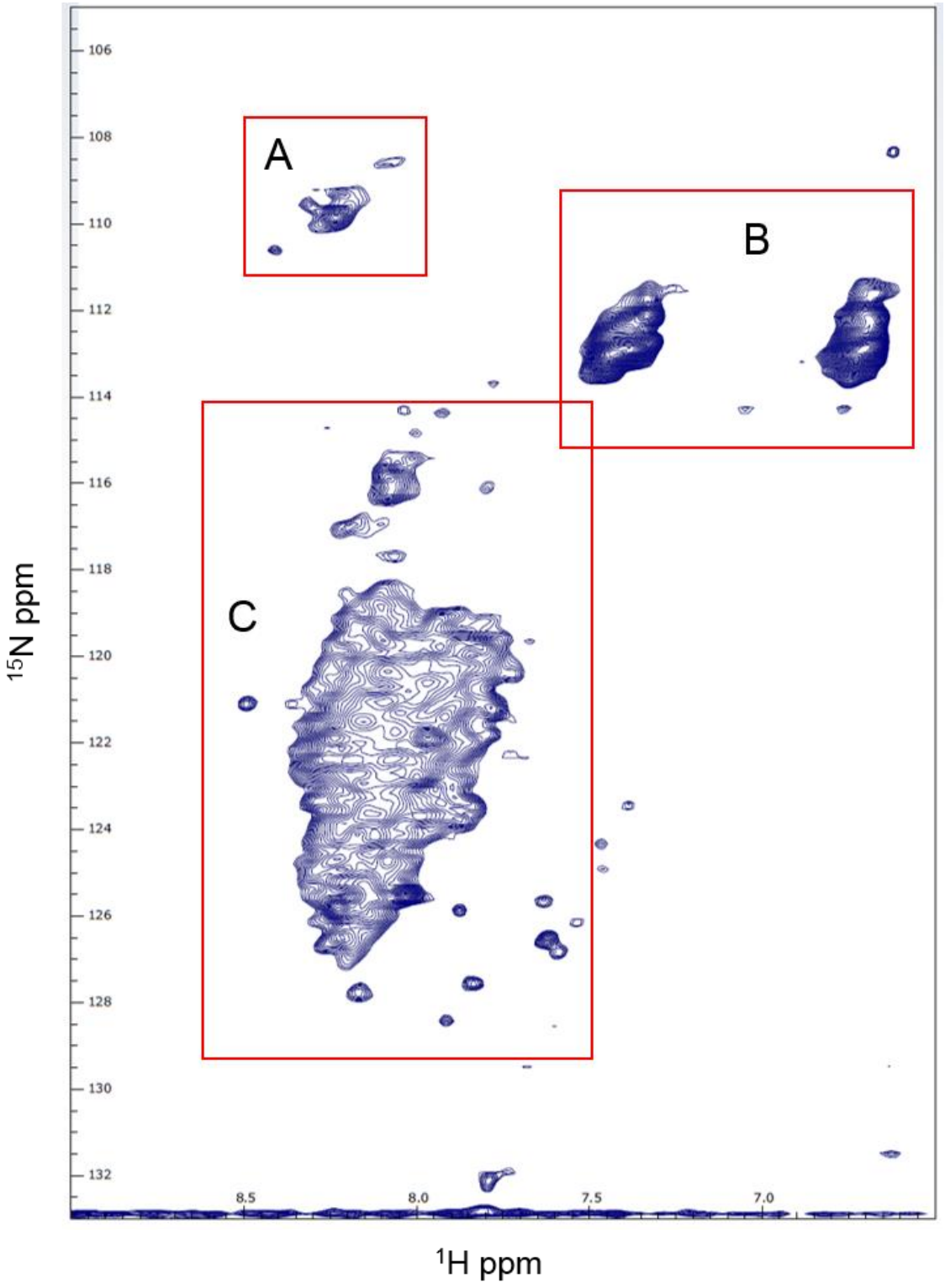

Fig 6.8: Two-dimensional ^{1}H–^{15}N HSQC NMR spectrum of PinLip, showing wide and unresolved peaks for the disordered protein sample. Three main area have been identified A) Glycine residue region, B) Side chain resonances, C) Unresolved overlapping peak.

From the result shown in Fig. 6.8 the protein remains to appear unfolded by ^{15}N-HSQC. Double ^{13}C ^{15}N labelled PinLip was used to try to obtain better NMR spectrum (Fig. 6.9).

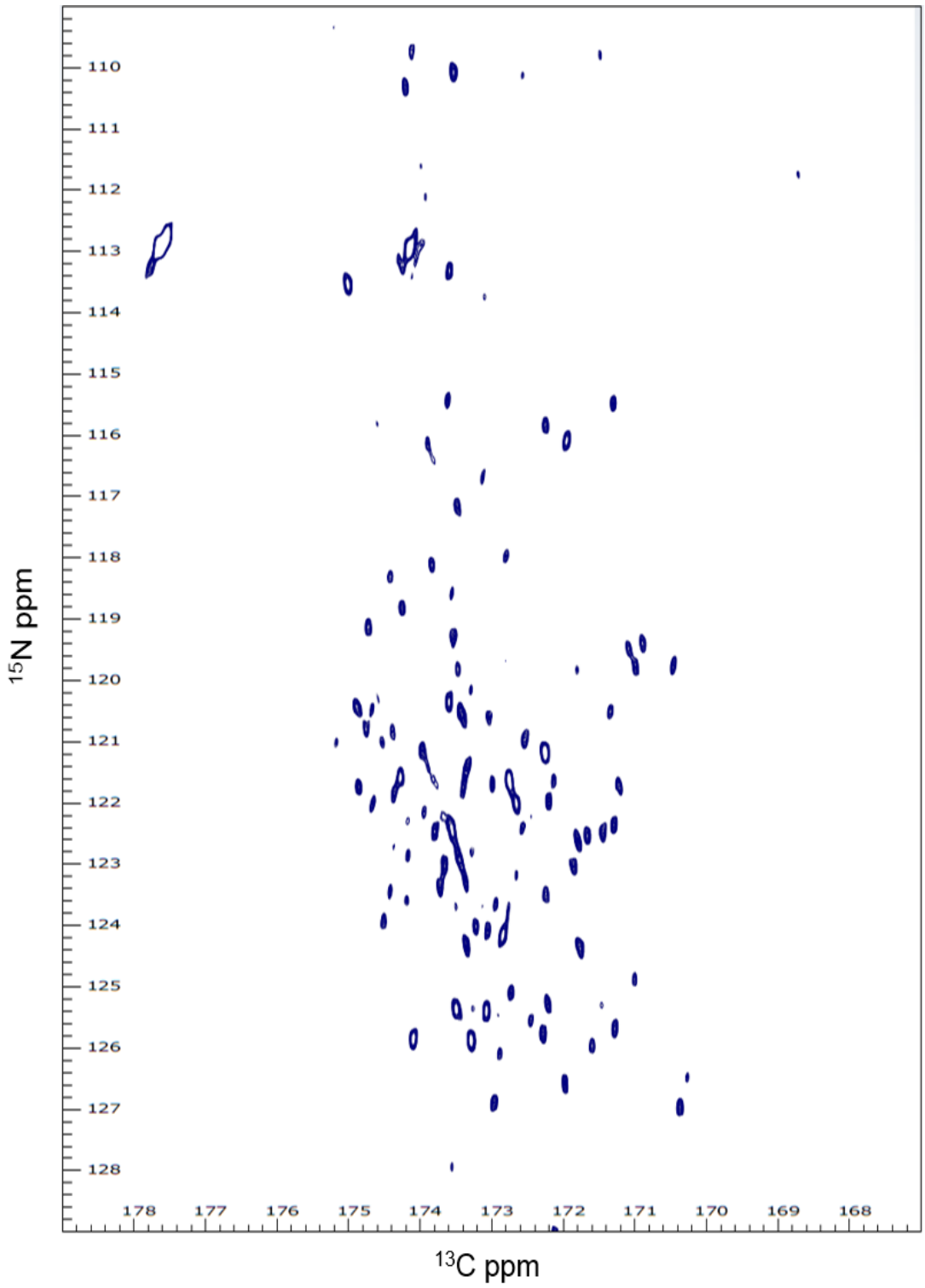

Fig. 6.9: PinLip C-CON NMR spectrum showing ~120 discrete peaks out of 378 residues. Each peak corresponds to the correlation of a NH to the CO of the previous residue.

Carbon-Carboxylic Carbon Nitrogen correlation (C-CON) correlates CO to the N atom, signal detection is significantly improved when using a ^{13}C detection probe. This may offer an alternative route to studying the protein, but conditions need to be optimised to obtain better quality spectra. Fig. 6.9 shows ~120 peaks out of 378 residues meaning still a significant portion of the protein is not visible. Current

efforts are aimed at improving the spectrum by adding stabilising compounds that will reduce the level of conformational flexibility. Peak detection will need to be improved up to >70% of total residues for backbone assignment.

6.3.3 Molecular modelling

To date, no 3D structure is available for PinLip, crystallisation trials and NMR studies are still in progress. The generation of a homology model would be useful for structural/functional analysis of this enzyme.

As described in section 6.2.4, three different types of web-based homology software were used for the generation of the PinLip model. I-TASSER (Zhang, 2008), Phyre^2 (Kelley et al., 2015) and SWISS-MODEL (Arnold et al., 2006). Only the I-TASSER results are reported as the resulting model appeared the most accurate. The templates were identified searching for homologous proteins in the PDB. 3NGM (*Gibberella zeae* Lipase) 3TGL (*R. miehei* Lipase) and 4L3W (*R. microspores* Lipase), structures were chosen as the templates. Multiple sequence alignment was performed with these template proteins by the treading algorithm LOMETS (Wu and Zhang, 2007), to identify sequence alignments of structural motifs. The alignment results revealed and an overall low sequence conservation of PinLip with the other lipase structures (Table 6.1) with only a few motifs highly conserved.

Table 6.1: The top 10 threading templates used by I-TASSER. Identity 1 is the percentage sequence identity of the templates in the threading aligned region with the query sequence. Identity 2 is the percentage sequence identity of the whole template chains with the query sequence. Norm. Z-score is the normalised Z-score of the threading alignments. Alignment with a Normalised Z-score >1 mean a good alignment and *vice versa*.

Rank	PDB hit	Identity 1 (%)	Identity 2 (%)	Coverage	Norm. Z-score
1	3NGM	21	20	0.77	1.43
2	3NGM	21	20	0.73	2.17
3	3NGM	20	20	0.74	1.64
4	3TGL	24	21	0.67	3.64
5	3NGM	21	20	0.73	2.55
6	3NGM	19	20	0.75	2.11
7	4L3W	24	20	0.67	3.04
8	3NGM	23	20	0.72	2.38
9	3NGM	22	20	0.73	1.46
10	3NGM	0	20	0.74	2.31

A total of five three-dimensional (3D) models were generated by I-TASSER; among them, the best model was selected based on its C-Score value. Out of the five predicted models, the most accurate structure had a maximum C-score (-1.72) and 10.7 ± 4.6 Å RMSD. The quality of the predicted structures was analysed by SAVes server (Procheck, Verify-3D (Laskowski et al., 1993; Eisenberg et al., 1997). The validation of the results also included the evaluation of the Psi/Phi Ramachandran plots.

The best model selected by the I-TASSER server as judged by the C-score value resulted in being the one with the overall higher quality. The Psi/Phi Ramachandran plots (Lovell et al., 2003) (Fig.6.10) calculated with RAMPAGE (Lovell et al., 2003) showed that 84.3% of the residues were present in the most favoured regions; 8.8 % in the additionally allowed regions and 6.9% in the outlier region. The analysis of the residues in the outlier region showed that 15 residues out of 25 were found in loop regions of the protein (Fig 6.13). The catalytic serine was found in the outlier regions of the Ramachandran plot as has been observed in other α/β hydrolase enzymes due the constrained position of this residue required for its catalytic activity (Derewenda et al., 1992; Noble et al., 1993 Nardini et al., 2000).

Overall these results indicate a poor model, however considering the low identity of the templates sequence it was an expected result. Furthermore, the inherent disorder of a psychrophilic protein can be another cause of error in the modelling process. For the final 3D model, the best evaluation of the model was based on the highly conserved region of the active site and lipase lid.

The final 3D model is shown in Fig. 6.11.

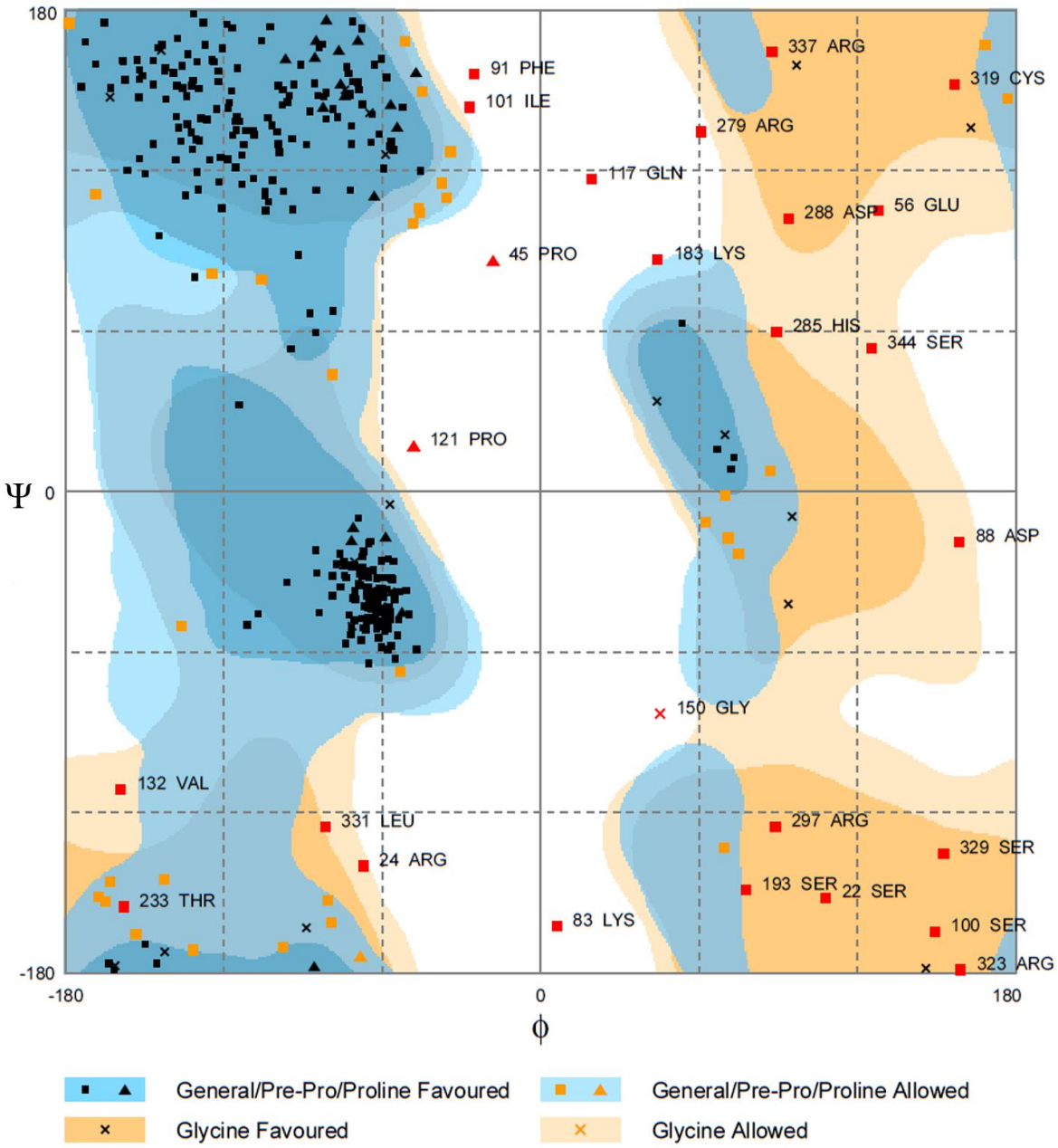

Fig. 6.10: The Ramachandran plot of the PinLip 3D model, 84.3% of the residues were present in the most favoured regions; 8.8 % in the additionally allowed regions and 6.9% in the outlier region. Outlier residues appear as red squares or triangle (proline) with labels. Image produced with the server RAMPAGE (Lovell et al., 2003).

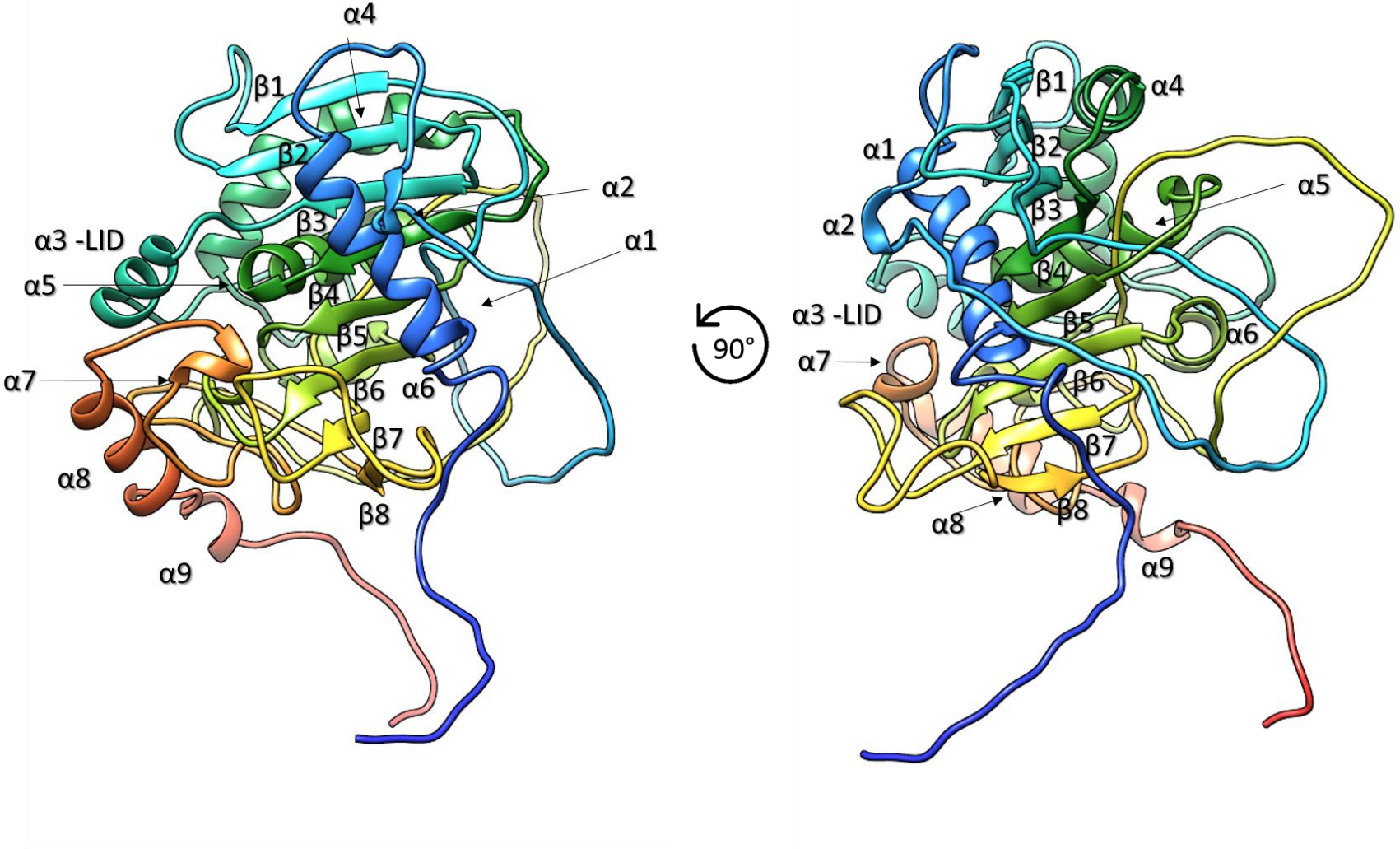

Fig. 6.11: The 3D model structure of PinLip lipase is represented in rainbow ribbon format from N-terminal (blue) to C-terminal (red) α-helices and β strands are labelled as α1–α9 and β1–β8, respectively. (Left) Side view of PinLip. (Right) View rotated 90° with respect to the left image. Image produced with UCSF Chimera (Pettersen et al., 2004).

The overall α/β fold is retained however the loop regions are not so well modelled. The secondary structure composition of the PinLip 3D model is represented by 39.4% α-helices, 35.9% loop regions and 24.5% β strands. A search for structural analogues with the DALI server identified the best match with extracellular lipase from *G. zeae* (PDB: 3NGM). Superposition of the PinLip model with *G. zeae* lipase shows the best aligned 151 residues having an RMSD of only 0.879 and all residues RMSD of 6.781. Furthermore, a structure-based sequence alignment of the PinLip model to the templates 3TGL (*R. miehei* Lipase), 3NGM (*G. zeae* Lipase) show that the most similar regions are limited to the central 180 amino acids of the sequence including the identical GXSXG motif and the Asp residue at the position preceding the catalytic histidine (Fig. 6.12).

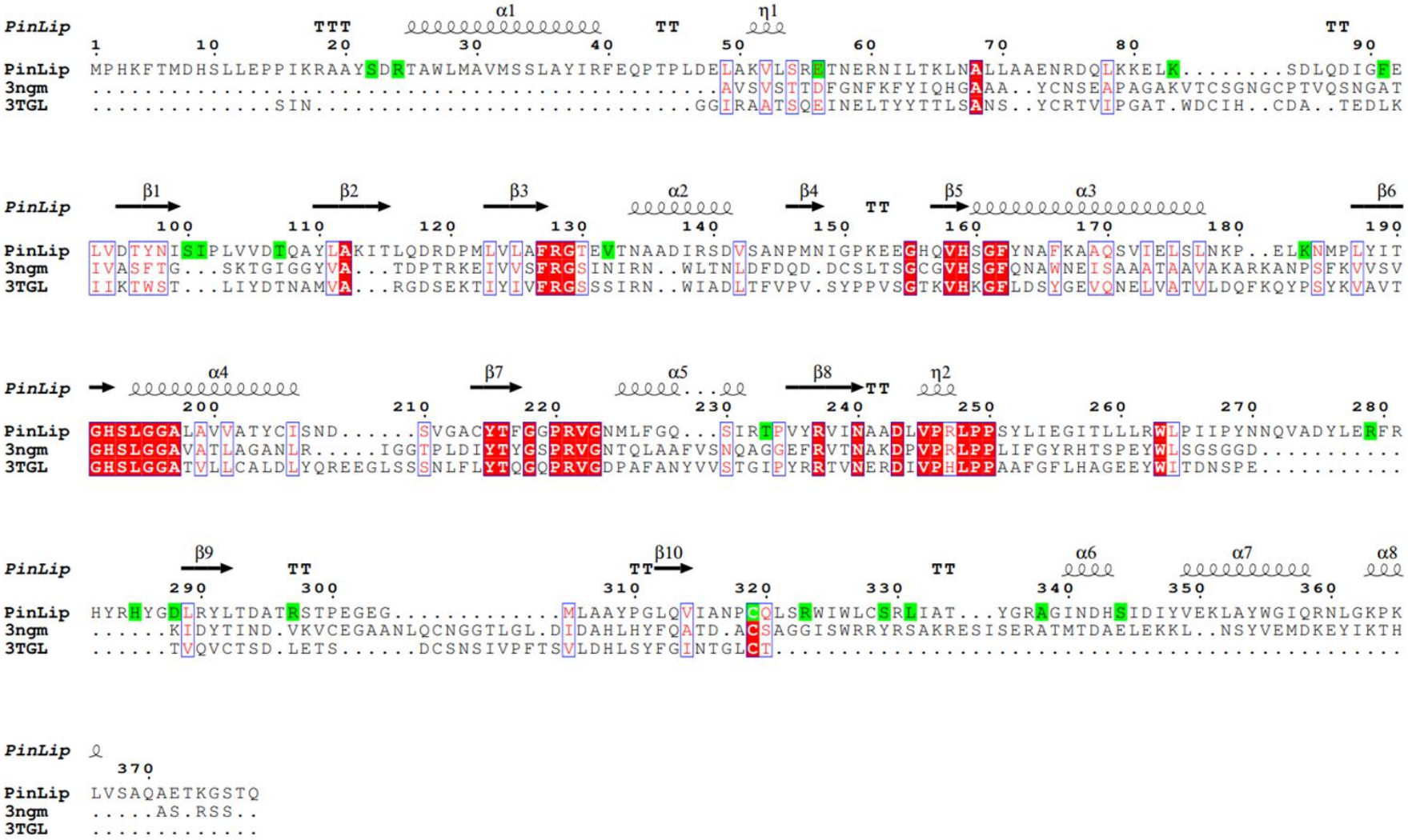

Fig 6.12: A representation of the alignment of the PinLip model with the PDB entries 3TGL and 3NGM. The secondary structure elements are presented on top of the sequence (helices with squiggles, β-strands with arrows and turns with TT letters, unmarked regions are loops) . The red boxes highlight sequence identity and light blue boxes similarity. The residue in yellow are indentified as outliers by the Ramachandran plot (Fig 6.10). The figure was produced using the program ENDScript 2.0 (Robert and Gouet, 2014).

6.3.3.1 Active site

The active site is located below α-helix α3 which constitutes the Lid domain. The conserved catalytic triad is composed of Ser193, Asp 243 and His 343. The catalytic serine is in a strained conformation and is located in a tight nucleophilic elbow at the end of strand β4 with the conserved lipase sequence Gly-His-Ser-Leu-Gly.

The catalytic triad was identified experimentally. As reported in section 5.3.1 the sequence homology between PinLip and the most closely related lipase structures was good enough for the identification of the catalytic serine and aspartic acid but too low for the identification of the histidine.

Three mutants were generated using site-directed mutagenesis (section 2.2.6.3) H282N, H285N and H343N. The three mutant enzymes were over-expressed and purified as described for the wild-type PinLip (section 5.2.3.2) and the lipase activity was evaluated. Out of the three mutants, only H343N showed loss of activity confirming the histidine 343 as the catalytic residue (Fig 6.13).

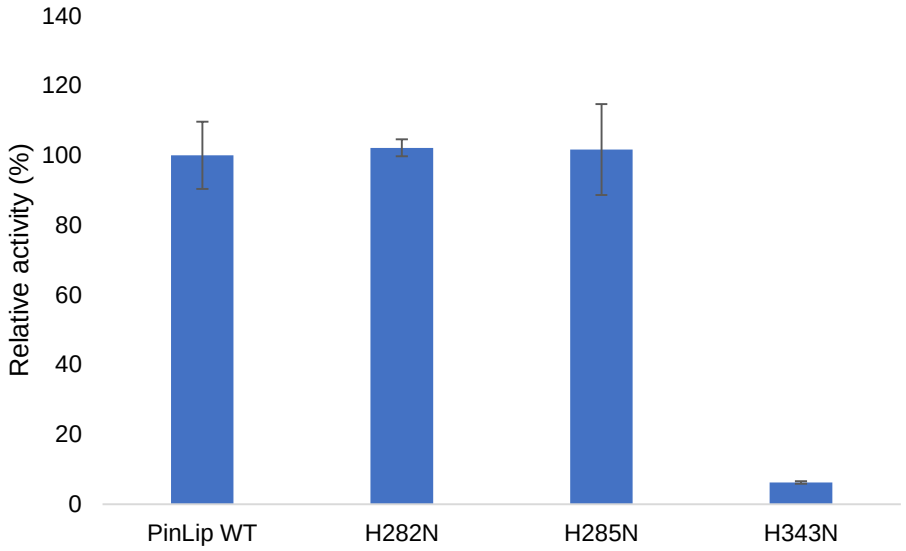

Fig 6.13: Activity towards pNP-laurate for the PinLip wild-type and the 3 mutant PinLip enzymes. The lipase activity assay was performed at 20 °C, pH 8.5. Activity of the wild-type enzyme was taken as 100%. The error bars display the standard deviation between three replicates.

This experimental data agrees with the 3D homology model generated for PinLip where the three catalytic residues are positioned in an arrangement ideal for catalytic activity (Fig. 6.14).

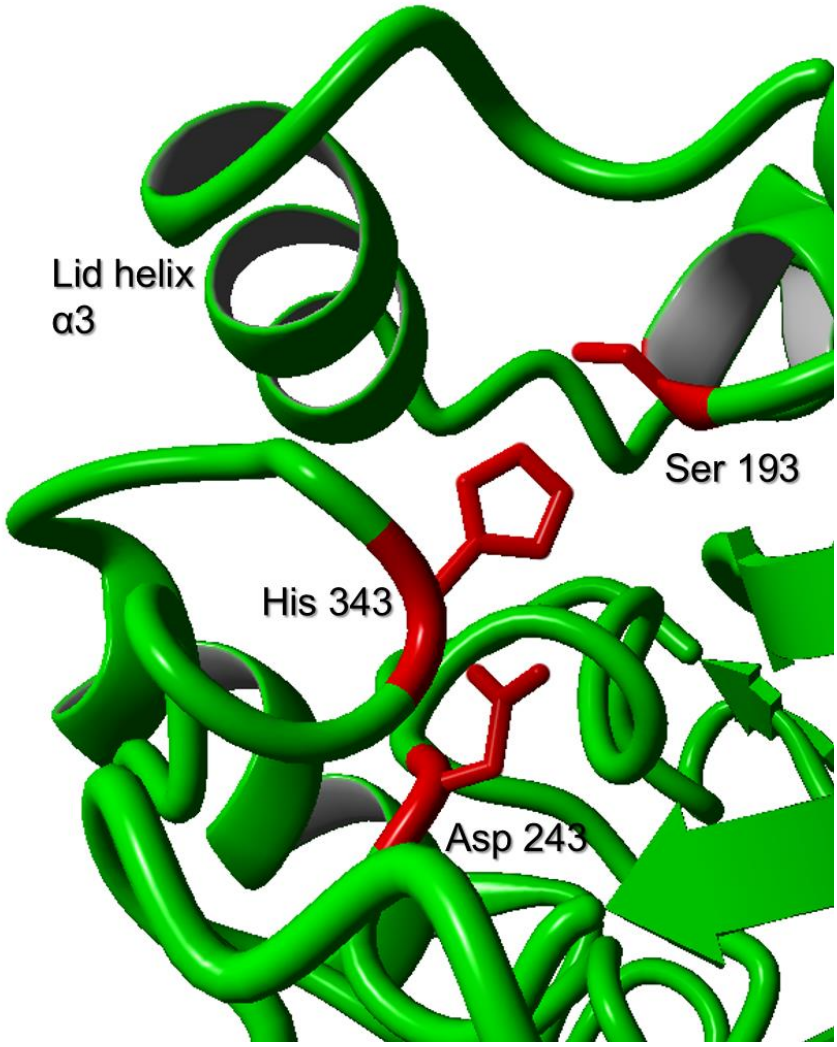

Fig. 6.14: The active site of PinLip as shown in the 3D model. The protein backbone is shown as a green ribbon with the catalytic triad residues shown in red. The image was produced with the program YASARA (Krieger et al., 2009).

The catalytic pocket is represented with the His343 properly positioned. The interatomic distances were checked in order to confirm the presence of stabilising hydrogens bonds. The His343 N^{ε} atom could form a hydrogen bond with the O^{γ} atom of Ser193 (2.7 Å), and the His343 N^{δ} atom could form hydrogen bonds to Asp243 (3.5 Å to $O^{\delta 1}$ and 2.7 Å to $O^{\delta 2}$).

This conformation of residues is typical of other enzymes that cleave ester bonds using this catalytic triad.

Ligand docking was attempted using the SWISS-DOCK server with ligands such butyric acid and valeric acid, however, the model has the lid helix in the closed conformation which prevented any molecules to be docked in the active site.

However, the ligand-binding site prediction meta-server COACH (Part of I-TASSER) generated five predictions for the active site pocket. All the five hits identified by the COACH meta server (Table 6.2) are based on lipase and esterase structures, also many of the suggested ligand binding residues sit in the catalytic pocket predicted by the model (Fig. 6.15).

Table 6.2: Ligand-binding site prediction meta-server COACH summary results table.

Rank	C-score	Cluster Size	Template	PDB number	Ligand name	Consensus Binding Residues
1	0.25	20	*T. lanuginosus* Lipase mutant S146A	1GT6A	Oleic acid	129; 130; 193; 194; 244; 245; 248; 340 ;343
2	0.07	5	*T. lanuginosus* Lipase	4GI1A	16-hydroxy-palmitic acid	109: 110; 111; 128; 130; 131; 138; 141; 142; 143; 159; 194; 198
3	0.04	4	*A. niger* Feruloyl esterase	2HL6A	CAPS	130; 131; 132; 133; 134; 135; 136; 193; 343; 344; 345
4	0.04	3	*T. lanuginosus* Lipase	4GHWB	Capric acid	141; 143; 159
5	0.04	3	*T. lanuginosus* Lipase	4KJXA	Lauric acid	109; 110; 111; 128; 129; 130; 131; 132; 134; 135; 194; 198

The best result was based on the *T. lanuginosus* lipase mutant S146A. This was used for prediction of the active site with the modelled oleic acid molecule as shown in Fig. 6.15. The lower ranking hits were excluded due to their very low C-score.

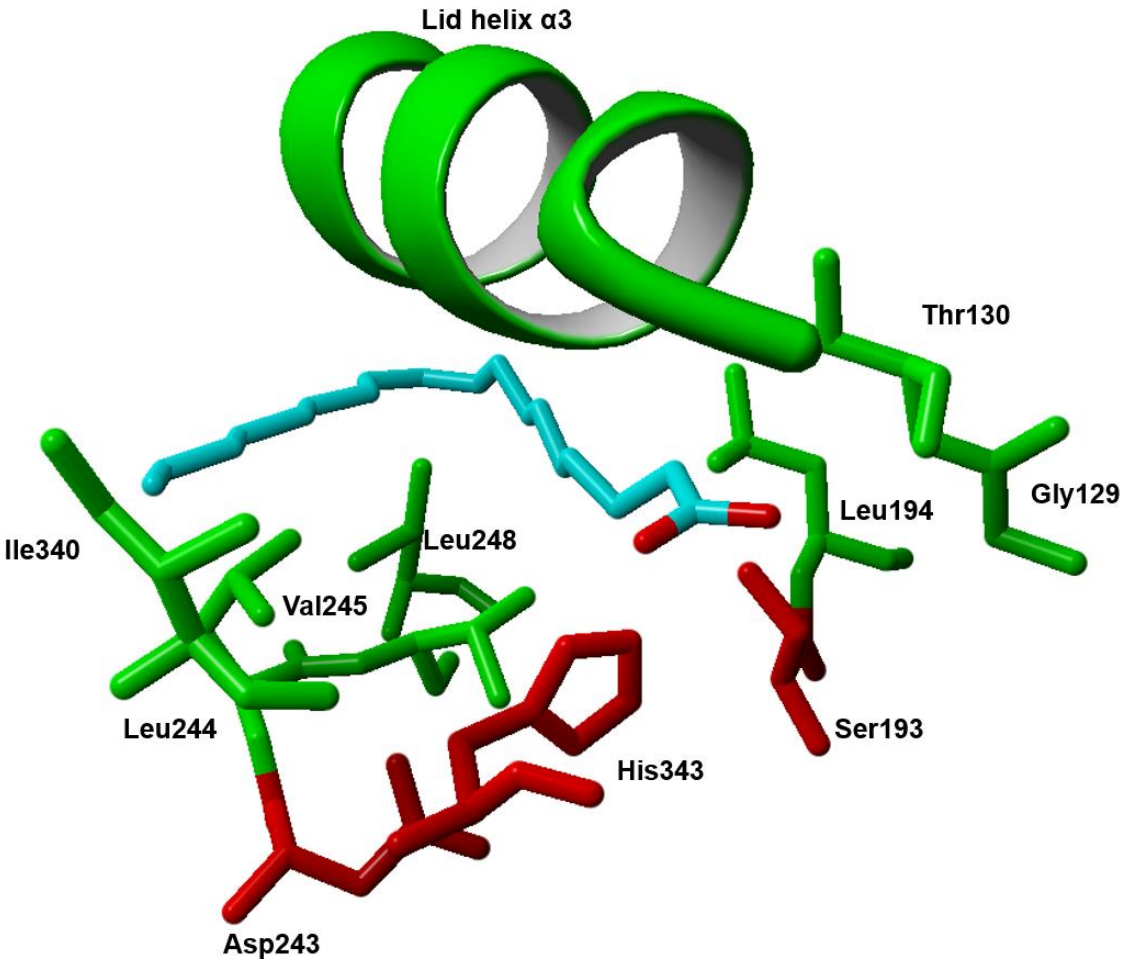

Fig. 6.15: The active site of PinLip with a molecule of oleic acid positioned in the active site. The catalytic triad residues are shown in red. The other residues involved in substrate stabilisation are shown in green. The secondary structure and the residues which are not predicted to directly interact with the substrate have been hidden for clarity. The image was produced using the program YASARA (Krieger et al., 2009).

This substrate binding cavity is 11 Å in width and, 15 Å in height. The bound oleic acid is trapped deeply within the binding groove with its carboxylic group lying near Ser193 (1.6 Å) and His343 (1.9 Å). The same active site structure can be observed in the templates 3NGM and 1GT6.

6.4 Discussion

In this chapter, the structural characterisation of PinLip has been attempted using several approaches.

It was not possible to obtain diffraction quality crystals suitable for X-ray structural determination despite the many conditions tested. It was however possible to obtain some ordered precipitates which could be further optimised if more time had been available. Both the CD and NMR spectroscopy results have shown that PinLip is at least partially unfolded, which is known to be detrimental to crystal formation (Derewenda, 2011; Deller et al., 2016).

The 1D ^{1}H NMR spectra showed a protein with elements of folded structure, as evidenced by the detection of down-shifted methyl peaks below 0 ppm (Fig. 6.5). These are peaks from methyl groups in the core of a folded protein shielded from the external solution conditions and therefore have a downfield chemical shift to surface methyl groups (normally found ~ 3 ppm in the ^{1}H dimension).

The ^{15}N-^{1}H HSQC for PinLip is very broad with overlapping peaks and only a few peaks are isolated with good resolution and dispersion. The broad spectrum indicates an unfolded protein or one with limited structure where the overlapping peaks are due to the residues experiencing the same local chemical environment, and therefore, having similar chemical shift values. Combined with the 1D ^{1}H NMR spectrum and CD data (Fig. 6.3), it appears that PinLip is in a molten globule state, exhibiting some structure but high levels of conformational flexibility and random coil.

PinLip may be in a molten globule state since the protein was found to be active even after the partial unfolding was confirmed and there are reports of active molten globule in the literature (Christensen et al., 2001; Vamvaca et al., 2004), which support this hypothesis. The preliminary double labelled C-CON NMR spectroscopy results were encouraging. The C-CON spectrum showed only 40% of the peaks expected for PinLip, indicating that much of the protein remains in conformational exchange, due to its flexibility and lack of defined structure.

Whilst only 40% of the residues were detectable, it is evident that carbon detection experiments are a significant improvement on previous NMR methods. This approach will be the method of further studies. The next step will be to

identify and optimise solution conditions where all peaks are observable to allow an in-depth conformational and structural determination and analysis.

With the obstacles presented by the experimental techniques the approach of homology modelling was employed. A 3D model of PinLip was generated using the server I-TASSER using three known lipase structures as templates (4L3W (*R. microspores* Lipase), 3TGL (*R. miehei* Lipase), 3NGM (*G. zeae* Lipase). The stereochemical quality of the optimised model shown only a portion of the residues in favourable positions (Veryfy3D) and the model was awarded a low C-score of –1.72. Despite scoring low, the Ramachandran Plot of the model was relatively good considering the low homology (~22%) of the PinLip compared to the templates used and the limitations of modelling and refinement methods (Fiser, 2010). The outlier residues were mainly identified in loop regions (Fig 6.13) with the exception of the catalytic Serine which is often constrained at an unusual angle due its catalytic activity (Derewenda et al., 1992; Noble et al., 1993 Nardini et al., 2000).

The comparison of the final model structure of PinLip with other lipases/esterases from different species shows that PinLip has a classic α/β-hydrolase fold with the lid helix protecting the highly conserved catalytic triad residues in its active site, which indicate a common catalytic mechanism. The main difference between the PinLip 3D model and comparable 3D structures like the *G. zeae* lipase or the *T. lanuginosus* lipase is the presence of extensive disordered loops in PinLip which are a characteristic of psychrophilic proteins. These disordered loops can be one of the reasons of the low score assigned to the PinLip model by the evaluation servers.

Other errors may be caused by the modelling software itself. All the homology protein software even the one that relies on an *ab initio* algorithm to generate the model 3D structure from scratch, such as I-TASSER uses the information present in the PDB. Psychrophilic structures are heavily under-represented in the PDB database (only 56 unique psychrophilic structure in the PDB so far). The use of thermophilic and mesophilic structures as templates for producing a model of a cold-adapted protein could be limited by low sequence homology and other structural differences. As mentioned in section 1.2.1, psychrophilic enzymes have evolved several mechanisms to be an efficient catalyst at cold temperature including extended surface loops, increased hydrophobic surface and decreased

ion electrostatic and aromatic interaction (De Maayer et al., 2014). As a result of the cold adaptation psychrophilic enzymes need to maintain the flexibility to be active at low temperature and are generally less thermostable than their mesophilic homologues.

The evaluation scoring systems used in the 3D modelling approach are biased towards mesophilic and thermophilic structural parameters because they rely on the available protein structures. A good quality homology model of the L-haloacid dehalogenase from the psychrophilic organism *P. ingrahamii* was generated by Novak (Novak et al., 2013) however this protein showed no obvious psychrophilic adaptations, suggesting it was acquired by the organism by horizontal gene transfer (Novak et al., 2013).

The final 3D PinLip model includes the lid helix (α3) in the closed conformation occluding the top of the active site pocket and the catalytic triad at the positions Ser193, Asp243 and His343. The model is reinforced by the experimental data confirming the role of His343 as a catalytic residue. The interatomic distances between the catalytic residues have been compared to known catalytic triads in other proteins and shown to be positioned within in the range for formation of stabilising hydrogens bonds. Furthermore, the binding site prediction meta server COACH predicted PinLip in complex with the oleic acid suggesting many of the residues within the active site are involved in the protein-ligand interaction. Lower scoring COACH predictions also suggested fatty acids as a substrate for PinLip including lauric and capric acid (Table 6.2) which are supported by the substrate specificity results (section 5.3.4.1).

Future study will include the continuation of the crystallisation trials and of the NMR spectroscopy experiments focusing on the stabilisation of PinLip in order to reduce the conformational stability. Also, it may be possible to perform *in silico* docking experiments deleting the PinLip lid helix to mimic an open conformation of the enzyme in order to facilitate the search for potential substrates.

Chapter 7 - Preliminary studies on the effect of formulation components on stability of Lipases

7.1 Background

As already mentioned in the previous chapters the single biggest market for lipase enzymes is in the laundry detergent industry. Despite the broad use of lipases in this industry, it is however unlikely that these enzymes perform at their best within the product formulations. When enzymes are placed in laundry detergent formulations they have to sustain harsh conditions such as a high surfactant or polymer concentrations, alkaline pH and chelating agents that can inhibit or denature the enzymes thereby defeating the purpose of positively adding them to the formulations (Zhang et al., 2014). Furthermore, it has already been shown (Chapter 3, 4, and 5) how the presence of a protease in the enzyme mix can be detrimental for the other enzymes.

This chapter focuses on the stabilisation of the lipase enzymes discussed in the previous chapters (PinLip, Lipex 16L, non-glycosylated Lipex, mono-glycosylated Lipex and tri-glycosylated Lipex) by the design of the added formulation in laundry products.

Modern laundry detergents are complex mixtures containing a variety of ingredients. A typical detergent composition is generally comprised of six groups of substances: surfactants, enzymes, bleaching agents, chelating agents and other minor additives such as dispersing agents, fabric softening clay, dye-transfer inhibiting ingredient, and optical brighteners (Yu et al., 2008). Lipases play an important role in laundry detergents as cleaning agents against fat and oily stains, but also as a “green ingredient”.

An ideal detergent enzyme should be stable at high pH and temperature, withstand oxidising and chelating agents, be effective at low concentrations and have a broad substrate specificity (Hemachander and Puvanakrishnan, 2000).

In this chapter, many formulation ingredients are tested on the lipases, in a range of concentrations chosen to mimic washing conditions. The stability of the lipases has been evaluated by differential scanning fluorimetry (DSF) where an increase of the measured melting temperature can be determined as having a positive effect regarding enzyme stability. Among the ingredients tested some are classic

chemical formulation ingredients while others are biological substitutes that are not yet present in commercial formulations.

Formulation design could be used to address both the problems of enzyme stability during storage and enzyme stability during wash performance and this chapter is focused on the latter. The ultimate goal of the studies described in this chapter is to understand the impact of the key formulation ingredients on the activity of different lipases. This information is crucial for Unilever for their development studies to establish the best compounds to be added in new sustainable formulation design.

7.2 Materials and Methods

All the formulation ingredients were kindly provided by Unilever.

7.2.1: Effect of single formulation ingredients on enzymes stability.

The enzyme samples were incubated in the presence of a selection of formulation ingredients including: surfactants, chelating agents, buffers and whitening agents (Table 7.1). The concentration of different ingredients tested ranged from 0.003% to 0.2% w/v. This concentration range was chosen to be representative of washing conditions in domestic laundry machines with 25 – 50 mL of laundry detergent formulation diluted in 40 L of water.

The DSF experiments were performed as described in section, 2.3.11.

Table 7.1: Function and name of the ingredients tested

Function	**Ingredient**
Anionic surfactant	Sodium laureth sulphate (SLES)
Anionic surfactant	Linear alkylbenzene sulphonate (LAS)
Non-ionic surfactant	Neodol
Polymer	EPEI (Sokalan HP20)
Whitening Agent	Tinopal CBS-CL
Buffering agent	Triethylamine
Biosurfactant mix	50/50 - Mono/Di rhamnolipid mix
Biosurfactant	Mono- rhamnolipid
Biosurfactant	Di- rhamnolipid
Biosurfactant	Mannosylerythritol lipid
Saponin	Escin
Chelating agent	Dequest 2010

7.3 Results and discussion

As already mentioned in Chapter 4, the melting temperature (T_m) of a protein is defined as the temperature at which the free energy of the unfolded and folded states is equal where half of the population is unfolded and the other half is folded.

The melting temperatures of all the enzymes used in this thesis without additives have been measured as controls (Fig. 4.13, Chapter 4 and Fig. 7.1).

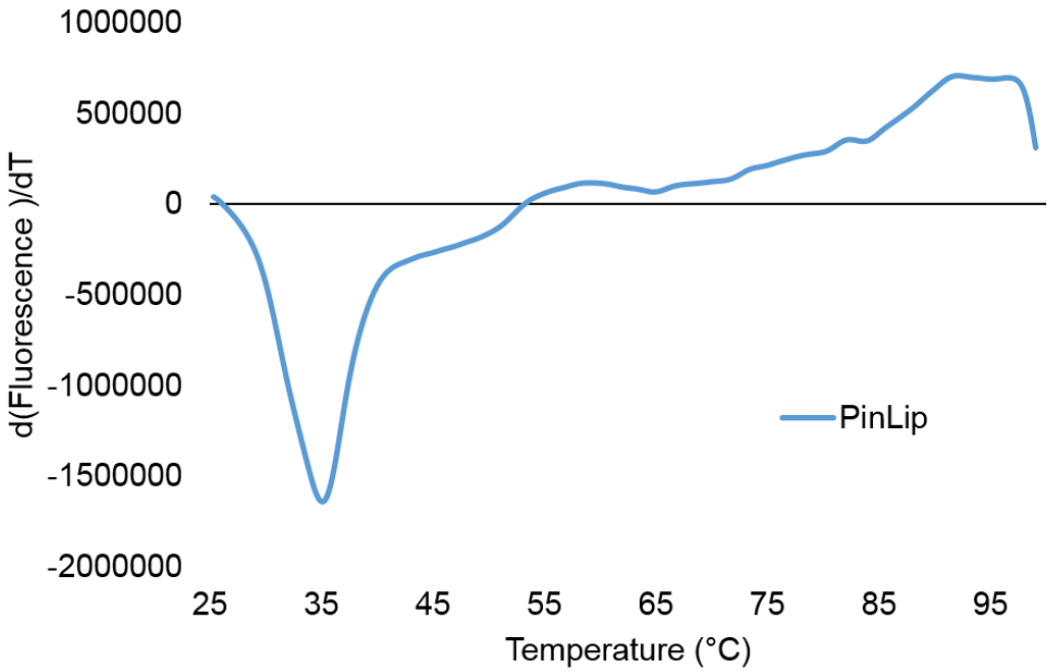

Fig. 7.1: Representation of the melting curve of the Pinlip. The characteristic shape of the raw data shows the derivative of the fluorescence with a progressive rise in fluorescence to a maximum, followed by a shallow decline. The minimum of the curve indicates the melting temperature of the protein.

While the four Lipex variants have T_m values higher than 68 °C (Fig. 4.13, Chapter 4) the cold-adapted PinLip has a T_m of 37.3 °C. To evaluate the effect of the formulation ingredients on the stability of the protein the T_m has been evaluated with these enzymes in the presence of the ingredients in a range of concentrations chosen to mimic that used in the laundry wash. An increase in T_m shows a positive stabilising effect while a decrease is indicative of destabilisation of the enzyme (Table 7.2, 7.3 and 7.4).

Table 7.2: Melting temperature values for Lipex 16L and non-glycosylated Lipex in the presence of different laundry formulation ingredients. T_m values higher than the control are highlighted. (Nd data were impossible to obtain with the DSF technique due complete destabilisation of the enzyme in the presence of the ingredient).

		Lipex 16 L		**Non-glycosylated Lipex**	
Compounds	Concentration range tested (%)	T_m (°C)	Concentration for maximum stability (%)	T_m (°C)	Concentration for maximum stability (%)
Enzyme only		69.3 ± 0.3		69.4 ± 0.5	
SLES	0.003 - 0.03	69.8 ±0.3	0.012	Nd	Nd
LAS	0.003 - 0.03	70.9 ±0.2	0.006	Nd	Nd
Neodol	0.003 - 0.03	69.8 ± 0.1	0.003	Nd	Nd
EPEI (Sokalan HP20)	0.003 - 0.03	69.8 ± 0.2	0.03	72.1 ± 0.2	0.03
Tinopal CBS-CL	0.003 - 0.03	69.6 ± 0.1	0.003	71.0 ± 0.7	0.003
Triethylamine	0.003 - 0.03	69.2 ± 0.3	0.003	71.5 ± 0.3	0.003
50/50 Mono/Di rhamnolipid mix	0.003 - 0.2	97.8 ± 0.6	0.2	96.7 ± 0.4	0.2
Mono-rhamnolipid	0.003 - 0.2	91.8 ± 0.4	0.2	92.2 ± 0.5	0.2
Di- rhamnolipid	0.003 - 0.03	70.5 ± 0.2	0.006	73.9 ± 0.2	0.0012
Mannosylerythritol lipid	0.003 - 0.03	Nd	Nd	Nd	Nd
Escin	0.003 - 0.03	69.5 ± 0.7	0.003	Nd	Nd
Dequest 2010	0.003 - 0.03	70.1 ± 0.5	0.012	72.7 ± 0.1	0.015

Table 7.3: Melting temperature values for mono-glycosylated Lipex and tri-glycosylated Lipex in the presence of different laundry formulation ingredients. T_m values higher than the control are highlighted. (Nd data were impossible to obtain with the DSF technique due complete destabilisation of the enzyme in the presence of the ingredient).

		Mono-glycosylated Lipex		**Tri-glycosylated Lipex**	
Compounds	Concentration range tested (%)	T_m (°C)	Concentration for maximum stability (%)	T_m (°C)	Concentration for maximum stability (%)
Enzyme only		69.8 ± 0.2		73.0 ± 0.1	
SLES	0.003 - 0.03	70.3 ± 0.1	0.012	74.2 ± 0.1	0.015
LAS	0.003 - 0.03	70.6 ± 0.2	0.009	73.9 ± 0.1	0.009
Neodol	0.003 - 0.03	70.2 ± 0.2	0.003	74.5 ± 0.1	0.003
EPEI (Sokalan HP20)	0.003 - 0.03	71.3 ± 0.1	0.03	73.1 ± 0.2	0.03
Tinopal CBS-CL	0.003 - 0.03	73.2 ± 0.1	0.003	73.3 ± 0.1	0.003
Triethylamine	0.003 - 0.03	70.8 ± 0.2	0.003	72.8 ± 0.1	0.003
50/50 Mono/Di rhamnolipid mix	0.003 - 0.2	95.4 ± 0.1	0.2	95.3 ± 0.1	0.2
Mono- rhamnolipid	0.003 - 0.2	90.2 ±0.1	0.2	93.2 ± 0.1	0.2
Di- rhamnolipid	0.003 - 0.03	71.7 ± 0.3	0.012	76.5 ±0.2	0.015
Mannosylerythritol lipid	0.003 - 0.03	Nd	Nd	Nd	Nd
Escin	0.003 - 0.03	Nd	Nd	Nd	Nd
Dequest 2010	0.003 - 0.03	70.2 ± 0.1	0.015	72.7 ± 0.2	0.015

Table 7.4: Melting temperature values for PinLip in the presence of different laundry formulation ingredients. T_m values higher than the control are highlighted. (Nd data were impossible to obtain with the DSF technique due complete destabilisation of the enzyme in the presence of the ingredient).

	PinLip		
Compounds	Concentration range tested (%)	T_m (°C)	Concentration for maximum stability (%)
Enzyme only		37.3 ± 0.2	
SLES	0.003 - 0.03	36.5 ± 0.3	0.003
LAS	0.003 - 0.03	33.3 ± 0.3	0.01
Neodol	0.003 - 0.03	Nd	Nd
EPEI (Sokalan HP20)	0.003 - 0.03	42.9 ± 0.2	0.01
Tinopal CBS-CL	0.003 - 0.03	43.2 ± 0.1	0.01
Triethylamine	0.003 - 0.03	42.8 ± 0.1	0.01
50/50 Mono/Di rhamnolipid mix	0.003 - 0.2	Nd	Nd
Mono- rhamnolipid	0.003 - 0.2	Nd	Nd
Di- rhamnolipid	0.003 - 0.03	35.7 ± 0.1	0.003
Mannosylerythritol lipid	0.003 - 0.03	Nd	Nd
Escin	0.003 - 0.03	34.6 ± 0.1	0.003
Dequest 2010	0.003 - 0.03	Nd	Nd

From the results in Table 7.2 and 7.3 it is clear that all of the four Lipex variants showed a similar trend with the same ingredients causing either an increase or a decrease in T_m across all of the Lipex variants. Most of the ingredients had a small positive effect on the enzymes T_m values with an increase in temperature from 0.3 to 1.5 °C. However, two ingredients increased the T_m of all the Lipex variants by over 20 °C, reflecting a large stabilisation effect. The two ingredients having this effect are both rhamnolipids, a type of biosurfactant already discussed in section 5.3.5, in particular both of the ingredients contain mono-rhamnolipids and since the di-rhamnolipids alone do not show the same positive effect, it can be deduced that the mono-rhamnolipids are responsible for the improved stability. Unilever is interested in the use of rhamnolipids since they are efficient as natural emulsifiers which are promising for their application in detergent compositions, laundry products, shampoos, and soaps (Parry et al., 2012). The data from these DSF experiments combined with the NMR data obtained with non-glycosylated Lipex in the presence of different components of laundry formulations by the group of Dr Alfonso De Simone at Imperial College (data not shown) have been used by Unilever to design a set of novel laundry formulations

focused on enzyme activity and stability improvements. NMR is used to monitor the protein unfolding in the presence of the different additives. These experiments are continuing with the goal to obtain laundry formulations that have improved cleaning performance and that do not compromise enzyme activity.

The data shown in table 7.4 with the cold-adapted PinLip shows that only three ingredients (EPEI, Tinopal CBS-CL, and Triethylamine) have a positive effect on enzyme stabilisation. The EPEI is a stabilising polymer and foaming agent which is known to have a positive effect on enzyme stability and is used in laundry formulation (Fuk-Pong Man and Killeen, 2013; López-Gallego et al., 2005; Brus et al., 2004; Gopalkrishnan et al., 2000). On the contrary tinopal CBS-CL and triethylamine are not expected to have this type of effect which will require further investigation. However, since even small increases of the T_m are indicative of having a stabilising effect on protein(Cimmperman and Matulis, 2011), these ingredients can be used to create an improved formulation for the psychrophilic PinLip enzyme to improve its wash performance even further.

Interestingly PinLip seems to be negatively affected by most of the biosurfactant components. However the wash performance experiments (Section 5.3.5.1) have shown that the PinLip performed particularly well in combination with biosurfactants based on rhamnolipid and mannosylerythritol lipid at low temperature. To explain these differences, more experiments will be needed and the PinLip stability in the presence of biosurfactant should be evaluated by other techniques such as CD and NMR spectroscopy.

8. Summary and Future work

8.1 Summary

This thesis has used a range of protein stabilisation techniques to improve the activity and stability of different lipases for their industrial applications in laundry and household care products.

The CLEAs technology has been used to obtain a more stable version of a popular commercial enzyme, Lipex 16L. The method is exquisitely simple and amenable to rapid optimisation. The improved protocol introduced in this thesis involves an activation step designed to lock the enzyme in the "open lid conformation" and a step to control the end point of the crosslinking reaction. The Lipex CLEA produced by this method has been shown to result in smaller aggregates (1.85 ± 0.28 μm), that are more stable in the presence of protease and are more active (129.7%) than the free enzyme. The overall product yield using this process is relatively low (< 60%) and requires further optimisation for a commercial process to be economically viable. This methodology could be applied to help stabilise other enzymes that are used in commercial detergents.

The effect of an increased number of glycosylation sites on the surface of proteins with regards to their stability has been studied in this thesis. Three Lipex variants were produced, a non-glycosylated, a mono-glycosylated (wild type) and a tri-glycosylated enzyme were investigated with regards to their stability. The commercial Lipex 16L was used as a comparison. The first two Lipex variants were obtained by cloning the Lipex enzyme and expressing it in *E. coli* and *P. pastoris.* The third was obtained by mutating the Lipex gene to introduce two new glycosylation sites (N37 and N99) within the protein and over-expression in *P.pastoris.* This has allowed the study of the effect of high mannose glycosylation on the enzyme stability. The three enzyme variants were characterised for activity and stability. The overall activity was found to be lower than the commercial Lipex 16L. The DSF data have proved that the tri-glycosylated Lipex is the most stable variant with a T_m shift of + 4 $^{\circ}$C which demonstrates a direct stabilisation effect relative to the abundance of glycan on the surface of the enzyme which is in agreement with other previous studies (Benoit et al., 2006; Deshpande et al., 2008; Zou et al., 2013; Han et al., 2014). The improved stabilisation does not

affect the lipase activity but does improve the resistance of the tri-glycosylated Lipex to degradation by proteases in the detergent formulation.

A new novel cold-adapted lipase has been characterised, and its industrial applicability has been evaluated. The lipase from the psychrophilic bacteria *P. ingrahamii* (PinLip) has been cloned into a pLATE31 vector with a C-terminal His-tag and over-expressed in *E coli.* The enzyme was purified by nickel affinity and gel filtration chromatography and biochemically characterised. The recombinant PinLip showed activity towards short and medium chain fatty acids. The optimal temperature for activity of the PinLip was 20 °C. The wash performance studies at low temperature (20°C) towards two different fat stains showed an SRI up to 10 points higher than the commercial benchmark lipase, Lipex 16L. The PinLip showed improved performance when combined with two types of biosurfactants developed by Unilever from rhamnolipids and mannosylerythritol lipids (MELs) with an activity increase of 37.1 and 29.3% respectively. These biosurfactants have good potential to substitute chemical surfactants in the future. However, new formulation design is necessary in order to produce a complete formulation that can be tested with psychrophilic enzymes. The PinLip crystallisation trials were unsuccessful, yet ordered precipitates have been obtained. The CD and NMR spectroscopy results showed that PinLip is partially unfolded, which is known to be detrimental to crystal formation, however, the preliminary double labelled C-CON NMR spectroscopy showed an improvement in the signal using a ^{13}C detection probe compared to the signal obtained with the ^{15}N. However only ~120 peaks out of 378 residues could be identified, and further protein stabilisation is necessary to achieve a good quality spectrum. Some insight into the structure of the PinLip can be gained from the 3D model of the enzyme generated by the server I-TASSER. While presenting a classic α/β hydrolase fold, a lid helix and well-positioned catalytic triad, the PinLip model also shows extensive, flexible loop regions which are characteristic of other psychrophilic proteins (De Maayer et al., 2014).

Finally, all of the lipases studied in this thesis have been studied with regards to their stabilisation in different laundry formulations. DSF was used to investigate the effects of the formulation components on enzyme stability. The detergent compounds tested were a mixture of classic formulation ingredients and novel biosurfactants. All the Lipex variants showed an increase in stability with the two

ingredients containing mono-rhamnolipid, the 50/50 mono/di rhamnolipid mix and mono-rhamnolipid alone with an increase in T_m of over + 20 °C. The PinLip was not stabilised by the same components that had a positive effect on the Lipex variants. Indeed, all of the ingredients tested except for three had an adverse impact on PinLip stability reflecting the difference between cold adapted and thermophilic enzymes. Among the three components with a positive stabilising effect (EPEI, Tinopal CBS-CL, and Triethylamine) only the EPEI, a polymer, had a stabilising function while the other two compounds, a whitening and buffering agent, respectively were not expected to have such effects. Further experiments need to be carried out to understand the rationale behind these results.

8.2 Future work

With the increasing demand of enzymes for Biocatalysis, the need for methods to stabilise proteins for different industrial applications will increase. This thesis gives some new insights into protein stabilisation techniques that could be applied not only in the laundry detergent industry but to other industrial applications. There are many ways in which this project can be developed.

The CLEAs production protocol could be further optimised in order to increase the total product yield, for a more cost-effective and economically viable process. This could be achieved by increasing the cross-linking time and/or the concentration of cross-linker or using a different bivalent crosslinker such as dextran polyaldehyde. The cross-linking efficiency and activity needs to be carefully balanced as excessive cross-linking will have a negative impact on enzyme performance. The CLEAs technology could also be applied to the cold-adapted PinLip in order to improve its stability.

Regarding the effect of glycosylation on the stability of Lipex, the results can be considered a starting point for further investigation into how to improve both the activity and the stability of the lipase enzymes. More glycosylation sites could be introduced into the enzyme and expression in different eukaryotic hosts (mammalian and insect cells) could be considered. This would allow a study of how the composition of the different glycans added by the various host cells could impact on the recombinant enzyme's stability. Mammalian glycoproteins often have a *complex* type of branched *N*-glycans with terminal sialic acids, while insect cell glycoproteins usually have simpler side chains, with few mannose residues that lack the final sialylation typical of mammal systems (Shi and Jarvis, 2007).

Chapters 5 and 6 were dedicated to the characterisation of the novel cold-adapted lipase PinLip. Future studies could include NMR spectroscopy experiments focusing on the stabilisation of PinLip to reduce its conformational instability. This could allow further assignment of the residues of this protein to provide information on it's 3D structure. The PinLip could be used as a model enzyme to understand further cold adaption. Such a model is important to help to engineer psychrophilic enzymes for industrial applications. If compounds are

found that could stabilise the PinLip, these could be incorporated into further crystallisation trials. Also, the ordered precipitates already obtained could be used for further optimisation of the crystallisation conditions. Future investigations could include the generation of different mutant enzymes with shorter surface loops. It is proposed that the shortening of the flexible loops could be the key to a more stable enzyme scaffold. Identification of the predicted loop flexibility of the wild-type enzyme could be determined from the model of PinLip already obtained using the I-TASSER server. A series of different mutant enzymes could be designed based on the model and information from sequence alignments with related enzymes. These mutant enzymes could be analysed for increased stability while maintaining their activity using a variety of techniques including CD, DSF and stability in commercial detergent formulations. Mutant proteins which could have a more rigid scaffold while maintaining the flexibility in the enzyme active site required for activity at cold temperatures would be important new lipases for commercial applications. Regarding the application of PinLip in the laundry detergents, the over-expression protocol needs to be optimised in order to reach a higher yield of protein required for industrial applications.

The experiments to test different formulation ingredients on lipase stability have suggested a clear stabilisation effect of the Lipex enzyme by mono-rhamnolipid based biosurfactants. Future experiments could address Lipex long-term storage stability and Lipex stability in the presence of a protease in formulation with biosurfactants.

The application of enzymatic processes to replace traditional chemistry for many other applications in bio-refinery, biofuels cells, and detergents, for example, has driven the need for an increased understanding of enzyme stability and stabilisation (Littlechild, 2015). The results obtained in this thesis have shown several valid methods to improve the stability of different lipase enzymes while maintaining their catalytic potential, which has direct importance for industrial applications. The further characterisation of the intrinsically unstable psychrophilic lipase, PinLip, could improve our understanding of the mechanism of protein stability, thereby resolving one of the main bottlenecks in many industrial enzyme applications.

9. Bibliography

Abdou, A. M. (**2003**). Purification and Partial Characterization of Psychrotrophic *Serratia marcescens* Lipase. *Journal of Dairy Science*, *86*(1), 127–132.

Aghajari, N., Van Petegem, F., Villeret, V., Chessa, J.-P., Gerday, C., Haser, R., and Van Beeumen, J. (**2003**). Crystal structures of a psychrophilic metalloprotease reveal new insights into catalysis by cold-adapted proteases. *Proteins: Structure, Function, and Bioinformatics*, *50*(4), 636–647.

Ahern, T. J., Casal, J. I., Petsko, G. A., and Klibanov, A. M. (**1987**). Control of oligomeric enzyme thermostability by protein engineering. *Proceedings of the National Academy of Sciences of the United States of America*, *84*(3), 675–9.

Ahmad, M., Hirz, M., Pichler, H., and Schwab, H. (**2014**). Protein expression in *Pichia pastoris*: recent achievements and perspectives for heterologous protein production. *Applied Microbiology and Biotechnology*, *98*(12), 5301–5317.

Alford, J. A., and Pierce, D. A. (**1963**). Production of Lipase by *Pseudomonas fragi* In A Synthetic Medium. *Journal of Bacteriology*, *86*, 24–9.

Alquati, C., De Gioia, L., Santarossa, G., Alberghina, L., Fantucci, P., and Lotti, M. (**2002**). The cold-active lipase of *Pseudomonas fragi*: Heterologous expression, biochemical characterization and molecular modeling. *European Journal of Biochemistry*, *269*(13), 3321–3328.

Altschul, S. F., Gish, W., Miller, W., Myers, E. W., and Lipman, D. J. (**1990**). Basic local alignment search tool. *Journal of Molecular Biology*, *215*(3), 403–410.

Altschul, S., Madden, T., Schaffer, A., Zhang, J., Zhang, Z., Miller, W., and Dj, L. (**1997**). Gapped BLAST and PSI- BLAST: a new generation of protein database search programs. *Nucleic Acids Res*, *25*(17), 3389–3402.

Anobom, C. D., Pinheiro, A. S., De-Andrade, R. A., Aguieiras, E. C. G., Andrade, G. C., Moura, M. V., … Freire, D. M. (**2014**). From structure to catalysis: Recent developments in the biotechnological applications of lipases. *BioMed Research International*, *2014*.

Apweiler, R. (**1999**). On the frequency of protein glycosylation, as deduced from analysis of the SWISS-PROT database. *Biochimica et Biophysica Acta -*

General Subjects, *1473*(1), 4–8.

Arnold, K., Bordoli, L., Kopp, J., and Schwede, T. (**2006**). The SWISS-MODEL workspace: A web-based environment for protein structure homology modelling. *Bioinformatics*, *22*(2), 195–201.

Asherie, N. (**2004**). Protein crystallization and phase diagrams. *Methods*, *34*(3), 266–272.

Babu, J., Ramteke, P. W., and Thomas, G. (**2008**). Cold active microbial lipases: Some hot issues and recent developments. *Biotechnology Advances*, *26*(5), 457–470.

Bajpai, D and Mishra A. (**2016**). Sustainable Biosurfactant. In *Sustainable Inorganic Chemistry* (pp. 181-189). Wiley

Balcão, V. M., and Malcata, F. X. (**1998**). On the performance of a hollow-fiber bioreactor for acidolysis catalyzed by immobilized lipase. *Biotechnology and Bioengineering*, *60*(1), 114–123.

Benkert, P., Tosatto, S. C. E., and Schomburg, D. (**2008**). QMEAN: A comprehensive scoring function for model quality assessment. *Proteins: Structure, Function, and Bioinformatics*, *71*(1), 261–277.

Benoit, I., Asther, M., Sulzenbacher, G., Record, E., Marmuse, L., Parsiegla, G., … Bignon, C. (**2006**). Respective importance of protein folding and glycosylation in the thermal stability of recombinant feruloyl esterase A. *FEBS Letters*, *580*(25), 5815–5821.

Berka, R. M., Rey, M. W., Brown, K. M., Byun, T., and Klotz, A. V. (**1998**). Molecular characterization and expression of a phytase gene from the thermophilic fungus *Thermomyces lanuginosus*. *Applied and Environmental Microbiology*, *64*(11), 4423–4427.

Berman, H. M., Westbrook, J., Feng, Z., Gilliland, G., Bhat, T. N., Weissig, H., … Bourne, P. E. (**2000**). The Protein Data Bank. *Nucleic Acids Research*, *28*(1), 235–42.

Biermann, M., Lange, F., Piorr, R., Ploog, U., Rutzen, H., Schindler, J., and Schmid, R. (**1987**). Synthesis of Surfactants. In *Surfactants in Consumer Products* (pp. 23–132). Berlin, Heidelberg: Springer Berlin Heidelberg.

Bordenave, G. (**2003**). Louis Pasteur (1822–1895). *Microbes and Infection*, *5*(6), 553–560.

Borges, N., Ramos, A., Raven, N. D. H., Sharp, R. J., and Santos, H. (**2002**). Comparative study of the thermostabilizing properties of mannosylglycerate and other compatible solutes on model enzymes. *Extremophiles*, *6*(3), 209–216.

Borrelli, G. M., and Trono, D. (**2015**). Recombinant lipases and phospholipases and their use as biocatalysts for industrial applications. *International Journal of Molecular Sciences*, *16*(9), 20774–20840.

Breezee, J., Cady, N., and Staley, J. T. (**2004**). Subfreezing growth of the sea ice bacterium "*Psychromonas ingrahamii*". *Microbial Ecology*, *47*(3), 300–304.

Brena, B. M., and Batista-viera, F. (**2006**). Immobilization of Enzymes A Literature Survey. *Methods in Biotechnology: Immobilization of Enzyme and Cells, 2nd Edition*, 15–30.

Bretthauer, R. K., and Castellino, F. J. (**1999**). Glycosylation of *Pichia pastoris* - derived proteins. *Biotechnology and Applied Biochemistry*, *30*(3), 193–200.

Brown, A. J. (**1902**). XXXVI.—Enzyme action. *Journal of the Chemical Society, Transformation*, *81*(0), 373–388.

Brus, C., Petersen, H., Aigner, A., Czubayko, F., and Kissel, T. (**2004**). Physicochemical and Biological Characterization of Polyethylenimine-graft-Poly(ethylene glycol) Block Copolymers as a Delivery System for Oligonucleotides and Ribozymes. *Bioconjugate Chemistry*, *15*(4), 677–684.

Brzozowski, A. M., Savage, H., Verma, C. S., Turkenburg, J. P., Lawson, D. M., Svendsen, A., and Patkar, S. (**2000**). Structural origins of the interfacial activation in *Thermomyces (Humicola) lanuginosa* lipase. *Biochemistry*, *39*(49), 15071–15082.

Buenger, J., and Driller, H. (**2004**). Ectoin: An Effective Natural Substance to Prevent UVA-Induced Premature Photoaging. *Skin Pharmacology and Physiology*, *17*(5), 232–237.

Bulter, T., Alcalde, M., Sieber, V., Meinhold, P., Schlachtbauer, C., and Arnold, F. H. (**2003**). Functional expression of a fungal laccase in *Saccharomyces cerevisiae* by directed evolution. *Applied and Environmental Microbiology*, *69*(2), 987–95.

Buzzini, P., Branda, E., Goretti, M., and Turchetti, B. (**2012**). Psychrophilic yeasts from worldwide glacial habitats: Diversity, adaptation strategies and biotechnological potential. *FEMS Microbiology Ecology*, *82*(2), 217–241.

Cao, L., van Rantwijk, F., and Sheldon, R. A. (**2000**). Cross-Linked Enzyme Aggregates: A Simple and Effective Method for the Immobilization of Penicillin Acylase. *Organic Letters*, *2*(10), 1361–1364.

Casanueva, A., Tuffin, M., Cary, C., and Cowan, D. A. (**2010**). Molecular adaptations to psychrophily: the impact of “omic” technologies. *Trends in Microbiology*, *18*(8), 374–381.

Cereghino, J. L., and Cregg, J. M. (**2000**). Heterologous protein expression in the methylotrophic yeast *Pichia pastoris*. *FEMS Microbiology Reviews*, *24*(1), 45–66.

Cereghino, G. P., Cereghino, J., Ilgen, C., and Cregg, J. M. (**2002**). Production of recombinant proteins in fermenter cultures of the yeast *Pichia pastoris*, *Molecular Biotechnology 13*(4), 329–332.

Chaplin, M. (**2014**). The use of enzymes in detergents. Web page : http://www1.lsbu.ac.uk/water/enztech/detergent.html

Choo, D., Kurihara, T., Suzuki, T., and Soda, K. (**1998**). A Cold-Adapted Lipase of an Alaskan Gene Cloning and Enzyme Purification and Characterization, *Applied Environmental Microbiology 64*(2), 1–7.

Christensen, K., Bose, H. S. H., Harris, F. M. F., Miller, W. L. W., and Bell, J. D. (**2001**). Binding of Steroidogenic Acute Regulatory Protein to Synthetic Membranes Suggests an Active Molten Globule. *Journal of Biological*, *20*(18), 17044–17051.

Ciulla, R. A., Burggraf, S., Stetter, K. O., and Roberts, M. F. (**1994**). Occurrence and Role of Di-myo-Inositol-1,1’-Phosphate in *Methanococcus igneus*. *Applied and Environmental Microbiology*, *60*(10), 3660–4.

Cimmperman, P., and Matulis, D. (**2011**). Protein thermal denaturation measurements via a fluorescent dye. *Biophysical Approaches Determining Ligand Binding to Biomolecular Targets: Detection, Measurement and Modelling*, (22), 247–273.

Clair, N. L. St., and Navia, M. A. (**1992**). Cross-linked Enzyme Crystals as Robust Biocatalysts. *Science*, (2), 7314–7316.

Cornish-Bowden, A. (**2013**). The origins of enzyme kinetics. *FEBS Letters*, *587*(17), 2725–2730.

Cui, J. D., and Jia, S. R. (**2015**). Optimization protocols and improved strategies

of cross-linked enzyme aggregates technology: current development and future challenges. *Critical Reviews in Biotechnology*, *35*(1), 15–28.

Czichocki, G., Dautzenberg, H., Capan, E., and Vorlop, K.-D. (**2001**). New and effective entrapment of polyelectrolyte-enzyme-complexes in LentiKats. *Biotechnology Letters*, *23*(16), 1303–1307.

D'Amico, S., Collins, T., Marx, J.-C., Feller, G., and Gerday, C. (**2006**). Psychrophilic microorganisms: challenges for life. *EMBO Reports*, *7*(4), 385–389.

D'Amico, S., Marx, J.-C. C., Gerday, C., Feller, G., D'Amico, S., Marx, J.-C. C., … Feller, G. (**2003**). Activity-stability relationships in extremophilic enzymes. *Journal of Biological Chemistry*, *278*(10), 7891–7896.

D'Arcy, A., Villard, F., and Marsh, M. (**2007**). An automated microseed matrix-screening method for protein crystallization. *Acta Crystallographica Section D Biological Crystallography*, *63*(4), 550–554.

da Costa, M. S., Santos, H., and Galinski, E. A. (**1998**). An overview of the role and diversity of compatible solutes in Bacteria and Archaea (pp. 117–153). Springer Berlin Heidelberg.

Damaso, M. C. T., Almeida, M. S., Kurtenbach, E., Martins, O. B., Pereira, N., Andrade, C. M. M. C., and Albano, R. M. (**2003**). Optimized Expression of a Thermostable Xylanase from *Thermomyces lanuginosus* in *Pichia pastoris*. *Applied and Environmental Microbiology*, *69*(10), 6064–6072.

Datta, S., Christena, L. R., and Rajaram, Y. R. S. (**2012**). Enzyme immobilization: an overview on techniques and support materials. *3 Biotech*, 1–9.

De Maayer, P., Anderson, D., Cary, C., and Cowan, D. A. (**2014**). Some like it cold: Understanding the survival strategies of psychrophiles. *EMBO Reports*, *15*(5), 508–517.

De Rose, S. A., Novak, H., Dowd, A., Singh, S., Lang, D. A., and Littlechild, J. (**2017**). Stabilization of a Lipolytic Enzyme for Commercial Application. *Catalysts*, *7*(3), 91.

De Simone, G., Menchise, V., Alterio, V., Mandrich, L., Rossi, M., Manco, G., and Pedone, C. (**2004**). The Crystal Structure of an EST2 Mutant Unveils Structural Insights on the H Group of the Carboxylesterase/Lipase Family. *Journal of Molecular Biology*, *343*(1), 137–146.

Delaglio, F., Grzesiek, S., Vuister, G. W., Zhu, G., Pfeifer, J., and Bax, A. (**1995**). NMRPipe: a multidimensional spectral processing system based on UNIX pipes. *Journal of Biomolecular NMR*, *6*(3), 277–93.

Deller, M. C., Kong, L., and Rupp, B. (**2016**). Protein stability: A crystallographer's perspective. *Acta Crystallographica Section:F Structural Biology Communications*, *72*, 72–95.

Derewenda, U., Brzozowski, A. M., Lawson, D. M., and Derewenda, Z. S. (**1992**). Catalysis at the interface: the anatomy of a conformational change in a triglyceride lipase. *Biochemistry*, *31 (5)*, pp 1532–1541.

Derewenda, Z. S. (**2011**). It's all in the crystals... *Acta Crystallographica Section D: Biological Crystallography*, *67*(4), 243–248.

Deshpande, N., Wilkins, M. R., Packer, N., and Nevalainen, H. (**2008**). Protein glycosylation pathways in filamentous fungi. *Glycobiology*, *18*(8), 626–637.

DeVries, A. L. (**1986**). Antifreeze glycopeptides and peptides: interactions with ice and water. *Methods in Enzymology*, *127*, 293–303.

DiCosimo, R., McAuliffe, J., Poulose, A. J., Bohlmann, G., Kumar, H., Satyanarayanan, T., … Langan, P. (**2013**). Industrial use of immobilized enzymes. *Chemical Society Reviews*, *42*(15), 6437–6474.

Dieckelmann, M., Johnson, L. A., and Beacham, I. R. (**1998**). The diversity of lipases from psychrotrophic strains of *Pseudomonas*: A novel lipase from a highly lipolytic strain of *Pseudomonas fluorescens*. *Journal of Applied Microbiology*, *85*(3), 527–536.

Domínguez de María, P., Fernández-Álvaro, E., Ten Kate, A., and Bargeman, G. (**2009**). Role of apparent pKa of carboxylic acids in lipase-catalyzed esterifications in biphasic systems. *Journal of Molecular Catalysis B: Enzymatic*, *59*(1–3), 220–224.

Donald van Slyke, B. D., Cullew, G. E., Armstrong, H. E., and Royal Sot, P. (**1913**). The Mode of Action of Urease and of Enzymes in General. *The Journal of Biological Chemistry 19*(2) 141 - 182.

Doscher, M. S., and Richards, F. M. (**1963**). The Activity of an Enzyme in the Crystalline State: Ribonuclease {S}. *The Journal of Biological Chemistry 238*(7), 2399–2406.

Edward, V. A., Pillay, P. ., Swart, P., and Singh, S. (**2015**). Immobilisation of xylanase from *Thermomyces lanuginosus* SSBP using Eudragit S-100. *South African Journal of Science*, *98*, 553–554.

Eisenberg, D., Lüthy, R., and Bowie, J. U. (**1997**). VERIFY3D: assessment of protein models with three-dimensional profiles. *Methods in Enzymology*, *277*, 396–404.

Estell, D. A., Graycar, T. P., & Wells, J. A. (*1985*). Engineering an enzyme by site-directed mutagenesis to be resistant to chemical oxidation. *Journal of Biological Chemistry*, 260(11), 6518–6521.

Feller, G. (**2007**). Life at low temperatures: Is disorder the driving force? *Extremophiles*. *11*(2), 211–216.

Feller, G. (**2013**). Psychrophilic enzymes: from folding to function and biotechnology. *Scientifica*, *2013*, 512840.

Feller, G., and Gerday, C. (**2003**). Psychrophilic enzymes: hot topics in cold adaptation. *Nature Reviews Microbiology*, *1*(3), 200–208.

Fernandes, M.L. M.; Krieger, N.; Baron, A.M.; Zamora, P.P.; Ramos, L.P.; Mitchell, D.A. (**2004**) Hydrolysis and synthesis reactions catalysed by *Thermomyces lanuginosa* lipase in the AOT/Isooctane reversed micellar system. *Journal of Molecular Catalasisys B: Enzymatic*, *30*, 43–49.

Fernandez-Fuentes, N., Rai, B. K., Madrid-Aliste, C. J., Eduardo Fajardo, J., and Fiser, A. (**2007**). Comparative protein structure modeling by combining multiple templates and optimizing sequence-to-structure alignments. *Bioinformatics*, *23*(19), 2558–2565.

Fernandez-Lafuente, R. (**2010**). Lipase from *Thermomyces lanuginosus*: Uses and prospects as an industrial biocatalyst. *Journal of Molecular Catalysis B: Enzymatic*, *62*(3–4), 197–212.

Fernandez-Lorente, G., Palomo, J. M., Mateo, C., Munilla, R., Ortiz, C., Cabrera, Z., … Fernandez-Lafuente, R. (**2006**). Glutaraldehyde Cross-Linking of Lipases Adsorbed on Aminated Supports in the Presence of Detergents Leads to Improved Performance. *Biomacromolecules*, *7*(9), 2610–2615.

Fields, P. A. (**2001**). Review: Protein function at thermal extremes: balancing stability and flexibility. *Comparative Biochemistry and Physiology. Part A, Molecular and Integrative Physiology*, *129*(2–3), 417–31.

Fields, P. A., Dong, Y., Meng, X., and Somero, G. N. (**2015**). Adaptations of protein structure and function to temperature: there is more than one way to “skin a cat.” *Journal of Experimental Biology*, *218*(12), 1801–1811.

Fiser, A. (**2010**) Template-based protein structure modeling. *Methods in Molecular Biology (Clifton, N.J.)*, *673*, 73–94.

Frenken, L. G. J., Egmond, M. R., Batenburg, A. M., and Verrips, C. T. (**1993**). *Pseudomonas glumae* lipase: Increased proteolytic stabifity by protein engineering. *Protein Engineering, Design and Selection*, *6*(6), 637–642.

Frueh, D. P., Goodrich, A., Mishra, S., and Nichols, S. (**2013**). NMR methods for structural studies of large monomeric and multimeric proteins. *Current Opinion in Structural Biology*, *23*(5), 734–739.

Fuk-Pong Man, V., and Killeen, Y. M. (**2013**). Foam stabilization with polyethyleneimine ethoxylates. Patent no WO2014084885 A1

Galante, Y. A., and Formantici, C. (**2003**). Enzyme applications in detergency and in manufacturing industries. *Current Organic Chemistry*, *7*(13), 1399–1422.

Garcia-Galan, C., Berenguer-Murcia, Á., Fernandez-Lafuente, R., and Rodrigues, R. C. (**2011**). Potential of Different Enzyme Immobilization Strategies to Improve Enzyme Performance. *Advanced Synthesis and Catalysis*, *353*(16), 2885–2904.

Gemmill, T. R., and Trimble, R. B. (**1999**). Overview of N- and O-linked oligosaccharide structures found in various yeast species. *Biochimica et Biophysica Acta - General Subjects*, *1426*(2), 227–237.

Georlette, D., Blaise, V., Collins, T., D’Amico, S., Gratia, E., Hoyoux, A., Marx, J,C., Sonan, G., Feller, G and Gerday, C. (**2004**). Some like it cold: Biocatalysis at low temperatures. *FEMS Microbiology Reviews*, *28*(1), 25–42.

Gerday, C., Aittaleb, M., Bentahir, M., Chessa, J. P., Claverie, P., Collins, T., D’Amico, S., Dumont, J., Garsoux, G., Georlette, D., Hoyoux, A., Lonhienne, T., Meuwis, M., and Feller, G. (**2000**). Cold-adapted enzymes: From fundamentals to biotechnology. *Trends in Biotechnology*.

Gilbert, J. A., Hill, P. J., Dodd, C. E. R., and Laybourn-Parry, J. (**2004**). Demonstration of antifreeze protein activity in Antarctic lake bacteria. *Microbiology*, *150*(1), 171–180.

Gopalkrishnan, S., Holland, R. J., Patterson, S., and Parker, E. J. (**2000**). Detergency boosting polymer blends as additives for laundry formulations. Patent no CA2146598A1

Gouka, R. J., Wilson, S., M., O. S. J. C., and Durrant, O. (**2011**). A review of psychrophilic enzymes and their potential for detergent applications., *VD11 0106*(0), 1–2.

Guauque Torres, M. D. P., Foresti, M. L., and Ferreira, M. L. (**2013**). Cross-linked enzyme aggregates (CLEAs) of selected lipases: a procedure for the proper calculation of their recovered activity. *AMB Express*, *3*(1), 25.

Günther, H. (**2013**). *NMR spectroscopy: basic principles, concepts and applications in chemistry*, Wiley

Gupta, P., Dutt, K., Misra, S., Raghuwanshi, S., and Saxena, R. K. (**2009**). Characterization of cross-linked immobilized lipase from thermophilic mould *Thermomyces lanuginosa* using glutaraldehyde. *Bioresource Technology*, *100*(18), 4074–4076.

Gupta, R., Rathi, P., Gupta, N., and Bradoo, S. (**2003**). Lipase assays for conventional and molecular screening: an overview. *Biotechnology and Applied Biochemistry*, *37*(Pt 1), 63–71.

Gurung, N., Ray, S., Bose, S., and Rai, V. (**2013**). A broader view: Microbial enzymes and their relevance in industries, medicine, and beyond. *BioMed Research International*, *2013*.

Hahn, E. L. (**1950**). Spin Echoes. *Physical Review*, *80*(4), 580–594.

Han, M., Wang, X., Ding, H., Jin, M., Yu, L., Wang, J., and Yu, X. (**2014**). The role of N-glycosylation sites in the activity, stability, and expression of the recombinant elastase expressed by Pichia pastoris. *Enzyme and Microbial Technology*, *54*, 32–37.

Hanahan, D. (**1983**). Studies on transformation of *Escherichia coli* with plasmids. *Journal of Molecular Biology*, *166*(4), 557–80.

Hardwood, J. (**1989**). The versatility of lipases for industrial uses. *Trend In Biochemical Science* (*Tibs)* (14), 125.

Hasan, F., Shah, A. A., and Hameed, A. (**2006**). Industrial applications of microbial lipases. *Enzyme and Microbial Technology*, *39*(2), 235–251.

Hemachander, C., and Puvanakrishnan, R. (**2000**). Lipase from *Ralstonia*

pickettii as an additive in laundry detergent formulations. *Process Biochemistry*, *35*(8), 809–814.

Homaei, A. A., Sariri, R., Vianello, F., and Stevanato, R. (**2013**). Enzyme immobilization: an update. *Journal of Chemical Biology*, *6*(4), 185–205.

Hoyoux, A., Jennes, I., Dubois, P., Genicot, S., Dubail, F., Franç Ois, J. M., Gerday, C. (**2001**). Cold-Adapted ᴺʟ-Galactosidase from the Antarctic Psychrophile *Pseudoalteromonas haloplanktis*. *Applied And Environmental Microbiology*, 67(4), 1529–1535.

Hwang, T. L., and Shaka, A. J. (**1995**). Water Suppression That Works. Excitation Sculpting Using Arbitrary Wave-Forms and Pulsed-Field Gradients. *Journal of Magnetic Resonance, Series A*, *112*(2), 275–279.

Illanes, A., Cauerhff, A., Wilson, L., and Castro, G. R. (**2012**). Recent trends in biocatalysis engineering. *Bioresource Technology*, *115*, 48–57.

Iyer, P. V., and Ananthanarayan, L. (**2008**). Enzyme stability and stabilization-Aqueous and non-aqueous environment. *Process Biochemistry*, *43*(10), 1019–1032.

Jäckel, C., Kast, P., and Hilvert, D. (**2008**). Protein design by directed evolution. *Annu. Rev. Biophys.* Retrieved from

Jaeger, K. E., and Eggert, T. (**2002**). Lipases for biotechnology. *Current Opinion in Biotechnology*, *13*(4), 390–397.

Jaeger, K. E., Ransac, S., Dijkstra, B. W., Colson, C., van Heuvel, M., and Misset, O. (**1994**). Bacterial lipases. *FEMS Microbiology Reviews*, *15*(1), 29–63.

Jaeger, K. E., and Reetz, M. T. (**1998**). Microbial lipases form versatile tools for biotechnology. *Trends in Biotechnology*, *16*(9), 396–403.

Jaeger, K. E., Dijkstra, B. W., and Reetz, M. T. (**1999**). Bacterial biocatalysts: molecular biology, three-dimensional structures, and biotechnological applications of lipases. *Annual Review of Microbiology*, *53*, 315–351.

Janeček, S. (**1993**). Strategies for obtaining stable enzymes. *Process Biochemistry*, *28*(7), 435–445.

Jha, B., Svensson, M., Kronberg, B., and Holmberg, K. (**1999**). Titration Microcalorimetry Studies of the Interaction between *Humicola lanuginosa* Lipase and Ionic Surfactants. *Journal of Colloid and Interface Science*,

213(1), 262–264.

Ji, X., Chen, G., Zhang, Q., Lin, L., and Wei, Y. (**2015**). Purification and characterization of an extracellular cold-adapted alkaline lipase produced by psychrotrophic bacterium *Yersinia enterocolitica* strain KM1. *Journal of Basic Microbiology*, *55*(6), 718–728.

Jiewei, T., Zuchao, L., Peng, Q., Lei, W., and Yongqiang, T. (**2014**). Purification and Characterization of a Cold-Adapted Lipase from *Oceanobacillus* strain PT-11. *PLoS ONE*, *9*(7).

Ju, H., Jang, E., Ryu, B. H., Kim, T. D., Ryu, H., and Kim, T. D. (**2013**). Characterization and preparation of highly stable aggregates of a novel type of hydrolase (BL28) from *Bacillus licheniformis*. *Bioresource Technology*, *128*, 81–86.

Jung, S. K., Dae, G. J., Mi, S. L., Lee, J. K., Kim, H. K., Seong, E. R., … Seung, J. K. (**2008**). Structural basis for the cold adaptation of psychrophilic M37 lipase from *Photobacterium lipolyticum*. *Proteins: Structure, Function and Genetics*, *71*(1), 476–484.

Kanapathipillai, M., Lentzen, G., Sierks, M., and Park, C. B. (**2005**). Ectoine and hydroxyectoine inhibit aggregation and neurotoxicity of Alzheimer's β-amyloid. *FEBS Letters*, *579*(21), 4775–4780.

Karanicolas, J., and Kuhlman, B. (**2009**). Computational design of affinity and specificity at protein–protein interfaces. *Current Opinion in Structural Biology*, *19*(4), 458–463.

Kartal, F., Janssen, M. H. A., Hollmann, F., Sheldon, R. A., and Kilinc, A. (**2011**). Improved esterification activity of *Candida rugosa* lipase in organic solvent by immobilization as Cross-linked enzyme aggregates (CLEAs). *Journal of Molecular Catalysis B: Enzymatic*, *71*(3–4), 85–89.

Kartal, F., and Kilinc, A. (**2012**). Crosslinked aggregates of *Rhizopus oryzae* lipase as industrial biocatalysts: Preparation, optimization, characterization, and application for enantioselective resolution reactions. *Biotechnology Progress*, *28*(4), 937–945.

Kawahara, H. (**2002**). The structures and functions of ice crystal-controlling proteins from bacteria. *Journal of Bioscience and Bioengineering*, *94*(6), 492–6.

Kelley, L. A., Mezulis, S., Yates, C. M., Wass, M. N., and Sternberg, M. J. E. (**2015**). The Phyre2 web portal for protein modeling, prediction and

analysis. *Nat. Protocols*, *10*(6), 845–858.

Kennedy, J., Marchesi, J. R., and Dobson, A. D. (**2008**). Marine metagenomics: strategies for the discovery of novel enzymes with biotechnological applications from marine environments. *Microbial Cell Factories*, *7*, 27.

Kim, M. H., Kim, H. K., Lee, J. K., Park, S. Y., and Oh, T. K. (**2000**). Thermostable lipase of *Bacillus Stearothermophilus*: high-level production, purification, and calcium-dependent thermostability. *Bioscience, Biotechnology, and Biochemistry*.

Klibanov, A. M. (**1983**). Stabilization of enzymes against thermal inactivation. *Advances in Applied Microbiology*, *29*, 1–28.

Korman, T. P., and Bowie, J. U. (**2012**). Crystal Structure of *Proteus mirabilis* Lipase, a Novel Lipase from the *Proteus*/Psychrophilic Subfamily of Lipase Family I.1. *PLoS ONE*, *7*(12), 1–8.

Kranen, E., Detzel, C., Weber, T. and Jose, J.(**2014**). Autodisplay for the co-expression of lipase and foldase on the surface of *E. coli*: washing with designer bugs. *Microbial Cell Factories*, *13*(1), 19.

Krieger, E., Joo, K., Lee, J. J., Lee, J. J., Raman, S., Thompson, J., … Karplus, K. (**2009**). Improving physical realism, stereochemistry, and side-chain accuracy in homology modeling: Four approaches that performed well in CASP8. *Proteins: Structure, Function and Bioinformatics*, *77*(SUPPL. 9), 114–122.

Kuddus, M. (**2014**). Cold-active Microbial Enzymes. *Biochemistry and Physiology: Open Access*, *4*(1), 1–2.

Kumar, V., Singh, D., Sangwan, P., and Gill, P (**2014**). Global market scenario of industrial enzymes. *Industrial Enzymes: Trends, Scope and Relevance*, 173–196.

Laemmli, U. K. (**1970**). Cleavage of structural proteins during the assembly of the head of bacteriophage T4. *Nature*, *227*(5259), 680–5.

Laskowski, R. A., MacArthur, M. W., Moss, D. S., and Thornton, J. M. (**1993**). PROCHECK: a program to check the stereochemical quality of protein structures. *Journal of Applied Crystallography*, *26*(2), 283–291.

Lentzen, G., and Schwarz, T. (**2006**). Extremolytes: natural compounds from extremophiles for versatile applications. *Applied Microbiology and Biotechnology*, *72*(4), 623–634.

Lesk, A. M., and Chothia, C. H. (**1986**). The Response of Protein Structures to Amino-Acid Sequence Changes. *Philosophical Transactions of the Royal Society of London A: Mathematical, Physical and Engineering Sciences*, *317*(1540).

Linder, S., Schliwa, M., and Kube-Granderath, E. (**1996**). Direct PCR screening of *Pichia pastoris* clones. *BioTechniques*, *20*(6), 980–2.

Lippow, S. M., and Tidor, B. (**2007**). Progress in computational protein design. *Current Opinion in Biotechnology*, *18*(4), 305–311.

Littlechild, J. A. (**2015**). Enzymes from Extreme Environments and Their Industrial Applications. *Frontiers in Bioengineering and Biotechnology*, *3*(October), 1–9.

Littlechild, J., Novak, H., James, P., and Sayer, C. (**2013**). Mechanisms of Thermal Stability Adopted by Thermophilic Proteins and Their Use in White Biotechnology. In *Thermophilic Microbes in Environmental and Industrial Biotechnology* (pp. 481–507). Dordrecht: Springer Netherlands.

Liu, P., Wang, Y.-F., Ewis, H. E., Abdelal, A. T., Lu, C.-D., Harrison, R. W., and Weber, I. T. (**2004**). Covalent Reaction Intermediate Revealed in Crystal Structure of the *Geobacillus stearothermophilus* Carboxylesterase Est30. *Journal of Molecular Biology*, *342*(2), 551–561.

Lonhienne, T., Gerday, C., and Feller, G. (**2000**). Psychrophilic enzymes: revisiting the thermodynamic parameters of activation may explain local flexibility. *Biochimica et Biophysica Acta*, *1543*(1), 1–10.

López-Gallego, F., Betancor, L., Hidalgo, A., Alonso, N., Fernández-Lafuente, R., and Guisán, J. M. (**2005**). Co-aggregation of enzymes and polyethyleneimine: A simple method to prepare stable and immobilized derivatives of glutaryl acylase. *Biomacromolecules*, *6*(4), 1839–1842.

López-Serrano, P., Cao, L., Van Rantwijk, F., and Sheldon, R. A. (**2002**). Cross-linked enzyme aggregates with enhanced activity: Application to lipases. *Biotechnology Letters*, *24*(16), 1379–1383.

Lorenz, P., Liebeton, K., Niehaus, F., and Eck, J. (**2002**). Screening for novel enzymes for biocatalytic processes: Accessing the metagenome as a resource of novel functional sequence space. *Current Opinion in Biotechnology*, *13*(6), 572–577.

Lovell, S. C., Davis, I. W., Arendall, W. B., de Bakker, P. I. W., Word, J. M.,

Prisant, M. G., … Richardson, D. C. (**2003**). Structure validation by Cα geometry: ϕ,ψ and Cβ deviation. *Proteins: Structure, Function, and Bioinformatics*, *50*(3), 437–450.

Luft, J. R., and DeTitta, G. T. (**1999**). A method to produce microseed stock for use in the crystallization of biological macromolecules. *Acta Crystallographica Section D: Biological Crystallography*, *55*(5), 988–993.

Lutz, S. (**2010**). Beyond directed evolution—semi-rational protein engineering and design, *Current Opinion in Biotechnology*, *21*(6), 734–43.

Macauley-Patrick, S., Fazenda, M. L., McNeil, B., and Harvey, L. M. (**2005**). Heterologous protein production using the Pichia pastoris expression system. *Yeast*, *22*(4), 249–270.

Maiangwa, J., Ali, M. S. M., Salleh, A. B., Rahman, R. N. Z. R. A., Shariff, F. M., and Leow, T. C. (**2015**, March). Adaptational properties and applications of cold-active lipases from psychrophilic bacteria. *Extremophiles*.

Margesin, R., and Häggblom, M. M. (**2007**). Thematic issue: Microorganisms in cold environments. *FEMS Microbiology Ecology*, *59*(2), 215–216.

Margesin, R., Hämmerle, M., and Tscherko, D. (**2007**). Microbial activity and community composition during bioremediation of diesel-oil-contaminated soil: Effects of hydrocarbon concentration, fertilizers, and incubation time. *Microbial Ecology*, *53*(2), 259–269.

Margesin, R., and Schinner, F. (**1994**). Properties of cold-adapted microorganisms and their potential role in biotechnology. *Journal of Biotechnology*, *33*(1), 1–14.

Martinelle, M., Holmquist, M., and Hult, K. (**1995**). On the interfacial activation of *Candida antarctica* lipase A and B as compared with *Humicola lanuginosa* lipase. *Biochimica et Biophysica Acta - Lipids and Lipid Metabolism*, *1258*(3), 272–276.

Martins, L. O., and Santos, H. (**1995**). Accumulation of Mannosylglycerate and Di-myo-Inositol-Phosphate by *Pyrococcus furiosus* in Response to Salinity and Temperature. *Applied and Environmental Microbiology*, *61*(9), 3299–303.

Mateo, C., Palomo, J. M., Fernandez-Lorente, G., Guisan, J. M., and Fernandez-Lafuente, R. (**2007**). Improvement of enzyme activity, stability and selectivity via immobilization techniques. *Enzyme and Microbial Technology*, *40*(6), 1451–1463.

Maurer, K. H. (**2004**). Detergent proteases. *Current Opinion in Biotechnology*, *15*(4), 330–334.

Mehta, A. (**2010**).Microbial Protease and their Industrial Application. In *Industrial Exploitation of Microorganisms* (pp. 199-226). I.K. International Publication House.

Meyer, H. P., Eichhorn, E., Hanlon, S., Lütz, S., Schürmann, M., Wohlgemuth, R., and Coppolecchia, R. (**2012**). The use of enzymes in organic synthesis and the life sciences: perspectives from the Swiss Industrial Biocatalysis Consortium (SIBC). *Catalysis Science and Technology*, *3*(1), 29–40.

Migneault, I., Dartiguenave, C., Bertrand, M. J., and Waldron, K. C. (**2004**). Glutaraldehyde: Behavior in aqueous solution, reaction with proteins, and application to enzyme crosslinking. *BioTechniques*, *37*(5), 790–802.

Mohamad, N. R., Marzuki, N. H. C., Buang, N. A., Huyop, F., and Wahab, R. A. (**2015**). An overview of technologies for immobilization of enzymes and surface analysis techniques for immobilized enzymes. *Biotechnology and Biotechnological Equipment*, *29*(2), 205–220.

Mollania, N., Khajeh, K., Ranjbar, B., and Hosseinkhani, S. (**2011**). Enhancement of a bacterial laccase thermostability through directed mutagenesis of a surface loop. *Enzyme and Microbial Technology*, *49*(5), 446–452.

Montesino, R., García, R., Quintero, O., and Cremata, J. A. (**1998**). Variation in N-linked oligosaccharide structures on heterologous proteins secreted by the methylotrophic yeast *Pichia pastoris*. *Protein Expression and Purification*, *14*(2), 197–207.

Morgan-Kiss, R. M., Priscu, J. C., Pocock, T., Gudynaite-Savitch, L., and Huner, N. P. A. (**2006**). Adaptation and acclimation of photosynthetic microorganisms to permanently cold environments. *Microbiology and Molecular Biology Reviews : MMBR*, *70*(1), 222–52.

Morita, T., Fukuoka, T., Imura, T., and Kitamoto, D. (**2009**). Production of glycolipid biosurfactants by basidiomycetous yeasts. *Biotechnology and Applied Biochemistry*, *53*(1), 39.

Morita, T., Fukuoka, T., Imura, T., and Kitamoto, D. (**2015**). Mannosylerythritol Lipids: Production and Applications. *Journal of Oleo Science, 64*(2), 133–141.

Mulligan, C. N. (**2005**). Environmental applications for biosurfactants. *Environmental Pollution*. *133*(2), 183–198.

Nardini, M., and Dijkstra, B. W. (**1999**). Alpha/Beta hydrolase fold enzymes: The family keeps growing. *Current Opinion in Structural Biology*, *9*(6), 732–737.

Nardini, M., Lang, D. A., Liebeton, K., Jaeger, K. E., and Dijkstra, B. W. (**2000**). Crystal structure of *Pseudomonas aeruginosa* lipase in the open conformation. The prototype for family I.1 of bacterial lipases. *Journal of Biological Chemistry*, *275*(40), 31219–31225.

Nevalainen, K. M. H., Te'o, V. S. J., and Bergquist, P. L. (**2005**). Heterologous protein expression in filamentous fungi. *Trends in Biotechnology*, *23*(9), 468–474.

Niehaus, F., Bertoldo, C., Kähler, M., and Antranikian, G. (**1999**). Extremophiles as a source of novel enzymes for industrial application. *Applied Microbiology and Biotechnology*, *51*(6), 711–729.

Nietlispach, D. (**2005**). Suppression of anti-TROSY lines in a sensitivity enhanced gradient selection TROSY scheme. *Journal of Biomolecular NMR*, *31*(2), 161–166.

Noble, M. E. M., Cleasby, A., Johnson, L. N., Egmondb, M. R., and Frenkenb, L. G. J. (**1993**). The crystal structure of triacylglycerol lipase from *Pseudomonas glumae* reveals a partially redundant catalytic aspartate, *3312*(1), 123–128.

Nomenclature Committee of the International Union of Biochemistry and Molecular Biology (NC-IUBMB). Classification and Nomenclature of Enzymes by the Reactions they Catalyse. Retrieved October 28, 2017, from http://www.sbcs.qmul.ac.uk/iubmb/enzyme/rules.html

Novak, H.R. (**2012)**. *Biochemical and strucutural charcterisation of dehalogenases from marine bacteria*. PhD Thesis, University of Exeter

Novak, H. R., Sayer, C., Panning, J., and Littlechild, J. (**2013**). Characterisation of an l-Haloacid Dehalogenase from the Marine Psychrophile Psychromonas ingrahamii with Potential Industrial Application. *Marine Biotechnology*, *15*(6), 695–705.

Ó'Fágáin, C. (**2003**). Enzyme stabilization—recent experimental progress. *Enzyme and Microbial Technology*, *33*(2–3), 137–149.

Page, R. (**2008**). Strategies for improving crystallization success rates. *Methods*

in Molecular Biology (Clifton, N.J.), *426*(3), 345–62.

Paiva, A. L., Balcão, V. M., and Malcata, F. X. (**2000**). Kinetics and mechanisms of reactions catalyzed by immobilized lipases. *Enzyme and Microbial Technology*, *27*(3), 187–204.

Parry, N. J., Parry, A. J., Peilow, A. C., and Stevenson, P. S. (**2012**). Combinations of Rhamnolipids and Enzymes for Improved Cleaning. Patent no WO2012010406A1.

Pasteur, L. M. (**1858**). Oeuvres de Pasteur / réunies par Pasteur tome 3.

Pauling, L. (**1946**). Molecular Architecture and Biological Reactions. *Chemical and Engineering News*, *24*(10), 1375–1377.

Persichetti, R., Clair, N., and Griffith, J. (**1995**). Cross-linked enzyme crystals (CLECs) of thermolysin in the synthesis of peptides. *Journal of the American Chemical Society*, *117*(10), 2732–2737

Peters, G. H., Svendsen, A., Langberg, H., Vind, J., Patkar, S. a., and Kinnunen, P. K. J. (**2002**). Glycosylation of *Thermomyces lanuginosa* lipase enhances surface binding towards phospholipids, but does not significantly influence the catalytic activity. *Colloids and Surfaces B: Biointerfaces*, *26*(1–2), 125–134.

Petersen, S. B., Harald Jonson, P., Fojan, P., Petersen, E. I., Neves Petersen, M. T., Hansen, S., … Hough, E. (**1998**). Protein engineering the surface of enzymes. *Journal of Biotechnology*, *66*(1), 11–26.

Pettersen, E. F., Goddard, T. D., Huang, C. C., Couch, G. S., Greenblatt, D. M., Meng, E. C., and Ferrin, T. E. (**2004**). UCSF Chimera - A visualization system for exploratory research and analysis. *Journal of Computational Chemistry*, *25*(13), 1605–1612.

Phillips, R. S., Vita, A., Spivey, J. B., Rudloff, A. P., Driscoll, M. D., and Hay, S. (**2016**). Ground-State Destabilization by Phe-448 and Phe-449 Contributes to Tyrosine Phenol-Lyase Catalysis. *ACS Catalysis*, *6*(10), 6770–6779.

Piette, F., D'Amico, S., Mazzucchelli, G., Danchin, A., Leprince, P., and Feller, G. (**2011**). Life in the cold: a proteomic study of cold-repressed proteins in the antarctic bacterium *Pseudoalteromonas haloplanktis* TAC125. *Applied and Environmental Microbiology*, *77*(11), 3881–3.

Pinholt, C., Fanø, M., Wiberg, C., Hostrup, S., Bukrinsky, J. T., Frokjaer, S., … Jorgensen, L. (**2010**). Influence of glycosylation on the adsorption of

Thermomyces lanuginosus lipase to hydrophobic and hydrophilic surfaces. *European Journal of Pharmaceutical Sciences*, *40*(4), 273–281.

Pompon, D., and Nicolas, A. (**1989**). Protein engineering by cDNA recombination in yeasts: shuffling of mammalian cytochrome P-450 functions. *Gene*, *83*(1), 15–24.

Posorske, L. H. (**1984**). Industrial-scale application of enzymes to the fats and oil industry. *Journal of the American Oil Chemists' Society*, *61*(11), 1758–1760.

Powell, K. A., Ramer, S. W., Del Cardayr, S. B., Stemmer, W. P. C., Tobin, M. B., Longchamp, P. F., and Huisman, G. W. (**2001**). Directed evolution and biocatalysis. *Angewandte Chemie - International Edition*, *40*(21), 3948–3959.

Quiocho, F. A., and Richards, F. M. (**1964**). Intermolecular Cross Linking of a Protein in the Crystalline State: Carboxypeptidase-a. *Proceedings of the National Academy of Sciences of the United States of America*, *52*, 833–839.

Rees, D. C., and Robertson, A. D. (**2001**). Some thermodynamic implications for the thermostability of proteins. *Protein Science : A Publication of the Protein Society*, *10*(6), 1187–94.

Reetz, M. T. (**2013**). Biocatalysis in organic chemistry and biotechnology: Past, present, and future. *Journal of the American Chemical Society*, *135*(34), 12480–12496.

Rehm, T., Huber, R., and Holak, T. A. (**2002**). Application of NMR in Structural Proteomics. *Structure*, *10*(12), 1613–1618.

Riaz, M., Rashid, M. H., Sawyer, L., Akhtar, S., Javed, M. R., Nadeem, H., and Wear, M. (**2012**). Physiochemical properties and kinetics of glucoamylase produced from deoxy-d-glucose resistant mutant of *Aspergillus niger* for soluble starch hydrolysis. *Food Chemistry*, *130*(1), 24.

Richardson, J. S., and Richardson, D. C. (**1989**). The de novo design of protein structures. *Trends in Biochemical Sciences*, *14*(7), 304–309.

Riley, M., Staley, J. T., Danchin, A., Wang, T. Z., Brettin, T. S., Hauser, L. J., Land, M,L. and Thompson, L. S. (**2008**). Genomics of an extreme psychrophile, *Psychromonas ingrahamii*. *BMC Genomics*, *9*, 210.

Robert, X., and Gouet, P. (**2014**). Deciphering key features in protein structures

with the new ENDscript server. *Nucleic Acids Research*, *42*(W1), W320–

Rodrigues, D. F., and Tiedje, J. M. (**2008**). Coping with our cold planet. *Applied and Environmental Microbiology*, *74*(6), 1677–86.

Rodrigues, R. C., Berenguer-Murcia, Á., and Fernandez-Lafuente, R. (**2011**). Coupling chemical modification and immobilization to improve the catalytic performance of enzymes. *Advanced Synthesis and Catalysis*, *353*(13), 2216–2238.

Rodrigues, R. C., Godoy, C. a., Volpato, G., Ayub, M. a Z., Fernandez-Lafuente, R., and Guisan, J. M. (**2009**). Immobilization-stabilization of the lipase from *Thermomyces lanuginosus*: Critical role of chemical amination. *Process Biochemistry*, *44*(9), 963–968.

Ryu, H. S., Kim, H. K., Choi, W. C., Kim, M. H., Park, S. Y., Han, N. S., … Lee, J. K. (**2006**). New cold-adapted lipase from *Photobacterium lipolyticum* sp. nov. that is closely related to filamentous fungal lipases. *Applied Microbiology and Biotechnology*, *70*(3), 321–326.

Sarda, L., and Desnuelle, P. (**1958**). Actions of pancreatic lipase on esters in emulsions. *Biochimica et biophysica acta*, *30*(3), 513–521.

Schmid, R. D., and Verger, R. (**1998**). Lipases : Interfacial Enzymes with Attractive Applications. *Angewandte Chemie International Edition*, *37*(12), 1608–1633.

Schmidt, M., and Bornscheuer, U. T. (**2005**). High-throughput assays for lipases and esterases. *Biomolecular Engineering*, *22*(1–3), 51–56.

Schneider, C. A., Rasband, W. S., and Eliceiri, K. W. (**2012**). NIH Image to ImageJ: 25 years of image analysis. *Nature Methods*, *9*(7), 671–5.

Schoemaker, H. E., Mink, D., and Wubbolts, M. G. (**2003**). Dispelling the Myths--Biocatalysis in Industrial Synthesis. *Science*, *299*(5613).

Schoevaart, R., Wolbers, M. W., Golubovic, M., Ottens, M., Kieboom, A. P. G., Van Rantwijk, F., … Sheldon, R. A. (**2004**). Preparation, optimization, and structures, of cross-linked enzyme aggregates (CLEAs). *Biotechnology and Bioengineering*, *87*(6), 754–762.

Schrag, J. D., Li, Y., Cygler, M., Lang, D., Burgdorf, T., Hecht, H.J., Schmid, R., Schomburg, D., Rydel, T,J., Oliver., J,D., Strickland, L.C., Dunaway, M., Larson., S.B., Day, J and McPherson, A. (**1997**). The open conformation of a *Pseudomonas* lipase. *Structure*, *5*(2), 187–202.

Schwarz, R. T., and Datema, R. (**1980**). Inhibitors of protein glycosylation. *Trends in Biochemical Sciences*, *5*(3), 65–67.

Schwede, T. (**2013**). "Protein Modeling: What Happened to the Protein Structure Gap?" *Structure 21*(9), 1531–1540.

Sekhon Randhawa, K. K., and Rahman, P. K. S. M. (**2014**). Rhamnolipid biosurfactants-past, present, and future scenario of global market. *Frontiers in Microbiology*, *5*, 454.

Shah, S., Sharma, A., and Gupta, M. N. (**2006**). Preparation of cross-linked enzyme aggregates by using bovine serum albumin as a proteic feeder. *Analytical Biochemistry*, *351*(2), 207–13.

Sharma, R., Chisti, Y., and Banerjee, U. C. (**2001**). Production, purification, characterization, and applications of lipases. *Biotechnology Advances*, *19*(8), 627–662.

Sheldon, R. A. (**2007**). Cross-linked enzyme aggregates (CLEAs): stable and recyclable biocatalysts. *Biochemical Society Transactions*, *35*(Pt 6), 1583–1587.

Sheldon, R. A., Schoevaart, R., and Van Langen, L. M. (**2005**). Cross-linked enzyme aggregates (CLEAs): A novel and versatile method for enzyme immobilization (a review). *Biocatalysis and Biotransformation*, *23*(3–4), 141–147.

Shi, X., and Jarvis, D. L. (**2007**). Protein N-glycosylation in the baculovirus-insect cell system. *Current Drug Targets*, *8*(10), 1116–25.

Shirai, K., and Jackson, R. L. (**1982**). Lipoprotein lipase-catalyzed hydrolysis of p-nitrophenyl butyrate. Interfacial activation by phospholipid vesicles. *The Journal of Biological Chemistry*, *257*(3), 1253–8.

Siddiqui, K. S., and Cavicchioli, R. (**2006**). Cold-Adapted Enzymes. *Annual Review of Biochemistry*, *75*(1), 403–433.

Silva, Z., Borges, N., Martins, L. O., Wait, R., da Costa, M. S., and Santos, H. (**1999**). Combined effect of the growth temperature and salinity of the medium on the accumulation of compatible solutes by *Rhodothermus marinus* and *Rhodothermus obamensis*. *Extremophiles : Life under Extreme Conditions*, *3*(2), 163–72.

Sinclair, A. M., and Elliott, S. (**2005**). Glycoengineering: The effect of

glycosylation on the properties of therapeutic proteins. *Journal of Pharmaceutical Sciences*, *94*(8), 1626–1635.

Singh, R.K. et al. (**2013**). From protein engineering to immobilization: promising strategies for the upgrade of industrial enzymes. *International Journal of Molecular Science* 14(1), 1232–77.

.

Spahn, C., and Minteer, S. D. (**2008**). Enzyme Immobilization in Biotechnology. *Recent Patents on Engineering*, *2*(3), 195–200. Stetter, K. O. (**1996**). Hyperthermophilic procaryotes. *FEMS Microbiology Reviews*, *18*(2–3), 149–158.

Stetter, K. O. (**2006**). Hyperthermophiles in the history of life. *Philosophical Transactions of the Royal Society of London. Series B, Biological Sciences*, *361*(1474), 1837-42–3.

Struvay, C., and Feller, G. (**2012**). Optimization to low temperature activity in psychrophilic enzymes. *International Journal of Molecular Sciences*, *13*(9), 11643–11665.

Suzuki, T., Nakayama, T., Kurihara, T., Nishino, T., and Esaki, N. (**2001**). Cold-active lipolytic activity of psychrotrophic *Acinetobacter sp.* strain no. 6. *Journal of Bioscience and Bioengineering*, *92*(2), 144–148.

Svendsen, A., Clausen, I. G., P, Shamkant A., and Erik, G. (**1991**) Lipase variants. Patent no WO 1992005249 A1.

Trincone, A. (**2013**). *Marine Enzymes For Biocatalysis : Sources, Biocatalytic Characteristics And Bioprocesses Of Marine Enzymes.* Elsevier Science.

Turcu, M. C. (**2010**). *Lipase-cataly approaches towards secondary alcohols : intermediates for enantiopure drugs*. Phd Thesis University of Turku.

Turner, N. J. (**2009**). Directed evolution drives the next generation of biocatalysts. *Nature Chemical Biology*, *5*(8), 567–573.

Uchiyama, T., and Miyazaki, K. (**2009**). Functional metagenomics for enzyme discovery: challenges to efficient screening. *Current Opinion in Biotechnology*, *20*(6), 616–622.

Vamvaca, K., Vögeli, B., Kast, P., Pervushin, K., and Hilvert, D. (**2004**). An enzymatic molten globule: efficient coupling of folding and catalysis. *Proceedings of the National Academy of Sciences of the United States of America*, *101*, 12860–12864.

Vassilenko, K. S., and Uversky, V. N. (**2002**). Native-like secondary structure of molten globules. *Biochimica et Biophysica Acta - Protein Structure and Molecular Enzymology*, *1594*(1), 168–177.

Verger, R. (**1997**). “Interfacial activation” of lipases: Facts and artifacts. *Trends in Biotechnology*, *15*(1), 32–38.

Verschueren, K. H. G., Seljee, F., Rozeboom, H. J., Kalk, K. H., and Dijkstra, B. W. (**1993**). Crystallographic analysis of the catalytic mechanism of haloalkane dehalogenase. *Nature*, *363*(6431), 693–698.

Vieille, C., and Zeikus, G. J. (**2001**). Hyperthermophilic Enzymes: Sources, Uses, and Molecular Mechanisms for Thermostability. *Microbiology and Molecular Biology Reviews*, *65*(1), 1–43.

Visuri, K., and Klibanov, A. M. (**1987**). Enzymatic production of high fructose corn syrup (HFCS) containing 55% fructose in aqueous ethanol. *Biotechnology and Bioengineering*, *30*(7), 917–920.

Vivoli, M., Novak, H. R., Littlechild, J. A., and Harmer, N. J. (**2014**). Determination of protein-ligand interactions using differential scanning fluorimetry. *Journal of Visualized Experiments*, (91), 51809.

Vulfson, E.N. (**1994**).Industrial Application of Lipases In *Lipases — their structure, biochemistry and application* (pp.271-288). Cambridge University Press.

Vyas, V. K., Ukawala, R. D., Ghate, M., and Chintha, C. (**2012**). Homology Modeling a Fast Tool for Drug Discovery: Current Perspectives. *Indian Journal of Pharmaceutical Sciences*, *1*(1), 1–17.

Wang, M., Qi, W., Yu, Q., Su, R., and He, Z. (**2010**). Cross-linking enzyme aggregates in the macropores of silica gel: A practical and efficient method for enzyme stabilization. *Biochemical Engineering Journal*, *52*(2), 168–174.

Wenda, S., Illner, S., Mell, A., and Kragl, U. (**2011**). Industrial biotechnology—the future of green chemistry? *Green Chemistry*, *13*(11), 3007.

Wolff and Showell (**1997**).Application of Lipases in Detergents. In *Enzymes in Detergency* (pp. 93-106). Dekker.

Wu, L., Sun, Q., Sugawara, H., Yang, S., Zhou, Y., Mccluskey, K., Ma, J. (**2013**). Global catalogue of microorganisms (gcm): a comprehensive database and information retrieval, analysis, and visualization system for microbial resources. *BMC Genomics*, *14*.

Wu, S., and Letchworth, G. J. (**2004**). High efficiency transformation by electroporation of Pichia pastoris pretreated with lithium acetate and dithiothreitol. *BioTechniques*, *36*(1), 152–154.

Wu, S., and Zhang, Y. (**2007**). LOMETS: A local meta-threading-server for protein structure prediction. *Nucleic Acids Research*, *35*(10), 3375–3382.

Yu, Y., Zhao, J., and Bayly, A. E. (**2008**). Development of Surfactants and Builders in Detergent Formulations. *Chinese Journal of Chemical Engineering*, *16*(4), 517–527.

Zelinski, T., and Waldmann, H. (**1997**). Cross-Linked Enzyme Crystals (CLECs): Efficient and Stable Biocatalysts for Preparative Organic Chemistry. *Angewandte Chemie International*.

Zeng, X., Xiao, X., Wang, P., and Wang, F. (**2004**). Screening and characterization of psychrotrophic, lipolytic bacteria from deep-sea sediments. *Journal of Microbiology and Biotechnology*, *14*(5), 952–958.

Zhang, J., Zhang, Y., Li, W., Li, X., and Lian, X. (**2014**). Optimizing detergent formulation with enzymes. *Journal of Surfactants and Detergents*, *17*(6), 1059–1067.

Zhang, Y. (**2008**). I-TASSER server for protein 3D structure prediction. *BMC Bioinformatics*, *9*(1), 40.

Zou, S., Huang, S., Kaleem, I., and Li, C. (**2013**). N-glycosylation enhances functional and structural stability of recombinant β-glucuronidase expressed in *Pichia pastoris*. *Journal of Biotechnology*, *164*(1), 75–81.

10. Appendix

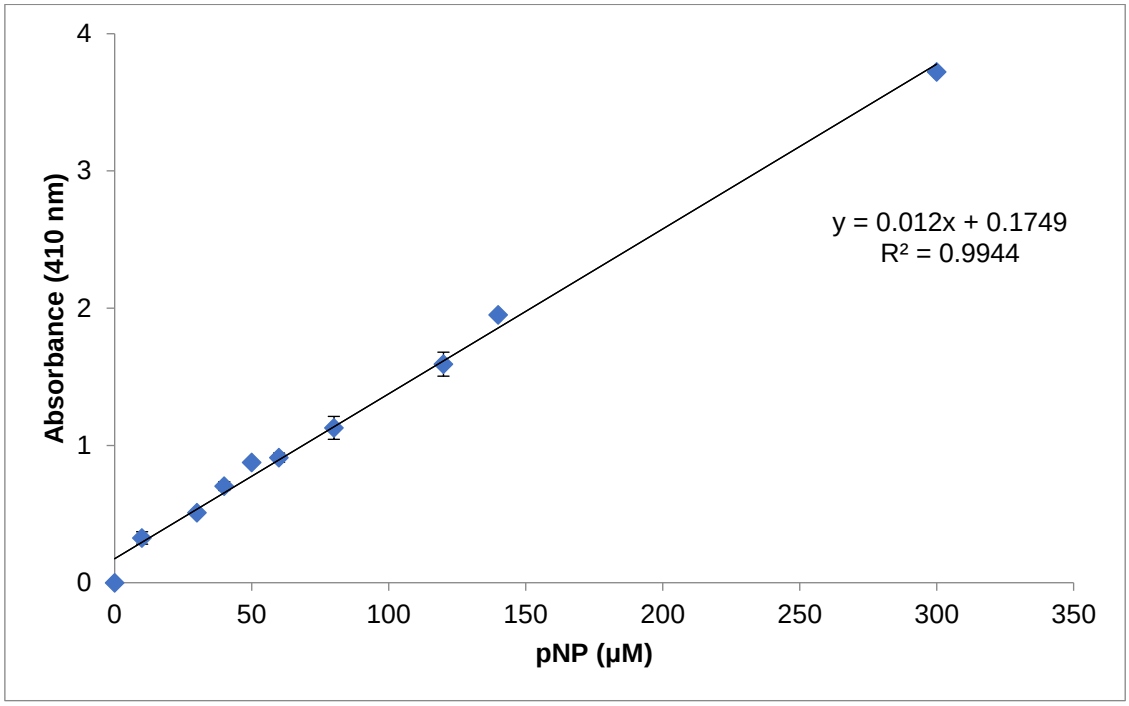

Fig 10.1: The pNP standard curve

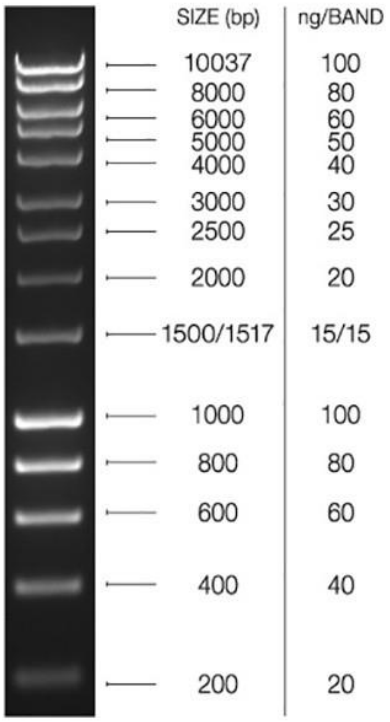

Fig.10.2: DNA gel ladder (Hyperladder 1, Bioline)

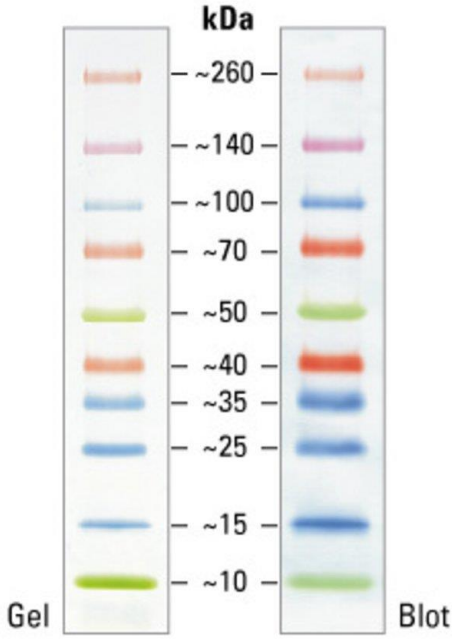

Fig.10.3: Protein gel ladder (Spectra Broad Range Multicolor, Thermo Fisher)

10.1 Sequences

Lipex gene sequence

CAGTGGTGGTGGTGGTGCTCGAAATGCAGCTGGCACGACAGGTTTCCCGACTGGAA
AGCGGGCAGTGAGCGGAAGGCCCATGAGGCCAGTCTTGTGCTCCAGGTACCCAGACAGG
TGCCAATCAGACCAAAATACCACAGATGTGCCGGAATATCCGGAATGTTCGGCTGATTA
TTACCACCGGTCGCATCAATACCTTCAATTTTCACAATATCACGACGACGAACCGGAAC
CAGGGTGCCGCTTTTAATCCAATATTCCGGACTGCTATGGCTATAACCAAATTCACGCG
GAGGCAGACGCGGAACAATATCATTGGTATGGGTAATACGATACAGGGTGCCACCGGTC
TGAACGGTCAGAAATTCTGCAAATGCACGATTACCAACACGCGGTGCACCATAGCTAAA
CACATCAATATCATAACCATTACCACGCAGATCGGCACCCGCAACGGTGGCCAGTGCAC
CACCCAGGCTATGACCGGTAAAAACAACACGATAATCCGGATGTTCACGAACTGCATCT
TCAACTTTCTGACGCAGGGTATCTGCAACGCTACGCCAGCTGCTGGTAAAACCATCATG
ACCACGACAACCGCTACAAATATCGTTGATCTCTTTCAGATCAAAGTTCAGATTGCCAA
TCCAATTTTCAATGCTACGGCTACCACGAAAGCTCAGAACAATCAGTTTGTTGGTATTA
TCCAGTGCCAGAAAACCGGTAACATCACCAACACCGCTATCTTCAAAGCTATACAGAAA
GGTTGCATCTGCTTTTTCAACTTCCGGACATGCATTACCGGTGCAGGTAATATTGGTGC
CTGCCGGTGCATCGTTATTTTTGCCACAATATGCTGCTGCGCTATACTGTGCAAACAGG
TTAAACTGATTAAACAGGTCCTGGCTAACTTCACGATCCGAATTAATTCCGATATCCAT
GGCCATCGCCGGCTGGGCAGCGAGGAGCAGCAGACCAGCAGCAGCGGTCGGCAGCAGGT
ATTTCAT

PinLip gene sequence

ATGCCGCACAAATTTACCATGGATCATAGCCTGCTGGAACCGCCTATTAAACGTGCAGC
ATATAGCGATCGTACCGCATGGCTGATGGCAGTTATGAGCAGCCTGGCATATATTCGTT
TTGAACAGCCGACACCGCTGGATGAACTGGCAAAAGTTCTGAGCCGTGAAACCAATGAA
CGTAACATTCTGACCAAACTGAATGCACTGCTGGCAGCAGAAAATCGTGATCAGCTGAA
AAAAGAACTGAAAAGCGATCTGCAGGATATCGGTTTTGAACTGGTTGATACCTATAACA
TTAGCATTCCGCTGGTTGTTGATACCCAGGCATATCTGGCAAAAATTACCCTGCAGGAT
CGTGATCCGATGCTGGTTCTGGCATTTCGTGGCACCGAAGTTACCAATGCAGCAGATAT
TCGTAGTGATGTTAGCGCAAATCCGATGAATATTGGTCCGAAAGAAGAAGGTCATCAGG
TTCATAGCGGCTTTTATAACGCATTTAAAGCAGCACAGAGCGTGATTGAACTGAGCCTG
AATAAACCGGAACTGAAAAACATGCCGCTGTATATTACCGGTCATAGTCTGGGTGGTGC
ACTGGCAGTTGTTGCAACCTATTGTATTAGCAATGATAGCGTTGGTGCCTGCTATACCT
TTGGTGGTCCGCGTGTTGGTAATATGCTGTTTGGCCAGAGCATTCGTACACCGGTTTAT
CGTGTTATTAATGCAGCCGATCTGGTTCCGCGTCTGCCTCCGAGCTATCTGATTGAAGG
TATTACACTGCTGCTGCGTTGGCTGCCGATTATTCCGTATAATAACCAGGTTGCAGATT
ACCTGGAACGCTTTCGTCATTATCGCCATTATGGTGATCTGCGTTATCTGACCGATGCA
ACCCGTAGCACACCGGAAGGTGAAGGTATGCTGGCTGCATATCCGGGTCTGCAGGTTAT
TGCAAATCCGTGCCAGCTGAGCCGTTGGATTTGGCTGTGTAGCCGTCTGATTGCCACCT
ATGGTCGTGCAGGTATTAATGATCATAGCATCGATATCTATGTCGAAAAACTGGCCTAT
TGGGGTATTCAGCGTAATCTGGGTAAACCGAAACTGGTTAGCGCACAGGCAGAAACCAA
AGGTTCAACCCAGGAGTGGCAGGGCGGGGCGGGCCATCACCATCACCACCACGGCTAA

Lipex 16L Amino acid sequence

The natural glycosylation site NXS/T is underlineded

EVSQDLFNQFNLFAQYSAAAYCGKNNDAPAGTNITCTGNACPEVEKADATFLYSFEDSG
VGDVTGFLALDNTNKLIVLSFRGSRSIENWIGNLNFDLKEINDICSGCRGHDGFTSSWR
SVADTLRQKVEDAVREHPDYRVVFTGHSLGGALATVAGADLRGNGYDIDVFSYGAPRVG
NRAFAEFLTVQTGGTLYRITHTNDIVPRLPPREFGYSHSSPEYWIKSGTLVPVRRRDIV
KIEGIDATGGNNQPNIPDIPAHLWYFGLIGTCL

PinLip Amino acid sequence

MPHKFTMDHSLLEPPIKRAAYSDRTAWLMAVMSSLAYIRFEQPTPLDELAKVLSRETNE
RNILTKLNALLAAENRDQLKKELKSDLQDIGFELVDTYNISIPLVVDTQAYLAKITLQD
RDPMLVLAFRGTEVTNAADIRSDVSANPMNIGPKEEGHQVHSGFYNAFKAAQSVIELSL
NKPELKNMPLYITGHSLGGALAVVATYCISNDSVGACYTFGGPRVGNMLFGQSIRTPVY
RVINAADLVPRLPPSYLIEGITLLLRWLPIIPYNNQVADYLERFRHYRHYGDLRYLTDA
TRSTPEGEGMLAAYPGLQVIANPCQLSRWIWLCSRLIATYGRAGINDHSIDIYVEKLAY
WGIQRNLGKPKLVSAQAETKGSTQ

10.2 Cloning maps

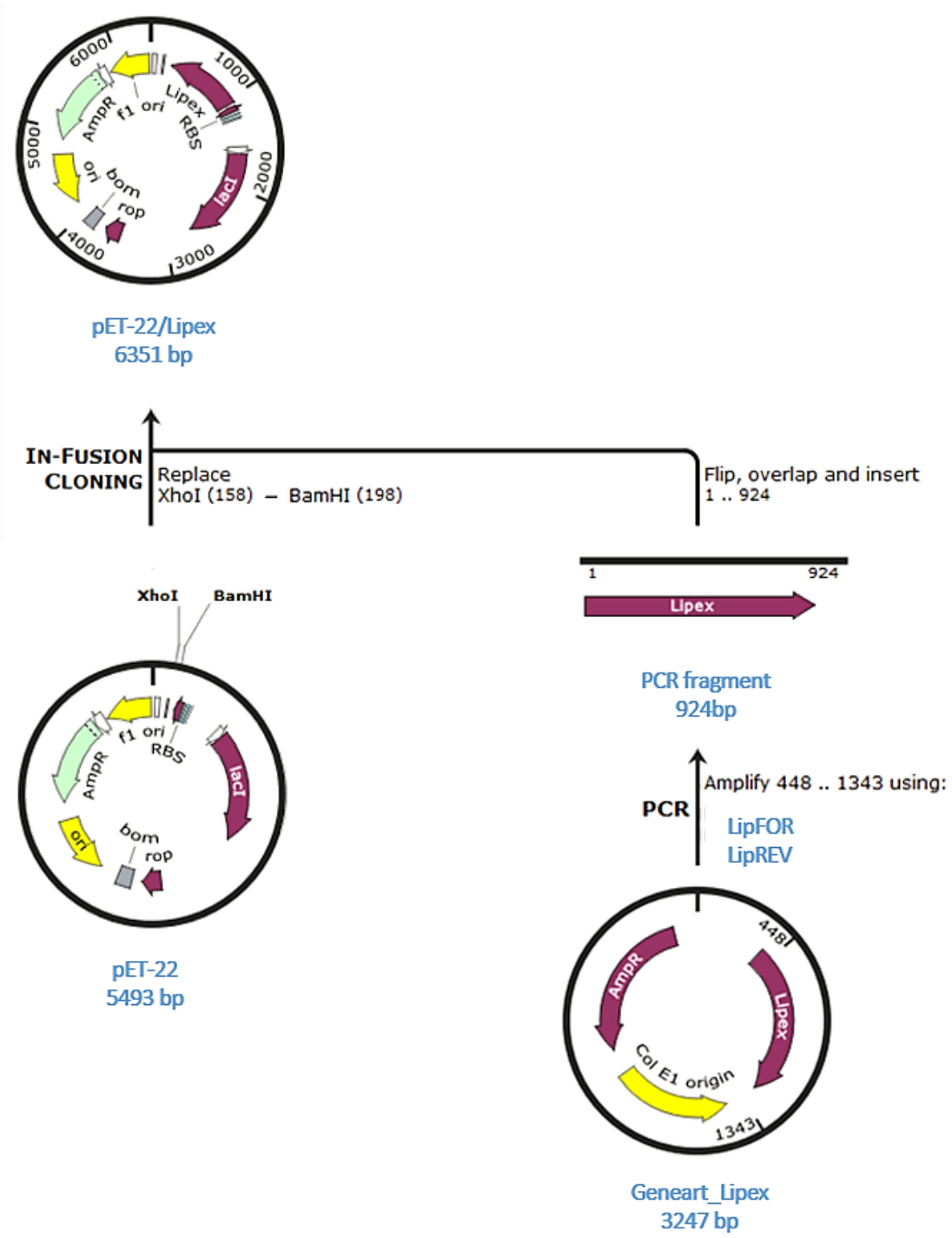

Fig 10.4: Lipex cloning in pET-22b Image obtained with SnapGene software (from GSL Biotech; available at http://www.snapgene.com/).

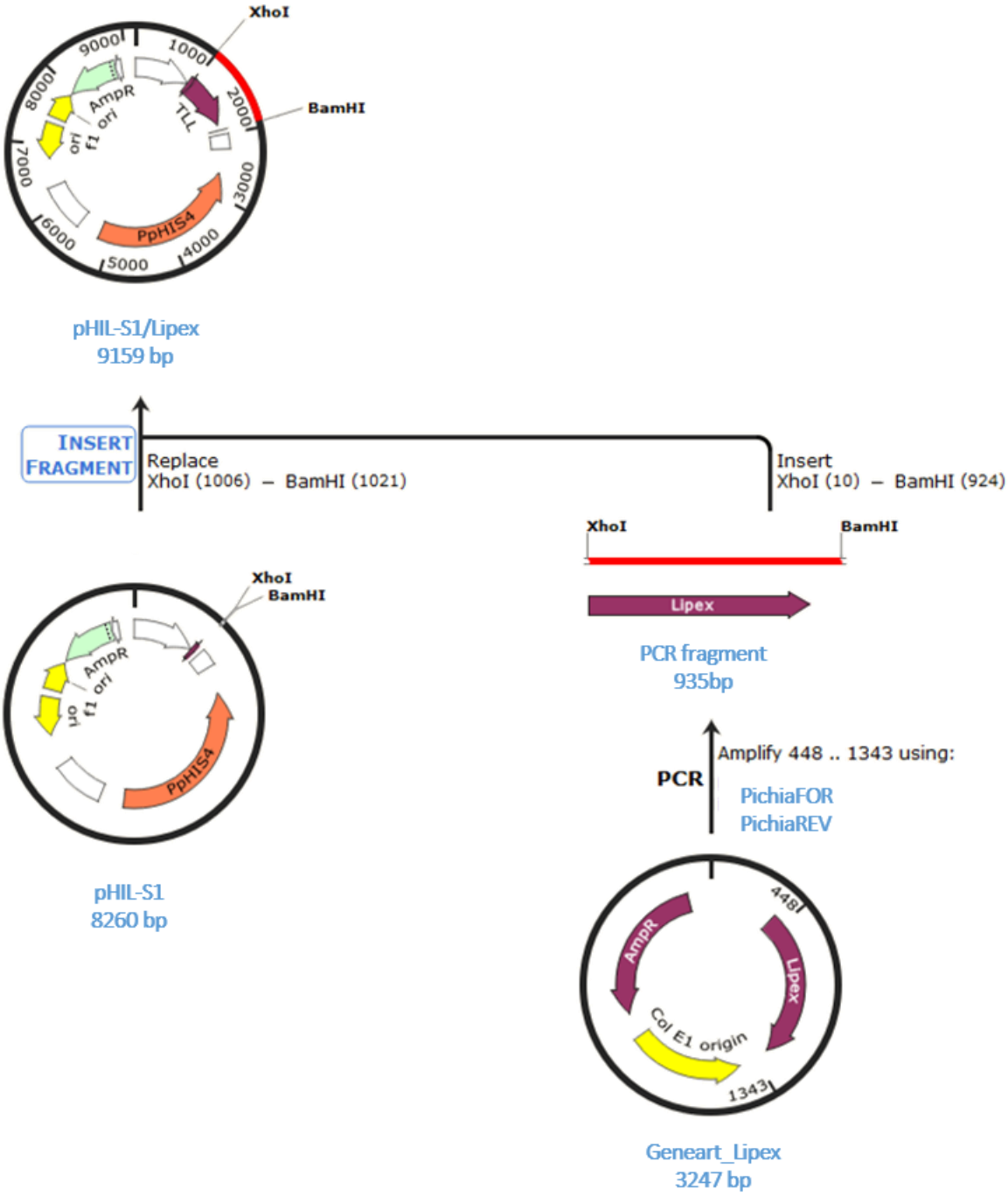

Fig 10.5: Lipex cloning in pHIL-S1. Image obtained with SnapGene software (from GSL Biotech; available at http://www.snapgene.com/).

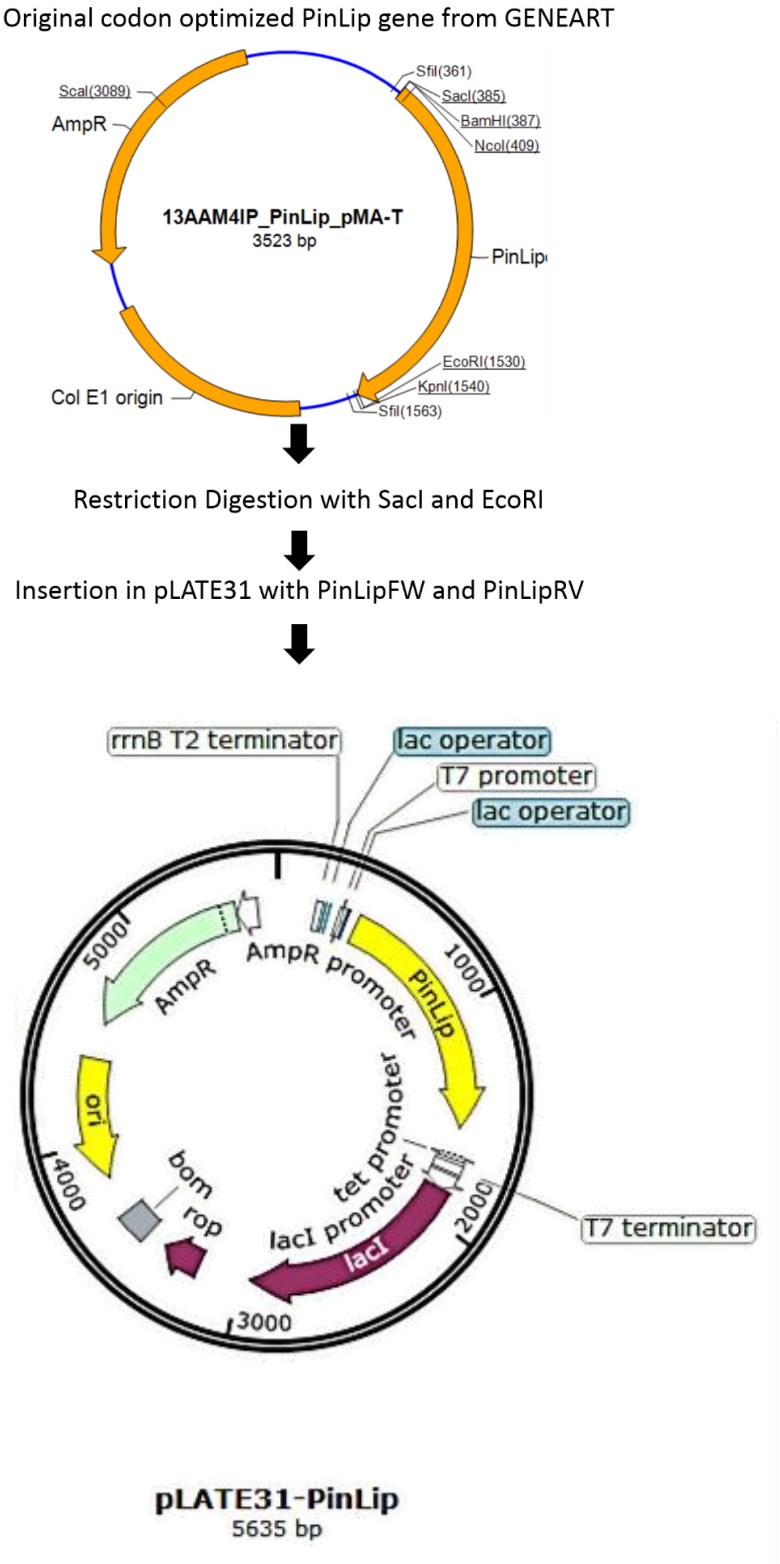

Fig 10.6: PinLip cloning into pLATE31

10.3 List of patents

De Rose, S.A.; Lang, D.A.; Littlechild, J.; Novak, H.; Singh, S. **Patent: WO2017/036901** Improved wash compositions. Published 09/03/2017 Full text available at https://patentscope.wipo.int/search/en/detail.jsf?docId=WO2017036901

De Rose, S.A.; Lang, D.A.; Littlechild, J.; Novak, H.; Singh, S. **Patent: WO2017/036902** Detergent compositions with lipase and biosurfactant. Published 09/03/2017 Full text available at https://patentscope.wipo.int/search/en/detail.jsf?docId=WO2017036902

De Rose, S.A.; Dowd, A.; Lang, D.A.; Littlechild, J.; Novak, H.; Parry N.J.; Singh, S. **Patent: WO2017/036915** Liquid Detergency Composition Comprising Protease and Non-Protease Enzyme. Published 09/03/2017 Full text available at https://patentscope.wipo.int/search/en/detail.jsf?docId=WO2017036915

De Rose, S.A.; Dowd, A.; Lang, D.A.; Littlechild, J.; Novak, H.; Parry N.J.; Singh, S. **Patent: WO2017/036916** Process to manufacture cross-linked enzyme aggregates. Published 27/04/2017 Full text available at https://patentscope.wipo.int/search/en/detail.jsf?docId=WO2017036916

De Rose, S.A.; Dowd, A.; Lang, D.A.; Littlechild, J.; Novak, H.; Parry N.J.; Singh, S. **Patent: WO2017/036917** Liquid detergency composition comprising lipase and protease. Published 09/03/2017 Full text available at https://patentscope.wipo.int/search/en/detail.jsf?docId=WO2017036917